Integrating spatio-temporal environmental models for planning ski runs

Nederlandse Geografische Studies / Netherlands Geographical Studies

ISSN 0169-4839

Netherlands Geographical Studies 311

Integrating spatio-temporal environmental models for planning ski runs

Karin Pfeffer

Utrecht 2003

Koninklijk Nederlands Aardrijkskundig Genootschap/
Faculteit Ruimtelijke Wetenschappen, Universiteit Utrecht

This publication is identical to a dissertation submitted for the title of Doctor at Utrecht University, the Netherlands. The public defense of this thesis took place on February 21, 2003.

Promotores:

Prof. Dr. P.A. Burrough	Utrecht University
Ao. Prof. Dr. B. Bauer	University of Vienna

Co-promotor:

Dr. Th.W.J. van Asch	Utrecht University

ISBN 90-6809-349-5

Printed in the Netherlands by Labor Grafimedia b.v. - Utrecht

CONTENTS

List of Figures

List of tables

1 INTRODUCTION

1.1 Context

During the last 30 years ski run construction has been one of the major human activities affecting the Alpine environment. The impact of skiing on environmental factors and processes, caused by the establishment of ski pistes, the maintenance of ski pistes and skiing itself, has been intensively studied (Cernusca, 1977; Cernusca, 1986; Mosimann, 1985). Human interference in the mountains continues to this day, driven by social and economical forces linked to the action of skiing and skiing facilities.

For instance, the number of visitors to one of the ski areas of the Austrian Tyrol increased from 204.000 per year in 1960 to 4 million per year in 2001, while the number of nights spent in one of these areas reached nearly 24 million (Figure 1.1).

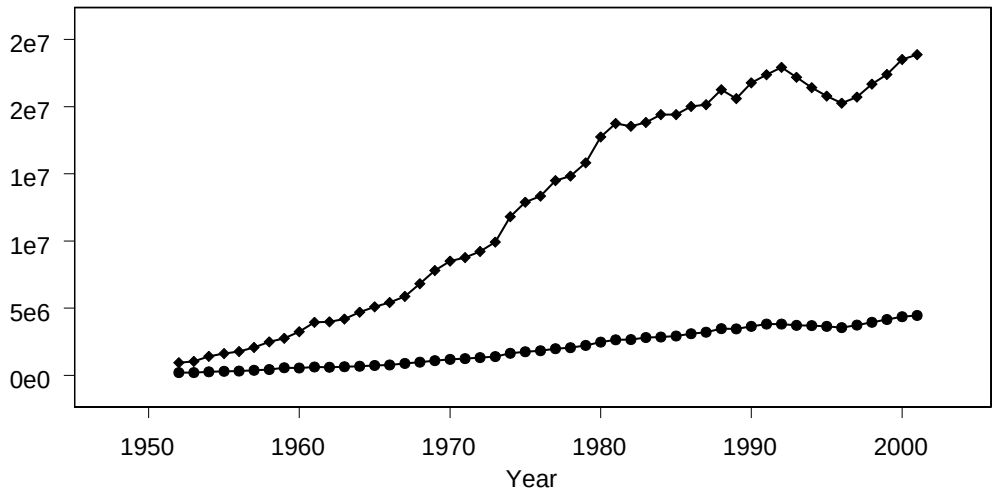

Figure 1.1 Development of winter tourism in Tyrol, Austria, from the winter 1951/52 to the winter 2001/2002. The dots indicate the number of visitors to a ski area in Tyrol, while the diamonds denote the number of nights spent in one of the ski areas. The drop from 1994 to 1997 was caused by a lack of snow. (Source: http://www.tirol.gv.at/statistik; Weber, 2000)

In addition, there is a trend in replacing old ski lifts with modern ones with a higher transport capacity, establishing new ski lifts in existing built up areas and integrating several ski areas to ski regions. For example, since 1990, the transport capacity has increased by 16.9 percent in the period 2000 to 2002 (Weber, 2002).

Further, and this is mainly caused by global warming, areas in higher alpine regions are going to be made accessible to skiing (Figure 1.2) since ski areas in lower areas suffer frequently from a lack of snow (Güthler, 2002). From the 155 projects in the year 2000, 25 projects aimed at opening natural areas to ski areas and 48 at the integration of smaller ski areas to skiing regions, also called ski arena.

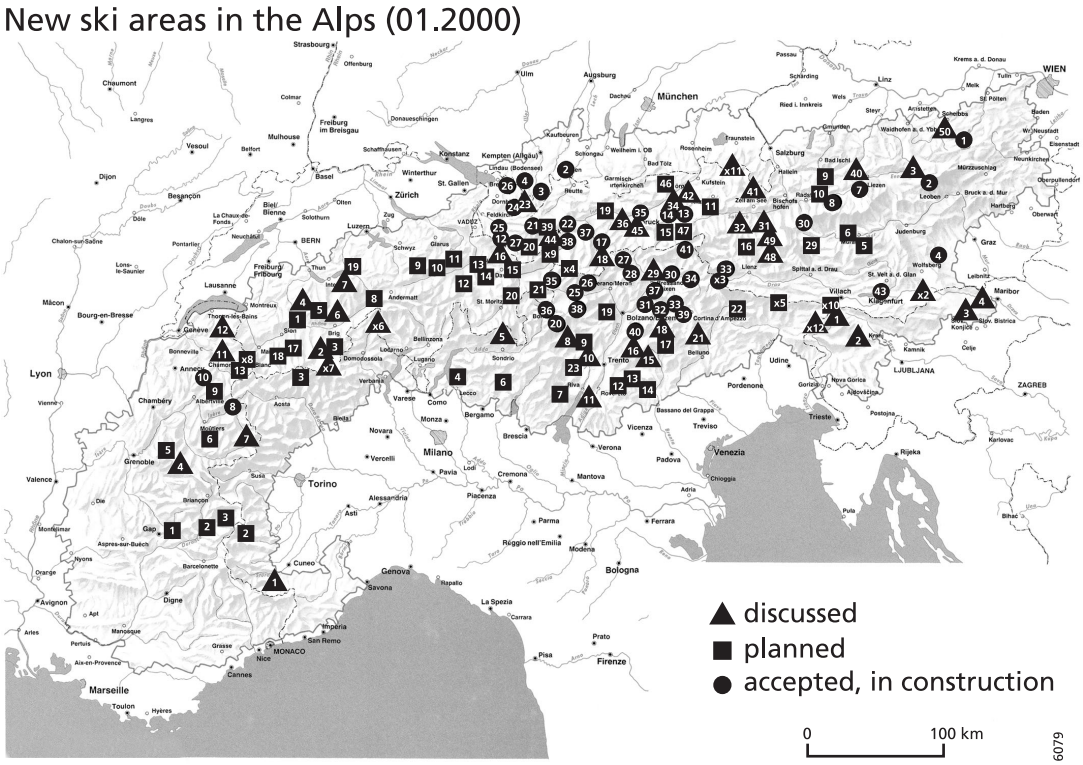

Figure 1.2 Planned ski areas in the Alps, as a consequence of global warming for the greater part located in higher areas. (Source: Bundesministerium für Umwelt, Jugend und Familie, 1996)

The continuous increase in skiing infrastructure and winter tourism takes place despite an awareness of the sensitivity of the alpine environment and possible consequences of ski run construction (Cernusca, 1990; Tappeiner et al., 1998). Therefore efficient tools are needed for evaluating the suitability of projects with respect to environmental quality. This was one objective of the GETS-project, which is a European research network for the application of **G**eomorphology and **E**nvironmental Impact Assessment to **T**ransportation **S**ystems. GETS was funded by the European Union (GETS Contract No. ERBFMRXCT970162). The main purpose of the project was to develop and improve methods and tools to facilitate the assessment of the impact of a transportation project on the environment and to communicate the results of the research to public authorities. The work described in this thesis was part of the research program of the GETS-project (http://www.feweb.vu.nl/gis/research/gets).

While other case studies in the GETS-project looked at the geomorphological and environmental impact possibly caused by a new motorway or railway, the case study described in this thesis explored the environmental suitability of a new cable car, ski lifts and ski pistes. The aim was to develop new methods and tools to improve and facilitate the procedure of an environmental impact assessment for skiing facilities. Discussions with experts in the field of environmental impact assessment and the planning of infrastructure in mountainous areas encouraged the development of a generic methodology to characterise environmental factors and processes and their interactions in a quantitative way. This methodology should be capable of integrating multiple concerns that are relevant for the establishment of infrastructure in an alpine area. The current

understanding of environmental processes supported by powerful computer hardware and software and data acquisition by remote sensing (RS) leads one to expect that selecting the best places to establish ski runs is reasonably easy. But data sets in mountainous regions are sparse, and data are difficult to collect in rugged terrain. So it is questionable if with normally available data and modelling it is possible to optimise the choice of sites. To be able to tackle this problem one needs to combine the understanding of environmental processes, data collection and analysis and socio-economic factors.

In this thesis the research question concerning only the physical environmental constraints and the associated requirements will be elaborated in great detail, the social and economical objectives have not been included.

1.2 Key elements and key processes of an alpine area

The alpine environment is a vulnerable, complex system, which is very sensitive to any kind of change, both of natural and artificial origin. Artificial origin concerns all direct and indirect changes caused by human activities. Important environmental factors which control the response of the environmental system to a change or which are subject of a change are biotic factors such as vegetation, animals and natural biotopes, the soil, the relief, geomorphologic features, geological conditions, the water balance, meteorological conditions and the visual appearance of the landscapes. For example, though soil formation in the mountains is for the greater part controlled by the slope geometry and the extreme climatic conditions, it is also determined by the underlying bedrock and the presence of vegetation. Conversely, the soil type and soil properties determine the vegetation that may develop at a certain site. Geological conditions also have an influence on the development of geomorphologic forms, the topography of a terrain and the triggering of mass movements. Both soil, underlying bedrock and vegetation influence hydrological characteristics like infiltration to the soil, soil moisture, percolation to the underground and many more. Besides, all these interactions are driven by meteorological conditions such as rain, temperature or solar radiation.

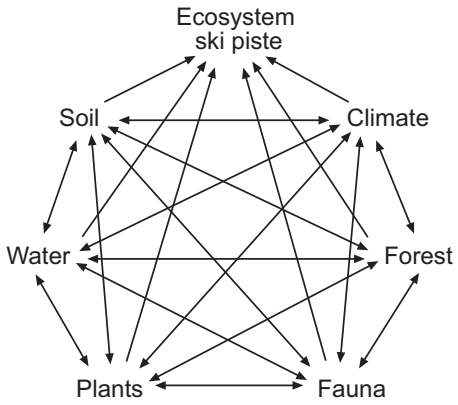

Figure 1.3 Interaction between selected geo factors which are sensitive to the establishment of skiing, maintenance of ski pistes and skiing itself.

Thus the alpine environment is a complex cause-effect system (Figure 1.3), where the change of one factor may evoke multiple consequences of different relevance.

When planning an environmentally sound ski run, all cause-effect relations should be known. However, the alpine area is often heterogeneous in many aspects, so it is nearly impossible to capture the entire environmental information at the appropriate scale. Therefore relevant key elements and key processes need to be identified.

1.3 Motivation

Planning skiing facilities demands taking many decisions. Principally, the need for making a decision is driven by the demands and perceived dissatisfaction. Causes for dissatisfaction could be long waiting times at the ski lift, high density of skiers on the ski runs, lack of demanding ski runs or high risk of avalanches on the road to a facility. For example the ski area of Sölden, which was also used as the case study for this thesis, has three areas dedicated to ski pistes. These are Hochsölden, Gaislachkogl and the glacier area. In former times the ski pistes at the glacier could only be reached via a mountain road that was in danger of avalanches. In times of heavy snow the road had to be closed, and there was no other means to reach the glacier from the village of Sölden. Furthermore, there are many easy ski pistes, but the conditions for advanced skiers were unsatisfactory for the size of the ski area. These two causes for dissatisfaction, but also the desire to be in a competitive position, stimulated the design of a project called *Golden Gate to the Glacier*, which incorporated both the establishment of an easy access to the glacier by cable car and the adaptation of a steep mountain to expand the possibilities for advanced skiers.

Usually the main decision that has to be made for this kind of land use planning is: "*Where is the new development going to be*?" and this decision is supposed to be based both on the demands and the site conditions of the project area including its surroundings. In the specific case of Sölden the location of the new development was reasonably clear, so the main decisions were related to 1) environmental justification, 2) how to solve the water supply and the transport of sewage water, and 3) the need for mitigation measures with respect to the risk of avalanches and rock falls. While the design of mitigation measures was based on geo-technical methods, the impact on the environmental quality was assessed qualitatively on the basis of the current situation just like "According to the vegetation survey the impact of the new development is expected to be very low" or "The soils in the project area are assumed to be capable of buffering the excess of surface runoff at the ski pistes and their surroundings". So in reality, and not only in the case of the Sölden ski area, but also in other areas, the decision for the *where* is mainly driven by the demands rather than natural hazard for which mitigation measures can be designed and the maintenance and sustainability of environmental quality. This example shows two aspects where improvements could take place, 1) to tailor site selection to both the demands and environmental quality including natural hazards and 2) to assess environmental quality quantitatively in order to facilitate the comparison of different sites for a new development and to illustrate the impact as a sum of all possible effects.

In the current procedure for planning ski runs the assessment of the potential impact and therefore the analysis of site conditions is controlled by the legal framework, which gives the conditions that have to be met. Accordingly, the elements of the environmental system such as vegetation, soil, bedrock or water balance are evaluated separately in correspondence with the legal guidelines. However, to compare different locations for a new development, in this thesis termed alternatives, and to understand the response of an integrated system such as the environmental system, the individual site characteristics need to be systematically brought together.

1.4 Definitions of terms

In the environmental literature there are several terms whose meaning may differ with context. In order to avoid confusion this section is devoted to provide a clear definition of the terms as used in this thesis.

Environmental criteria: An environmental criterion represents a concern that should be met with a new development. For example if we are concerned about the maintenance of rare plant species, an environmental criterion may be "minimal impact on rare plant species" when making a new development.

Spatio-temporal environmental models: Spatio-temporal environmental models are dynamic or forward models, which are capable of simulating an environmental process in space and time (Karssenberg, 2002). Environmental processes are those that are controlled both by natural causal factors and human interference.

Multicriteria analysis: Multicriteria analysis is the analysis and aggregation of several concerns or factors that may have an effect on the decision-making process for a new development or strategy. Environmental criteria are often measured on different scales. In addition, they can have different importance for the decision-making situation and they may be either a benefit or cost for the environment or the participants. Therefore standard procedures such as standardisation, weighting methods and aggregation methods are often used to synthesise the overall impact of alternatives.

Alternatives: The word alternative is used for a possible solution, in this thesis a possible site for a future ski run.

Ski run or *ski piste*: A ski run or ski piste is a defined area in mountainous terrain that was made accessible for skiing activities. In this thesis the terms ski run and ski piste are used synonymously.

1.5 Objectives of the thesis

For locating an environmentally sound ski run we need to have insight in the environmental system of the respective environment, i.e. the alpine environment, and specifically, information about cause-effect relations between environmental factors and processes and the future ski run. Having this knowledge enables one to figure out *the environmental criteria that are important for the planning of ski runs in an alpine area*. For example, the investigation of cause-effect relations can be achieved by field

observations and field experiments. These methods provide data to compare ski runs that have been established in the past with natural areas having similar site characteristics. The analysis of the impact caused by a ski piste with respect to site characteristics makes it possible to specify vulnerable site conditions. These kinds of impact studies have been carried out for different aspects and sites as made explicit in the literature review in Chapter 2, which gives a comprehensive overview of impacts that may have been caused by the establishment of ski pistes, the maintenance of ski pistes and skiing itself. In order to identify the impacts likely to be caused by the ski pistes in the study area and to obtain data for the environmental characterisation of that area, data were also collected in the field (Chapter 4), to a large extent acquired by students of Utrecht University, the Netherlands.

Conversely, the understanding of the environmental system and its response to human activities can be gained by environmental models (Hardisty, 1993; Goodchild et al., 1993; Jakeman et al., 1995; Jørgensen, 1996; Wesseling et al., 1996; Karssenberg, 2002). These are commonly used to represent environmental processes by mathematical expressions. Up to now this kind of model has been merely used as an "independent" tool for different purposes such as risk assessment, forecasts of natural hazards or in environmental management and water management. But *what is actually the benefit of spatio-temporal modelling in the choice for locating new ski runs?* And, moreover, *which problems do we encounter when using them for the planning of socio-economic infrastructure in an alpine area with respect to data, modelling concept and application?* These questions are tackled in Chapter 3, giving a theoretical introduction to the decision model proposed in this thesis. This is continued in Chapter 6, which provides a general outline of the environmental models used in this thesis, including the modelling principles and requirements for the proposed decision framework. In addition, these questions are considered in the subsequent chapters, which are devoted to the technical description of the snow model and the hydrological model (Chapter 7), the erosion model and the stability model (Chapter 8) and the plant growth model (Chapter 9).

When planning ski runs one needs detailed spatial information on site conditions such as topography, vegetation or soil, especially when we want to use environmental models. However, in alpine areas, the availability of spatial and temporal information is sparse, and moreover, high-resolution data are expensive and difficult to collect. *Nevertheless, is it possible to generate appropriate thematic maps by an automatic procedure if we know the environmental factor such as the presence of plant species or soil type at several locations spread over the space?* This objective will be discussed in more detail in Chapter 5, which proposes a mapping procedure for mapping alpine vegetation using derivatives of a digital elevation model and vegetation observations collected in the field.

Usually, when carrying out an environmental impact assessment, the environmental suitability of a defined set of alternatives is evaluated, while there might be better solutions with the same socio-economic satisfaction. Moreover, using optimisation techniques, searching for an optimal solution from an infinite number of solutions, would make it possible to tailor site selection towards the maximum benefit in the light of the environment. *Is it feasible to implement optimisation techniques to improve the choice for locating a new ski run with respect to the given decision situation,*

available environmental data and computer power? What are the benefits and which constraints do we have to take into account? The theoretical aspects of this question are introduced in Chapter 3, while the application is partly addressed in Chapter 6 and then made explicit in the last chapter of the analysis (Chapter 10), which brings together the various elements of the decision model. The various parts are 1) environmental criteria expressing a specific concern with respect to the choice for locating a new ski run, 2) models, namely statistical models or environmental models, to supply a measure for a certain environmental criterion, and 3) possible solutions for locating the new ski run. To be able to select the best solution from the set of feasible solutions and to communicate the result to the decision maker, we need to compress the given information to an understandable result. Multicriteria analysis is a useful method for combining several indicator values in the decision making process. However, since we are working with spatio-temporal models providing maps for different moments, the questions arises, whether *it is possible to apply traditional techniques of multicriteria analysis (Janssen, 1992; Malczewski, 1999) to spatio-temporal data and which trade-offs are involved when trying to compress the information.* The theoretical framework with respect to this concern is also described in Chapter 3, while the procedure to compress the detailed information supplied by the individual models will be extensively explored in Chapter 10. Since the procedure to compress the information requires many decisions in which uncertainty is involved, the sensitivity of the outcome of the multicriteria analysis needs to be analysed (Chapter 11). This thesis will be completed with the discussion and conclusion of the presented research (Chapter 12).

2 ENVIRONMENTAL IMPACT OF SKI PISTES AND SKIING

2.1 Introduction

The establishment of ski pistes and ski lifts, the action of skiing and maintenance of ski runs (Ries, 1996) may cause considerable environmental impact. An impact on an environmental system arises where human development changes the system from its normal position into another state (Beinat et al., 1999). The impact can be both a positive or a negative response to the interaction and is often irreversible. However, the negative consequences are those that people are concerned about. This chapter reviews the human actions that are responsible for causing environmental impact in a ski area along with their possible effects.

2.2 Human actions causing environmental impact in a ski area

The artificial modification of mountain slopes, particularly deforestation and the disturbance of the soil cover and the soil profile, was very common in the earliest development of ski runs. Negative effects on the environment were usually neglected. However, the effects were rather severe especially in higher areas, where natural restoration is restricted by the extreme climatic situation and constrained conditions for vegetation and re-growth. Numerous studies in the early nineteen eighties investigated the adverse effects caused by skiing facilities, such as the destruction of the soil profile (Mosimann, 1983), the development of different erosion features (Mosimann, 1980, 1981, 1983, 1985), the disturbance of the ecosystem (Cernusca, 1977, 1979, 1986, 1990) and the degradation of vegetation (Schauer, 1980, Grabherr, 1985). These studies showed the great importance of the problem and demonstrated increased awareness. The perception of the negative effects on the environment changed society's view and encouraged the inclusion of consideration of the environmental sensitivity in the planning of new socio-economic infrastructure. For example, when surface corrections are made these days, the upper layer of the soil can be taken off, stored at the edge of the area, and afterwards replaced. Still, for this procedure the soil type must be appropriate (Cernusca, 1977).

Nevertheless, as noted in the introduction, the demand for skiing and attractive skiing facilities increases, continuing the impact caused by new skiing facilities, the action of skiing and the management of ski slopes. However, human activities are not always disadvantageous. For example revegetation of established ski runs is essential to increase the protective function of vegetation and to improve the aesthetic view.

In the following sections I examine the range of human activities and their effects, in particular those caused by the destruction of the ground cover and the soil, the degradation of geomorphologic forms, deforestation, slope preparation, including the production of artificial snow, and skiing itself.

2.2.1 Surface corrections – the disturbance of soil, vegetation and geomorphologic features

Surface corrections are terrain modifications to remove large irregularities in the slope over a short distance and single obstacles at the surface such as outcropping rocks. This may involve the degradation of vegetation, soil and geomorphologic features. The term vegetation refers to alpine grassland, heaths and meadows, but not to forest. The negative impact induced by deforestation is addressed in Section 2.2.2.

The evolution of skiing to a sport for the masses has increased the demand for wide smooth ski runs because of their large capacity for skiing and easier slope preparation with artificial snow and piste caterpillars (Mosimann, 1986), and it called for additional facilities. Proper ski piste conditions enhance the achievement of a certain quality standard for the ski piste such as the Tyrolean standard – "Pistegütesiegel" (Giessübel, 1985), favouring safety standards and socio-economic benefits. However, alpine slopes are mostly quite rough, and therefore the slopes need to be smoothed to provide the conditions skiers and the skiing companies want, which may induce adverse effects on environmental factors and processes.

Prevailing site conditions determine the degree and type of interference. In lower areas, below the timber line, which oscillates around 2000 m, surface corrections mainly concern the forest, soil, vegetation cover and single obstacles in the landscape such as big stones or a group of trees (Ries, 1996). In areas above the timber line, geomorphologic features, for example morainic arcs, rock glaciers or outcropping bedrock, are the main targets to be destroyed in the landscape, although the disturbance of soil properties and alpine vegetation is not out of the question either. This may include disturbance of vegetation density, species composition and species variety.

The impacts on the environment depend both on the degree of human interference and the geo-ecological characteristics of an area (Giessübel, 1988; Mosimann, 1981). For instance, disturbance of the protective vegetation cover and smoothing the slope create favourable conditions for the generation of overland flow and consequent soil erosion, as addressed by Grabherr (1985) and Mosimann (1985). However, the impact also depends on the underlying material (Giessübel, 1988) and the thickness of a soil. Impermeable rock layers such as schist or marl can be more hazardous than if the underlying material is porous or has a high water storage capacity, as for example limestone or morainic material, which may buffer the risk of saturated overland flow.

2.2.1.1 The destruction of geomorphologic forms and its impact on the environment

The destruction of geomorphologic forms can have an impact on the behaviour of natural processes and on the scientific, socio-economic, educational, cultural and scenic value of a landscape. The various values of a landscape are described in more detail in Carton et al. (1993) and Bergonzoni et al. (1995).

Geomorphologic forms have specific characteristics and a certain position in the environmental system. Hence the destruction of geomorphologic forms may have an unfavourable impact on the environment. For instance, morainic materials or rock glaciers are essential buffers for the geo-hydrologic system because of their high water

storage capacity along with a slow release of water to the surroundings. The cumulative effect of the decrease of the water storage capacity and the creation of long smooth concave slopes create favourable conditions for surface runoff or avalanche tracks because such a smooth surface cannot slow down the motion of snow and water masses. The induced impact on the environment can for example be expressed as "the increase in area susceptible to surface runoff" or "the change of the size of run-out zones of avalanches".

The destruction of geomorphologic forms also has an impact on the scientific value of an area. An example for this kind of impact is the degradation of a frontal moraine of the "Gepatsch" glacier in the Tyrolean Alps, Austria, caused by the road construction to the skiing centre near the "Weissespitz" mountain (Grabherr, 1985). The removal of the surface deposits reduced the volume of the moraine by 50 % and disturbed the primary succession of plants, which had established after the retreat of the glacier in about 1850. The moraine was one of the few moraines in the Eastern Alps below the timberline. Another example is the blasting of a well-developed rock glacier in the ski area of Sölden, Austrian Alps, for the creation of a wide and steep ski run to increase the attractiveness of the ski area (Figure 2.1). In both cases evidence on geomorphologic evolution has been destroyed in favour of skiing facilities.

It is rather subjective to evaluate this type of impact, since it is difficult to ascribe monetary values to geomorphological forms. However, there are attempts to describe this impact by indicators and to integrate it in the framework of an environmental impact assessment (Marchetti and Rivas, 2001; Panizza and Piacente, 1996). Also geomorphologists believe it is important to integrate the geomorphologic impact in the planning of socio-economic projects in order to better understand how the landscape may be able to absorb these changes.

Figure 2.1 Degradation of a rock glacier in the Sölden ski area (1999) – left side of the mountain in the centre: destroyed; right side: no disturbance.

2.2.1.2 Effects caused by degradation of soil and vegetation

The soil has essential chemical, physical and biological properties, which are relevant for other biotic and abiotic factors and processes. For instance soil thickness, soil structure and the soil profile determine hydrologic characteristics such as water storage capacity, hydraulic conductivity and plant-available water capacity. The soil also provides additional resources for the development and growth of vegetation, specifically nutrients and oxygen. It is a habitat for soil organisms, which are important elements for soil formation. Vegetation protects the slope from erosion and landslides by interception, evapotranspiration, increased infiltration and deep rooting, and it guards the soil from intensive radiation. Surface corrections to create a smooth ski run and the action of skiing imply the degradation of soil and vegetation, in particular the removal of the soil or soil patches, soil compaction, disturbance of vegetation and even continuous destruction of the sward (Cernusca, 1977; Schönthaler, 1985; Ries, 1996; Grabherr, 1985; Watson, 1985). Soil compaction is for the greater part caused by heavy machines such as caterpillars and piste caterpillars. These changes have an impact on the soil properties, the biomass production, the composition of plant species and the hydrologic system, thereby increasing the risk of land degradation, especially erosion.

Hydrologic changes are to a large extent caused by the removal of soil material that can store a reasonable amount of water such as fine material or organic substances, the disturbance of the soil profile and soil compaction. Together with vegetational changes these have an impact on the water balance, specifically on the amount of water available for infiltration and the potential infiltration capacity. For example, studies in the Sölden ski area (Thonon, 2001) or in the Hohe Tauern region (Bunza, 1989) have shown that the soil on ski runs is more compacted than the soil of natural areas and that less water could infiltrate. A low infiltration capacity is one of the causal factors for triggering overland flow after heavy rain or snowmelt. It must be noted that the overland flow is also controlled by factors other than the infiltration capacity such as soil profile, soil cover and the slope. The effects are rather severe if harmful surface corrections take place on shallow soils with a low holding water capacity where overland flow is already favoured by the initial conditions (Mosimann, 1985).

Soil aggregates of the upper soil layer contain fine material, organic substances, subterranean organs of certain plant species and soil organisms and they are well known for their high water holding capacity. The destruction of them decreases the water retention of the soil and therefore the plant-available water, and further it encourages a rapid drainage to the underground. The rapid drainage of water to the underground and the lack of a protective vegetation cover increase the risk of desiccation (Cernusca, 1977), thereby constraining both soil formation and the restoration of vegetation. This is likely followed by additional adverse effects such as different erosion features, which will further be discussed in a latter paragraph of this section.

The disturbance of a well-developed humus layer and subterranean organs of plant species decreases the available nutrients and inhibits the regeneration of disturbed plants from these organs (Grabherr, 1985). The decrease in nutrients, plant-available water and limited resources of natural seeds affect the regeneration of the vegetation cover after the establishment of a ski run or after a skiing season; they also affect the species composition and therefore the biomass production. The total impact on the vegetation is

the sum of the impacts due to different soil conditions, as just discussed, and the direct destruction of the vegetation (Grabherr, 1985; Schauer, 1980). The negative response of individual species to ski run construction and skiing in alpine grassland and dwarf shrubs was for example analysed by Grabherr (1985).

These days much effort is devoted to the revegetation of disturbed ski pistes (Holaus, 1994), but species characteristic for a certain environment and rare species may be lost due to the lack of commercially available seed mixtures adapted to alpine conditions (Mosimann, 1985) and the new environmental conditions. Successful regeneration also depends on the growth characteristics of indigenous plant species. For instance the re-establishment of *Carex curvula* is nearly impossible because its lateral spread is low and reproduction by seeds hardly occurs (Grabherr, 1985). The use of common species for revegetation, which are able to grow in any environment, reduces the number of indicator species reflecting particular environmental conditions, but has satisfactorily established a protective vegetation cover in lower areas at about 1600 m. The success of revegetation is highly influenced by the environmental suitability of the seed mixture because species have their "biological" limits. (Gissübel, 1988). For example, Badany and Schönthaler (1982, cit. in: Grabherr, 1985) showed that the establishment of *Festuca rubra*, a grass species which forms the major component of all seed mixtures for use in high altitudes, was constrained by extreme environmental conditions such as a shorter growth period, low temperatures and the low nutrient availability. The restoration of dense vegetation cover in higher areas is less successful because soil formation and the growth of vegetation is restricted by the extreme climatic situation and constrained growing conditions. At these locations it takes a long time to compensate for the damage caused by terrain modifications such as flattening small humps, filling up depressions and the total removal of the upper soil layer and the vegetation cover (Grabherr, 1985; Mosimann, 1985). This was confirmed by Badany and Schöntaler (cit. in Grabherr, 1985), who showed that the restoration of natural or semi-natural grasslands and dwarf shrub heaths of the higher lying regions above the timberline is usually unsatisfactory. Besides altitude there may be regional differences in topography, climate and other environmental factors that influence the development of vegetation.

The impact on vegetation has various consequences. On the one hand it increases the risk of hazardous processes, on the other it affects the originality of an area, the aesthetic view (see Figure 2.2, p. 28) and agricultural production (Mosimann, 1986). An example is the loss of colourful low-nutrient grasslands, or of typical species such as the pink flowering *rhododendron*. The shift from species-rich into species-poor grasslands decreases the feeding value of the grass and therefore the agricultural production, and is therefore an unfavourable effect for local farmers (Pfiffner, 1977; Köck and Schnitzer, 1980; Wyl, 1982; all cit. in Grabherr, 1985).

Another consequence of surface corrections, as already mentioned in a previous paragraph, is the initiation of soil erosion. Erosion features on ski runs or in their surroundings have been reported many times (Mosimann, 1980, 1981, 1983, 1985; Schönthaler, 1985; Ries, 1996), above all in the early phases of ski piste constructions, when people were less aware of possible consequences. An example is the research in the ski area Crap Sogn Gion/Laax (France), where a detailed analysis was carried out to map the negative impact on the risk of erosion (Mosimann and Luder, 1980). The increase in

erosion is caused by the cumulative effect of the decrease in water holding capacity and the lower infiltration rate, degradation of the protective vegetation cover, the disturbance of the soil profile and the creation of long smooth slopes. The lower water holding capacity and the lower infiltration rate may be related to soil compaction, thinner soils, degradation of vegetation including forest, and land use changes (Cernusca, 1977; Mosimann, 1985; Giessübel, 1988). Such a land use change is for example the change from woodland to ski run (c.f. Section 2.2.2). The greatest erosion is associated with long, concave hollows in the direction of the slope, which are moist throughout the year (Mosimann, 1985). Prevailing erosion features are rill and gully erosion, especially when the soil surface is bare, but also caused by wheel tracks (Giessübel, 1988). Surface runoff and erosion not only cause the shift of material, they also constrain the regeneration of vegetation (Mosimann, 1985) because seeds, soil stabilisers and fertilisers might be washed out by overland flow, and the eroded and deposited material might bury plants, which might inhibit the germination of colonising plants at the foot of the slope or in depressions. This effect is more severe above 2200 m of elevation, where growing conditions are not optimal. Moreover, it prohibits the restoration of a stable soil due to the recurrent degradation processes (Schönthaler, 1985). Erosion may also have an impact on the surroundings, for instance by supplying large sediment loads to the torrents in the downstream area (Mosimann, 1985).

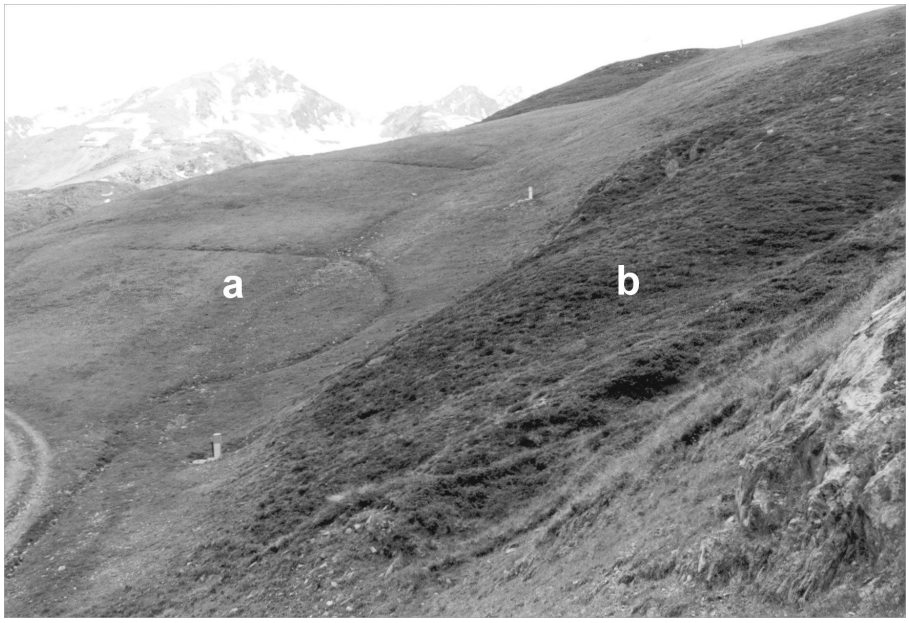

Figure 2.2 Ski piste after a skiing season, showing the vegetation difference between a) ski piste, and b) natural area.

The consequences of land degradation and the interaction between individual geo-ecological factors show that the construction of ski runs requires a detailed analysis of natural processes in an alpine area to understand the cause-effect relations and to prevent or minimise the negative effects of ski piste constructions.

2.2.2 Negative effects induced by deforestation

Traditionally, skiing took place on slopes that were suitable for this activity. With the development of skiing to a sport for the masses, forested areas were converted into ski runs because the natural potential of the alpine environment could not satisfy the demand. An extra section is devoted to the impact of deforestation on the alpine environment, since deforestation is mainly enhanced by the demand for more ski runs, and not by irregularities at the slope surface. Cernusca (1977) was one of the first scientists to draw attention to the impact of skiing on the landscape, especially with respect to deforestation.

A forest has crucial functions for the alpine environment. First, it buffers meteorological factors such as wind, temperature above the soil surface and incoming radiation. Of all ecosystems it absorbs most incoming energy and has the lowest reflection rate. Deforestation implies a change in the energy input, whose impact differs from the size of the deforested area and the shape and the aspect of the new ski slope. If the deforested area is quite small, the effect only concerns the local climate. The clear-cut of a large area may be followed by a significant change of the energy balance. Trees located on wind-protected south-facing edges of a deforested ski run are susceptible to sunburn due to exposure to strong radiation, which is intensified by the sharp transition from ski run to forest. The effect can be mitigated by planting shrubs at the sensitive side. A well-established vegetation cover would mitigate the effect of intensive radiation. However, newly created ski runs are mostly bare or have a sparse vegetation cover. The creation of a ski run through a forest creates favourable conditions for the wind speed and the wind direction. This can be disadvantageous for the trees at the edges of the ski run. The impact on the temperature mainly affects the microclimate and is thus negligible.

Second, a forest is a good manager of the water balance (Mosimann, 1986) because of the high storage capacity of the soil, for the greater part caused by the large content of fine pores and organic materials and the high potential infiltration rate, and the high rate of evapotranspiration, which favours both biomass production and the consumption of water from lower soil layers. The consumption of water from the lower soil creates space for new rainwater. Thus deforestation along with the physical disturbance of the soil profile and the soil structure reduces infiltration to the soil and the water storage capacity (Giessübel, 1988), thereby exposing the soil to the danger of surface runoff and erosion, though in correspondence with the prevailing substrate, and the risk of flooding. The change in the water balance restricts growth conditions for the new developed grass cover after deforestation because of fast draining pores, enhanced by the degradation of the upper soil layer which consists to a large extent of fine pores and organic material, and the decrease in water retention reduces the amount of plant-available water, especially in periods with little rain.

Further, the forest provides a natural protection against the risk of mass movements such as landslides and snow avalanches. For that reason deforestation, and therefore also the removal of stabilising roots, affects the stability of a slope (Dorren, 2002). The creation of smooth ski runs through the forest introduces favourable conditions for the motion of avalanches and overland flow. Additional measures have to be taken to protect a slope from instability and to protect any settlements down slope against avalanches and flooding.

Negative consequences for the energy balance, the water balance, the soil

properties, the stability of the slope, the natural avalanche protection and the visual view follow the enlargement of the area for skiing. These effects can partly be offset by extra cost, for example by establishing artificial avalanche protection or intensive revegetation. Additionally, the impact can be minimised by an exact planning of the location of the ski pistes considering the slope, the aspect and the width of the ski run in the forest, the soil type and the underlying bedrock (Cernusca, 1977).

2.2.3 Slope preparation

The intensive use of ski runs requires regular slope preparation, in particular an even distribution of snow and in times of too little snow the addition of artificial snow. Both activities have advantages and disadvantages.

2.2.3.1 The impact of artificial snow

Spatial and temporal snow cover changes depend upon meteorological conditions and the location in the landscape. Because of the demand for skiing even in periods and areas with little snow, the production of artificial snow has become widespread in ski areas. This action favours the socio-economic situation, though it can have a number of negative effects. The direct impact involves the mechanical impact caused by the installation of devices for producing artificial snow and the associated environmental effects (Leicht, 1993). The indirect impact concerns the consequences with respect to the socio-economic situation because a continuous snow cover attracts more people over a larger period, more people consume more resources, produce more waste and sewage and require more socio-economic infrastructure, the construction of which causes new environmental impacts (Broggi and Willi, 1989; Leicht, 1993, Schatz, 1993). Moreover, adding artificial snow encourages levelling of ski pistes because flatter slopes facilitate the distribution of snow (Broggi and Willi, 1989).

In the following paragraphs various impacts on the environment induced by artificial snow production are addressed, in particular negative effects created by the installation of devices for producing artificial snow, the use of resources for producing artificial snow, the effects on the water balance of a slope and slope stability, direct consequences for vegetation, the impact on the soil properties, the disturbance of biotopes and habitats and the impact on landscape aesthetics.

Artificial snow production requires pipelines for the transport of surface water from the valley to higher regions and additional technology for the actual snow production. The installation of these devices has an impact on the vegetation cover and soil properties. This might increase the risk of erosion because the regeneration of a protective vegetation cover in higher areas is a long process and a compacted soil has less infiltration capacity, as discussed in Section 2.1.2. As any construction works, the installation may disturb the fauna, especially if the work is done in sensitive periods such as in breeding times. The mechanical impact can partly be compensated for, but it is impossible to reproduce the original situation.

Artificial snow production requires air, water and energy (Broggi and Willi, 1989;

Leicht, 1993; Schatz, 1990) and should only be carried out under certain meteorological conditions. Resources needed for snow production depend on the chosen technique, for example whether a high or low-pressure machine is used, the available resources and their characteristics. The amount of energy per year used for artificial snow production is generally negligible; according to Schatz (1990) it is 2-3% of the total annual energy consumption of a region. However, there may be problems if artificial snow is produced in periods of high-energy use and when energy resources are short (Broggi, 1989; Schatz, 1990). Up to now there are no explicit research results that question the amount of water used for snow production. Nevertheless, the withdrawal of surface water in periods of a low water table might impair the organisms of the surface water that is not frozen such as the main river in a valley (Broggi and Willi, 1989; Leicht, 1993, Schatz, 1990; Schatz, 1993).

The additional amount of snow added to the ski pistes might change the water balance of the local catchment because the extra amount of snow increases the volume of snowmelt water of the catchment in snowmelt periods. This might enhance overland flow, and is possibly followed by flooding and erosion (Broggi and Willi, 1989, Schatz, 1990; Cernusca, 1987; Cernusca et al., 1990; Leicht, 1993). In addition, an increase in snowmelt water endangers the stability of slopes, since slope instability is frequently related to periods of intensive snow melt (Leicht, 1993).

Compared with undisturbed natural snow, artificial snow can have a negative impact on vegetation due to its dense structure, formed by the rounded shape of artificial snow crystals, and therefore its longer duration on the surface. (Broggi and Willi, 1989; Kammer and Hegg, 1990; Leicht, 1993; Holaus and Partl, 1994; Schatz, 1993). The end of the snow melt period can be retarded by up to 25 days compared to natural, unprepared snow (Mosimann, 1987). A longer duration of the snow cover is associated with a later start of the regeneration of vegetation and therefore a shorter vegetation period (Kammer and Hegg, 1990). This prevents the flowering of spring species (Leicht, 1993) and implies a change of the species diversity and the vegetation cover, probably followed by less total biomass production and a higher risk of erosion (Cernusca 1989; Broggi and Willi, 1989; Kammer and Hegg, 1989; Schatz, 1993). Holaus and Partl (1994) believe that artificial snow can reduce biomass production. However, this is difficult to prove because of the high spatial variability of alpine site conditions and the dependency of biomass production upon a large set of parameters. The later start of the growing period affects the succession of meadow plants because meadows are often cut when plants are still developing (Krammer and Hegg, 1990). The longer duration of the snow cover, the low impermeability and the fact that soil organisms and plant roots consume oxygen when snow is still there cause a lack of oxygen, which is required by biotic organisms (Cernusca, 1989; Newesely et al., 1994; Newesely and Cernusca, 2000). The production of artificial snow depends on the wet bulb temperature, which is based on a certain proportion of temperature and relative humidity. If artificial snow has been produced under unsuitable conditions, for example above the wet bulb temperature of -3° C, it can enhance the formation of toxic gases and carbon dioxide between the bottom of the snow and the soil surface. This is because the production of artificial snow above this temperature creates very compact snow. Decay of vegetation (Broggi and Willi, 1989; Leicht, 1993; Cernusca, 1989) and lack of oxygen in the soils are possible consequences. More details about the effects of artificial snow on gas exchanges and oxygen deficiency

and their consequences on the environment can be found in Newesely et al. (1994), Newesely (1997), Newesely and Cernusca (2000).

The use of artificial snow also affects the available nutrients (Kammer and Hegg, 1990), the pH-value and average moisture of the soil. This is because, first, surface water has a different chemical composition to natural rain (Broggi and Willi, 1989; Leicht, 1993), second, less soil forms as a consequence of the lower biological activity of soil organisms likely caused by the longer duration of the snow cover and the saturation of the soil (Cernusca, 1987), and third, because of the increased amount of snow melt water (Kammer and Hegg, 1989). On the one hand these changes can be the cause for a shift of the species composition from nutrient-poor grassland and sub alpine grassland to nutrient-rich grassland with some common species (Schatz, 1993), on the other they can decrease the diversity of species (Kammer and Hegg, 1989). For example, species representative for dry and low-nutrient circumstances might be replaced by species that are characteristic for nutrient-rich and humid situations (Kammer and Hegg, 1989). Indicator species are endangered of being replaced by common species that do not reflect environmental conditions (Leicht, 1993; Kammer and Hegg, 1989).

The change of site conditions such as mean wetness index, species composition or nutrient content might change valuable biotopes. Together with the impact of noise (Leicht, 1993, Schatz, 1993) and light during snow production it might cause the migration of individual fauna, and therefore affect the variety of the fauna at those sites. The noise can also cause the wildlife to become aggressive. (Broggi and Willi, 1989; Schatz, 1990; Schatz, 1993).

Technical devices in the landscape such as pumping stations and the impoverishment of the vegetation cover disturb the landscape aesthetics (Broggi and Willi, 1989; Leicht, 1993). Another impact on the visual view is the longer duration of some snow bands in the landscapes, especially at the location of intensively used ski pistes (Leicht, 1993, Schatz, 1993). These are also the locations where the vegetation cover significantly reflects the intensive use.

In comparison to the numerous negative effects there are also some positive aspects: The maintenance of a continuous snow cover reduces the mechanical impact on vegetation and soil caused by the sharp edges of skis or the wheels of piste caterpillars (Broggi and Willi, 1989; Leicht, 1993, Schatz, 1990; Schatz, 1993). It also leads to approximately stable temperatures at the soil surface. This may reduce the risk of or even prohibit the freezing of plants and the soil (Leicht, 1993; Schatz, 1990; Schatz, 1993). Furthermore, it is not necessary to collect the snow from different areas to provide a continuous snow cover, thereby decreasing the pressure from piste caterpillars (Broggi and Willi, 1989; Leicht, 1993). The increase in soil moisture due to additional snowmelt water can have a positive effect on the biomass production in naturally dry areas because the shortage of soil moisture is partly compensated. (Broggi and Willi, 1989; Cernusca, 1989; Schatz, 1993). If the delay of the snow melt period is large, the benefit for biomass production due to better moisture conditions is offset by the shorter growing season. (Mosimann, 1987). The positive effect of the increase in soil moisture in naturally dry, but compacted ski pistes lasts just a few days because compacted soils have little plant-available water (Cernusca, 1989).

Ignoring the socio-economic benefit, the negative impact on the environment caused by artificial snow production is higher than the effect of mitigation. It is difficult

to draw general conclusions about the consequences implied by artificial snow because of its dependence on site characteristics. While additional melt water might favour biomass production in rather dry areas with a high water storage capacity, it might trigger overland flow on saturated compacted soils (Cernusca, 1989). However, socio-economic stakeholders press for the use of artificial snow, thus negative effects must be taken into account and controlled.

2.2.3.2 Slope preparation by piste caterpillars

Slope preparation by means of piste caterpillars implies snow compaction, as snow crystals are deformed and compressed. Daily temperature oscillations and therefore thawing and freezing processes at the snow surface along with slope preparation favour ice-formation there because free water particles are pressed into the pores of colder snow layers. The generation of an ice-layer is not necessarily an effect of artificial snow, but mostly it is thicker on ski runs that have been prepared using artificial snow due to a larger snow mass (Cernusca, 1989). The ice-layer plus the dense structure of the snow reduce the thermal protection, which might lead to freezing of vegetation and soil instead of protecting it from freezing. In addition, ice formation inhibits the supply of oxygen to the soil (Newesely et al., 1994, Newesely, 1997), which can damage fine plant roots, and consequently increases the risk of erosion (Cernusca, 1989). To this end damage of vegetation and change of soil properties as a consequence of freezing, oxygen deficiency or the generation of toxic substances is not only a matter of artificial snow, but can also occur below compacted natural snow.

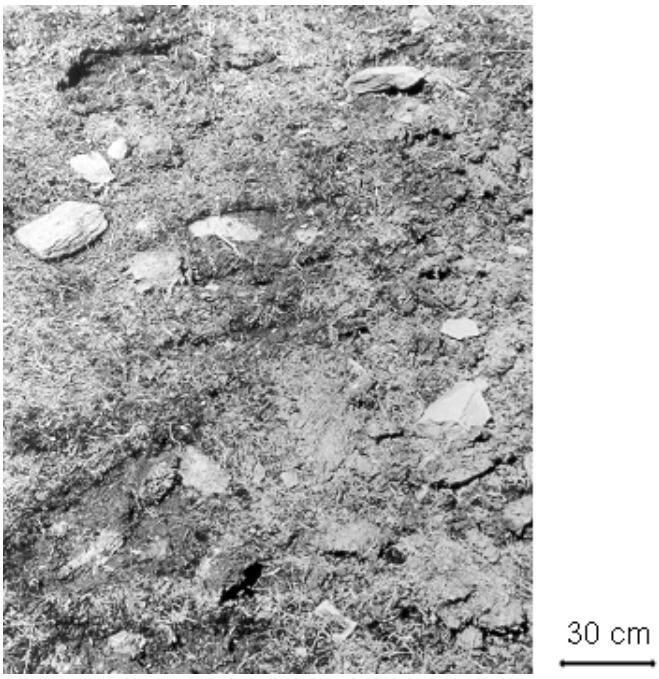

Figure 2.3 Impact on vegetation because of slope preparation.

Slope preparation is most critical at convex slopes or when the snow cover is very thin because there vegetation is in danger of being sliced off (Giessübel, 1988; Ries, 1996) or of being destroyed. The mechanical impact of wheels (Figure 2.3, page 33) favours the generation of rill erosion. (Grabherr, 1985).

2.2.3.3 The action of skiing and off piste skiing

Apart from the establishment and the maintenance of ski runs there is also the impact of skiing itself. On the one hand skiing contributes to the compaction of the snow cover, whose consequences are already discussed in the section slope preparation. On the other hand skiing causes a mechanical impact on soil and vegetation due to the sharp edges of the skis (Grabherr, 1985), especially in times of a thin snow cover. The slicing-off effect is less severe for plant species that regenerate from subterranean organs of plant species. Examples of such species include *Vaccinium gaultherioides* and *Phyteuma hemisphaericum*. In case of repeated disturbance rapid re-establishment by seed production or natural regeneration is not possible.

2.3 Discussion and conclusion

The review of literature and field observations show that the establishment of ski runs, the maintenance of skiing facilities and the action of skiing have an impact on the environment, which depends to a large extent upon the degree of interference and prevailing site conditions. The impact can partly be compensated for by mitigation measures such as revegetation and reforestation, artificial drainage trenches and artificial avalanche protection. However, it is impossible to re-establish the original conditions. Nevertheless, the pressure of skiing companies, local authorities and users continues because people like skiing and because ski areas are an important source of income for the local population in alpine areas. This necessitates the expansion and improvement of existing facilities and new developments. Therefore careful planning must precede new activities to keep the environmental impact as small as possible. This means the consideration of a number of criteria which are used to describe a given decision situation such as whether a new activity is environmentally justifiable. This is also related to the availability of appropriate methods and tools to measure the desirability of a new project with respect to the defined set of criteria focusing on the environmental suitability of the project.

In the literature much attention has been paid to the degradation of vegetation and soil, the triggering of overland flow and erosion and the impact of the addition of artificial snow and slope preparation on natural processes. This work has supported the identification of a number of aspects that should be incorporated in the planning of new ski runs: 1) minimise changes introduced by ski piste constructions, 2) minimise negative effects caused by producing artificial snow, 3) minimise risk of overland flow and triggering of additional natural hazards and 4) minimise risk of natural hazard.
The minimum number of changes can be achieved by first selecting naturally smooth slopes to minimise the area that might be affected by surface corrections; second,

minimising the destruction of valuable vegetation with respect to its scientific function and its relevance for the water balance and the ecological equilibrium; third, minimising the degradation of geomorphologic forms as they are important indicators for historic processes and since they have a certain position in the environmental system, fourth, providing easy accessibility for heavy machines to minimise the impact during construction works and slope preparation, and fifth, analysing the availability of a proper snow cover to protect the lower vegetation from freezing and being sliced off and to prevent the need of adding artificial snow. In order to keep the negative effects of artificial snow sufficiently low, it should only be added if environmental conditions are appropriate. This includes meteorological conditions such as a wet bulb temperature below –3 °C, appropriate soil properties, that is to say soils with a high water storage capacity and a high infiltration rate to buffer the additional amount of snow melt, and the presence of a vegetation cover that can handle the additional snow melt water. Triggering of overland flow and erosion can partly be prevented by choosing 1) the right slope and slope profile, 2) the presence of an adequate vegetation cover and the potential for revegetation, and 3) the consideration of the soil properties and the underlying material. For example long concave slopes are easy to ski on, but they enhance saturation at the foot of the slope. Thus a trade off has to be made between attractiveness for skiing and prevention of erosion. Furthermore shallow soils, steep slopes, impermeable soil layers and bare soils are unfavourable for new skiing facilities with respect to triggering of overland and erosion. If possible, new ski runs should be located outside hazardous zones; else mitigation measures have to be established to protect the infrastructure and its users, which are related to extra costs. In addition, the triggering of new hazards should be avoided. The potential for revegetation and the conservation of a certain species association is also important for the aesthetic view and the economic benefit of an alpine area, since these areas are frequently used for summer tourism and farming.

The analysis of possible consequences of ski pistes for the alpine environment demonstrated that the alpine system is complex and that the individual components are related with each other. It is difficult to define discrete independent criteria and it necessitates the need for an integrated assessment rather than the consideration of separate aspects apart from each other as is mostly done in practice. The need for an integrated assessment suggests the use of multicriteria analysis to support the integrated assessment of a defined set of criteria and the consideration of a multiple set of ski runs. The results of the multicriteria analysis can be used to assist the decision-making in the planning for new ski runs. The concept of multicriteria analysis, the definition of criteria, its requirements and how it can be used for the planning of new ski pistes will be addressed in the following chapters.

3 USING SPATIO-TEMPORAL ENVIRONMENTAL MODELS AND MULTICRITERIA DECISION MAKING FOR PLANNING SKI RUNS

3.1 Introduction

Chapter 2 provided a comprehensive overview of the environmental impacts of ski pistes; it showed that the development of ski areas is for the greater part controlled by user's demand and economic benefit, while neglecting the sensitivity of the alpine environment. Human interference in the mountain continues, however, because the action of skiing and associated skiing facilities have social and economical relevance. Additionally, thanks to the perception of the negative effects on environmental factors and processes, attention is paid to the environmental sensitivity when establishing ski runs. So a suitable balance is required between environmental, social and economic concerns. General concepts have already been developed to analyse the environmental suitability of a new development and in order to minimise the negative impact of a new activity. For example, in Switzerland and Austria people were brought together to design regulations to optimise ski run construction with respect to technical aspects, safety for the user and the impact on the environment. The compiled regulations (ÖAWV 1998; Felber et al. 1989), based on experiences of the past and expert knowledge, include both a description of possible impacts and directives that should be taken into account when planning a new project. Furthermore, Environmental Impact Assessment (EIA), which is an effective instrument to evaluate the environmental suitability of a new development by following a logical sequence of steps, has been introduced in the legislation of certain countries. However, the performance of an EIA adds extra costs and time to a new development and is therefore abandoned if it is not made obligatory.

The current decision procedure for a new project in Austria is based on a detailed study of the site conditions, including a qualitative description of the current situation and the expected impact on the environment. For the assessment of the risk of natural hazards, such as avalanches and rock fall, numerical models are often used (Salm and Gubler, 1990). In addition, technical plans are worked out for the drainage and wastewater treatment. The survey of the project area and the qualitative assessment of possible changes caused by the project are in most cases carried out by a professional planning agency. The planning proposal is submitted to the national authority in charge that takes the decision for the proposed project. This procedure has three shortcomings.

First, different aspects are often evaluated separately rather than in combination with one another. However, the alpine environment is a complex system, whose components are related to each other. The separate consideration of single aspects may cause underestimation or overestimation of some factors. Making a balanced decision requires a systematic decomposition of the complex system into meaningful attributes that can be systematically combined in an integrated assessment.

Second, mostly just one alternative is proposed to the decision maker who has to decide whether this development is environmentally justifiable. However, the fact that there might be another alternative with more suitable site conditions that would result in

the same socio-economic satisfaction is often ignored. The evaluation of multiple alternatives would assist in giving a more complete picture of the decision problem.

The environment is a dynamic system that varies in space and time. However, and this is the third shortcoming of the current practice, the assessment of the environmental suitability is mostly derived from a static analysis of the environment, in spite of the availability of more advanced techniques such as environmental models that are able to simulate spatial and temporal behaviour of environmental processes.

In order to overcome these shortcomings this chapter proposes a generic methodology to improve the decision making process for the planning of socio-economic infrastructure. The methodology addresses 1) the integration of multiple environmental attributes relevant for the choice of site for a new ski run using techniques of multicriteria analysis (MCA) (Janssen, 1992; Climaco, 1997; Beinat and Nijkamp, 1998; Malczewski, 1999; Van Herwijnen, 1999) such as the analytical hierarchical process (AHP) (Saaty, 1980), 2) the comparison of different ski runs with respect to the selected attributes, and 3) the use of spatio-temporal environmental models to generate useful information in order to characterise the possible sites for ski pistes.

After a short introduction to the theory of decision making and multicriteria analysis a general outline of the approach is given. This includes the description of the systematic analysis of the decision problem, the design of the decision making process, and its requirements such as data, tools and techniques.

The decision model is designed in such a way that it can be used to support the first investigation of potential sites for a new ski run.

3.2 Multicriteria decision making (MCDM)

Multicriteria decision making (MCDM) incorporates decision making and multicriteria analysis (MCA). MCA is the analysis of multiple elements to find a balanced solution for the problem tackled in the decision making process. Since much has been written on the theory of MCA, (Janssen, 1992; Climaco, 1997; Beinat and Nijkamp, 1998; Malczewski, 1999; Van Herwijnen, 1999) and decision making (Simon, 1960; Sprague, 1989; Cowlard, 1998), only the main concepts are addressed here, which are essential to understand the methodology proposed in this thesis.

3.2.1 General framework of decision making

A decision problem arises when an individual or a group of individuals perceive a difference between the current state and the desired state (Janssen, 1992). Examples of decision problems in a ski area are long waiting times at a ski lift, bad snow conditions on ski pistes at lower altitudes or the triggering of erosion features on the ski run. Decision making (DM) is a delicate and responsible assignment as the decision maker is concerned with taking the right decision on the basis of the available information to satisfy all aspects involved. Moreover it is a crucial issue in our society. Especially in the field of management science people perceive the need for systematic methods to solve decision problems. To this end several general decision models have been developed to structure

the decision making process (DMP) in a logical sequence of steps (Dewey, 1910; Simons, 1960; Mintzberg, 1976; Sol, 1982). A frequently used approach that has been adopted in Figure 3.1 is the one defined by Simon (1960), who suggested to structure the process of DM into three phases, namely intelligence, design and choice. The intelligence phase is concerned with the identification and the analysis of the decision problem that requires a solution. The design incorporates the intervention, development and analysis of possible courses of actions that can be taken. In the choice phase the course of action that satisfies the aspiration level is selected from those available. Simon's model clearly shows the main steps involved in solving a decision problem, but he does not address the support required to realise the individual steps of each phase. To this end, Simon's model needs to be extended with the component "evidence" (see Figure 3.1) (Cowlard, 1998), which involves both any kind of information such as data, knowledge and experience and the set of tools, methods and techniques to use the information in an efficient way.

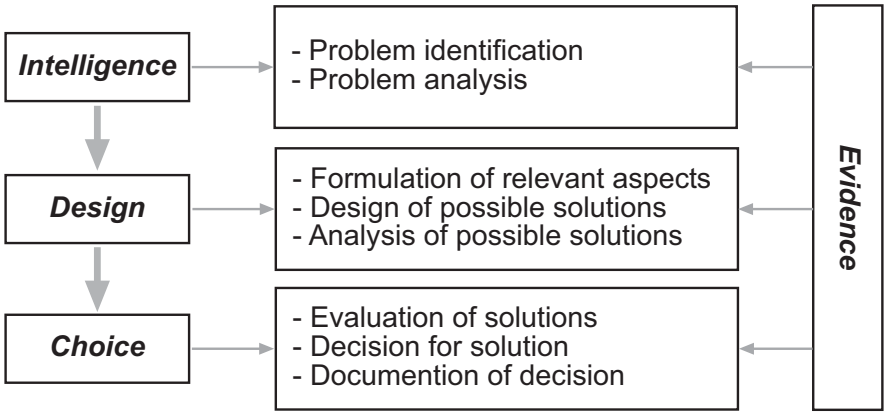

Figure 3.1 Systematic decomposition of the decision making process into three steps following Simon's decision model (1960); evidence is needed for every step of the decision (Cowlard, 1998).

3.2.2 Evidence

In general, decisions are made on the basis of the available information and knowledge about a certain issue or situation (Huxham and Sumner, 2000). Consequently, the use of adequate evidence is an essential component of the decision making process (DMP).

Research fields of the environmental sciences, advanced data acquisition techniques such as remote sensing, and methodology and software for spatio-temporal environmental modelling provide useful means for the analysis of the geographical space and the relation between society and the environment. The means involve, primary and secondary data, expert knowledge and scientific knowledge, concepts, methodologies and tools to facilitate the procedural steps in decision making.

Sources of primary data, that means data that are directly obtained in the field or by any other kind of survey, are field observations and field experiments, automatic measuring facilities such as weather stations or discharge gauges, aerial photographs and remotely sensed images, and historical records of natural events and site conditions.

Secondary data or modelled data are derived from primary data by integrating knowledge, underlying concepts and methodologies, in most cases supported by an appropriate tool. Expert knowledge is defined here as the knowledge gained by observing and monitoring a certain situation or a process and using the experience so obtained to establish cause-effect relations as for instance applied in the forecast of avalanches. Scientific knowledge is achieved by scientific research, for example by the investigation of the behaviour of hydrological processes or the analysis of the response of vegetation to changes in soil properties. In the field of decision making there is a wide range of concepts and methodologies for data analysis, evaluation, integration and documentation. Frequently used examples in DM are the analytical hierarchical process (AHP) approach (3.2.3), other techniques of multicriteria analysis (MCA) (3.2.4), environmental modelling (3.2.5), cost-benefit analysis (CBA) and environmental impact assessment (EIA). Tools used in MCDM are software packages such as Geographical Information Systems (GIS), programming languages or statistical software packages that facilitate the implementation of concepts and methodologies. The use of a certain type of evidence depends on the aim, the decision situation itself, the study area and the access to certain sources of information, tools, methods and techniques.

The approach proposed in this thesis deals with all procedural steps of decision making, thereby using AHP to analyse the decision problem, environmental modelling to structure the data and further techniques of MCA to combine them to useful information.

3.2.3 Analytical hierarchical process

A careful analysis of the problem and the perception of the whole decision situation are indispensable in rational decision making. Since decision problems are often rather complex and difficult to understand, appropriate methods are needed to capture the essential elements incorporated in the problem. A possible method that is frequently used in decision analysis is the analytical hierarchical process (AHP) approach (Saaty, 1980). It is a simple way within MCA to decompose the problem into smaller, understandable parts of hierarchical order to support comparative judgement and to synthesise priorities (Malczewski, 1999).

The decision problem for which a solution is needed forms the top of the hierarchy, sketched in Figure 3.2. The problem is decomposed into smaller parts, which express relevant concerns of the problem. These smaller parts are the *evaluation criteria*, standards, by which a proper decision can be made. In MCDM there are two types of criteria, which are also represented by different hierarchical levels, namely objectives and attributes. An *objective* conveys the desired state of the system which an individual or a group of individuals would like to achieve, while *attributes* are used to characterise the respective objective. Thinking of a ski area, an objective could be the increase of the social benefit, described by benefits related to ski runs, logistics and entertainment in the area. For each objective, a hierarchical decomposition is made into attributes, where the lowest level of attributes needs to represent measurable entities. For example, referring to the example above a measurable entity could be the waiting time at a ski lift or the number of ski runs. These measurable entities are defined here as *indicators*. A meaningful integration of underlying indicators provides an indication for the

achievement of the related objective. Principally, there is no restriction to the number of hierarchical levels, but generally it is advised not to have more than three levels (Belfroid et al., 1996). It can be concluded that using AHP in MCDM supports the analysis of the decision problem, it assists in finding the right balance between criteria, and in addition, it helps to synthesise the multitude of factors involved in the decision problem (Sharifi, 2002). Pairwise comparison (Saaty, 1980) of all possible criteria pairs at each level of the criteria tree supports the derivation of weights that are required for the balanced decision.

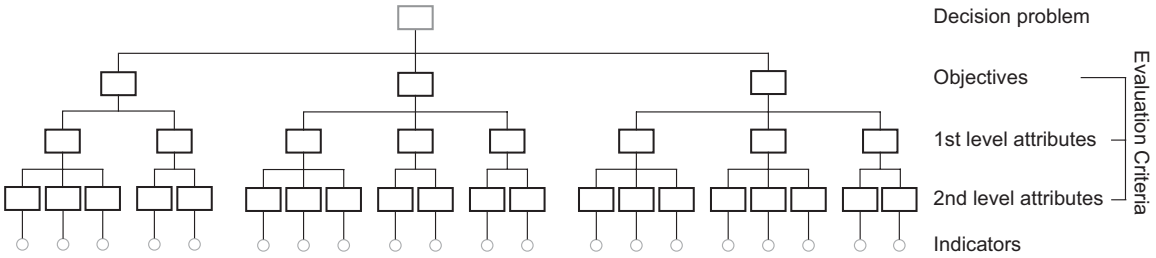

Figure 3.2 Systematic decomposition of the decision problem into objectives, attributes and indicators using AHP.

3.2.4 Multicriteria analysis (MCA)

The main aim of MCA is the integration of multiple criteria to synthesise the multitude of concerns involved in the decision problem as a measure to compare possible solutions (set of alternatives). To this end MCA requires a set of evaluation criteria, a set of alternatives and adequate techniques to implement the conceptual ideas. For instance a suitable set of evaluation criteria can be derived from a hierarchical structure such as illustrated in Figure 3.2. This tree structure is the basis for the search, selection and implementation of evidence, but especially for synthesising the multitude of factors.

The generation of alternatives is widespread. Examples are on the one hand different strategies or a combination of them, frequently used in finding solutions to reduce the emission level, and on the other spatial objects such as a point, line or polygon or any composition of these objects, typical for planning socio-economic infrastructure. Figure 3.3 shows the main elements of MCA, in particular a set of alternatives a_j for j=1,…,3 and a set of criteria c_i for i=1,…,4 to characterise each alternative, and how they are integrated for the final decision. Referring again to the ski run example, the decision for a ski run (a_j) could be based on the risk of natural hazard (c_1), the construction costs (c_2), the distance to other ski runs (c_3) and the ecological impact (c_4).

However, if we want to integrate different criteria, we might be confronted with three problems: First, indicators may have been measured on different scales as they are retrieved from different sources of evidence, Second, the set of evaluation criteria contains both *benefit* and *cost* criteria. A criterion is a *benefit criterion* if a high indicator value has a positive effect on the achievement of the objective, while it is a *cost criterion* when its impact is disadvantageous. And third, evaluation criteria may have different importance with respect to the achievement of a desired state and the general decision

situation. To overcome these weaknesses, standardisation (A in Figure 3.3) and weighting (B in Figure 3.3) are commonly used in MCA, the first to transform indicator values at once to a commensurate scale between 0 and 1 and to the same type of criterion, and the second to assign a priority to each evaluation criterion. Alternatives can be evaluated by comparing them with respect to each criterion (method C1 in Figure 3.3), defined as *non-compensatory evaluation*, or by considering the degree to which an objective is met by looking at the combined value of indicators, known as *compensatory technique* (method C2 in Figure 3.3). While the first approach is only feasible for a small number of criteria and alternatives, the latter one requires a meaningful aggregation of all evaluation criteria, where meaningful denotes the consideration of the importance of a criterion for the decision to be made. Since the decision analysis described in this thesis aims at the evaluation of multiple alternatives, the use of the *non-compensatory* evaluation is not feasible.

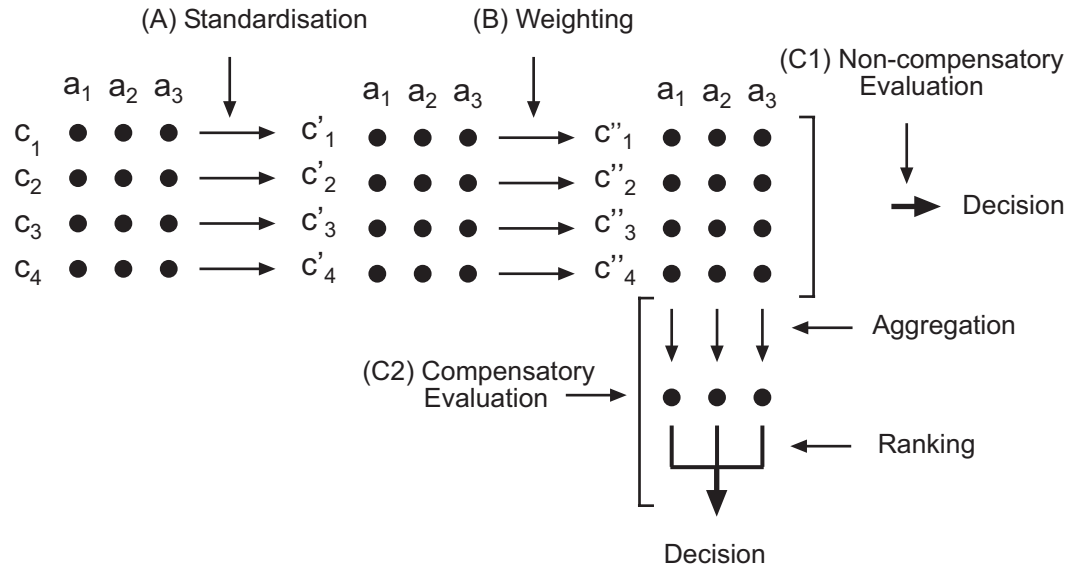

Figure 3.3 Transformation of the original decision matrix (array of a_j and c_i) by standardisation and weighting in order to facilitate the comparison of alternatives with respect to their performance. The columns of the first array represent the alternatives a_j for j=1,…,3 and the rows are the criteria c_i for i=1,…,4. c_i' are standardised criteria and c_i" are the result of weighting.

Malczewski (1999) and Sharifi (2002) give a comprehensive review of commonly used aggregation and combination techniques, how they can be implemented for a certain decision situation, their advantages and disadvantages. As there is no convention about the suitability of a certain method for a certain problem, it is common to test several possible techniques. The choice for a certain MCA technique needs to be tailored to the nature of the decision problem, its objectives and attributes. Moreover, since every MCA involves uncertainty to a certain degree because many choices have been made regarding the selection of MCA techniques and the assignment of weights, it is indispensable to carry out a sensitivity analysis to test the sensitivity of the ranking of the alternatives to the MCA techniques that have been used.

3.2.5 Spatio-temporal environmental models

An environmental model is a conceptual representation of a part of the landscape, including entities and processes above, at or below the land or water surface (Karssenberg, 2002). On the one hand environmental models can be analogue or physical models representing the part of the landscape with a miniature version of that part in the laboratory; on the other environmental models are mathematical models or numerical models using mathematical expressions to describe an environmental system. Mathematical models can be divided into statistical models using a descriptive approach to achieve the modelling aim, and process-based models striving to simulate the physical behaviour of a process. The broad range of process-based models contains different modelling approaches with respect to the factor time (static or dynamic), space (lumped or spatially distributed) and the representation of the process (empirical or physically based) (Obled, 1990). A process-based model may have any combination of the temporal concept, the spatial concept and the representation of the process. In this thesis an environmental model is a mathematical model (Figure 3.4) that consists of 1) a database which manages the input data and the model output, and 2) a model engine that is composed of a defined set of model equations, model parameters and model variables for each process under consideration.

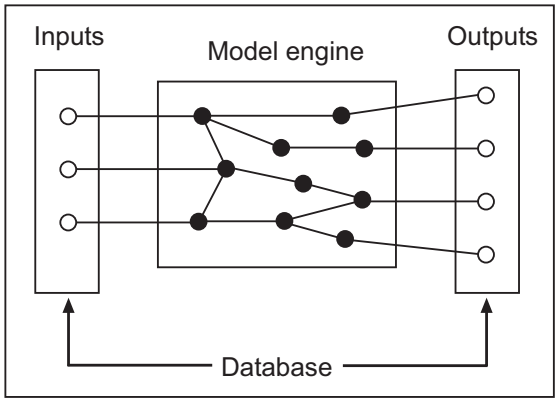

Figure 3.4 Structure of an environmental model. The left box and the right box represent the database and the box in the middle illustrates the interaction between model components and the database.

For the decision analysis described in this thesis we use mainly spatio-temporal environmental models which are dynamic models that apply rules of cause and effect forward in time to simulate the temporal change of physical systems of the landscape. In Equation 3.1 the concept of forward modelling is illustrated:

$$z(t+1) = f(z(t), i(t)) \qquad \text{for each } t \tag{3.1}$$

with *z(t)* the state of the variable *z* at the time *t*, *z(t+1)* the state of the variable z at some time later and *i(t)* is an external input to the system that may cause a change of the state

of the variable z between t and t+1. For example $z(t)$ is the water level in a closed bucket at time t and $i(t)$ is the input of rainfall to the bucket at time t; due to the input the water level of the bucket will rise and the new water level at a defined interval later is expressed by $z(t+1)$.

The integration of spatio-temporal environmental models in the decision analysis requires spatial information on site conditions, temporal records of data that are variable in time, scientific knowledge for model building and appropriate tools to implement the model concept. The output of these models may be a time series of spatial maps, a time series of non-spatial values, a spatial map or simply a non-spatial value.

The application of those models in MCDM has several advantages. For example, they represent processes as they are occurring in the landscape, and so spatial and temporal patterns of the properties can be included in the decision analysis. Furthermore, process-based models are a useful tool to understand the complex behaviour of an environmental system, they teach us how the system that has been modelled works. Dynamic or forward models also support the prediction of a future behaviour under various courses of action, for instance the response of the environment to the construction of new transport lines, and therefore they can be used for scenarios in MCDM in order to analyse the cause-effect relations. In addition, process-based models provide crisp values and therefore objective information for the integrated assessment. Moreover, environmental models are also a useful means to use the quantity of data in an efficient way, especially in times of advanced data acquisition techniques.

More details about the theoretical background of environmental modelling and model building can be found in Beck (1993), Hardisty (1993), Goodchild et al. (1993), Jakeman (1995), Jørgensen (1996), Van Deursen (1995), Wesseling et al. (1996), Burrough (1998), Karssenberg (2002) and Skidmore (2002).

3.3 Spatial MCDM

In standard multicriteria decision theory, a decision problem is evaluated in the 0^{th} dimension, which means that the performance of an alternative for a certain criterion is measured without any spatial component (Van Herwijnen, 1999). However, as many decision problems in society are related to the geographical space and due to the advances in the field of geographical information science, the consideration of the factor space became a sensible issue in spatial decision making. MCA techniques have been applied to spatially distributed data, either within a GIS environment or by coupling a GIS with software packages specially meant for MCA (Jankowski, 1995; Malczewski, 1999; Van Herwijnen, 1999).

In spatial decision problems alternatives can be characterised by a defined set of maps that provide information for each criterion, called criteria map. The creation of these maps is facilitated by the development of modern geographical information systems because they make it possible to store basic data in terms of basic geographic entities such as points, lines and areas, and also to transform, combine and display them as required according to the needs of the user (Burrough, 1989). The information content of these maps can be represented in either the raster (grid cell) or the vector (symbols and connected lines) form (Burrough, 1989; Burrough and McDonnell, 1998). With respect to

compensatory evaluation (Figure 3.3) Van Herwijnen (1999) proposed two paths for solving spatial decision problems, illustrated in Figure 3.5. In the first path the author suggested to aggregate the spatial information to a non-spatial value for each criterion separately (Function *g*). The result is a decision matrix that consists of a finite set of non-spatial values representing the characteristics of each alternative to which traditional MCA techniques, in particular standardisation, weighting and decision rules, may be applied. In the second path MCA techniques are applied to the individual attribute maps describing a criterion, which are consequently combined for each alternative (Function *f*), while still keeping the spatial component. This results in one map for each alternative, reflecting the performance of the alternative in space. Since decision rules are usually applied to single values, each map has to be aggregated to a single, non-spatial value, which represents the overall performance of each alternative. The main difference in the two approaches is the spatial aggregation. If we treat each criterion separately (Path 1), the selection of the spatial aggregation method may be tailored to the physical meaning of each criterion, while in the other approach (Path 2) spatial aggregation is constrained to one method because the spatial meaning of each criterion was eliminated due to the combination of them in an earlier stage. However, and this is only valid if spatial data have been stored in the raster form, path 2 will be more appropriate when considering every grid cell of a raster map as an alternative. More details about advantages and disadvantages of the two paths can be found in Van Herwijnen (1999) and Sharifi et al. (2002).

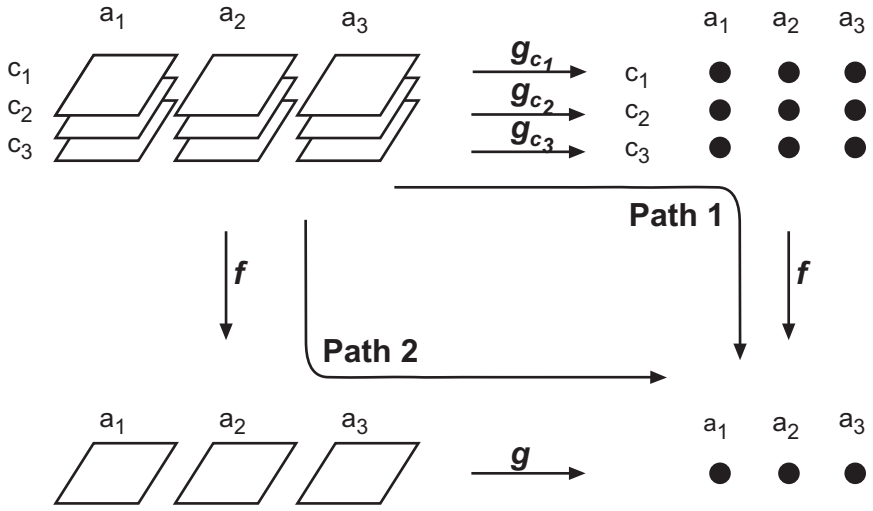

Figure 3.5 Two paths for solving spatial multicriteria analysis (Van Herwijnen, 1999). Function *g* is used for the aggregation of the spatial component, while the function *f* removes the explicit meaning of individual criteria because of the integration of them to a complex entity.

3.4 Spatio-temporal MCDM (stMCDM)

Spatio-temporal environmental models provide the decision maker with a set or stack of maps for different moments. This means that for each time step *t* for which the model has

been computed one or more maps are stored in the database to visualise environmental processes in space and time. These stacks of maps assist in understanding the processes described by environmental models, but the generated information is too complex to be directly used in a multicriteria evaluation. Since the aim of MCA is to compare a set of alternatives on the basis of an integrated assessment of evaluation criteria, the spatial and temporal information needs to be reduced to a single value, thereby removing the spatial and temporal components. Van Herwijnen presented two methods for aggregating spatial information to single values (Figure 3.5). In order to include the maps for different moments in the integrated assessment, the aggregation in time was added to Van Herwijnen's approach (Figure 3.6 and Figure 3.7). Aggregation in time means both the aggregation of maps and non-spatial values for different moments to one map or one value.

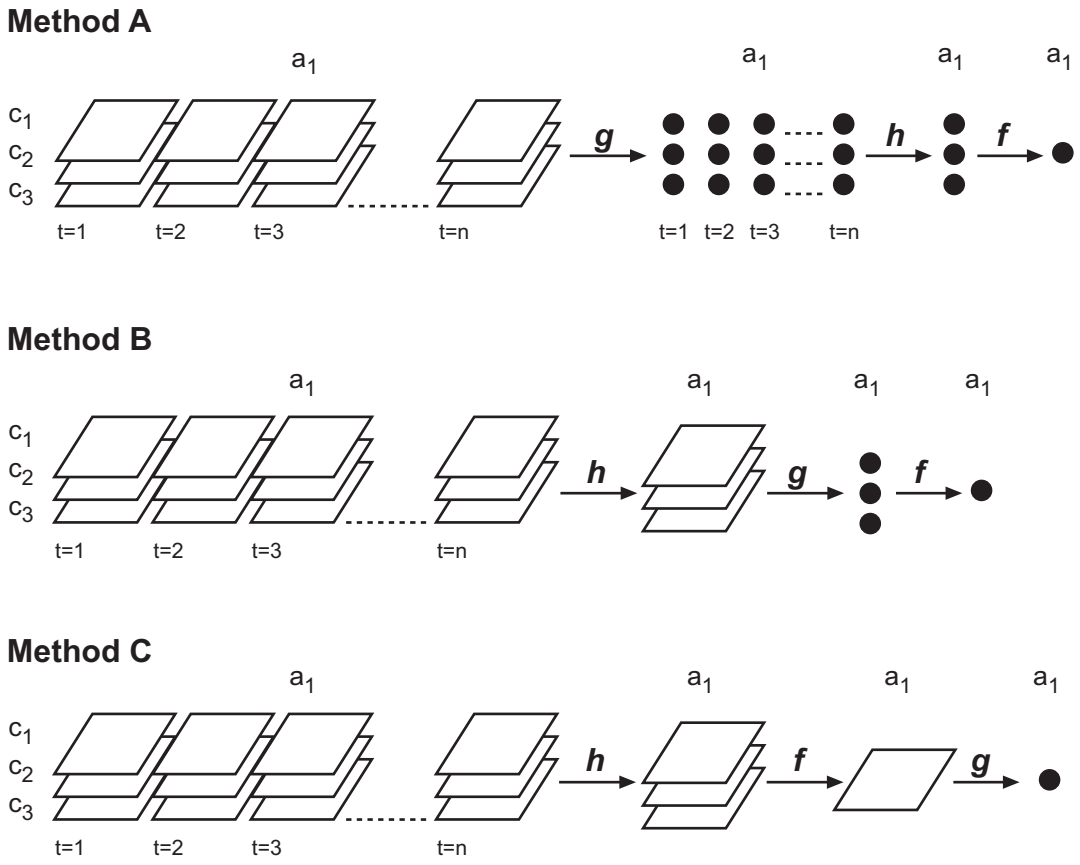

Figure 3.6 Transformation of spatio-temporal data to single values by various strategies (methods A, B and C). The starting point is a stack of dynamic maps for the three criteria c_1 to c_3 describing the alternative a_1. Function *f* represents the combination of criteria, *g* the spatial aggregation of a map to a non-spatial value and *h* the temporal aggregation of a time series of entities (maps or non-spatial values) to one entity.

To this end, three types of aggregation functions may be used for solving spatio-temporal decision problems, defined here as function *f*, *g* and *h*. The task of function *f* is to

integrate the defined set of criteria, either represented in form of maps or in form of non-spatial values, to one map or one value. Given, that a decision problem depends on three criteria, for example costs, view and slope, each represented by a map, function *f* combines the three maps to one map, thereby loosing the physical meaning of each environmental criterion. If those criteria are expressed by a single value, the output of function *f* will also be a single value.

Function *g* aggregates the spatially distributed information to a single value. For example, the slope map from the previous example shows for each spatial unit the corresponding slope. Applying function *g* to the slope map results in one value, which is representative for the slope of the area in consideration. Function *h* is the aggregation in time, the method that has been added to Van Herwijnen's approach in order to include temporal data in the decision analysis. For instance, a stack of maps representing the daily increase in biomass above soil surface could be aggregated to the total amount of biomass during one growing season, or from a time series representing the daily discharge at the outflow point, the maximum discharge could be extracted. Figure 3.6. shows the three aggregation methods, which have been applied to the same input. The input is a stack of maps for different moments, which represents the state of three environmental criteria for *n* time intervals, characterising one alternative (Figure 3.6). The methods differ in the sequence of the functions *f*, *g* and *h*. A simplified example is used to demonstrate the principles of each aggregation method:

A skiing company is concerned with finding a suitable location for a new ski run. Three criteria are assumed to control the choice for the location of the new piste, namely biomass production, the risk of erosion and satisfactory snow conditions. Each criterion has been described by a spatio-temporal environmental model, which results for each criterion in a map for each moment for which the respective model has been computed (i.e. a stack of dynamic maps). To be able to compare possible solutions, model results need to be transformed. The first method (Method A in Figure 3.6) suggests to remove first the spatial component (function *g*), second the temporal component (function *h*), and then the three criteria need to be combined (function *f*), for example by simple additive weighting (Malczewski, 1999). An example for the first two steps could be the number of days during the growing season that the amount of biomass at the ski piste exceeded the threshold that defines satisfactory biomass production. Spatial aggregation can be done by identifying the moments for which the amount of biomass was satisfactory. Counting the moments with a positive response the value for different moments is aggregated to a single measure.

In the second approach (Method B in Figure 3.6) the first two steps are reversed; the maps for different moments are first aggregated to one map (Function *h*), and second, the resulting map is transformed to a single value (Function *g*) that needs to be combined with the other criteria (Function *f*). For example, from the stack of maps describing the spatial distribution of erosion for each time step *t*, the maximum amount of erosion can be extracted for each location *s*. From this map one could compute the spatial average of the maximum erosion for the area in consideration.

The third method (Method C in Figure 3.6) is the same as the first part of the second approach (Function *h*), but then the criteria maps are first combined to one map, which represents information for three different criteria (Function *f*), and then spatial aggregation is applied to that synthetic map (Function *g*). For instance, the set of maps

providing information about the spatial distribution of snow could be transformed to one map indicating the total amount of snow during the winter season for each spatial unit in which the snow maps are divided. The temporal aggregation is followed by the integration of the snow map, the erosion map and the biomass map to one map, thereby removing the implicit meaning of each criterion. This results in a map that needs to be transformed to a single value to apply compensatory evaluation (c.f. 3.2.4) to the decision problem.

In the first and second approaches (A and B) both spatial aggregation and temporal aggregation may be tailored to the characteristics of the representative criterion. In the third approach only temporal aggregation may be adapted to the meaning of a criterion. The choice of aggregation method depends on the criteria in consideration and the meaning of the criteria for the specific decision problem. Again, there is no general rule for the best aggregation method. These three aggregation methods are combined in the general framework for spatio-temporal MCDM (stMCDM) (Figure 3.7).

Three alternatives, which are going to be analysed with respect to four criteria, are the starting point of the framework shown in Figure 3.7. Each criterion is represented by a stack of maps for different moments, describing the respective environmental process or state in space and time. In the framework possible aggregation and combination functions are elaborated with respect to the given input, using the aggregation function (*f*, *g* and *h*) and strategies (methods A, B and C) that have been illustrated in Figure 3.6.

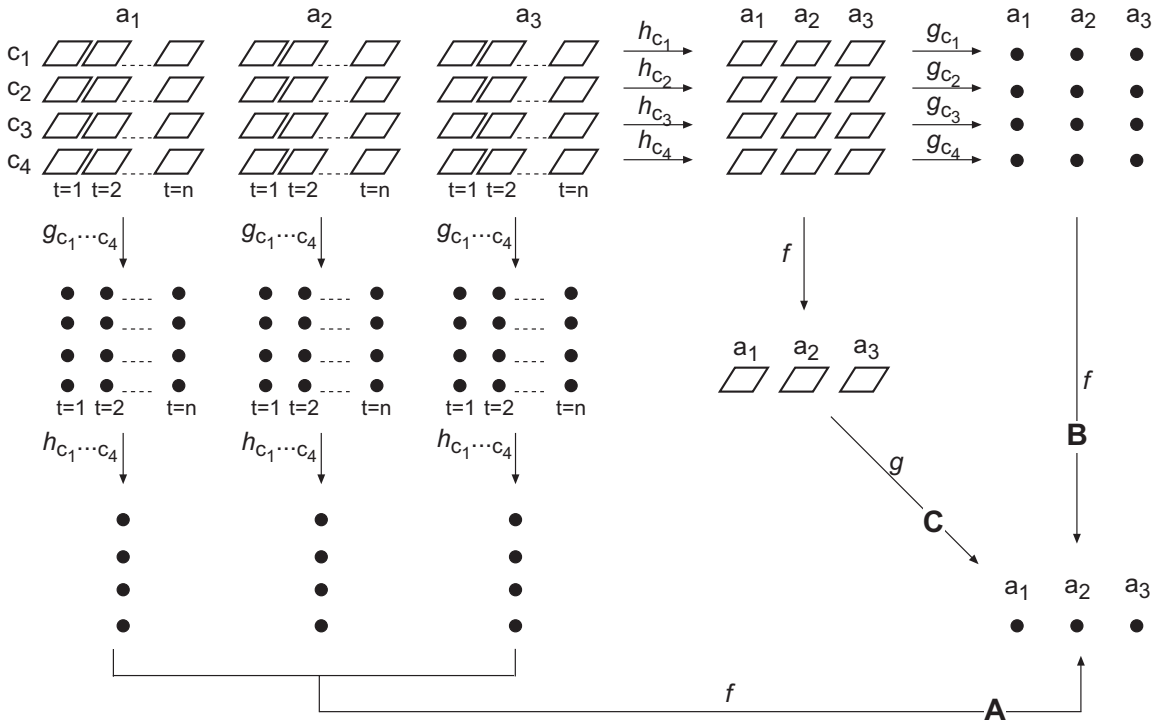

Figure 3.7 General framework for spatio-temporal MCDM (stMCDM). Function *f*, *g* and *h* correspond to the functions used in Figure 3.6 and represent possible aggregation paths for criteria maps $c_1,\ldots,c_4$ and the set of alternatives $a_1,\ldots,a_3$.

3.5 stMCDM for the planning of ski runs

For planning new ski runs the design of the decision model involves 1) problem analysis, 2) design of possible ski run alternatives, and 3) generation of information to evaluate the set of alternatives and to identify the alternative that fits most to the defined objectives.

3.5.1 Problem analysis

Ski runs are related to social, economical and environmental concerns. Political issues are supposed to be incorporated in these concerns. Table 3.1 gives a general overview of planning criteria, both objectives and first level attributes that might be considered when planning a new ski run according to social, economical and environmental interests. One should note that the definition of environmental criteria depends on the specific decision situation and therefore the situation needs to be thoroughly analysed.

Table 3.1 General approach for the planning of new ski runs (see also Figure 3.2).

Concern	Objective	1st level attributes
Society	Increase social benefit	- Ski run - Logistics - Entertainment in ski area
Economy	Increase benefit for local enterprises	- Ski run company - Logistics (Hotel and restaurants) - Shops
Environment	Minimise environmental disturbance	- Ecology - Land degradation - Snow conditions

This study focuses on the environmental part only, and therefore the evaluation of the socio-economic situation will be ignored. The review of possible environmental impacts of ski pistes and associated activities given in Chapter 2 showed that vegetation, soil, topography and precipitation, either in the form of rainfall or snow, play a central role in the planning of environmentally sound ski runs. This is because vegetation protects the slope from erosion and landslides, and it is important for the economic situation of alpine farmers, for the aesthetic view and for ecological research. Further, precipitation, topography and soil are relevant driving forces for the hydrologic system and therefore of processes such as overland flow, erosion or slope instability, which may degrade the landscape. If the aim is to construct a ski run that considers the sensitivity of the alpine environment, then the essential criteria need to be identified. Figure 3.8 illustrates the analytical decomposition of the decision problem into measurable elements considering the principles of the analytical hierarchical process (AHP) to achieve minimal overall disturbance when building a new ski run in an alpine area. The definition of the environmental attributes at the first level of the hierarchical structure, specifically vegetation, land degradation and snow conditions, originates from the environmental impacts identified in the literature review of Chapter 2 and field observations of the study area.

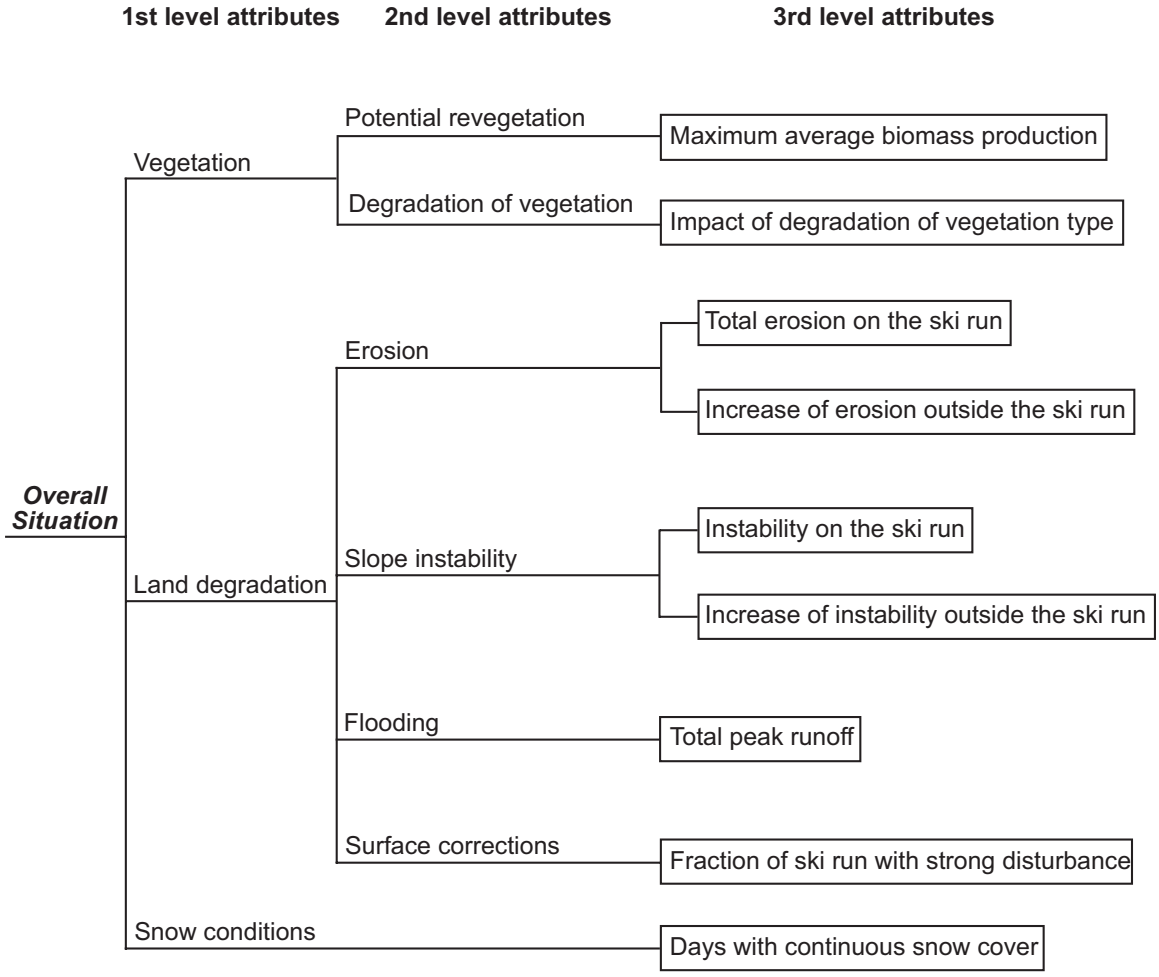

Figure 3.8 Hierarchical structure of environmental criteria to be considered in the planning of environmentally sound ski runs.

3.5.1.1 Vegetation

In the case study elaborated in this thesis the analysis of vegetation is related to two issues: first we are concerned about the destruction of special plant species which have a specific role in the alpine environment: they can be rare species, be important for the maintenance of the ecological balance, or they are a typical part of a certain vegetation community. This is partly based on the results of impact studies that often reported the shift of a species-rich vegetation community to a species-poor community (Grabherr, 1985; Schauer, 1980), caused by ski pistes. Further, bare ski pistes are highly prone to land degradation by shallow landslides and erosion because vegetation protects the slope from erosion and stabilises it. Attempts in some alpine ski areas to re-establish a grass cover similar to the original vegetation cover have partially been successful, to a large extent determined by the local growing conditions of an area. To this end we are aiming

to identify locations for possible ski runs where growing conditions are favourable to compensate for the impact on the original grass cover, and those, which are not habitats of valuable plant species. This involves the analysis of the spatial distribution of biomass production (kg/m^2) during an alpine growing season and the determination of the potential degradation of valuable vegetation at each potential site for a ski run. In this thesis, the degradation of valuable plants is indicated by a number between 1 and 9 according to the comparative scale introduced by Saaty (1980), also used for pairwise comparison, where 1 indicates little degradation and 9 serious impact.

3.5.1.2 Land degradation

Land degradation is a serious problem in an alpine environment, especially if residential areas or human constructions are endangered. In this thesis erosion, slope instability, flooding and the impact on the soil, regolith and bedrock due to surface corrections are considered as those criteria that capture the essential issues of land degradation in a ski area. Erosion caused by a ski piste can occur both on the ski piste, but also in its surroundings because in an alpine environment erosion is for the greater part triggered by surface runoff. Additionally, both hydrological processes and the erosion and deposition of sediments are spatial processes, which means that the processes are not only controlled by the mechanisms at the location in consideration, but also by the situation in the surroundings, i.e. the upstream area. Therefore, both the possible sediment loads (kg/m^2) on a potential site for a ski run and the erosion rate in the total catchment that has been selected for the decision analysis, are considered. The same procedure, that is to say the analysis of an environmental attribute on the potential ski run location and also in the total catchment, is applied to the analysis of the probable failure of slopes because slope instability is assumed to be related to hydrological conditions, and these conditions are controlled by the spatial interaction of influence factors. Slope instability is represented by the probability that parts of the potential ski run location might become unstable due to unfavourable conditions at that site. Flooding, caused by the hydrological situation of a catchment that contains the ski run, has been assigned to the criterion “land degradation” because it can have an enormous destructive power as for example shown by the flood disaster in the ski area of Sölden in 1987 (Aulitzky, 1988). However, one must note, that that disaster was rather caused by heavy rain events together with high snow melt rates than by the compacted surface of ski pistes. In the proposed decision framework flooding is represented by the peak runoff of the period that has been analysed. Additionally, man-made land degradation is appended to the attribute land degradation. This type of degradation addresses the impact caused by the removal of topographical irregularities of a potential ski run to create artificial smooth surfaces and is expressed as a change in the topographic elevation (m).

Referring to the concept of MCA, land degradation is a *cost criterion* (Section 3.2.4), thus the aim is to keep the degree of land degradation of all contributing environmental attributes as small as possible.

3.5.1.3 Natural snow conditions

Natural snow plays a major role in the alpine environment. Apart from its impact on the hydrological system, it controls the regeneration and the growth of vegetation because of its protective function for vegetation, both with respect to freezing and with respect to the mechanical impact. Furthermore, the duration of snow determines the length of the growing period. An adequate snow cover prevents the need for the addition of artificial snow, the negative impact of which was discussed in Chapter 2. In order to provide a measure for the *benefit criterion* "snow conditions", information about the spatial distribution and the duration of an adequate snow cover is needed (c.f. Chapter 7 and Chapter 10).

3.5.2 Identification of the best site for a ski piste

Figure 3.9 illustrates the general requirements to characterise a ski run from the environmental point of view. This includes the availability of useful information related to an alpine ski area and a method for the generation of potential ski run alternatives. Both conditions are related to the use of adequate evidence such as measured data, modelled data, methods, techniques and tools to characterise potential alternatives for possible ski runs.

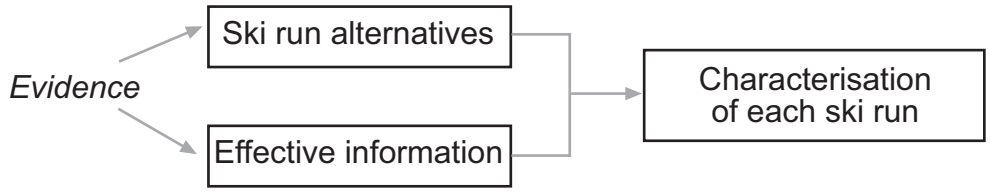

Figure 3.9 General requirements for the development and analysis of a set of ski runs. Effective information represents the information by which each ski run can be characterised.

3.5.2.1 Generation of potential ski pistes (alternatives)

Planning experience and functions provided by geographical information systems can be used to design a set of ski run alternatives. When dealing with maps in raster form (Burrough, 1989; Burrough and McDonnell, 1998), each single grid cell of a raster map may represent an alternative. However, this approach depends on the spatial resolution that is to say on the size of the grid cells in which the project area has been divided. If the grid cells of a raster map, representing individual alternatives, are reasonably small (< 50m), the number of alternatives can be very large. To reduce the number of grid cells to feasible grid cells only, often a constraint map is used (Malczewski, 1999), which excludes those areas that are not suitable for a specific development. Conversely, if the spatial resolution is coarse, a grid cell may cover an area that is larger than the area of the planned development. So, when choosing the grid cell approach, the size of the grid cells needs to be tailored to the size of the future development.

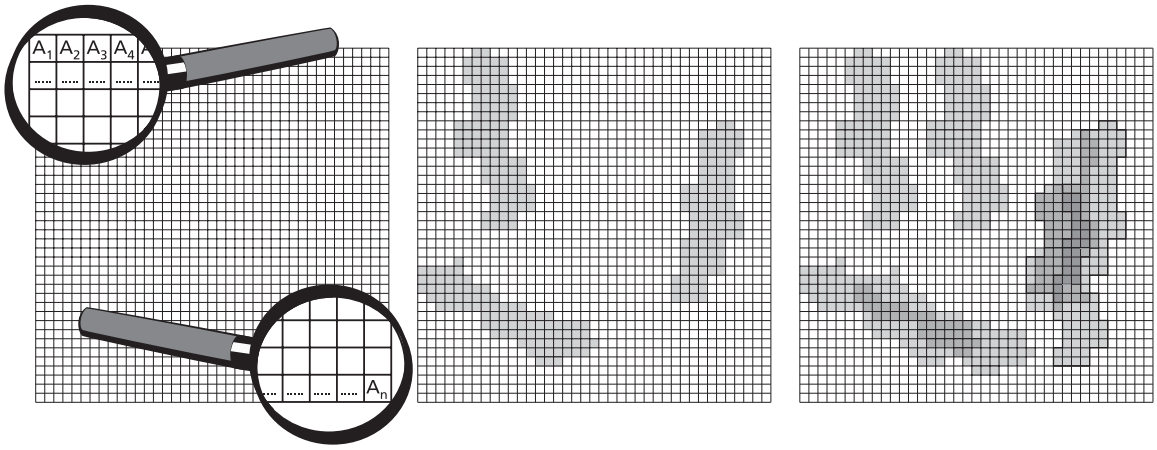

Figure 3.10 The left map represents the single grid cell approach, the map in the middle could be a proposal submitted by a private or public enterprise and the map to the right displays the idea of overlapping ski runs to optimise the search for a suitable site for a ski run.

Nevertheless, when dealing with spatial objects such as ski run polygons the single-grid-cell approach (left map of Figure 3.10) is not appropriate. First, and that was already tackled above, the aerial extent of a ski piste will hardly match the grid cell area, and second the topological contiguity is important for certain processes such as hydrological processes. Considering single grid cells as alternatives, the spatial interaction between the spatial units is ignored and the total impact of a potential later development of a ski run, which probably exceeds the size of a grid cell when using high resolution maps, cannot be taken into account. Moreover, it is not feasible from the operational point of view because the whole decision analysis would have to be repeated for every grid cell. To overcome these shortcomings we need to consider spatial object that represent the spatial extent of a ski run. On the one hand feasible alternatives for locating a new ski run can be provided by a public or private authority in charge, tailored to socio-economic demands (map in the middle of Figure 3.10). This approach aims at the identification of the more acceptable ski piste location from the finite set of alternatives that has been proposed by the authority in charge. The disadvantage of this approach is that other solutions than the proposed ones, which might be better from the environmental point of view, are not included in the decision analysis.

Conversely, one could use a computer model to generate a set of all possible locations for new ski runs within a defined domain with respect to the physical properties of the domain. As we are dealing with spatial objects larger than one grid cell and since we want to explore all spatial solutions representing possible ski pistes, alternatives overlap as shown in Figure 3.10, right map. Then it is possible to optimise the search for the more acceptable ski piste location within the defined domain according to the selected environmental criteria.

The decision framework proposed for this case study uses the principles of the modelling approach to create a finite set of possible ski runs for the alpine catchment in consideration. Therefore a computer model has been developed (ski run model) which generates possible ski pistes on the basis of the physical characteristics of the terrain

deduced from the DEM. The application of the ski run model for the decision analysis requires the consideration of three facts: 1) the catchment of a size of 3.44 km^2 is represented in the raster form (Section 3.3), which means that the catchment is divided into a finite number of grid cells, 2) areas of the alpine catchment which are not suitable for potential ski runs, such as slopes steeper than 27 º, were excluded from the search domain for possible ski pistes, and 3) the direction of the steepest downhill slope as determined from a gridded digital elevation model according to the D8 algorithm (Moore et al., 1993; Burrough and McDonnell, 1998; Burrough et al., 2001), also called local drain direction (*ldd*), defines the shape and direction of a potential ski piste. The main steps of the ski run model are:

1) Definition of the area that is suitable for ski pistes.
2) Selection of a feasible location from which a ski piste could start in the domain that has been defined in step 1.
3) Generation of a ski piste of a certain length and width from the starting point following the local drain direction as shown in Figure 3.11.
4) Application of a smoothing technique to the surface of the generated ski piste because a ski run with high irregularities of the slope over short distances is not feasible from the socio-economic point of view.

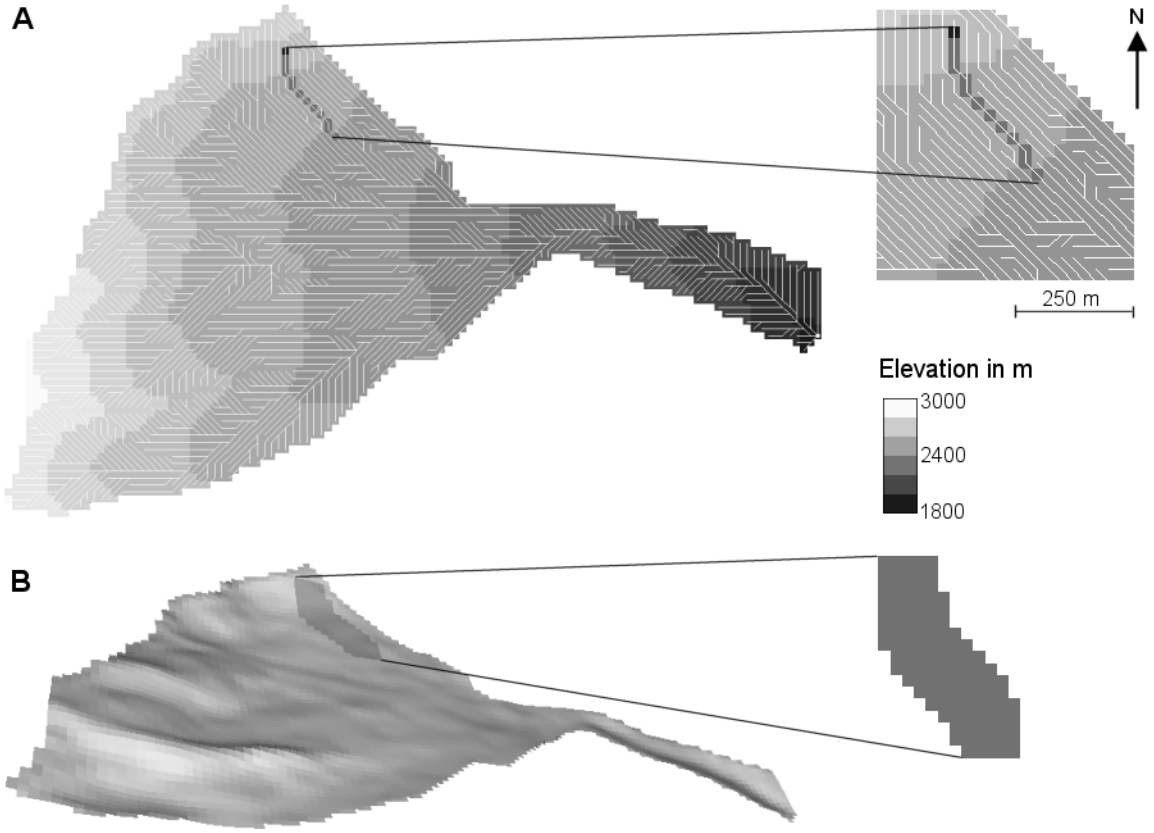

Figure 3.11 Part A shows the generation of a ski run from a feasible starting point that totally falls in the catchment; the ski run follows the physical shape of the terrain, indicated by the direction of the steepest slope down hill (white lines). Part B illustrates the final extension of the ski run.

For the smoothing block kriging (Burrough and McDonnell, 1998; Pebesma and Wesseling, 1998) was applied to the elevation data of the area of a possible ski piste and its surroundings. Block kriging is a method for interpolating data values from sample data using regionalized variable theory in which the prediction weights are derived from a variogram model. The average value of z over a block B, given by

$$z(B) = |B|^{-1} \int_B z(s)dx$$

with $|B|$ the block area, is approximated by

$$\hat{z}(B) = \sum_{i=1}^{n} \lambda_i \cdot z(s_i)$$

with $\sum_{i=1}^{n} w_i = 1$ and s_i the points that discretise the block B and where w_i are the weights for each point s_i, derived from the variogram. Block kriging was used to interpolate the elevation values for the total ski piste area on the basis of the sample data. Both the elevation of the grid cells at the edge of the simulated ski run polygon and the elevation of a finite number of grid cells within the area of the potential ski piste, selected according to a regular sampling scheme, were used as the sample data in order to define the variogram model to optimise the prediction weights. (Figure 3.12). In this case a spherical model was chosen with a range of 500 m. The block size of 40 m by 40 m and the radius of 500 m were determined by the evaluation of the characteristics of the surface interpolation. Block kriging assisted in generating a rather smooth surface, which is closer to the surface of a ski piste as requested by law or most skiers. Using a 3 by 3 window would smooth the surface on the base of original data values (i.e. the smoothing is an approximation of the original surface), however, big differences between close data values are decreased, but are not totally removed.

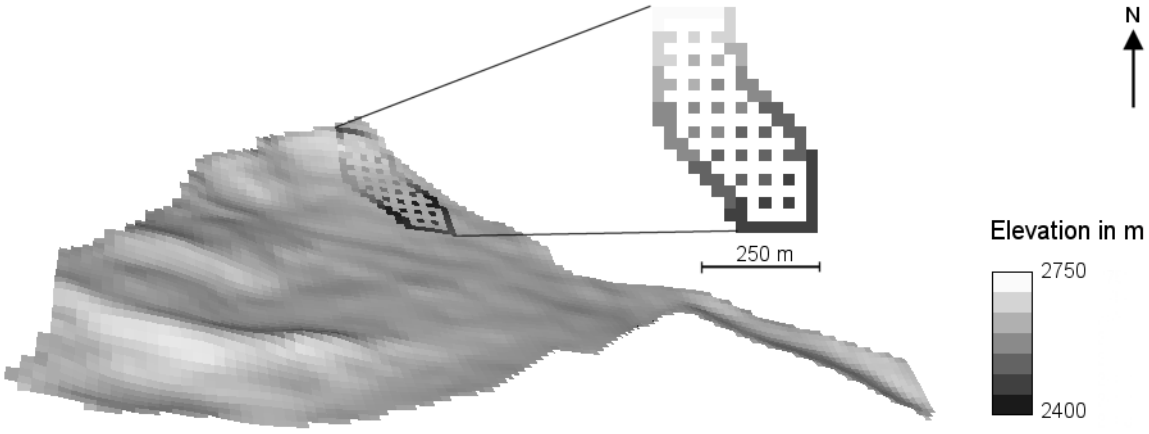

Figure 3.12 Subset of elevation data used to fit the variogram and to predict elevation data for the total ski run area.

The sequence of steps to generate a ski piste was applied to a defined set of starting points for which the generated ski piste falls completely within the domain (area suitable for skiing) defined in step 1. The identification of these points was done in a separate analysis. In order to determine the prediction weights, the same variogram was used for the smoothing of the surface of each ski run. All ski runs that are included in the decision analysis have the same spatial extent. When performing another analysis, a different width or length may be chosen.

3.5.3 The generation of effective information using spatio-temporal environmental models

The generation of effective information is related to the application of spatio-temporal environmental models (Section 3.2.5) to each ski run alternative to compute information in correspondence with the environmental criteria formulated in Figure 3.8.

Figure 3.13 gives a general overview of the individual steps to obtain the required information. These are 1) the design of possible ski runs by the ski run model as explained in Section 3.5.2, 2) environmental modelling, introduced in Section 3.2.5 and continued in the Chapters 6, 7, 8 and 9, and 3) the aggregation of the model results to single non-spatial values for each criterion as described in Section 3.4.

With respect to the selected environmental criteria environmental models were applied to each ski run alternative. These are spatio-temporal environmental models such as a snow model (Section 7.2), a hydrological model (Section 7.3), an erosion model (Section 8.1), a stability model (Section 8.2), a grass growth model (Chapter 9) and additionally a statistical vegetation model (Chapter 5) in order to generate the required information (Figure 3.8 and Figure 3.14). All models except for the vegetation type model access the same database.

The dynamic models are run sequentially, starting with the snow model, which simulates snow cover changes due to snow accumulation and snow melt. Snow melt is also required by the hydrological model, which computes water fluxes and states such as surface runoff to determine the amount of erosion, the peak discharge at the outflow point of the catchment and the height of the groundwater table required by the stability model. The stability model returns the probability that a slope might become unstable. The potential growth model uses the same solar radiation approach as the snow model and describes the growth of grass and sedge for one growing season. The statistical vegetation type model assists in mapping vegetation classes. Spatial and temporal model results describing environmental criteria are aggregated according to Figure 3.6, where the aggregation method is chosen according to the relevance of the criterion with respect to the environmental suitability of a development (c.f. Section 10.3). The study described in this thesis aimed at the development of models, which are simple enough for the use in practical applications such as the planning of ski runs in small alpine catchments, but rigorous enough to capture relative spatial differences of important environmental criteria.

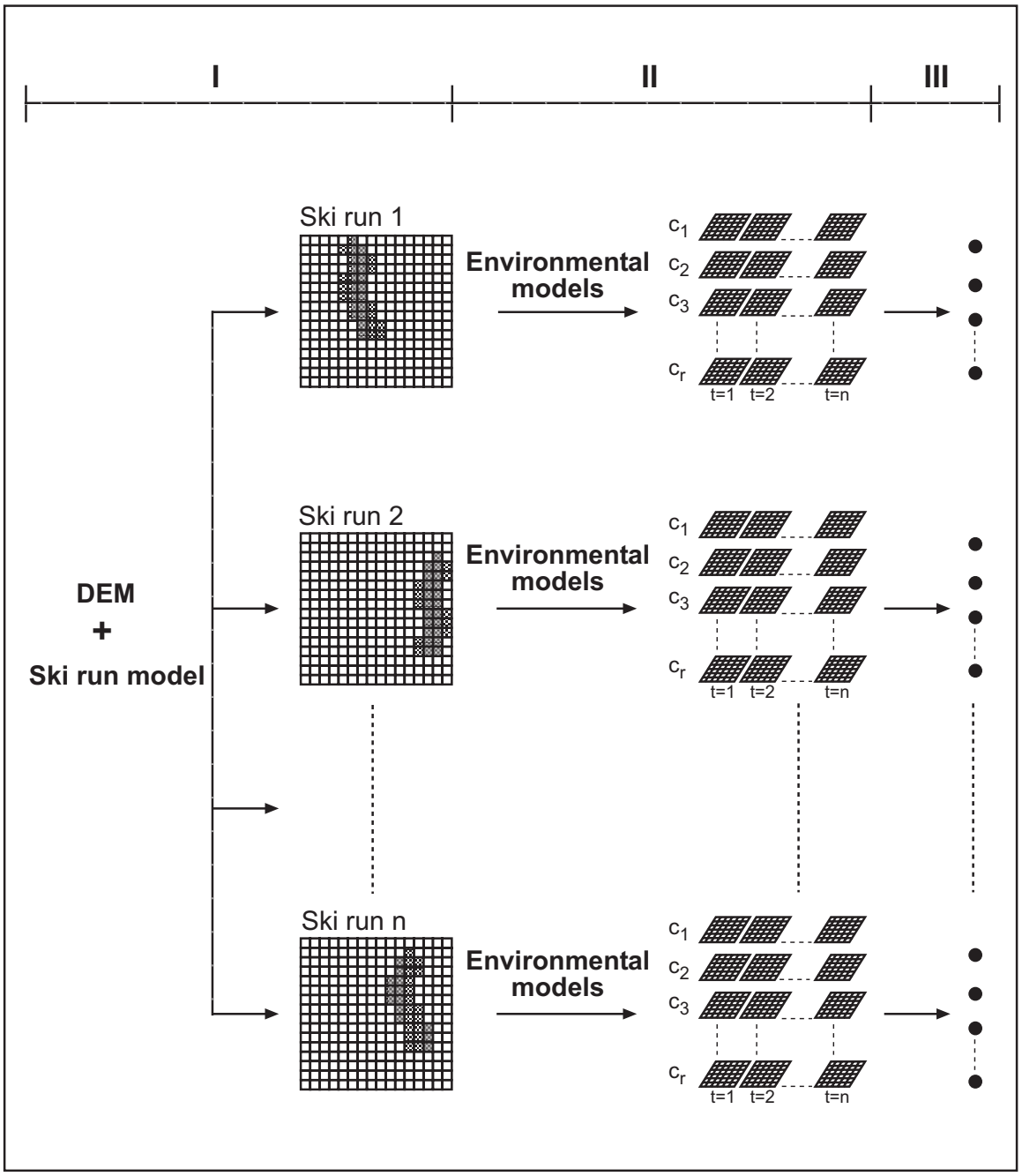

Figure 3.13 From ski runs to the characterisation of a ski run by a set of indicators, where step I represents the generation of ski runs, step II is the application of each environmental model to each alternative and step III reflects the aggregation of the spatio-temporal model output to a single value.

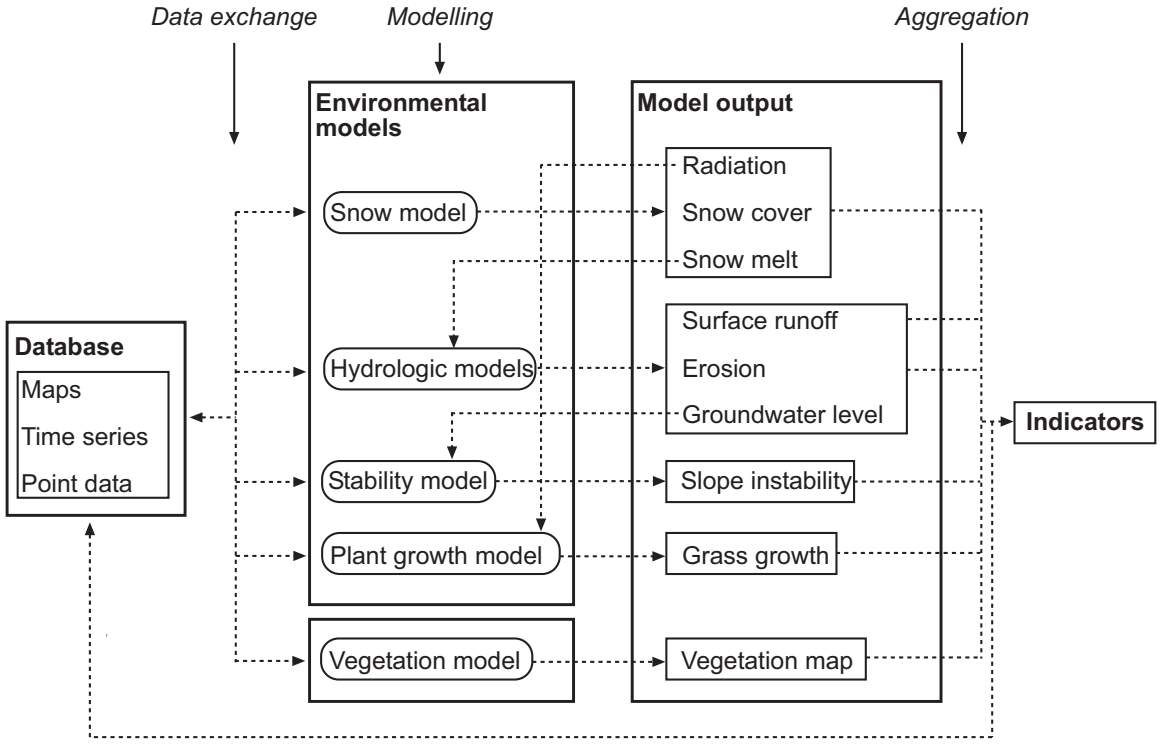

Figure 3.14 Communication between database, environmental models, intermediate model output and model output that is aggregated to indicators to be used for the MCA. The dashed line represents the flow of information.

3.5.4 Software environment

The PCRaster software package (PCRaster, 1996; Wesseling et al., 1996) was used as the general software environment. This is a raster GIS with an embedded modelling language. It supports both GIS functionality such as data storage, processing, evaluation and visualisation, but also static and dynamic modelling. Since the constructed model can be executed within the GIS environment, the communication between the database and the models is easy. However, PCRaster can also communicate with other software tools, which provide the user with additional functions apart from the tools provided by PCRaster. The embedded modelling language and the coupling with other software tools facilitate the data exchange between the individual models and enable the implementation of MCA techniques in a different software environment, such as the statistical software package Splus6. Additionally, dynamic models constructed in PCRaster can be tailored to the respective decision problem and the study area.

4 DATA, METHODS AND TECHNIQUES

4.1 General geographical information

The study area is located in the Ötztal (Figure 4.1), a north-south oriented valley in the region of Tyrol, on the upper western slopes of the village of Sölden, which is a popular ski area in the Austrian Alps. It covers an area of approximately 3.6 km^2, and has an elevation range from the timberline, at about 1900 m, up to 2650 m.

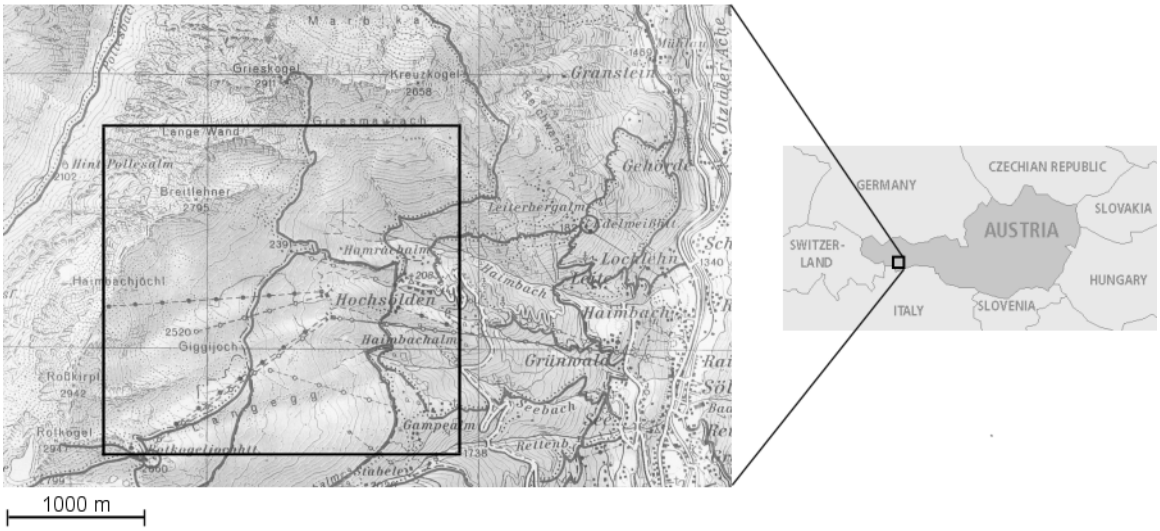

Figure 4.1 Geographical location of the study area, marked by the rectangle (Source: ÖK 1: 25000, BEV Austria);

Geologically, the study area belongs to the Ötztal massive, whose formation is the result of a sequence of processes going back more than 450 million years (Purtscheller, 1978). The present land formation is mainly determined by alpidic fold and uplift, degradation and glacial activity. Typical geomorphologic features are rock glaciers, protalus ramparts and talus cones, which occur predominantly at higher altitudes. The presence of morainic arcs, cirques, smooth land forms and a dominant cover of morainic deposits testify to the glacial activity. The underlying material consists for the greater part of different kinds of gneiss and schist of variscic and prevariscic origin. The amphibolites at the northern border of the study area originated from volcanic tuffs by metamorphism and are typical for the area to the north of Sölden. For further details about geomorphological characteristics the reader is referred to Ghinoi (1999).

Due to the rather homogeneous characteristics of the underlying material, the soil of the area consists largely of podzols, interspersed by loamy and marshy soils. These differences in soil type have an effect on the soil moisture and consequently on vegetation. However, it is difficult to trace these singularities due to the unpredictable occurrence of these soil differences and due to their short-range variation. Less extreme

climatic conditions and human interaction engender a greater and more developed content of soil organic material in the lower areas.

The Ötztal is an inner alpine valley with a dry climate characterised by an average annual precipitation of 700 to 800 mm in the valley, concentrated over few days of a year. The small amount of precipitation, especially in winter, is for the greater part caused by its location in a north-south valley. The area has large oscillations in temperature. At the lower boundary of the study area the mean yearly temperature is about 2° C with a minimum of –24.5° C and a maximum of 20° C. Higher areas receive more precipitation and are generally colder, since precipitation increases and temperature decreases with elevation (about 30% and 6° C per 1000 m respectively). The percentage of sunny days (more than 50%) favours tourism both in winter and summer.

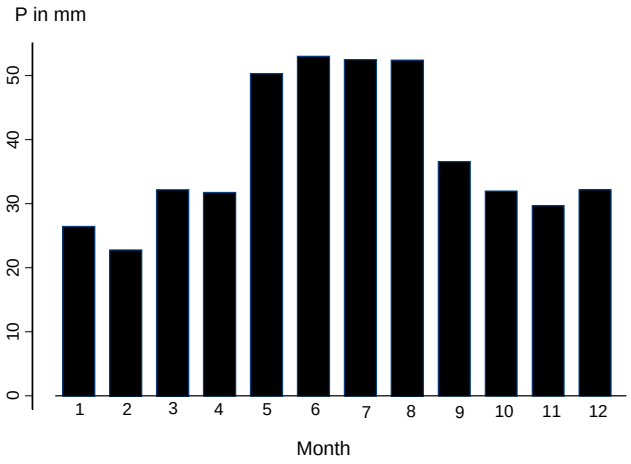

Figure 4.2 Monthly mean precipitation in mm for the period 1978-1997, recorded in the valley of Sölden.

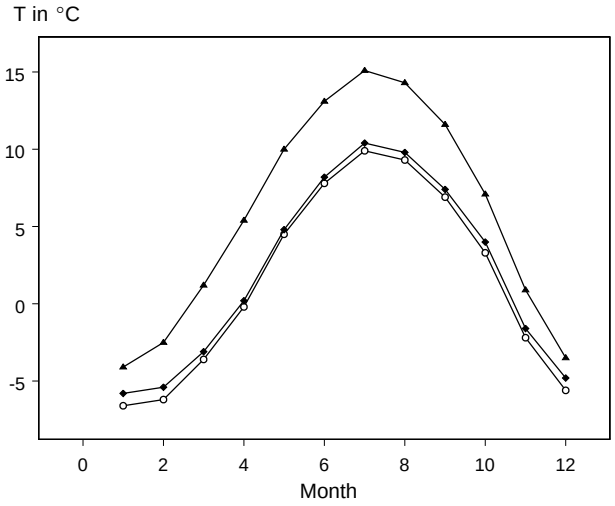

Figure 4.3 Monthly mean temperature in ºC for the period 1961-1990 for three locations in different elevations in the surroundings of Sölden: Längenfeld (1180 m, triangles), Vent (1906 m, diamonds) and Obergurgl (1950 m, open circles). The graphs clearly show the decrease in temperature with increasing elevation.

The vegetation of the area can be roughly divided into vegetation types at the ski piste, dwarf shrub heaths, alpine grassland dominated by sedge and different kind of grass and pioneer vegetation.

Figure 4.4 Vegetation in the upper part of a ski piste, mainly dominated by mosses and *carex curvula*

The wide smooth east-facing slopes above the timberline are intensively used, both for skiing in winter and hiking and grazing in the summer.

Much artificial snow is produced, particularly on the ski pistes below 2300 m (Figure 4.5, darker grey). This increases the capacity of the area for winter tourism, but it also affects natural processes like growth of the vegetation and the snowmelt rate. However, winter and summer tourism are the most important sources of income in that area.

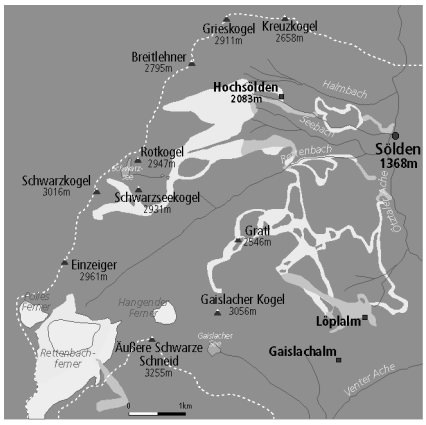

Figure 4.5 The light polygons show the distribution of ski pistes in the ski area of Sölden, including the glacier area; ski pistes, which are also subject to the addition of artificial snow in times of too little snow, are represented by the darker grey.

4.2 Terrain characteristics

Two separate digital elevation models of grid cells of 10 by 10 m and 25 by 25 m were generated from digital isolines in vector format having altitude intervals of 20 m (source: BEV Austria). First the isolines were rasterised to grid cells of 10 m and 25 m. Then linear interpolation was applied to calculate elevation values for the pixels between the isolines on the basis of the elevation values at the isolines (Ilwis, 1998). In order to derive the details from the topographical terrain, the 10 by 10 m digital elevation model was used for mapping vegetation types. However, since such a high-resolution digital elevation model is not appropriate for modelling in space and time because computing-time is related to the number of grid cells and time steps (c.f. Chapter 6), the 25 by 25 m digital elevation model was used for that analysis (c.f. Chapters 6, 7, 8 and 9).

Topographic attributes, in particular altitude, slope, planform curvature, profile curvature, (potential annual) solar radiation, distance to ridges, mean wetness index and mean sediment transport were derived from the digital elevation model (DEM) having a grid cell size of 10 m by 10 m using PCRaster (PCRaster, 1996; Wesseling et al., 1996). Slope was calculated on the basis of the elevation of its nearest neighbours in a 3 x 3 cell window. The third-order finite difference method was used, suggested by Horn (1981) and also used by Skidmore (1989). The curvature transverse to the slope direction and the curvature in the direction of the slope, defined as planform curvature and profile curvature, were determined according to the equations given by Zevenbergen (1987). The mean wetness index and the mean sediment transport were computed using the surface topology of the DEM as determined by the well-known D8 algorithm (Burrough and McDonnell, 1998; Moore et al., 1993). Received solar radiation in MJ/m^2, which is preferred to aspect because it is measured on a circular scale and is an ecologically more useful and interpretable variable (Burrough et al., 2001), was derived from the DEM with a radiation model implemented in PCRaster (Van Dam, 2001). All results were stored in raster maps having a grid cell size of 10 m, required for the mapping of vegetation types in an alpine area (c.f. Chapter 5).

4.3 Vegetation data

4.3.1 Vegetation species

During the summer of 2000 the occurrence of plant species in the study area was recorded at 223 plots, each representing an area of 10 m x 10 m. Plots were selected using a regular sampling scheme with a grid of 100 m x 100 m as a reference. All species growing on the sampling plot were recorded on the basis of a simple ordinal abundance scale ranging from 1 to 3, where 1 indicates just the presence of a plant species at that plot, 2 that a species occurred frequently and 3 that the sampling plot was dominated by a certain plant species. Species data were stored in tabular form. In total 147 species were identified, neglecting detailed specification of some grass species and all fungi and ferns. From the 223 sampling plots 208 sites were used for the analysis. The 15 samples that were rejected had heterogeneous environmental conditions within the grid cell. The

species table was used as the input to the detrended correspondence analysis described in Chapter 5. The results of the correspondence analysis and the correlation between the correspondence axis and the topographic attributes per sampling site, derived from the high resolution DEM, were used to map alpine vegetation types (c.f. Chapter 5).

The vegetation records show that the study area contains many common species, that is to say species that were found at many of the sampling sites. These common species (c.f. Appendix 1, Table A1.1), are known to be typical for alpine grassland and alpine heaths (Reisigl and Keller, 1987). Although each species has its own preferences, some species are rather tolerant. Tolerant species frequently occur on sites where conditions are not typical for them, making it difficult to identify an unambiguous correlation between these species and topographic attributes. On the other hand some species were recorded which were characteristic for sites with specific conditions like a certain elevation range, exposure or moisture content.

4.3.2 Growth measurements

In the summer of 2000, specifically from the beginning of June until the beginning of August, the development of biomass and sedge was measured in the field at seven locations, controlled by the given site conditions of the study area. The locations were selected according to differences in elevation, aspect, land use (i.e. ski run) and manuring. At each measuring location vegetation was totally cut at three sub plots of a size of 0.5 m^2 distributed over the area of the measuring location according to the raster shown in Figure 4.6. From each vegetation sample, a small part was sorted with respect to dead grass and sedge, sound grass and sedge and other biotic material. Both the sorted vegetation sample and the remaining part of the large sample were weighted, dried and weighted again. The results of the sorted sample were used to compute the fraction of dead grass and sedge, sound grass and sedge and remaining biotic material of the total vegetation sample. The extraction of the small sample was done because it was just not feasible to sort the total amount of vegetation that was cut at each sub plot. The amount of roots was also derived from those samples. Data so obtained were used to calibrate the vegetation data predicted by the plant growth model (c.f. Chapter 9).

Furthermore, the maximum height of the vegetation, the density of grass and sedge and the density of the total vegetation cover were estimated in the field and mapped for the total catchment.

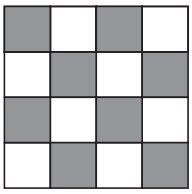

Figure 4.6 Sampling scheme for the acquisition of vegetation data, specifically the amount of the biomass of grass and sedge. Per observation and location three subplots of the large plot of a size of 8 m^2 were selected which were not adjacent but distributed over the area of the large plot to take into account the spatial variability of the plot.

4.4 Snow data

4.4.1 Data collection

In spring 2000 (23 May until 21 June) snow thickness, snow density and snow coverage were measured at 32 locations in the study area. These plots of a size of approximately 10 m by 10 m were selected according to stratified random sampling within a defined area. It was assumed that they were representative for a grid cell of 25 m by 25 m, since this spatial resolution was used for further analysis. The location of the measurement plots was georeferenced with a GPS (Garmin 12) and corrected according to field observations.

Per observation 10 snow samples were taken by means of pF-rings of a known volume (100 cm^3) to determine the average snow water equivalent of the plot, and at the same locations the thickness of the snow was recorded by means of a stick with a metric scale to estimate average snow thickness of the snow patch. The measurements were repeated every 2 to 3 days. Snow coverage per plot was estimated. Additionally, photographs were taken from fixed locations at different dates to get an idea of the change of the total snow cover in time.

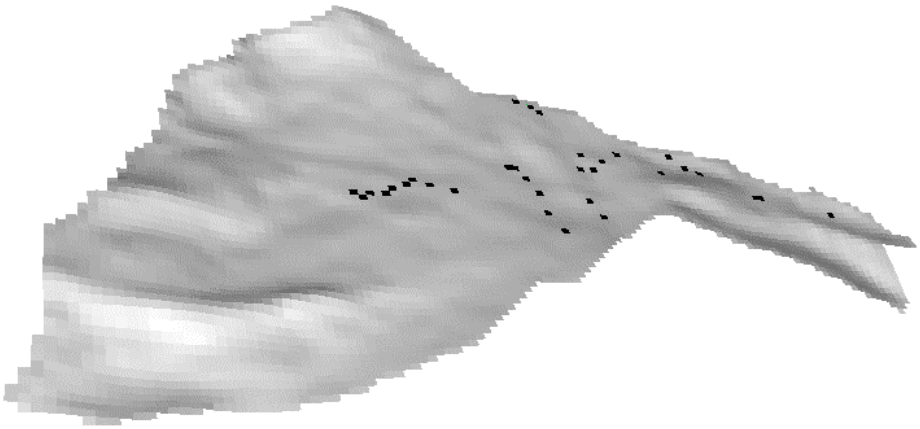

Figure 4.7 Measurement plots for taking snow samples (black dots) distributed over two catchments. Finally, only the big catchment was used for the analysis. Higher elevations were too difficult to access.

4.4.2 Data processing

For each measuring plot of a size of 10 by 10 m, the snow water equivalent (g water/plot) was derived from the measured snow thickness (cm), snow density (g/cm^3) and the fraction of the measuring plot that was covered with snow according to:

$$SWE = H \cdot \delta \cdot A \tag{4.1}$$

with, SWE the snow water equivalent (g water/plot), H the snow thickness (cm), δ the snow density (g/cm^3) and A the fraction of the grid cell that was covered with snow (-).

The observed snow water equivalent (SWE_o) for each observation and each measurement plot was used to calibrate the modelled snow water equivalent at these locations (c.f. Chapter 7, p. 105).

4.5 Hydrological measurements

4.5.1 Precipitation

Precipitation data stem from different sources, 1) data provided by public authorities, in particular the Hydrological Service of Austria, and 2) data measured in the field in the summer of 2000, specifically 24 June to 15 August 2002. Precipitation was also measured in the summer of 1999, but not used for the analysis described in this thesis. The hydrological service records daily precipitation in the valley of Sölden (Sölden-Schmiedhof; 1340m) by means of a non-recording rain gauge. The data are tested with respect to their reliability and published in the annual report of the hydrographical service of Austria, *Hydrographisches Jahrbuch von Österreich*. From the data acquired for every year since 1978, only 1999 and 2000 were considered in the analysis. Figure 4.2 has shown the mean monthly precipitation (mm) for a period of 20 years. The figure clearly shows that most precipitation falls during the summer.

For the measurements carried out in summer 2000, two types of precipitation gauges were used. First, a non-recording gauge consisting of a cylinder and a funnel at the top which was emptied after a rain event to determine cumulative rain fall, and second, an electronic data logger, in particular an Eijkelkamp tipping bucket (Eijkelkamp Agrisearch Equipment), which recorded continuously the increment of rainfall, depending of the size of the bucket. The cumulative rain gauges of different diameters were placed at five locations in the field to analyse the impact of elevation on rainfall and to test the reliability of the continuous rainfall records. So two of these rain gauges where placed at the same site as the tipping bucket, in particular one at 1950 m where also temperature was recorded, and one at 2290m, at the location of the main meteorological station. The difference in the diameter of the cumulative gauges was taken into account by dividing the measured amount of rainfall by the surface of the respective funnel. With the tipping buckets the software written for the electronic data logger did the conversion automatically. One switch of the tipping bucket was stored as 0.2 mm rain.

With respect to the general trend, precipitation increases with elevation (Kuhn and Pellet, 1989). For example Blöschl et al. (1991) defined an increase of 30 % per 1 km in their physically based snowmelt model. However, the general trend does not apply to all situations because it is also controlled by other effects. The presence of the other effects was clearly shown by the cumulative rainfall records, which were collected at different elevations after a rain event. These measurements showed that the relation of rainfall with elevation differs for each rainfall event (Figure 4.8).

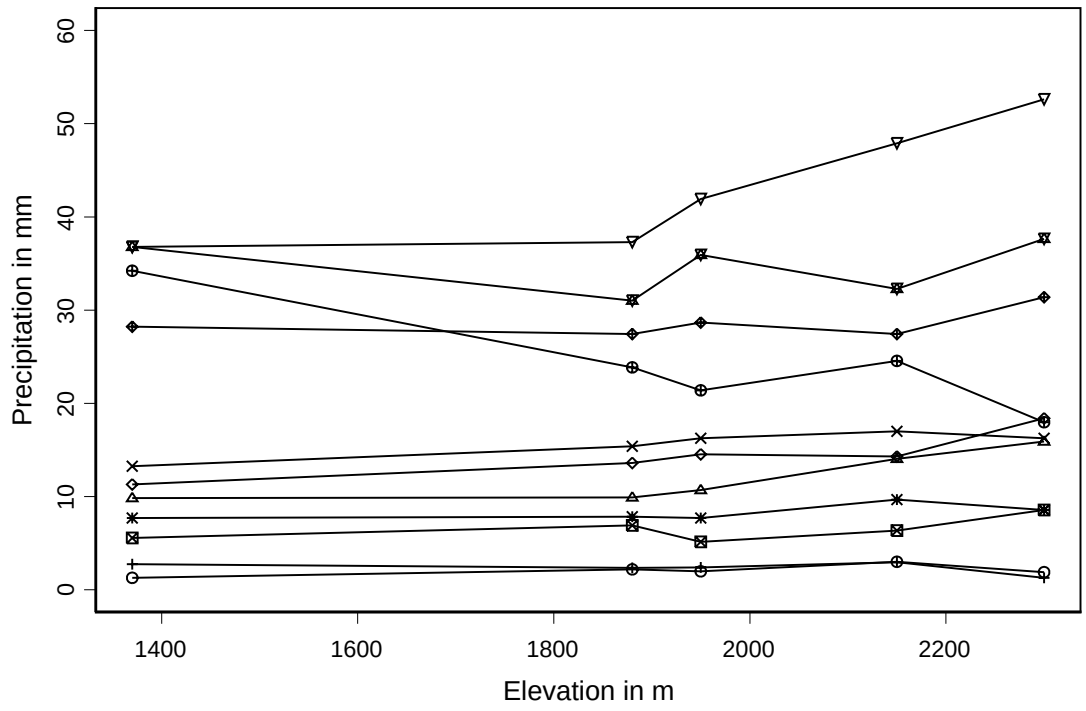

Figure 4.8 Precipitation-elevation relation of cumulative rainfall (mm), measured at different elevations (1370 m, 1880 m, 1950 m, 2150 m and 2300 m) by means of a cumulative rain gauge for different events. The different shape of the symbols represents the individual rain events and the location of a symbol the elevation of the measuring locations at which the cumulative rainfall (mm) was recorded.

4.5.2 Infiltration

The infiltration rate is controlled by the condition of the soil surface and the vegetation, soil properties such as porosity of the soil, hydraulic conductivity and the current soil moisture. For the research described in this thesis emphasis was put on the description of the infiltration in form of the hydraulic conductivity (*K*). The hydraulic conductivity was derived from artificial rainfall experiments using an Eijkelkamp rainfall simulator (Eijkelkamp Agrisearch Equipment). The advantage of this instrument for this research is the easy performance of the measurement and its size and weight because it can be easily transported in mountainous terrain. However, the measurement refers to a very small support since the area covered by the surface of the rainfall simulator is just 650.25 cm^2. To estimate hydraulic conductivity (*K*), the cumulative runoff, which was approved to be nearly constant from the beginning of the experiment, was plotted against the time. Then a linear regression was fit to the data, where the slope, divided by the surface of the plot, returned the *K* of the soil.

Rainfall experiments were carried out both in natural areas mainly covered with alpine heaths and on ski runs with different degree of disturbance. During the experiments runoff was observed to occur earlier on existing ski pistes than on the soil in natural areas.

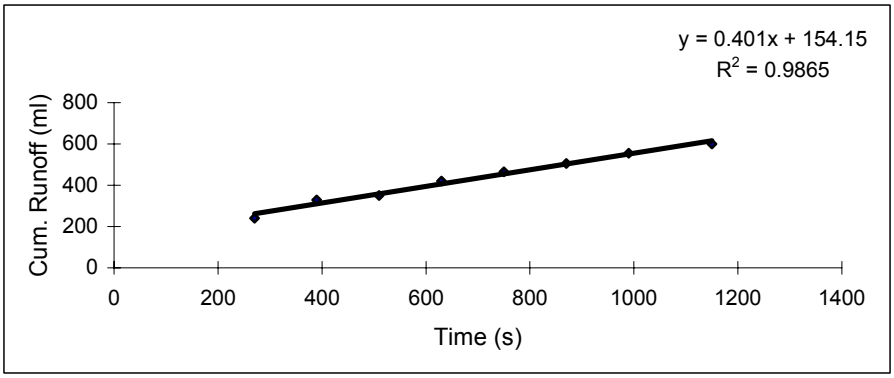

Figure 4.9 Derivation of the hydraulic conductivity from one rainfall experiment.

4.5.3 Discharge

Even though continuous discharge of the small mountain streams was one of the most important parameters in the hydrological analysis, it was not directly recorded. Instead continuous water level heights were recorded at a fixed location, and consequently continuous discharge data were derived by means of the rating curve, also called stage-discharge relationship (Shaw, 1994). The determination of continuous discharge consisted of three parts, 1) recording continuous water level, 2) measuring both the discharge and the corresponding water height for different situations, and 3) constructing the rating curve according to the results obtained in step 2.

Measuring continuous water level. Continuous water level was recorded in three catchments of the study area by means of water level sensors, specifically absolute pressure level sensor (KELLER transmitters 3.1). These sensors measured the hydrostatic pressure consisting of the pressure of the water column and the air pressure supplied to the water surface. In order to deduce the height of the water level from these measurements, air pressure needs to be subtracted from the hydrostatic pressure recorded by the sensor and converted to a metric dimension according to:

$$h_w = (p_w - p_a) \cdot c \qquad (4.2)$$

with, h_w the height of the water level (cm), p_w the hydrostatic pressure of the water column (mbar), p_a the force of the air pressure applied to the water surface (mbar), and c a constant to convert mbar to a metric dimension (1mbar ≈ 1cm). The water level was also measured manually to check the data recorded by the pressure device.

Sudden input method. The discharge of the mountain streams for different situations was measured by dilution gauging, in particular by the sudden input method. The principle of this method is, that a chemical solution of known concentration is added to the stream flow, while measuring the dilution of the concentration a certain distance further downstream by means of an EGV-meter. The discharge (l/s) of the individual mountain streams was derived from the measured concentrations.

Rating curve. The rating curve was constructed by plotting discrete discharge measurements of different situations, derived by the sudden input method, against the corresponding stage of the mountain stream (Figure 4.10). It is generally represented by (Shaw, 1994):

$$Q = a \cdot H^b \tag{4.3}$$

with, Q the discharge (l/s) measured by dilution gauging, H the corresponding relative water height (cm), and a and b are constants that had to be fit by the measured data. The rating curve was used to estimate the continuous discharge (l/s) with respect to the continuous water level recorded by the Keller transmitters. However, the rating curve was only valid for the data range that was covered by the sudden input method. The discharge time series so obtained was eventually used to calibrate the hydrological model (HE-model) for the first catchment, described in Chapter 7.

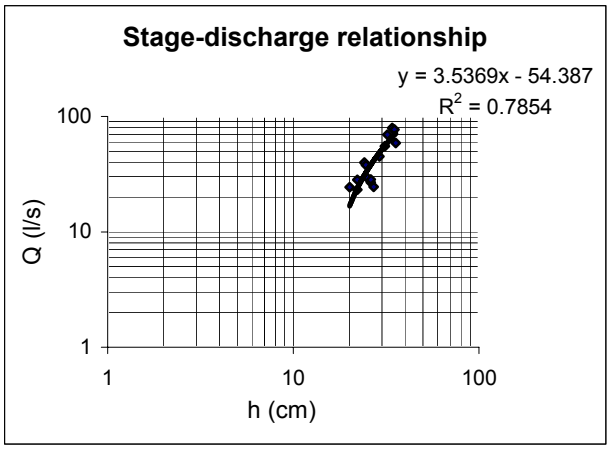

Figure 4.10 Rating curve to compute continuous discharge derived from dilution gauging. Dots along the fitted line represent the measurements (Source: Groenendijk and Koerts, 2001).

4.5.4 Saturated hydraulic conductivity

The saturated hydraulic conductivity is an important parameter for the determination of the groundwater height of an area, which is required for the estimation of the safety factor. To measure saturated hydraulic conductivity (K_s) in the field the inversed auger hole method was used (Kessler and Oosterbaan, 1974). This method consists of boring a hole to a given depth, filling it with water and measuring the rate of fall of the water level (Kessler and Oosterbaan, 1974). Applying the set of mathematical operations suggested by Kessler and Oosterbaan to the measured values, a K_s value could be computed for each measuring location (c.f. Cremer, 2001). For the hydrological model and the stability model a constant K_s was specified, however, based on the measured K_s values.

4.6 Soil measurements

4.6.1 Soil water content

In order to establish a soil water balance for the plant growth model, information about the soil water content was needed. Therefore soil samples were taken at several locations in the study area by means of pF rings, approximately 8 cm below the soil surface. To take into account the standard error, two samples, and not just one, were taken at those locations at which above ground biomass production was measured (Section 4.3.2). Furthermore, to incorporate the spatial variability, additional samples were collected at transects of 50 to 100 m. To derive the volumetric soil water content, the samples were first weighted, then dried under a considerable low temperature because of the high content of organic material, and eventually weighted once more. The difference between the weight of the wet sample and the dry sample supported the determination of the volumetric soil water content. This procedure was repeated for each moment, for which growth measurements took place. Besides, the average rooting depth was estimated at each measuring location.

4.6.2 Nutrient content

Another important input parameter to the plant growth model was the nutrient content. An estimate for the availability of nutrients was on the one hand derived from the knowledge whether an area was manured in the observed year. This knowledge was obtained both by visual interpretation of 120 locations in the area of consideration and by interviewing local people. On the other, soil samples were taken at the seven measurement location (4.3.2) and analysed with respect to the concentration of nitrate and ammonium by means of the autoanalyser (Whitehead, 1995).

4.6.3 Soil water retention curve

In order to establish the soil water balance of the plant growth model (Chapter 9), the soil water retention curve was required. Therefore soil samples were taken at 8 cm depth at the seven measurement locations, and for each sample the soil water content for different suctions, in particular for a suction of 0 cm, 100 cm and 16000 cm, was determined by means of the standard methods (Kutilek and Nielsen, 1994). These measurements supported the determination of percolation, transpiration and the restricted assimilation of carbohydrates.

4.6.4 Geotechnical measurements

Other important parameters for the determination of the safety factor are the cohesion of the soil (C, kN/m^2) and its angle of internal friction (φ, degrees). Therefore undisturbed

soil samples had to be collected in the field, and consequently analysed in the laboratory by means of the direct shear test (Cernica, 1995; Cremer, 2001; Strik, 2001). Carrying out this test for each sample, the shear stress τ (kN/m^2) and the shear strength σ (kN/m^2) could be determined for each sample. The angle of internal friction φ (degrees) and the soil cohesion c (kN/m^2) were obtained by plotting the shear stress of each sample against the shear strength and fitting a linear function through all the measurements. The slope of the function represented the angle of internal friction and the intercept denoted the cohesion (c.f. Cremer, 2001; Strik, 2001). To derive input parameters for the stability model (Chapter 8) the mean cohesion and the mean angle of internal friction were computed from the values of all samples.

5 MAPPING VEGETATION TYPES IN AN ALPINE AREA USING VEGETATION OBSERVATIONS AND DERIVATIVES OF A DIGITAL ELEVATION MODEL

Karin Pfeffer, Edzer J.Pebesma and Peter A. Burrough

Submitted to Landscape Ecology

5.1 Introduction

The establishment of socio-economic infrastructures such as ski runs in alpine areas may have considerable impact on the natural vegetation cover, going as far as the total removal of the natural vegetation. This should be avoided because the presence of vegetation protects the slope and reduces the risks of erosion and landslides. If the establishment of new infrastructure aims to use vegetation cover to minimise the environmental impact and the risk of natural hazards, then it is useful to know species associations and species preferences, to avoid the disturbance of ecologically valuable sites and to identify locations that can be easily revegetated (c.f. Chapter 3). Furthermore vegetation is crucial for many environmental processes such as hydrological processes, and therefore an important input to the environmental models used in this thesis. However, spatial information on site conditions is commonly lacking in mountain areas (Hörsch et al., 2002), and in most cases to satisfy planning criteria the mapping of vegetation has to be carried out from scratch.

For many years vegetation has been mapped by using information from the external aspects of the landscape, such as changes in elevation or rock type, and by manually drawing boundaries between dissimilar units. Initially, this procedure was carried out merely in the field. With the establishment and progress of aerial photography and satellite remote sensing, boundaries could be drawn by visual interpretation of images and updated by field visits. However, identifying vegetation associations and locating their boundaries according to visual changes in the landscape is rather subjective. Studies in related field disciplines have shown that even when using the same images, different scientists are likely to produce different thematic maps of the same study area (Bie and Beckett, 1973; Janssen and Middelkoop, 1991). Moreover, conventional mapping neglects short-range variation. Satellite images are a possible alternative for the direct retrieval of certain spatially distributed vegetation characteristics, but with current technology a clear identification of individual plant species other than trees is hardly possible (Franklin, 1995; Nagendra, 2001).

Conventional mapping of vegetation in the field, from aerial photographs or satellite images might be sufficient for projects at a regional scale. However, when considering projects at a local scale, for instance the design of an environmentally sound ski run, the spatial resolution of data obtained by aerial photo interpretation, generalised field mapping or data retrieved from satellite images is insufficient, especially for critical areas such as gullies and steep slopes. But high resolution vegetation data are expensive

and difficult to collect so other methods are needed that support the quick and inexpensive acquisition of a vegetation map with the right balance between data accuracy and costs.

It is well known that both plant growth and species composition of vegetation depend to a certain extent on ecological site factors such as elevation, slope, aspect of the slope (a surrogate for the amount of direct received solar radiation), slope curvature, soil moisture, or a meaningful combination of several of these. Today, these factors can be easily derived from a gridded digital elevation model (DEM), which may have any spatial resolution we need (Burrough et al., 2001). This enables the use of the derivatives of the digital elevation model to support the mapping of high resolution vegetation data, as shown by Gottfried et al. (1998), Tappeiner et al. (1998), Burrough et al. (2001), and Hörsch et al. (2002). These studies, however, merely examined the deterministic relations between vegetation data (species and types) and the derived topographic attributes, but the interactions between the spatially correlated structures of the vegetation and geographical distribution of the ecological factors were hardly addressed. As Bio (2000) has shown for individual species, however, the spatial correlation structures of plant species response should be an integral part of exploratory data analysis and mapping. The inclusion of species-site factor relations and spatial interactions in a mapping campaign may provide useful extra information at a high spatial resolution, compared to the conventional techniques already mentioned.

Accordingly, the aim of this study is to develop and test a quick and reliable procedure for moderate to high resolution vegetation mapping in Alpine areas where access is difficult and field data collection is expensive. Our source data are ecological site attributes computed from a high resolution, continuous, gridded digital elevation model (DEM) derived from large scale maps, and vegetation species abundance collected in the field. Since the actual vegetation patterns are not only determined by topography, but from a complex interaction between historical and recent environmental, human and disturbance factors (Hörsch et al., 2002) and interactions among species such as competition, we also incorporate the spatial autocorrelation structures of field observations of the vegetation data to improve the information content.

Figure 5.1 gives a flowchart of the procedures used. In stage 1, ecologically important derivatives are computed for each grid cell of the DEM (Chapter 4, Section 4.2). Because of time constraints, species abundance data cannot be collected for each individual cell on the DEM, but must be collected from a much smaller sample of quadrats of equal shape and size (Chapter 4, Section 4.3.1). These quadrats are located in the terrain with reference to a lower resolution grid. Detrended correspondence analysis (DCA) is used to reduce these vegetation scores to a limited number of major axes (Jongman et al., 1995).

In stage 2 we use multiple linear regression to relate the DCA axes scores to the primary and secondary topographical attributes that were computed for the sampled quadrats. The spatial correlation structures of the regression residuals at the sampled quadrats are then examined using semivariograms (Burrough and McDonnell, 1998; Pebesma and Wesseling, 1998).

In stage 3, we combine the regression models and semivariograms to carry out a universal kriging interpolation of the DCA scores from the sampled quadrats to the whole area covered by the DEM. The DCA vegetation scores are classified into vegetation

classes using *k*-means clustering (MacQueen, 1967): these classes are used to allocate all grid cells to classes in a map of vegetation that covers the whole area.

In this chapter we describe the mapping procedure in detail and demonstrate its application to the study area. The end result of the work is a detailed vegetation map that can be used for multicriteria decision making that should lead to improvements in the planning of new ski runs (Pfeffer et al., 2002).

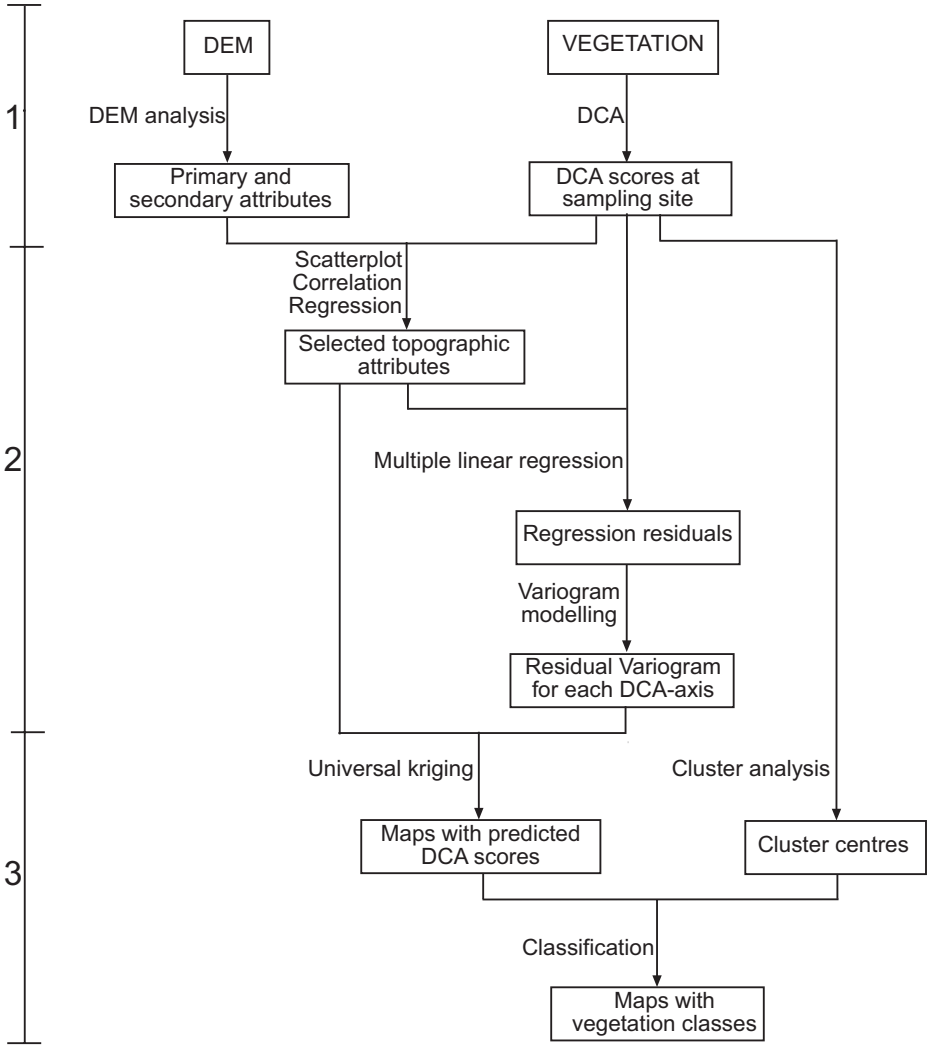

Figure 5.1 Flowchart of mapping procedure; the numbers 1, 2 and 3 indicate the different stages of the mapping procedure.

5.2 Vegetation Data reduction

Detrended correspondence analysis (DCA) (Jongman et al., 1995) was used to reduce the 147 recorded species (Chapter 4) to four independent ordination axes. This ordination technique constructs a theoretical variable that best explains the species data by

maximising the dispersion of species scores, and DCA also corrects for the arch effect by detrending (Jongman et al., 1995). The ordination identified those sites with similar plants and those species that tend to occur together.

We used the computer program Canoco 4.02 (Ter Braak and Smilauer, 1998) to carry out DCA. Table 5.1 illustrates the importance of each ordination axis with respect to the original vegetation pattern as indicated by the eigenvalue. The four extracted axes explain only one fifth of the total variation of the species data, so a large part of the variation in the occurrence pattern of plant species is unexplained. The eigenvalues show, however, that the explained variability in the vegetation data is for the greater part expressed by the first two dimensions; these do not give a clear separation of the species along one single axis, however, for which the eigenvalue should be above 0.5 (Jongman et al., 1995). The small amount of explained variation is partly caused by the use of abundance data whose frequency was measured on a simple abundance scale instead of actual count data. Also, the species data are generally rather noisy (Ter Braak, 1998) due to complex interactions between numerous influence factors (Hörsch et al., 2002). In addition the tolerance of plants to their typical growing conditions and the occurrence of many common species might have disturbed a clear response to the theoretical variable constructed by DCA.

Table 5.1 Summary table of DCA applied to vegetation data.

	DCA1	DCA2	DCA3	DCA4	Dispersion of all EV*
Eigenvalue (EV)	0.432	0.195	0.119	0.098	4.186
Cumulative percent of dispersion	10.32	14.98	17.82	18.05	
Range of DCA scores	[-1.9; 2.9]	[-2.4; 4.8]	[-3.0; 6.0]	[-5.1; 5.2]	

*: Dispersion of all eigenvalues (EV) represents the total variance in the species data

The range of the DCA scores along the first ordination axis is rather small compared to the ranges along subsequent ordination axes; it does not have outlying values as found in subsequent axes. It seems that the first ordination axis reflects the major pattern of common species, while subsequent axes account for rare species, because sites with extreme scores in the subsequent axes contain rare species.

5.3 Mapping of vegetation classes

5.3.1 Outline

To map vegetation classes we need to combine topographic information with vegetation data. As already explained in the introduction, the starting points are topographic attributes derived from the DEM (Chapter 4) and reduced vegetation data in the form of DCA scores (Figure 5.1). The mapping approach covers two main stages, regression and residuals analysis (stage 2 in Figure 5.1), and derivation of vegetation classes from both DCA scores and topographic attributes (stage 3 in Figure 5.1). First, the correlation between vegetation scores and topographic attributes is identified and the spatial

dependence of the scores is modelled. Second, DCA scores are estimated for unsampled locations from the DCA scores at observed locations, using the topographic attributes specified in the first part and the spatial dependence of the observation points (universal kriging). Then *k*-means cluster analysis is applied to the DCA scores at the observed locations, resulting in cluster centres that were used to convert the predicted DCA maps to vegetation classes that characterise specific species associations.

5.3.2 Regression analysis and selection of variables

Different techniques were used to identify those topographic variables that have an impact on the extracted vegetation axes in a spatial context. First a visual interpretation of the species-topography relation was performed on the basis of scatter plots of topographic attributes against extracted vegetation axes and bivariate correlations. Figure 5.2 shows the scatter plot of elevation against the scores of DCA 1. Several non-linear transformations of the topographic attributes were explored in a vain attempt to enhance the linearity of their relationship to the DCA scores. Table 5.2 shows that height, slope, solar radiation, profile curvature of the slope, mean wetness index and mean sediment transport play the main role in explaining the variation in the DCA scores.

Table 5.2 Pearson correlations of DCA axes with single topographic attributes.

	Axis 1	Axis 2	Axis 3	Axis 4
Elevation (m)	0.762	-0.089	-0.155	0.125
Slope (degrees)	-0.580	-0.217	-0.123	-0.083
Planform curvature ($m^{-1} \cdot 100$)	0.048	0.127	-0.063	-0.114
Profile curvature ($m^{-1} \cdot 100$)	0.073	-0.061	0.027	0.149
Solar radation (MJ/m^2)	-0.259	-0.143	-0.523	-0.056
Ridge proximity (ln (m))	0.130	0.043	-0.058	0.039
Mean wetness index (ln_e)	0.267	0.252	-0.042	-0.002

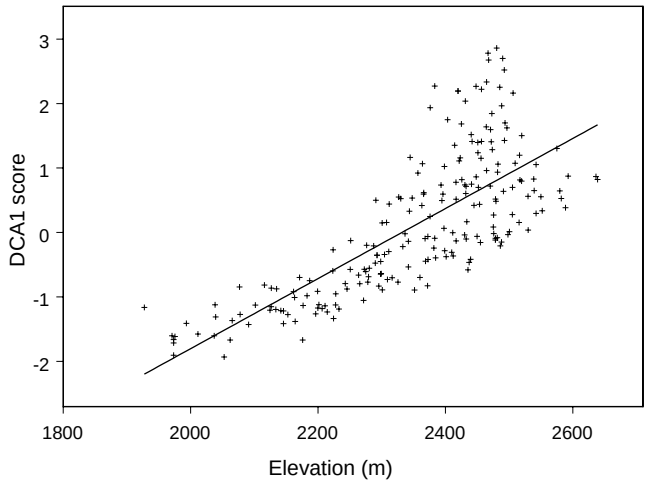

Figure 5.2 Scatter plot of elevation against scores of DCA 1 (for further scatter plots see Appendix 2).

Since mean wetness index and mean sediment transport were highly correlated, the sensitivity of the species-environment relation to the exclusion of either of them was tested. The exclusion of one of those attributes hardly changed the species-environment relation. Assuming that mean wetness index has a higher impact on the occurrence of vegetation species than mean sediment transport, sediment transport was excluded from the further analysis.

To select a relevant subset of the topographic variables for linear regression, for each DCA axis a stepwise variable selection was carried out using the statistical software package SPSS 10.0. Table 5.3 shows the topographic attributes that were selected for each axis. For example elevation, slope and solar radiation are relevant variables in explaining the variation in the first DCA axis.

Table 5.3 Selected topographic attributes to explain the variance in each vegetation axis.

Dependent variable	Independent variables	Multiple R^2
DCA1	DEM, Slope, Solar radiation	0.7466
DCA2	Mean wetness index, DEM, Slope	0.1095
DCA3	Solar radiation	0.2733
DCA4	Profile curvature	0.0221

5.3.3 Residual analysis

Linear regression between the vegetation axes and the selected topographic attributes resulted in regression residuals for each vegetation axis. We used variogram analysis (Burrough and McDonnell, 1998; Pebesma and Wesseling, 1998) to analyse the spatial structure in these regression residuals. To model spatial correlation, we fitted the spherical model,

$$\gamma(\mathbf{h}) = \begin{cases} c_0 + c_1\left(\dfrac{3\mathbf{h}}{2a} - \dfrac{1}{2}\left(\dfrac{\mathbf{h}}{a}\right)^3\right) & \text{for } 0 < \mathbf{h} < a \\ c_0 + c_1 & \text{for } \mathbf{h} \geq a \\ \gamma(0) = 0 & \text{for } \mathbf{h} = 0 \end{cases} \qquad (5.1)$$

where γ(h) is the semivariance, a is the range of the variogram defining the spatial scale of variation, $\mathbf{h}$ the lag, and c_0 the nugget variance which represents the spatially uncorrelated part of the variance without spatial component, and with c_1 the maximum value of the semivariance.

Table 5.4 displays the parameters for the fitted variogram models. Figure 5.3 shows the residual variograms for each vegetation axis, computed with the computer program Gstat, which supports geostatistical modelling, prediction and simulation (Pebesma and Wesseling, 1998).

Table 5.4 Variogram parameters for each DCA axis. Variogram models for DCA 1, 3 and 4 are effectively linear.

	c_0	c_1	a
DCA 1	0.11	1.33	10823
DCA 2	0.42	0.80	612
DCA 3	0.48	3.49	12779
DCA 4	0.58	1.23	2522

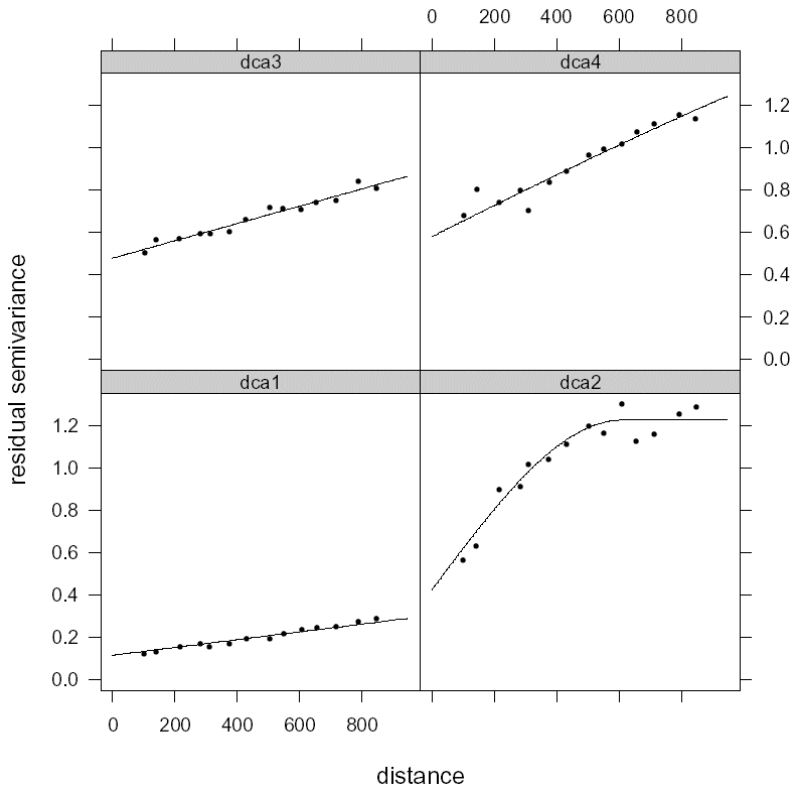

Figure 5.3 Fitted variogram for each extracted ordination axis DCA 1, DCA 2, DCA 3 and DCA 4.

5.3.4 The spatial prediction of vegetation scores

The prediction of vegetation scores at unobserved locations was based on the DCA scores at the observed locations and the results of the regression and residual analysis. To predict DCA scores at unobserved locations we used universal kriging because this addresses both spatial dependence of the observations and their linear relation to topographic attributes. Universal kriging models the DCA scores at all locations $Z(x)$ as the sum of an unknown intercept β_0, a non-stationary trend and an intrinsically stationary error $\varepsilon(x)$ (Cressie, 1993), where the trend is modelled as a linear function of known base functions $f_j(x)$ and unknown constants β_j:

$$Z(x) = \beta_0 + \sum_{j=1}^{p} f_j(x)\beta_j + \varepsilon(x) \qquad (5.2)$$

The topographic attributes that were identified in stepwise linear regression (Table 5.3) were used as base functions. The spatial dependence in the error term $\varepsilon(x)$ was modelled by the variogram of the residuals for each vegetation axis. It is assumed that the weighted least square residual variograms, shown in Figure 5.3, can be used for universal kriging of the DCA scores. As an example, the model for the first vegetation axis is:

$$Z(x) = \beta_0 + D_{elev}(x)\beta_{elev} + D_{slope}(x)\beta_{slope} + D_{rad}(x)\beta_{rad} + \varepsilon(x) \qquad (5.3)$$

where D_{elev}(x) and D_{slope}(x) and D_{rad}(x) are the selected base functions, expressing that elevation, slope and solar radiation are significantly correlated with the first vegetation axis. β_0 is an unknown intercept, and β_{elev}, β_{slope} and β_{rad} are unknown constants.

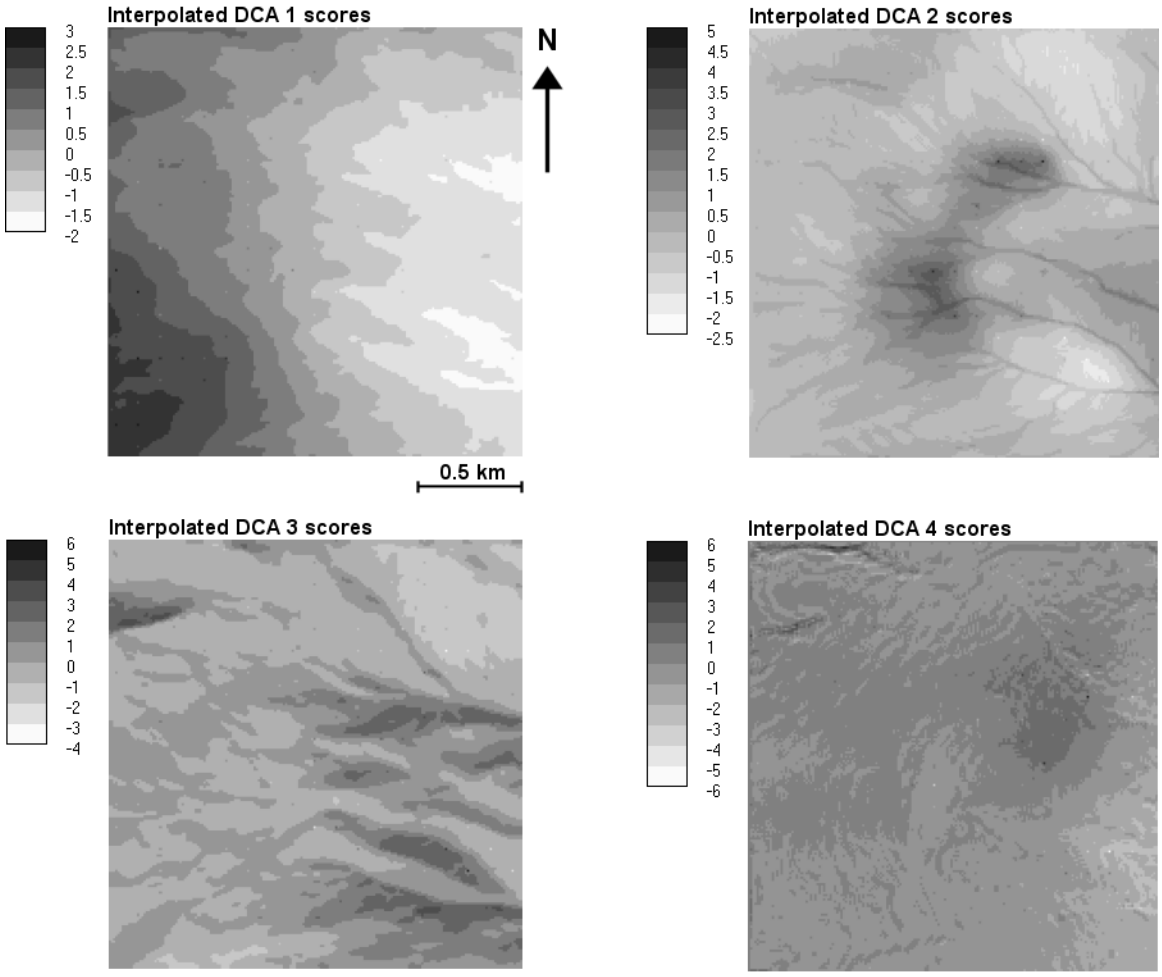

Figure 5.4 Maps with predicted DCA scores obtained with universal kriging.

Universal kriging of the four vegetation axes on the basis of DCA scores, selected topographic attributes and the fitted residual variograms in Figure 5.3 was done with Gstat (Pebesma and Wesseling, 1998).

The four maps of resulting predicted DCA scores are shown in Figure 5.4. They clearly reflect the trend of the base functions specified for each ordination axis.

5.3.5 Cluster analysis and classification of predicted DCA scores

Cluster analysis was applied to standardised and weighted DCA scores at the sampled locations. The scores were standardised to zero mean and variances equal to their corresponding eigenvalue to include that each vegetation axis explains a certain amount of variation.

Cluster analysis requires the specification of the number of vegetation clusters, which in this case was chosen such that it matched the impression obtained in the field and general knowledge about growing preferences of alpine vegetation. The clustering was repeated for several numbers of classes to explore the correspondence of computed vegetation clusters with the impression obtained in the field. Eventually we concluded that in this case seven classes suffice to reflect vegetation variability due to variation in elevation, slope, aspect, average wetness, land use and the location of the timber line.

k-means clustering (MacQueen, 1967) was used to create a legend for a vegetation map with the seven classes. This classification technique was chosen because it is possible to compute class centres and dispersion from the data. It can also allocate individual observations to the classes once they have been defined. The vegetation clusters of the observation locations are shown on the left hand of Figure 5.5.

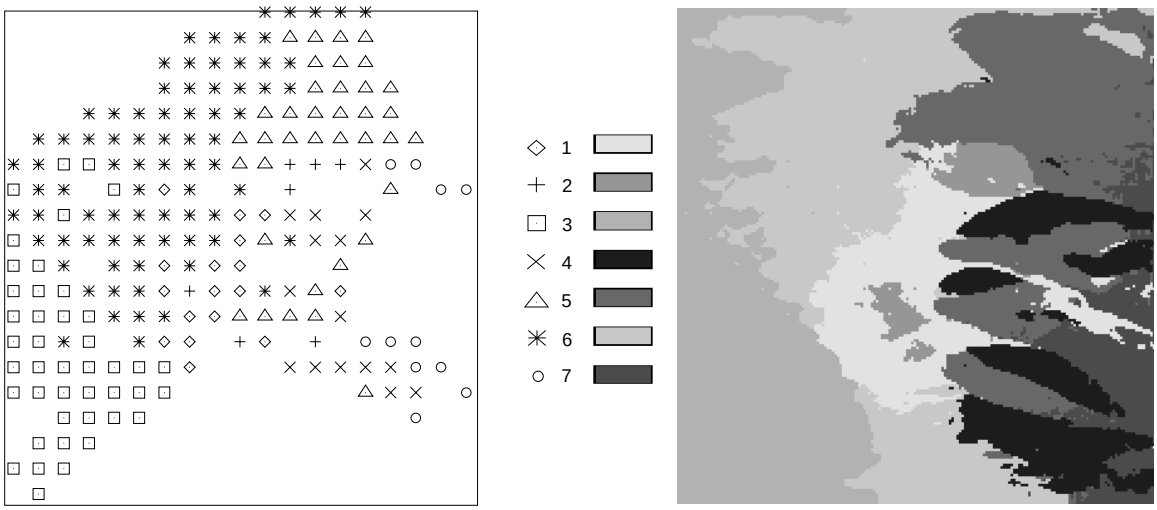

Figure 5.5 Clusters assigned to observations (left) and classification of the predicted DCA scores (right).

These cluster centroids were used to classify the transformed and weighted predicted (kriged) DCA scores to one of the seven vegetation classes, where the scores of the prediction maps were standardised and weighted in the same way as the DCA scores at the sampling sites. The vegetation class map so obtained is shown on the right hand of Figure 5.5. Cluster analysis and the classification of the predicted DCA scores (Figure 5.4) to a vegetation class were done with SPSS 10.0.

5.4 Interpretation of vegetation classes

Each vegetation class was defined by sampling sites having a similar species composition and topographic attributes that were identified to have an impact on the observed species. To analyse the ecological representation of each computed vegetation class, the class membership of the sampling sites was linked to the original table of field data with species records per sampling site. This allowed the identification of common and typical species for each vegetation class, listed in Table A1.2 and Table A1.3 (c.f. Appendix 1).

It seems that vegetation classes 1 and 2 were mainly determined by the presence of species that have not been observed at other locations, for the greater part reflected by extreme values along the second DCA axis, and rather homogeneous site conditions at the sampling site and its neighbouring area. Frequently observed species of class 1 are common for revegetated ski runs and alpine meadows. Locally observed species in this class are species which are usually found in moist areas. The occurrence of these species such as *Trifolium badium* can be explained by the presence of small water outlets due to the presence of impermeable soil layers (loamy spots), which are source areas for the mountain rivers. These sites have a high mean wetness index, and are also areas where snowmelt water creates marshy soils in the snowmelt period. Class 2 represents species which are characteristic for alpine grassland in the Central Alps. Additionally, it contains species introduced by the use of this area for farming, for example *Geranium pratense* or *Chrysanthemum leucanthemum*, but also species with a rather low frequency at other sites. The higher east-facing slopes at the south-western part of the study area, mainly assigned to skiing, were occupied by class 3. Due to the extreme growing conditions, caused by the elevation and the impact of skiing, the species diversity is rather low. It is covered by moss species such as *Polytrichium* and *Pohlia nutans*, grass and lichen species, interspersed with some flowers such as *Primula glutinosa* and *Sibbaldia procumbens*. Class 4, which for the greater part covers north-facing slopes until an elevation of 2250 m, was created by the significant correlation of the first and third vegetation axis with solar radiation and the specific species pattern of sites at north-facing slopes below 2250 m, in particular species of alpine heaths dominated by Rhododendron. South-facing slopes, ranging from 2000 until 2500 m were assigned to class 5. The creation of that class is mainly determined by the similar species composition of the observed locations and the topographic uniformity of that area with respect to aspect and slope. It is dominated by alpine species that are characteristic for these slopes above 2000 m, with a gradual change from alpine heaths dominated by *Erica* to *Nardetum* and *Curvuletum*, interspersed with *Juniper*, *Campanula barbarta*, *Lotus cornulates* and *Antennaria dioeca* in the lower elevation ranges of that class. Class 6 mainly occupies

east-facing slopes and south-facing slopes above 2350 m. These gentle slopes with little planform and profile curvature cover a large part of the natural area, but they are also a part of the ski runs, and they contain walking paths. The observed species composition of class 6, consisting of *Nardus stricta, Carex, Polytrichium, Cladonia rangifera, Centraria islandica* and other lichens, interspersed with some common flowers such as *Homogynae alpina, Trifolium alpinum, Leucanthemopsis alpina* and *Geum repens*, is characteristic for the site conditions of that alpine area together with the human interference including grazing. The occurrence of tree species in the lower area of the study area, related to elevation, determined the configuration of class 7. This class also indicates the location of the timberline.

5.5 Consistency of vegetation classes

When reducing multiple vegetation species to vegetation axes, the observation at each observed location is represented by a set of scores, which is used to measure similarity to other observation locations. Thus the DCA scores and maps derived from the DCA scores depend on the whole set of observations included in the analysis. To analyse the sensitivity of the mapping procedure to sampling variability, the whole procedure for mapping vegetation types was repeated five times, each time for a different subset containing 80 percent of the whole data set. The configuration of the subsets is based on a random division of all observed locations into a five groups, where each group contained 20 percent of the full data set. For each subset one group was excluded. From Figure 5.6 one can see how different the map attained for each of the subsets (Figure 5.6b-5.6f) is from the reference map (Figure 5.5, repeated in 5.6a). The subset maps show that predicted DCA scores cluster largely according to a common spatial pattern. However, the clusters differ in size, shape and spatial pattern. A cluster that is dominant in the original map may disappear, if it is part of a very small cluster containing few data points with an excentric species composition. Table 5.5 shows that in every submap 50 to 65 percent of all grid cells correspond to the reference map of vegetation classes of Figure 5.5.

Table 5.5 Success rate of classification.

Classified sub maps	Success rate in %
Sub map1	61.5
Sub map2	49.8
Sub map3	53.4
Sub map4	53.3
Sub map5	62.9

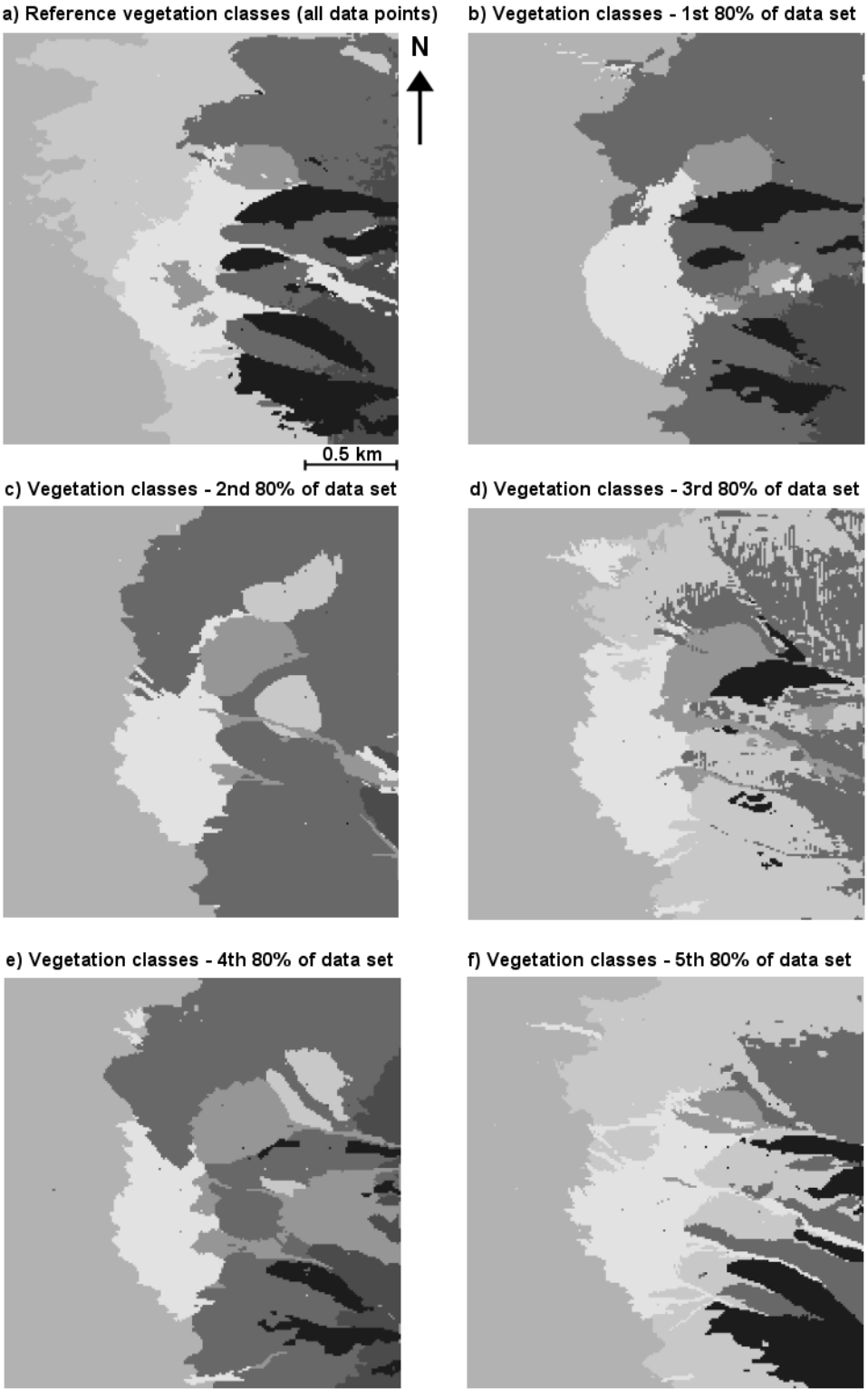

Figure 5.6 Consistency of vegetation classes: Vegetation classes using the full data set and vegetation classes using subsets containing 80% of the full data set. Grey scales were assigned such that maximal visual correspondence to the reference map was obtained.

5.6 Discussion

Vegetation is the result of a complex interaction of historic and recent natural processes and human interaction, and it is impossible to completely explain the response of the vegetation to a limited set of attributes. Additionally, some species are quite tolerant with respect to varying conditions, thus there will never be a perfect species-environment correlation. However, the analysis of the correlation between vegetation and topographic attributes showed that about one third of the vegetation pattern that was encompassed by the extracted vegetation axes could be explained by a set of the selected topographic attributes. Thus the overall influence of topography on the spatial pattern of alpine vegetation types was evident, despite the impact of natural and artificial disturbance factors. The expected correlation of alpine vegetation especially with elevation and solar radiation was explicitly reflected by the first and third vegetation axes (c.f. Table 5.2; Appendix 2). The integration of additional environmental attributes, for instance soil variables, may increase the species-environment correlation. In our case this information was not available.

The identified correlation of vegetation and topographic attributes made it possible to map vegetation at unobserved locations using the established relation between vegetation and topography as also reported in other studies (Gottfried et al., 1998; Burrough et al., 2001; Hörsch et al., 2002; Meentemeyer and Moodry, 2000), but with the differences, that we addressed spatial correlation among sampling sites, thus optimising spatial predictions. Spatial correlation of the observations adds useful information especially in areas with spatially variable species composition, but homogeneous site conditions. The sample variograms of the DCA score regression residuals showed that there are other spatial structures in the vegetation data in addition to a pattern explained by topography with a dominant long-range correlation.

Choosing a finer resolution of the sampling scheme might result in a more accurate description of the vegetation pattern, but it is also more costly. A very fine resolution mapping such as used in the vegetation study by Gottfried et al. (1998) requires a very detailed digital elevation model and a sophisticated global positioning system to georeference the precise location of the sampling plots in the field. These conditions are not appropriate for socio-economic planning, where a suitable balance must be found between the cost of data collection and data accuracy (Meentemeyer and Moodry, 2000). However, our procedure could be improved by including intermediate samples in areas where topography varies quickly over short distances, or by stratified sampling, where sampling density increases with vegetation variability in attempt to find the right balance between data accuracy and costs.

The DCA scores, and therefore the generation of vegetation classes, are determined by the samples included in the analysis. The incidence of a few samples having an excentric species composition, possibly caused by local differences of sites conditions, will cause extreme DCA scores along one of the vegetation axes. When classifying the DCA scores, samples with excentric scores will be assigned to single classes. Therefore fewer classes remain for the bulk of observations. This happened in the classification of the second subset of the DCA scores (Figure 5.6c), where one sample had very exceptional DCA scores because of the occurrence of species that were not found at another location. This sample occupied one class and therefore only six classes

were left to classify the other sites of the study area. The comparison of the computed vegetation classes using the whole data set with the classes derived from a random subset showed that the classification procedure is quite sensitive to which samples are included and it is wise to have an equal distribution of samples over units with dissimilar topographic conditions.

5.7 Conclusion

This chapter shows that the procedure proposed is a useful approach for the rapid mapping of vegetation under the given circumstances. It integrates the established relation between spatial information on site conditions and abundance of plant species, measured on a simplified abundance scale, with the spatial structure in the vegetation data. It was confirmed that topographic variables have an overall influence on the spatial pattern of alpine vegetation, and that this information can be used to map vegetation. DCA supported the illustration of the variability of the species composition at observed locations. The comparison of the vegetation classes so obtained with the original data set showed that the general structure of the vegetation pattern was encompassed by the derived classes. The consistency of the mapping procedure was shown by repeating the procedure for different subsets of the vegetation data. A strong persistence of the large-scale features indicates the necessity for further research with respect to short-range features.

The vegetation map so obtained was used in the integrated assessment for planning ski runs elaborated in Chapter 10.

6 UNIFICATION OF PROCESS-BASED MODELS OF ENVIRONMENTAL PROCESSES

6.1 Introduction

As shown in the literature review (Chapter 2) ski pistes have a clear impact on the environmental system. The establishment and maintenance of ski pistes, and the action of skiing itself involve deforestation, surface corrections, degradation of vegetation, soil compaction and the addition of artificial snow, causing an increase in overland flow, triggering of erosion, and slope instability. Clearly, for improvements to be made in the planning of ski runs in alpine terrain a good understanding of the environmental system and the response of environmental processes to a new development is necessary. This requires the acquisition of knowledge about each individual environmental process that has a direct or indirect relation with a ski piste, such as hydrological processes, hazardous processes and the growth of grass, but we also need to understand the interaction between these processes. The range of the responses of an environmental process to a change in site conditions caused by a potential ski run can be analysed with process-based models. Examples are a process-based hydrological model that predicts overland flow for different infiltration capacities or a grass-growth model that is able to determine CO_2-assimilation for different radiation intensities or soil moisture conditions.

When evaluating scenarios in such a sensitive environment like the Alps we also have to consider the spatial variation due to the heterogeneity of site conditions such as soil type, vegetation cover or topographic attributes. Also, temporal variation occurs as a result of varying inputs to the system like rainfall and solar radiation. To incorporate the spatial and temporal dynamics of a process in scenarios we need to use environmental models that can make spatial and temporal predictions; in this thesis these are termed spatio-temporal environmental models (Chapter 3).

The most important environmental criteria identified in Chapter 3 (Figure 3.8) for planning ski runs, having spatial and temporal variation, are the 1) duration of the snow cover, controlled by the input of new snow and the snow melt rate, 2) the peak runoff at the outflow point of the catchment, influenced by the snow melt rate and the input of rainfall, 3) the occurrence of erosion driven by the kinetic energy of rainfall and overland flow, 4) the triggering of slope instability due to a raise in pore pressure, and 5) the growth of grass, stimulated by solar radiation.

This chapter defines the principles for modelling these environmental processes whose results will be used in the framework for multicriteria decision making to optimise the planning of ski runs. This includes 1) principles of model building, in particular the modelling approach, data requirements versus data availability together with the feasibility of model application, and 2) the efficient implementation of these models with respect to their use for multicriteria analysis.

6.2 Principles of model building

The use of spatio-temporal process-based models to predict the environmental response to ski pistes is related to 1) the modelling approach - the models should capture the essential environmental processes to identify the impacts likely to be caused by a potential ski run and to select locations that are least vulnerable, 2) input data - the models should be applicable with easily available environmental data so that they can also be used in areas other than those they are built for, and 3) computer run-time - it should be possible to run the models on a personal computer within a feasible time span, since many runs may be needed to evaluate different scenarios. In the following sections the modelling conditions and related issues are further explained.

6.2.1 Modelling approach

In computer-based environmental modelling there are principally different approaches to represent an environmental process, namely physically based models and empirical models. Physically based models describe a process by mathematical equations, which are derived from physical laws. If proper data are available, this physically based approach may provide a rather accurate description of the process. Empirical models approximate the physical behaviour of a process according to observed phenomena. Model equations of empirical models can be derived using knowledge of the main physical processes, the purpose for which a model is used, the characteristics of the study area to which the model is applied, the availability of information on site conditions and other influence factors. For example, among the numerous snow melt models of different complexity that have been developed in the last 25 years (Braun, 1991; Sambles and Anderson, 1994; Blöschl et al., 1991; Kustas et al., 1994), *physically based models* utilise the energy balance to model the snow melt process (Anderson, 1976; Leavesley, 1989; Blöschl and Kirnbauer; 1991; Blöschl et al., 1991; Sambles and Anderson, 1994; Tarboton, 1994; Tarboton and Luce, 1996; Marks et al. 1998; Marks et al. 1999; Kustas et al., 1994; Kuchment, 1996; Braun, 1991; Singh et al., 1997), while empirical models, in snow hydrology termed as *index models,* assume that the snow melt process can be captured by a function of one or more calibration factors and the corresponding *index variable* such as temperature or solar radiation which are the parameters in the equation (Sambles and Anderson, 1994; Albert and Krajeski, 1998; Dingman, 2002). The energy balance supports the physical description of snow processes, however, it is a complex and data hungry approach; the forcing data are hardly available for the study area and much less over a river catchment or a region (Anderson, 1976). In addition, information about local snow properties must be known. Index models are a useful tool if data are sparse and if regional snow melt data are required. However, they lack the physical consideration of the melt process and they need to be calibrated with site-specific melt factors. Similar principles hold for hydrological models. Besides the division into physically based models and empirical models, the issue of spatial scale and temporal resolution are crucial driving forces representing a hydrological process in a computer model. The spatial scale refers to the size of the catchment and the size of the units or

grid cells in which the catchment is divided. In hydrological catchment modelling a catchment is considered as one unit or divided in representative units having similar characteristics or in grid cells of a certain size where calculations are carried out for each grid cell.

The temporal resolution denotes the length of the modelling period and the length of a time step, and therefore the number of time steps. There are event-based models simulating the response of a hill slope or catchment to a single event using very short time steps such as seconds or minutes. Other hydrological models use continuously varying data and larger time steps.

Well known rainfall-runoff models are the PRMS-model (Leavesley et al., 1983), SHE model (Abott, et al., 1986), Topmodel (Beven, 1997), Eurosem (Morgan et al. 1998, Rhineflow model (Van Deursen and Kwadijk, 1993) or Lisflood (De Roo et al., 1998). The SHE-model and the Eurosem model consider small-scale processes and are typical examples of data-hungry and run-time intensive models. Both require data that cannot be expected to be generally available, especially not in an alpine environment. Moreover, Eurosem describes hydrological processes for events using very small time steps, which are not feasible if we also want to analyse the seasonal behaviour. In other hydrological models, often developed for single applications, hydrological processes are described by standard modules such as the interception model by Rutter (1971), Green-Ampt-model for infiltration (Green and Ampt, 1911), Penman-Monteith (Monteith, 1965) for evapotranspiration or kinematic wave for routing (Chow, 1988), which are known to produce quite reasonable results. However, they require geo-hydrological information and small-scale data, which most probably have to be acquired in the field. On the other hand field data collection within socio-economical planning is limited by available resources, which implies that it is not possible to implement these kinds of procedures in hydrological models to be used for this kind of decision model. Simple models like the Rhineflow model can be easily implemented; however, it is designed for a large river catchment using time steps of a month. Since we want to analyse the dynamics of an alpine catchment within a season or a year rather than the response to a single event and because of the difficulty and expense of fulfilling the data requirements of physically based or complex empirical models including the virtual impossibility of collecting these data at several locations in the catchment to be spatially representative, it was not possible to adapt one of the existing models for modelling snow and hydrological processes.

The approach followed in this thesis when constructing the individual models aims at building empirical models that are robust enough to be run with not too many input data and within a reasonable time span, but rigorous enough to capture the essential processes relevant for planning, in particular for the evaluation of site conditions and the estimation of a set of impacts.

6.2.2 Data

The environmental models described in Chapters 7, 8 and 9 are designed in such a way that they can be used with standard available data such as a digital elevation model

derived from digital isolines with 20 m spacing, which is also a common distance of topographic isolines in rough terrain, daily rainfall records which are expected to be available for almost every alpine area, meteorological data from automatic meteorological stations in the surroundings which are being increasingly used for avalanche forecasts, and data that can be collected with reasonable effort within a planning procedure. Detailed vegetation maps and soil maps are usually not available for higher regions because those areas are not regarded as potential areas for farming. As a result, those maps can be generated on the basis of regional small-scale maps and expert knowledge. Moreover, mapping procedures can be applied to generate more detailed maps. For example, vegetation types were mapped using vegetation samples and derivatives of the digital elevation model (c.f. Chapter 5). In the case that these detailed maps are available, general data can be replaced by the more accurate data. The same holds for other model inputs and parameter values. For instance, the stability model requires information about the angle of internal friction and cohesion, which have been measured in the field (Chapter 4) for this study. If these values are not available, general values from literature (Mulder, 1991; Lee et al., 1983) can be used.

Nevertheless, for the plant growth model, some site-specific data need to be collected in the field, but the expenses required for data collection are assumed to be acceptable within the proposed decision model.

6.2.3 Computer run-time

Computer run-time depends on the modelling approach used for the description of the environmental process, the spatial and temporal resolution for which the model computes the set of mathematical equations and the software and hardware used. In this thesis the term spatial resolution is used for the division of the catchment into grid cells of a certain size, while temporal resolution refers to the length of a time step.

The spatial resolution, a grid cell size of 25 m by 25 m, is related to the derivation of the digital elevation model from digital isolines with 20 m spacing and the computing time required to carry out the set of mathematical operations for all grid cells and all time steps. The temporal resolution depends on the specific process to be modelled, the modelling aim and the feasible computer-run time. For example, there is no point in selecting a short time step for modelling groundwater level, which responds slowly to changes of environmental factors; conversely, a shorter time step is required for processes that react immediately to an input characterised by a high temporal variability such as rain. The length of the modelling period is determined by 1) the seasonal characteristics of a process and their relevance in the impact assessment, and 2) technical issues, described in more detail in Section 6.3.

Since the aim of this research is to provide a tool that can be easily applied in the first stage of a planning process, the model run-time has to be adjusted to the computational power of a standard modern PC, which means that the scenarios can be performed within a reasonable time span. PC's are standard but their computational power is very dependent on CPU-speed and memory, which differs a lot with each PC.

6.3 Model implementation

Model implementation involves computer programming, resulting in an executable model with available input data (see Section 6.2.2). Therefore special software is needed. In this thesis all spatio-temporal process-based models have been constructed using the dynamic spatial modelling language of the PCRaster software package (PCRaster, 1996; Wesseling et al., 1996; Karssenberg, 2002), which also represents the general software environment for the application of the spatio-temporal multicriteria decision making methodology described in Chapter 3. With respect to model implementation there are four important issues: 1) the original data are stored in a common data base to keep the spatial and temporal scale flexible, 2) the individual models are linked with each other to make efficient use of the output of one model as input to another, 3) the set of operations defined in a model script are carried out for each grid cell of a map and each time step, which is computed for each possible ski run location, and 4) the model tree, which consists of all models had to generate the attribute maps required for the multicriteria analysis. To this end tools are needed to generate the required model input for each model from the original data or intermediate model results. This incorporates a spatial model to specify the spatial scale, an interpolation tool that can create time series files with a certain start time, end time and length of the time step, and a conversion model to adjust the time step of an intermediate model result if required. The spatial model consists of standard procedures that can be performed with the cartographic modelling tool of PCRaster (PCRaster, 1996). For example the operation *resample* can adjust the map boundaries and the spatial resolution. The spatial model ensures that the location attributes of the individual maps correspond; otherwise the model cannot be executed. So the modeller is restricted to the same spatial scale for all maps and all models. To generate time series files, which are data files that assign the correct data value to a time step, a specific program was written that interpolates the original time series data to a time series with a fixed time step. The interpolation of all temporal data but rain is done using inverse distance interpolation. Rainfall records with small time steps are summed to determine the amount of rain for a larger time step; otherwise they are divided into equal partitions to cover the time steps for which no records are available. The interpolation tool is applied to all temporal data to generate the suitable time series file for each environmental model, which enables the modeller to fit the temporal resolution to the demands of the individual models and the modelling aim.

Another issue of model implementation refers to the communication between the models. On the one hand models are using different time steps in correspondence to the process they are describing. On the other hand models are using input data, which are the output of hierarchically higher models using another time step. Therefore conversion routines have to be inserted between the different model runs to convert the time step of the model result to the temporal resolution required by the subsequent model. This implies that the sequence of maps, also called a dynamic stack of maps, showing the spatial distribution of an environmental attribute for each time step, has to be converted to a dynamic stack of maps required by the subsequent model according to the respective time step.

6.4 Model tree

In order to model the environmental processes identified in Section 6.1 according to the model output required for the estimation of the impact and the evaluation of site conditions (see also Chapter 3, Figure 3.8), a set of spatio-temporal process-based models was developed, which are hierarchically related to each other (Figure 6.1; Chapter 3, Figure 3.14). The snow model (SN-model) sits on the top of the hierarchy and creates important inputs to the hydrological models, specifically the hydrological model (HS-model) for calculating slope instability (ST-model) and the hydrological model (HE-model) for predicting erosion (ER-model), but also to the potential growth model (PG-model).

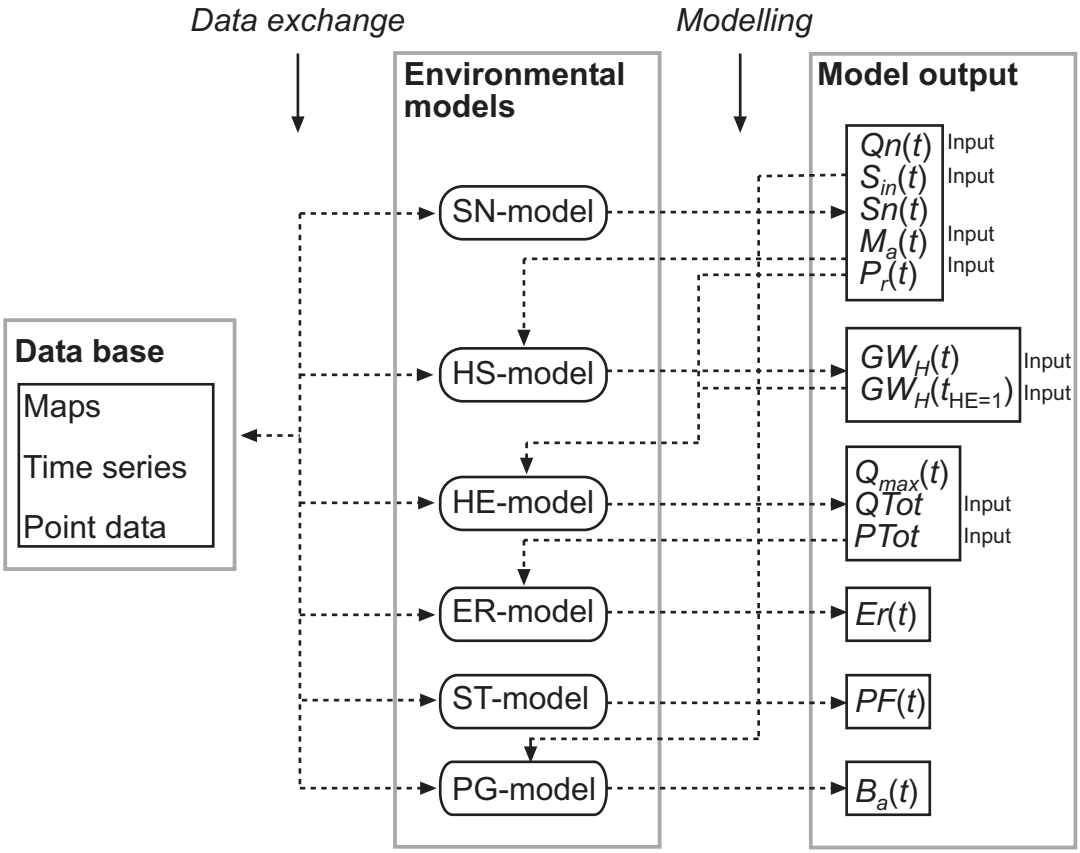

Figure 6.1 Hierarchical structure of the models, i.e. snow melt model (SN), hydrological model (HS) required by stability model (ST), hydrological model (HE) needed by erosion model (ER) and plant growth model (PG), to generate input data for the multicriteria analysis, with t at time t, t_{HE} the time step of the HE-model, $Q_n(t)$ net radiation (J·m^{-2}·time step^{-1}), $S_{in}(t)$ incoming shortwave radiation (J·m^{-2}·time step^{-1}), $Sn(t)$ snow thickness (m), $M_a(t)$ the melt rate (m/time step), $P_r(t)$ the rain flux (m/time step), $GW_H(t)$ the groundwater level, $GW_H(t_{HE})$ the groundwater level at t_{HE}=0, $Q_{max}(t)$ the peak discharge (l/s), $QTot$, the total discharge of the snow melt period (m), $PTot$ the total rainfall of the snow melt period (m), ER erosion (kg/m^2), $PF(t)$ the likelihood of unstable cells and $B_a(t)$ the biomass above the soil surface (kg/m^2).

Figure 6.2 shows the relationship of the individual models, the modelling period of each model and the time step selected for each model.

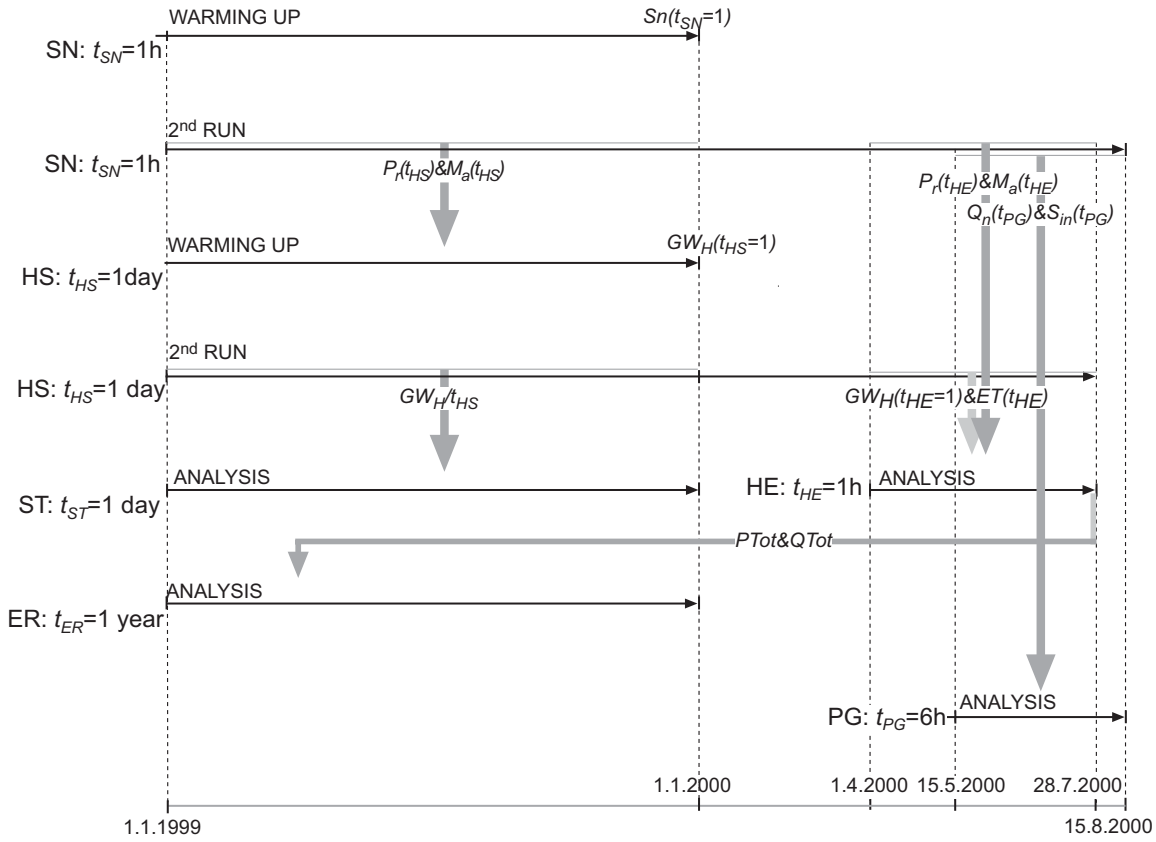

Figure 6.2 Relationship and temporal scale of all models, with t at time t, t_{SN} the time step of the snow model (SN), t_{HE} the time step of the hydrological model (HE) needed by the erosion model (ER), t_{HS} the time step of the hydrological model (HS) required by the stability model (ST), t_{ST} the time step of the ST-model, t_{ER} the time step of the ER-model, t_{PG} the time step of the plant growth model (PG), $Q_n(t)$ net radiation ($J \cdot m^{-2} \cdot$time step^{-1}), $S_{in}(t)$ incoming short wave radiation ($J \cdot m^{-2} \cdot$time step^{-1}), $Sn(t)$ snow thickness (m), $M_a(t)$ the melt rate (m/time step), $P_r(t)$ the rain flux (m/time step), $GW_H(t)$ the groundwater level, $GW_H(t_{HS}=1)$ the groundwater level at $t_{HS}=1$, $GW_H(t_{HE}=1)$ the groundwater level at $t_{HE}=1$, $QTot$, the total discharge of the snow melt period (m), $PTot$ the total rainfall of the snow melt period (m).

The total modelling period of this study covers 19.5 months. The snow model (SN-model) was run twice. First it was computed for one year, denoted as the warming up run, to generate the snow cover map which is used in the second model run as the initial snow cover map ($Sn(t=0)$. This approach is needed since insufficient measurements are available to derive the initial snow thickness from the snow measurements. The second model run starts at the same time as the first model run and covers the total modelling period. The choice for the time step of the snow model is that the snow melt process varies during the day with respect to meteorological conditions. It is represented by an

hourly time step selected for the radiation model, which is a part of the SN-model. The SN-model generates input data for each time step of the HS-model, the HE-model and the PG-model, in particular melt rates (M_a/time step) and rain flux (P_r/time step) for the first two and radiation maps *(S_{in}*/time step*)* for the latter. The dynamic stack of maps with an hourly time step is converted to the temporal resolution required by the individual models. The hydrological models (HS-model and HE-model) differ for the greater part in the time step and some concepts that are related to the length of the time step, also explained in Chapter 7 (Section 7.3.1).

The main aim of the HS-model is to model the spatial and temporal variation of the groundwater level, required by the stability model (ST-model) and to generate input data for the HE-model. Since groundwater recharge is a slower process than processes above the surface, a daily time step was chosen. As a consequence, the ST-model uses the same time step. The ST-model is executed for one year to take into account all seasonal effects of the groundwater level on slope stability. Just like the SN-model, the HS-model is run two times. First, and this is again the warming up phase, to generate the initial map of groundwater height ($GW_H(t_{HS}=0)$), which can be used as the initial groundwater level map in the second model run, starting at the same time as the first model run. The second model run is devoted to the generation of groundwater level maps (GW_H/time step) for the ST-model and to provide the HE-model with the groundwater level map at the start of the snow melt period of the second modelling year ($GW_H(t_{\mathrm{HE}}=0)$) and evapotranspiration (*PET*/time step). The start of the HE-model is considered as the start of the melting season. The HE-model is only run for the snow melt season since this season is regarded as the most critical period of a hydrological year for the generation of overland flow. It uses an hourly time step to represent the fast response of hydrological processes above the surface to changes in the input to the surface such as rain and snow melt water, provided by the SN-model. The erosion model (ER-model) derives the hydrological information from the HE-model to compute erosion on an annual basis (in Figure 6.2 *PTot* and *QTot*). The PG-model predicts potential grass growth for one growing season. It is executed every 6 hours to capture the impact of the day-time (morning, afternoon, night) on the biomass production. It is solely linked to the SN-model which provides incident solar radiation maps.

6.5 Outline

This chapter provided the basic principles of the spatio-temporal process-based models used to predict a potential set of environmental impacts and to describe environmental conditions at the site in consideration. The following chapters, Chapters 7, 8 and 9, present the technical details of the individual models. Chapter 7 deals with the description of the hydrological issues, which involves the characterisation of the hydrological system in an alpine area, the description of snow accumulation and snow melt, the identification of relevant hydrological processes with respect to the modelling conditions and the site characteristics and how the physical behaviour of these processes can be translated to mathematical equations in the SN-model, the HE-model and the HS-model. The aim of the snow model is to assess the duration of a certain snow cover to compare a set of ski

runs with respect to their snow conditions. Model results of the HS-model are not used for the multicriteria analysis, but by the ST-model. The HE-model generates both input data for a subsequent model, the ER-model, and provides data for the assessment of the impact of a potential ski run on the discharge. This is followed by Chapter 8, which addresses the modelling of hazardous processes. Among natural hazards that are likely to occur in an alpine area only erosion and slope stability are taken into account. The risk of avalanches was considered in a different study using a statistical approach (Ghinoi, 2002). The ER-model and the ST-model are derived from existing models, in particular from the Morgan-Morgan-Finney-model (2001) to compute annual erosion and the PROBSTAB-model (Van Beek, 2002) to assess the probability of landslide activity in a Mediterranean environment. The erosion model computes annual erosion loads and the stability model calculates the probability that a slope might become unstable, both at the ski run location and for the total catchment. With respect to multicriteria decision making these two models aim at the assessment of the degree of land degradation. The last chapter of Part D, Chapter 9, deals with the technical description of the plant growth model, which was developed by Frings (2001) and Castenmiller (2001). It derives data about incoming solar radiation from the SN-model, calculates the biomass production of grass and sedge, and it is used to identify potential areas with reasonable growing conditions to prevent natural hazard and to compensate the visual impact of ski runs on vegetation. The integration of the model output is discussed in Chapter 10.

7 HYDROLOGICAL MODELLING

7.1 Introduction

The hydrology of an alpine area is especially important for initiating hazardous processes such as the triggering of erosion, slope instability and flooding. These consequences may interfere with people, residential areas or infrastructure, but hydrology also controls other environmental processes such as biomass production or economical issues. Therefore, when assessing the environmental suitability of an alpine site for a new development, it is useful to know the dynamics of the hydrological system at the site including its response to any change. The hydrologic system can be divided into three sub systems: 1) the atmospheric water system that incorporates precipitation, interception, evaporation and transpiration, 2) the surface water system including overland flow and channel flow, and 3) the subsurface water system that involves infiltration, percolation to the groundwater, subsurface flow and groundwater flow. The individual components of the sub systems are controlled by the spatial information on site factors such as vegetation, soil, geology, topography, meteorological conditions and the location in the geographical space. In rugged terrain topographic attributes are crucial driving forces as they direct the flow of the water according to the surface topology in the direction of the steepest slope downhill, they influence soil formation and the development of vegetation and they have an indirect impact on the amount, the form and the spatial distribution of precipitation.

The annual hydrologic cycle of an alpine area is driven by snow accumulation and snow melt. In winter, when temperatures are below zero, precipitation falls as snow and is stored in the seasonal snow cover. During that season a part of the snow pack is lost to the atmospheric water system, but there is hardly any interaction with the surface water system and the subsurface water system. In addition the mountain streams are mostly frozen. As a result the winter base flow is very low. In spring, when temperatures and solar radiation are rising, snow melts, and the surface water system and the subsurface water system are activated, affecting the soil moisture and increasing the discharge of the mountain streams, which will reach their peaks in periods of rapid snow melt. After the snow melt season until the start of the winter the input to the surface is merely rain, mist and dew, and the discharge of the mountain rivers decreases.

The snow model (SN) and the hydrological models (HE and HS) describe the dynamics of the hydrologic system in an alpine area according to the modelling conditions addressed in Chapter 7. This chapter is divided in two parts: The first part (7.2) discusses snow processes, and the second part (7.3) deals with hydrological aspects. In each part a description will be given of the underlying theory and model structure; it explains how the specific processes and states can be expressed by mathematical equations with respect to the use of the proposed models in the framework of multicriteria decision making. The illustration of the model components is followed by the description of how the models have been calibrated. At the end of each part results are shown which are required for the decision model discussed in Chapter 3.

7.2 Snow model (SN)

7.2.1 Introduction to snow modelling

The analytical framework (Chapter 3, Figure 3.8) for the planning of environmental sound ski runs addresses both the spatial distribution of a continuous snow cover and the occurrence of hydrologically driven land degradation. Accordingly, the snow model aims to estimate 1) spatial and temporal variation of the snow cover driven by topographic heterogeneity and the spatial and temporal variation of meteorological conditions, and 2) the prediction of the timing and the amount of snow melt water released to the hydrological system. Snow cover changes are controlled by snow accumulation, snow metamorphism and snow melt, driven by meteorological factors such as air temperature, net radiation, relative humidity, wind, vapour pressure and precipitation. Snow metamorphism refers to the change of snow properties such as snow compaction due to the impact of external forces and internal heat fluxes. The snow cover varies in structure and thickness due to the input of fresh snow, the heat fluxes at the snow surface, and the energy fluxes in the pack and heat fluxes at the snow-soil interface. Among the variety of snow models which differ in the processes being considered, the approach to how processes are represented, the spatial scale, and the study area they have been designed for, there are point models that aim at the physical representation of snow processes at one location (Anderson, 1976; Blöschl and Kirnbauer, 1991; Albert and Krajeski, 1998), spatially distributed models using an empirical approach for the description of snow processes (Cazorzi and Fontana, 1996; Coughlan and Running, 1997; Williams and Tarboton, 1999; Daly et al., 2000), spatially distributed physically based snow models (Blöschl et al., 1991, Sambles and Anderson, 1994; Marks et al. 1999; Kuchment et al., 2000) and snow melt models that are linked to runoff models (Leavesely et al., 1983; Martinec and Rango, 1998). Most of these models focus on the description of snow accumulation and the snow melt process. The metamorphism of the snow pack and processes changing the properties of the snow itself have often been ignored due to the complexity of these processes, insufficient data, and the large spatial and temporal variability of the properties of the snow to be modelled. Before explaining the snow model implemented for the case study, a short introduction to snow processes and how they can be described is given.

Snow accumulation. Snow accumulation is the increase of the snow cover thickness due to the input of fresh snow. In many snow models snow accumulation is assumed to be a function of precipitation and air temperature: precipitation falls as snow if the air temperature is below a certain temperature threshold, otherwise precipitation is rain. The threshold value depends on local meteorological conditions, so a wide range of values has been used, for instance from -1° C to 3° C (Todini, 1995; Tarboton et al., 1996), from –1° C to 7° C (Braun, 1991), or above 0° C (Kuchment et al., 2000), 0.5° C (Cazorzi and Fontana, 1996; Albert and Krajeski, 1998) and 1° C (Bell and Moore, 1998; Fontaine et al., 2002). Accordingly, snow fall can be described by:

$$P_s(t) = P(t) \qquad \text{if } T_a(t) < T_c \tag{7.2.1}$$

with, $P_s(t)$ the amount of snow fall (m/time step) at time t, $P(t)$ the amount of precipitation (m/time step) at time t, $T_a(t)$ the actual air temperature (ºC) at time t and T_c the temperature threshold (ºC) below which all precipitation is snow.

Alternatively, snow accumulation can be retrieved from measurements in the field (Chang and Li, 2000) or from remotely sensed images (Blöschl and Kirnbauer, 1992; Balk and Elder, 2000; Tappeiner et al., 2001) using statistical models such as regression models or neural networks. Although these approaches are useful in other situations, they have disadvantages when applied in the proposed framework for decision making described in Chapter 3. Field measurements provide an accurate description of snow properties such as snow thickness, snow profile and snow structure. However, they just represent the conditions at a point at a certain moment and do not cover a continuous area and time span. Additionally, manual field data collection is constrained by accessibility, weather conditions and time and moreover, it is very costly. As such, those field data are mostly not feasible in the framework of decision making for socio-economic infrastructure. Time series of remotely sensed images (Blöschl, 1992; Elder, 1998; Turpin, 1999) can be applied to improve the spatial and temporal resolution. For example satellite images are useful for the retrieval of the snow covered area including snow properties, but their potential to derive temporal changes may be restricted by cloudiness and long intervals between the records; radar images on the other hand are independent from the cloud cover, but the retrieval of accurate information from them is very difficult because of radar shadow effects (Lillesand and Kiefer, 1994). So the availability of potential high-resolution time series of remotely sensed images is limited, which is a weakness if short-time temporal changes are required. Since the spatial and temporal components play a crucial role for the description of the dynamic behaviour of a process, the use of a spatio-temporal process based model is a useful alternative for the determination of snow accumulation because snow accumulation can be estimated for all locations and for all time steps, requiring a feasible number of data. Field measurements of the snow thickness and remote sensing images can additionally be used to derive snow parameters and to verify model predictions.

Snow melt. Because of the importance of the snow melt rate for socio-economic purposes such as hydro-power generation or domestic use, predictions of the snow melt rate have received much attention. As already explained snow melt can be described by the physically based approach implementing the energy balance or by an empirical model using the index approach (Sambles and Anderson, 1994). An example of the index approach is the degree-day index (Kustas et al., 1994), where the decrease of the snow thickness (cm) is equated to the product of the difference between the average temperature of a day and the base temperature and the degree-day factor:

$$M_{DDI}(t) = a \cdot (T_a(t) - T_b(t)) \qquad (7.2.2)$$

with, $M_{DDI}(t)$ the melt rate of snow (cm snow/day) according to the degree-day index, t the time (day), a the degree-day factor (cm $\cdot$ºC$^{-1}\cdot$day^{-1}), $T_a(t)$ the average daily air temperature (ºC) and T_b the base temperature (ºC), usually 0º C.

Knowing the total energy that can be gained by the snow pack at time t, snow melt can be expressed physically in terms of (Sambles and Anderson, 1994):

$$M_{EB}(t) = \frac{Q(t)^*}{L_f \cdot \rho_w} \cdot 1000 \qquad (7.2.3)$$

with, $M_{EB}(t)$ the melt rate (mm per time step) at time t, $Q^*(t)$ the total energy gained by the snow pack (J· m^{-2}·time step^{-1}) at time t described by the energy balance, L_f the latent heat of fusion (J/kg) and ρ_w the water density (kg/m^3). The total energy gained by the snow pack ($Q^*(t)$, J· m^{-2}·time step^{-1}) at time t is controlled by the energy balance according to (Anderson, 1976; Blöschl et al., 1991; Sambles and Anderson, 1994):

$$Q^*(t) = Q_n(t) + Q_s(t) + Q_l(t) + Q_g(t) + Q_p(t) - Q_m(t) \qquad (7.2.4)$$

with, $Q_n(t)$ the net radiation (J· m^{-2}·time step^{-1}) , $Q_s(t)$ the sensible heat flux(J· m^{-2}·time step^{-1}), $Q_l(t)$ the latent heat flux(J· m^{-2}·time step^{-1}), $Q_g(t)$ the heat flux from the ground (J· m^{-2}·time step^{-1}), $Q_p(t)$ the heat flux of precipitation (J· m^{-2}·time step^{-1}), and $Q_m(t)$ the internal energy change in the snow pack (J· m^{-2}·time step^{-1}). As already mentioned, the energy balance requires many data; the minimum data requirement for its application are air temperature, incoming solar radiation, vapour pressure and wind speed (Leveasely, 1989; Rohrer, 1990). In addition, information about local snow properties should be known. Because of the difficulty and expense of fulfilling the data requirements of the energy balance approach, it is not a feasible method to be applied in the SN-model that can be used with the usually available data to support the planning of environmental sound ski runs.

Additional processes, which may be important when modelling snow melt at a point location, are the impact of rain on the snow and the snow melt (Kuchment et al., 1996; Singh et al., 1997; Marks et al., 1998), the flow of water through a snow pack (Albert and Krajeski, 1998) and snow metamorphism. However, just as with the energy balance, many data are needed to model these processes and therefore it is not easy to include them in a snow model with respect to the modelling conditions that were defined in the previous chapter. Moreover, it is assumed that these processes are of minor importance when modelling snow melt at this spatial scale.

While topographic maps, aerial photographs of different years and daily precipitation records at one location are expected to be usually available, continuous meteorological data from several meteorological stations in the study area such as relative humidity or wind speed are normally not at one's disposal. The same is true for solar radiation, but this can be overcome by applying models to compute potential incident solar radiation. Data to characterise the snow cover development are not generally acquired, but may partly be derived from a time series of aerial photography or satellite images if available for that area.

To this end a multi-variable index approach (Sambles and Anderson, 1994) was implemented in the SN-model to meet the data requirements, the effect of rain on the snow melt and the effect of different radiation intensities due to the variation of topographic attributes characteristic for alpine terrain.

7.2.2 Building the snow melt model (SN)

Alpine terrain is characterised by heterogeneous site conditions, but the available data are not always sufficient to represent all heterogeneity. The snow melt model should

- be spatially distributed, simulating changes of snow cover and snow melt through time.
- include those processes, which are essential for predicting snow cover development and snow melt at a feasible resolution, thereby ignoring processes which are of minor importance. This is because of the aim to investigate relative spatial differences due to topographic heterogeneity rather than defining absolute spatially distributed snow melt rates as, for instance, is required for the assessment of the profitability of a future hydro-power stations.
- be a model that meets the general modelling conditions specified for all spatio-temporal process-based models (c.f. Chapter 6).

The snow model consists of three components: 1) the meteorological model to allow for the altitudinal dependence of temperature and precipitation, 2) a radiation model (Van Dam, 2001) to include spatial variability of radiation intensities due to topographical differences, and 3) the snow model simulating snow accumulation and snow melt. Figure 7.1 illustrates the main components of the snow model.

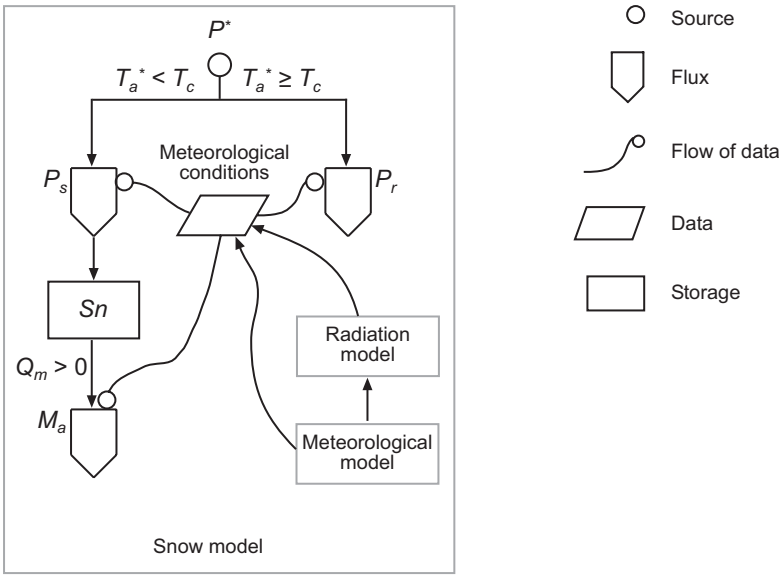

Figure 7.1 Modelling structure of the snow model; with P^* the precipitation (m), T_a^* air temperature (ºC), T_c temperature threshold (ºC), P_s snow (m water slice), P_r rainfall (m), Sn snow thickness (m water slice), Q_m melt energy (J·m^{-2}·time step^{-1}) available for snow melt and M_a the melt rate (m/time step).

Meteorological model. The meteorological model predicts air temperature and precipitation data at all altitudes on the basis of continuous data of temperature and precipitation that were recorded at two measuring locations at different elevations. It is assumed that elevation has a linear relation with temperature and precipitation. Therefore a linear regression with elevation was used within each Thiessen polygon (Burrough and McDonnell, 1998), representing the two rain zones surrounding the measuring locations. Additional effects of factors related to other topographic attributes such as aspect of the terrain is not included. It is assumed that air temperature decreases linearly with increasing elevation. For each grid cell, air temperature is determined by the air temperature measured at the nearest measurement location and the elevation difference between the elevation of the cell and nearest measurement location:

$$T_a^*(t) = T_a(t) - H_{rel} \cdot L_T \tag{7.2.5}$$

with, $T_a^*(t)$ the relative temperature (°C) at time t (hours) at the grid cell in consideration, $T_a(t)$ the measured air temperature (°C) at time t, H_{rel} the topographic elevation (m) of the grid cell minus the elevation of the measurement location and L_T (°C/m) the lapse rate (Section 7.2.3, Table 7.1) defining the decrease of temperature with elevation. Precipitation is supposed to increase linearly with elevation according to:

$$P^*(t) = P(t) + P(t) \cdot H_{rel} \cdot L_p \tag{7.2.6}$$

with, $P^*(t)$ the precipitation (m/time step) at time t (hours), $P(t)$ the measured precipitation (m/time step) at time t at the measurement location nearest to the grid cell and L_P (m/m) the empirically derived lapse rate (Section 7.2.3, Table 7.1) defining the increase of precipitation with elevation.

For each grid cell, the temperature at the grid cell determines whether precipitation falls as snow or rain:

$$\begin{aligned} &P_r(t) = P^*(t) \qquad \text{if } T_a^*(t) \geq T_c \\ &P_s(t) = 0 \\ &P_r(t) = \ 0 \qquad\quad \text{if } T_a^*(t) < T_c \\ &P_s(t) = P^*(t) \end{aligned} \tag{7.2.7}$$

with, $P_r(t)$ rainfall (m/time step) at t, $P_s(t)$ snow fall (m water slice/time step) at t, T_c is the critical temperature (°C) specifying the threshold for the transition from rain to snow and which is kept constant for all time steps. $T_a^*(t)$ and $P^*(t)$ are the air temperature (°C) and the precipitation (m/time step) at each grid cell equivalent to the terms in Equation 7.2.5 and 7.2.6, respectively.

Radiation model. The radiation model computes net radiation (Q_n, J·m^{-2}·time step^{-1}) as a function of topographic attributes, elevation and inclination of the sun above the horizon, meteorological conditions and the location of the cell in consideration. Net radiation $Q_n(t)$ (J·m^{-2}·time step^{-1}) at time t is (c.f. Van Dam, 2001):

$$Q_n(t) = S_{in}(t) - S_{out}(t) + L_{in}(t) - L_{out}(t) \quad (7.2.8)$$

with, $S_{in}(t)$ (J·m^{-2}·time step^{-1}) and $L_{in}(t)$ (J·m^{-2}·time step^{-1}) the incoming shortwave and longwave radiation respectively, and $S_{out}(t)$ (J·m^{-2}·time step^{-1}) and $L_{out}(t)$ (J·m^{-2}·time step^{-1}) the outgoing shortwave and longwave radiation, respectively, all at the grid cell in consideration. The amount of shortwave radiation is controlled by the proportion of the incident energy that is reflected and the presence of clouds according to:

$$S_{in}(t) - S_{out}(t) = S_{in}(t) \cdot (1 - A) \cdot (1 - Cl(t)) \quad (7.2.9)$$

with, *Cl(t)* the cloud cover (fraction) controlling the amount of incoming radiation and *A* the Albedo defining the reflectance from the ground surface (Section 7.2.3, Table 7.2). For example snow has a very high surface albedo value, which reduces the energy for heating up the snow pack. The absorption of solar radiation at the Earth's surface leads to heating up, which in turn, leads to the emission of longwave radiation. The amount of emission is defined by the Stefan-Boltzman law (Henderson-Sellers and Robinson, 1994). While a part of the longwave radiation travels downwards and is received as incoming longwave radiation ($L_{in}(t)$, J·m^{-2}·time step^{-1}), the other part, specifically outgoing longwave radiation ($L_{out}(t)$, J·m^{-2}·time step^{-1}), is emitted upwards or leaves the atmosphere. Incoming longwave radiation (L_{in}, J·m^{-2}·time step^{-1}) is for the greater part determined by air temperature and actual vapour pressure (Henderson-Sellers and Robinson, 1994):

$$L_{in}(t) = \varepsilon \cdot \sigma \cdot \left(T_a^*(t) + 273.15\right)^4 \cdot \left(0.61 + 0.05 \cdot \sqrt{e_a}\right) \cdot \left(1 + 0.17 \cdot Cl(t)\right) \quad (7.2.10)$$

with, ε the average emissivity of the land cover (Section 7.3.2, Table 7.2), σ Stefan-Boltzman constant (J·m^{-2}·K^{-4}·time step^{-1}) (Table 7.1), $T_a^*(t)$ the air temperature (ºC), Equation 7.2.5, and $e_a(t)$ (mbar) the actual vapour pressure. The actual vapour pressure depends on relative humidity and the saturated vapour pressure:

$$e_a(t) = RH(t) \cdot e_s(t) \quad (7.2.11)$$

with, $RH(t)$ the relative humidity (fraction) and $e_s(t)$ (mbar) the saturated vapour pressure. It is assumed that measured relative humidity is representative for the total catchment. Saturated vapour pressure ($e_s(t)$, mbar) is determined by:

$$e_s(t) = 6.107 \cdot e^{\frac{17.27 \cdot T_a^*(t)}{T_a^*(t) + 237.3}} \quad (7.2.12)$$

Outgoing longwave radiation ($L_{in}(t)$, J·m^{-2}·time step^{-1}) is given by:

$$L_{out}(t) = \varepsilon \cdot \sigma \cdot \left(T_a^*(t) + 273.15\right)^4 \quad (7.2.13)$$

Snow model. Temporal snow cover changes are determined by snow accumulation and snow melt. For each grid cell, the snow thickness ($Sn(t)$, m water slice) at time t is:

$$Sn(t) = Sn(t-1) + P_s(t) - M_a(t) \tag{7.2.14}$$

with, $Sn(t\text{-}1)$ the snow thickness (m water slice) at the previous time step, $P_s(t)$ snow fall (m water slice/time step) at time t and $M_a(t)$ the actual snow melt rate (m water slice/time step), Equation 7.2.17.

Potential snow melt ($M_p(t)$, m/time step) at time step t is the amount of snow that can potentially be melted by the positive energy input to the snow pack within one time step. It is modelled according to the multiple-variable index approach (Sambles and Anderson, 1994). For each grid cell, $M_p(t)$ is a function of the heat flux of temperature, net radiation and the heat flux of rain:

$$M_p(t) = a_r \cdot \left(\max(T_a^*(t) - T_b, 0)\right) + m_q \left(Q_r(t) + Q_p(t)\right) \tag{7.2.15}$$

with, a_r the restricted degree factor to determine the snow melt rate (m water slice·ºC^{-1}·time step^{-1} (Section 7.2.3, Table 7.1), $T_a^*(t)$ the relative air temperature, Equation 7.2.5, above 0° C, max(x,y) an operation that assigns the maximum value of x and y, so max($T_a^*(t)$-T_b,0*)* assigns the maximum value of ($T_a^*(t)$-T_b) and 0, T_b the base temperature at which it is assumed that snow melt takes place (Section 7.2.3, Table 7.1), defined to be 0º C, m_q the transformation factor to convert energy (J·m^{-2}·time step^{-1}) to snow melt depth (m water slice) (Section 7.2.3, Table 7.1), $Q_n(t)$ the average positive net radiation (J·m^{-2}·time step^{-1}), Equation 7.2.8, and $Q_p(t)$ the energy supplied by rainfall (J·m^{-2}·time step^{-1}). The energy supplied by rain is calculated as a function of water characteristics and rain (Kuchment et al., 1996; Singh et al., 1997; Marks et al., 1998):

$$Q_p(t) = (1/3600) \cdot D_w \cdot C_w \cdot T^*(t) \cdot P_r^*(t) \tag{7.2.16}$$

with, D_w the water density (kg/m^3) and C_w the specific heat of water (J·kg^{-1}·°C^{-1}) and $P_r^*(t)$ the rain (m). For each grid cell, actual snow melt $M_a(t)$ (m/time step) during one time step t is:

$$M_a(t) = \min\left(M_p(t), Sn(t)\right) \tag{7.2.17}$$

where min (x,y) assigns the minimum value of x and y, so $M_a(t)$ is equivalent to the lower value of $M_p(t)$ and $Sn(t)$.

7.2.3 Model implementation

The SN-model, containing Equations 7.2.5 to 7.2.17, was written using the dynamic modelling language of PCRaster (PCRaster, 1996; Wesseling et al., 1996). It is computed for all grid cells of the defined catchment and the number of time steps of the modelling period specified in Chapter 6, Figure 6.2. Required input data are the digital elevation model, a ground cover or vegetation cover map (Chapter 5) and meteorological data such as precipitation, temperature, relative humidity and cloudiness. The ground cover map is required for the estimation of the albedo and the emissivity in times when there is no snow because radiation data calculated by the SN-model are also used by the PG-model. Table 7.1 gives an overview of model parameters and Table 7.2 shows parameter values for emissivity and surface albedo in correspondence to the land cover.

Table 7.1 Calibration parameters and other model input.

Parameter	Symbol	Unit	Value	Source
Temperature lapse rate	L_T	ºC/m	0.005	calibrated
Precipitation lapse rate	L_P	m/m	0.00055	calibrated
Temperature threshold	T_c	ºC	1.5	calibrated
Restricted degree index	a_r	$m \cdot ºC^{-1} \cdot \text{time step}^{-1}$	7.10^{-5}	calibrated
Conversion factor	m_q	$m \cdot J^{-1} \cdot m^{-2} \cdot \text{time step}^{-1}$	9.10^{-8}	calibrated
Density of water	D_w	kg/m^3	998	Jansen (1977)
Melt energy	*MeltQ*	J/kg	334000	Jansen (1977)
Specific heat of water	C_w	$J \cdot kg^{-1} \cdot ºC^{-1}$	4180	Jansen (1977)
Base temperature	T_b	ºC	0	Kustas et al. (1994)

Table 7.2 Values defining surface albedo and emissivity with respect to land cover following suggestions by Henderson-Sellers and Robinson (1994).

Land cover	Surface Albedo (-)	Emissivity (-)
Alpine grass	0.2	0.95
Alpine heaths	0.18	0.96
Forest	0.14	0.98
Bare/rock	0.23	0.93
Snow	0.8	0.98

The model generates data that are to a large extent an input to subsequent models. These are rainfall ($P_r(t)$, m/time step) and actual snow melt rate ($M_a(t)$, m/time step) for each grid cell and corresponding time step, required by the HS-model and the HE-model, potential incident solar radiation, $S_{in}(t)$ ($J \cdot m^{-2} \cdot \text{time step}^{-1}$), for each grid cell and corresponding time step, needed by the PG-model, and the spatial and temporal changes of snow thickness, $Sn(t)$ (m water slice/time step), used by the evaluation model. The evaluation model prepares the input data for the multicriteria analysis. It aggregates the model results to non-spatial values used for the evaluation and comparison of ski runs.
Figure 7.2 represents the spatial distribution of the snow cover in the beginning of the

actual melt period. It clearly reflects the dependence of the snow thickness on elevation, in particular an increase of snow thickness with elevation and the early disappearance in lower elevations, for the greater part caused by the increase in precipitation and higher temperatures in lower altitudes. The typical development of snow water equivalent (m^3) in time, in particular the increase of snow water equivalent during the winter period and the decrease in the melting season, is illustrated for one location by the graph in the middle of Figure 7.3.

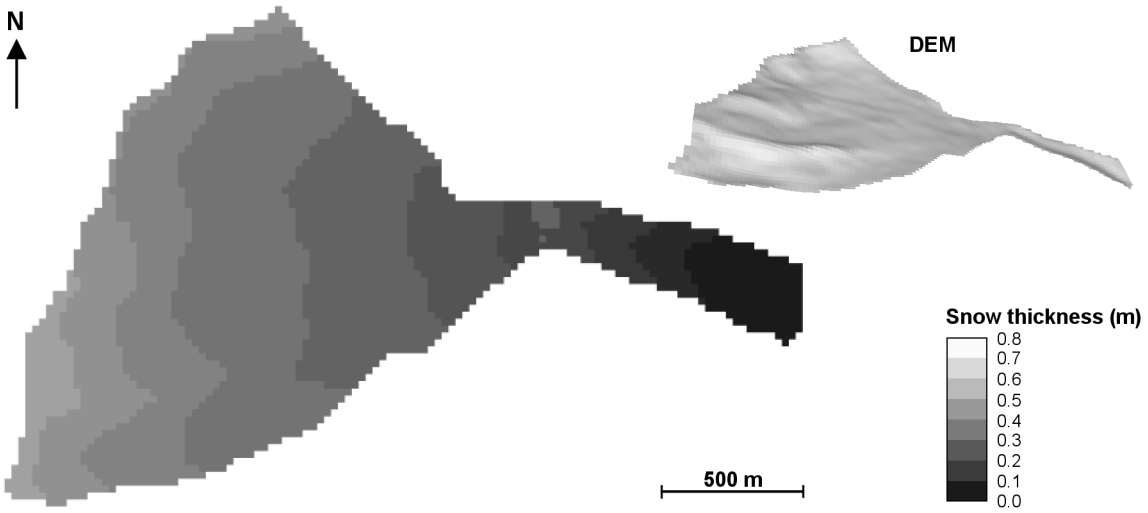

Figure 7.2 Spatial distribution of the snow cover at the start of the snow melt period. The gradual change from dark grey to light grey illustrates the increase of the snow thickness (m water slice) with elevation caused by the dependence of temperature, precipitation and radiation on topographical attributes.

For each potential ski run, the number of days with a sufficient snow cover is derived from the spatial distribution and temporal variation of snow thickness during one year. Usually one would expect that higher locations are more favourable because of the increase of snow with elevation. However, it is not only the number of days with snow that counts, but also the number of days that are snow free to achieve satisfactory growing conditions for vegetation. The optimal location for a potential ski run that satisfies both the protection of vegetation during the skiing period and the regeneration of vegetation is elaborated in Chapter 10.

The melt rate (m water slice/time step) of snow, reported for the same location as the snow cover development, is shown in the lower graph of Figure 7.3. It is for the greater part determined by the energy available for snow melt and the presence of snow. For the same location, the top graph of Figure 7.3 shows the snow fall (m water slice/time step). Maps of the melt rate and the rain flux, having a time step of one hour, are converted to the respective time step of the HE-model and the HS-model because they are input to these models.

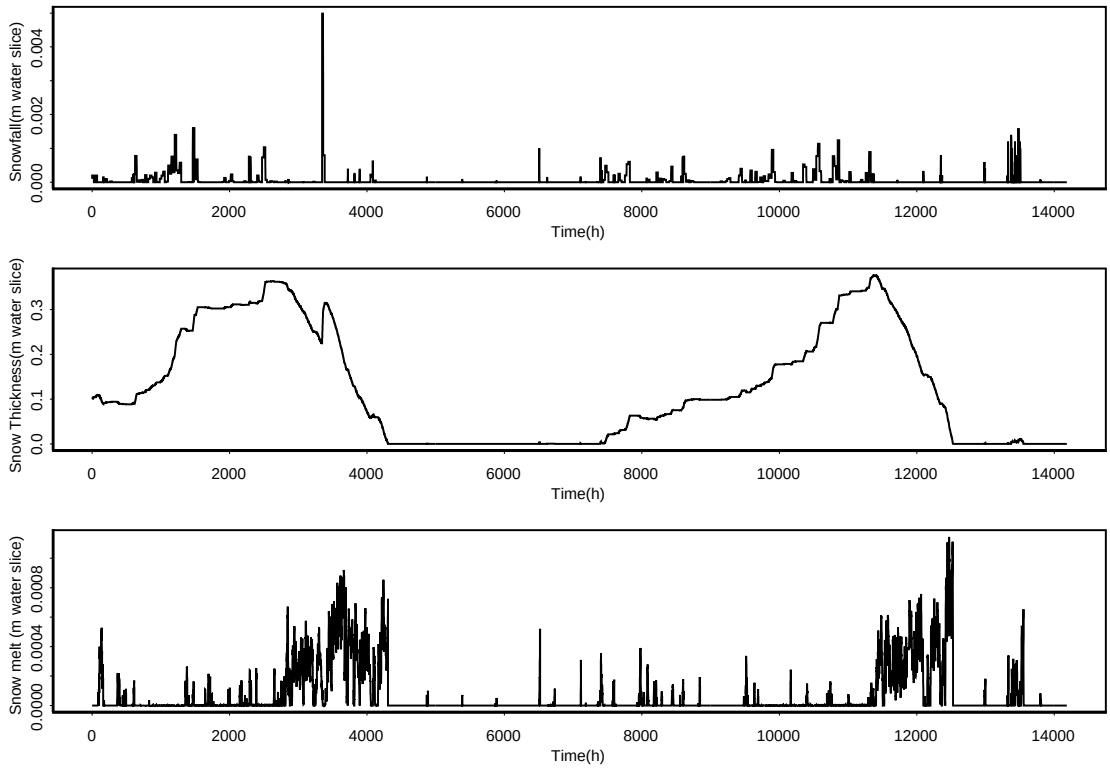

Figure 7.3 For the total modelling period, the upper figure shows snow fall (m water slice/h), the figure in the middle displays snow cover development (m water slice), and the lower one represents the hourly melt rate (m water slice/h), all reported for the same location at an elevation of 2300 m.

7.2.4 Model calibration

The snow model was calibrated using the measured snow water equivalent (*SWE*, m^3) at 32 locations (Chapter 4). For each grid cell, snow water equivalent represents the water volume present in the snow cover of a cell. Five model parameters, specifically the lapse rate to calculate air temperature (L_T, Eq. 7.2.5), the lapse rate to calculate precipitation (L_P, Eq. 7.2.6), the temperature threshold below which precipitation is assumed to be snow (T_c, Eq. 7.2.7), the restricted degree index a_r (Eq. 7.2.15), and the energy conversion factor, m_q (Eq. 7.2.15), were selected to achieve correspondence between measured snow water equivalent and predicted snow water equivalent for the snow melt period from 23 May 2000 until 21 June 2000. After each calibration run the modelled snow water equivalent at time t, in particular $Sn(t) \cdot CA$ (m^3) with $Sn(t)$ calculated by Equation 7.2.9 and CA the cell area of a grid cell, and the measured snow water equivalent were compared for each time step for which an observation was available. For each location the average mean square error (*MSE*, Eq. 7.2.18) was calculated with respect to all observations, and additionally, the average mean square error of all locations together was determined on the bases of the average mean square error for each location. For each measurement location, the mean square error (*MSE*) is:

$$MSE = \frac{\sum_{m=1,\ldots,k} \left(SWE_c(t_m) - SWE_o(t_m)\right)^2}{k} \qquad (7.2.18)$$

with, t_m, m=1,...k, the time step with a measurement of the snow water equivalent, $SWE_o(t_m)$ (m^3), k *the* number of observations at a measurement location and $SWE_c(t_m)$ (m^3) the calculated snow water equivalent at time t_m. Calibration parameters were tuned with respect to two aspects: 1) visual correspondence of the modelled snow water equivalent and the measured snow water equivalent, 2) minimal average mean square error of all locations together. In the first run, starting values for each calibration parameter were defined according to literature values, which resulted in unsatisfactory correspondence. In the following runs four parameters were kept constant while the parameter for which a better result was expected was changed. In total 30 runs were needed to achieve satisfactory model calibration. Comparing starting values of the calibration parameters with the final calibration result, the model output was most sensitive to the precipitation lapse rate (L_P, Eq. 7.2.6), followed by the temperature threshold (T_c, Eq. 7.2.7) and the restricted degree factor (a_r, Eq. 7.2.15).

Comparing the calibration plots of modelled snow water equivalent with measured snow water equivalent, the fit of observations located in higher altitudes was fair, but model predictions for the locations in lower altitudes, which may be covered with artificial snow in times of too little snow, were unsatisfactory. Therefore a rule-based approach was used to take into account the addition of artificial snow. The approach incorporates that snow is added during the skiing season if the natural snow water equivalent drops below a certain threshold and if the conditions of snow production, in particular that the wet bulb temperature (Henderson-Sellers and Robinson, 1994) is below -3 ºC, are met. This resulted in an average mean square error of 0.00990435 for all location, and the average mean error at each location ranges between 0.006 and 0.152. Appendix 3 of this thesis shows the correspondence between model predictions (SWE_c) and observations of snow water equivalent (SWE_o) of selected plots.

7.2.5 Discussion and conclusions

The aim of the snow model was to assess spatial differences of the snow cover and to describe the impact of the snow melt on the hydrological system. The calibration of plots has shown that the modelled snow water equivalent and the measured snow water equivalent correspond well despite the error involved in the input data, the omission of internal snow processes and the assumptions made to assess snow accumulation and snow melt. These assumptions are that at a certain temperature precipitation is snow, and snow melt is a function of temperature, net radiation and the heat flux of rain. The reasonable model results show that the temperature threshold and the multi index approach are useful methods to describe snow cover changes at this spatial scale. However, the lapse rate to extrapolate precipitation data to unobserved locations, determined by model calibration, was fairly high compared to other studies (Blöschl et al., 1991). When we used a realistic value for the increase of precipitation with elevation,

the measured snow water equivalent was clearly higher than the modelled snow water equivalent. Keeping the realistic regression factor and decreasing the melt factor caused snow to remain at locations that are usually snow free for a couple of months. One reason for the small snow water equivalent predicted by the model could be the error involved in precipitation records; for example that in the valley, the only location for daily records of precipitation which formed the main input for the snow cover development, no precipitation was recorded while there was precipitation in higher elevations. Another reason could be the use of constant melt factors for the total modelling period to transfer energy input to melt rates, while in reality the melt factor varies with snow properties; for instance wet snow requires less energy to be melted than dry snow. Additionally, meteorological data from a neighbouring meteorological station, which were used in periods for which no data were measured in the field, were assumed to be representative for the study area and a constant fraction was taken for the annual cloud cover (Table 7.1). Moreover, internal snow processes and displacement of snow by wind drift were totally neglected, and snow samples were taken on a ski slope, which is regularly subject to slope preparation and snow compaction, so there is a lot of water in the snow pack and more energy is needed to melt the snow pack. In the planning of ski pistes the displacement of snow by wind drift is an important process, however, it is very difficult to include this process in the snow model because of the unpredictability of wind.

Modelling snow accumulation with a spatio-temporal process based model generated approximate snow cover data because of multiple influence factors such as measurement errors in the input data, interpolation of recorded input data to unobserved locations and the definition of a constant temperature threshold (T_c, Eq. 7.2.7), while the threshold may be different for varying weather conditions. Nevertheless, it turned out to be a useful method to describe snow accumulation in space and time and to identify spatial differences with respect to the physical shape of a terrain.

The multiple index approach requires fewer input data than the energy balance, commonly used for point applications, but it still requires data that are usually not available such as cloud cover or continuous air temperature and relative humidity data. So assumptions had to be made, increasing the error of the final prediction.

Snow was described in terms of water slice instead of a porous medium. On one hand this facilitated the estimation of the snow cover development, but on the other it was not possible to include internal snow processes and to consider the effect of albedo and emissivity with changing snow properties.

The uncertainty involved in the individual components of the model could be compensated by adjusting calibration parameters and incorporating a rule-based approach for the addition of artificial snow to achieve maximal correspondence between modelled snow water equivalent and measured snow water equivalent, thus the snow model is a useful tool be used for a comparative study in the planning of new ski runs, where the aim is to identify relative spatial differences rather than to determine absolute snow melt rates, for example as required for hydro-power generation, or to assess the amount of water for domestic use. Nevertheless, when applied to another study area, calibration parameters need to be fitted to the new circumstances.

7.3 Hydrological model

with Derek Karssenberg

7.3.1 Introduction

For the purpose of this thesis the main aim of hydrological modelling is to predict hydrologically driven land degradation, in particular flooding, erosion and slope instability. In order to predict erosion, overland flow is an important component of the hydrological model as it is the main process that triggers erosion. The main causes of overland flow in the area may be 1) periods with heavy rainfall, and 2) high rates of snow melt in spring. To capture both processes, a hydrological model (HE-model) was developed with a time step of one hour. This model was run over a period of 17 weeks representing the melting period. It is assumed that the main erosion occurs in this period, and that the results of this period are representative for a whole year. In principle, a shorter time step and a longer model run-time, for example a whole year, would be better, but this is not feasible from the viewpoint of model run-times within the decision model (c.f. Chapter 6). The same model computes the maximum discharge at the outflow point of the catchment representing the sensitivity of the catchment to flooding. A slightly modified version of the one-hour time step model was used for calculating groundwater levels, which are important for slope instability. It is assumed that slope stability is related to the pore pressure imposed by the groundwater level, which is seen to be controlled by infiltration to the soil and groundwater flow. This model (HS-model) uses a daily time step, sufficient to represent temporal changes in the groundwater system. Since this model uses a longer time step than the HE-model, it is possible to run it for a whole year, resulting in run-times that are still feasible for the analysis such as few hours to a day.

There are many ways to describe the mechanism of the hydrological system and its components. With respect to the aim of hydrological research the models differ in the representation of the process, the spatial scale and the temporal resolution. Models range from very simple, mostly empirical models using a black box approach to complicated physically based models based on the laws of physics. But none of the existing rainfall-runoff models and standard procedures to describe hydrological processes could meet the data requirements and the conditions with respect to spatial and temporal support of the prediction that have been defined for a hydrologic model to be used for multicriteria decision making to support the planning of ski runs (c.f. Chapter 6). So there was no realistic alternative to be implemented for this study. To this end hydrological processes have had to be represented in this thesis by empirical models that fit both the time step used and the available data.

Figure 7.4 shows the underlying model structure that was developed to describe the mechanism of the hydrological system of a small watershed in the mountains.

Interception by vegetation (7.3.2), evapotranspiration (7.3.3) to the atmosphere, infiltration to the soil (7.3.4), saturated overland flow (7.3.5) and groundwater flow (7.3.6) along the bedrock were regarded as important hydrological components to be

included in the model. The following Sections 7.3.2 to 7.3.6 discuss the components of the modelling scheme, and Section 7.3.7 explains the implementation and calibration of the HE-model and HS-model.

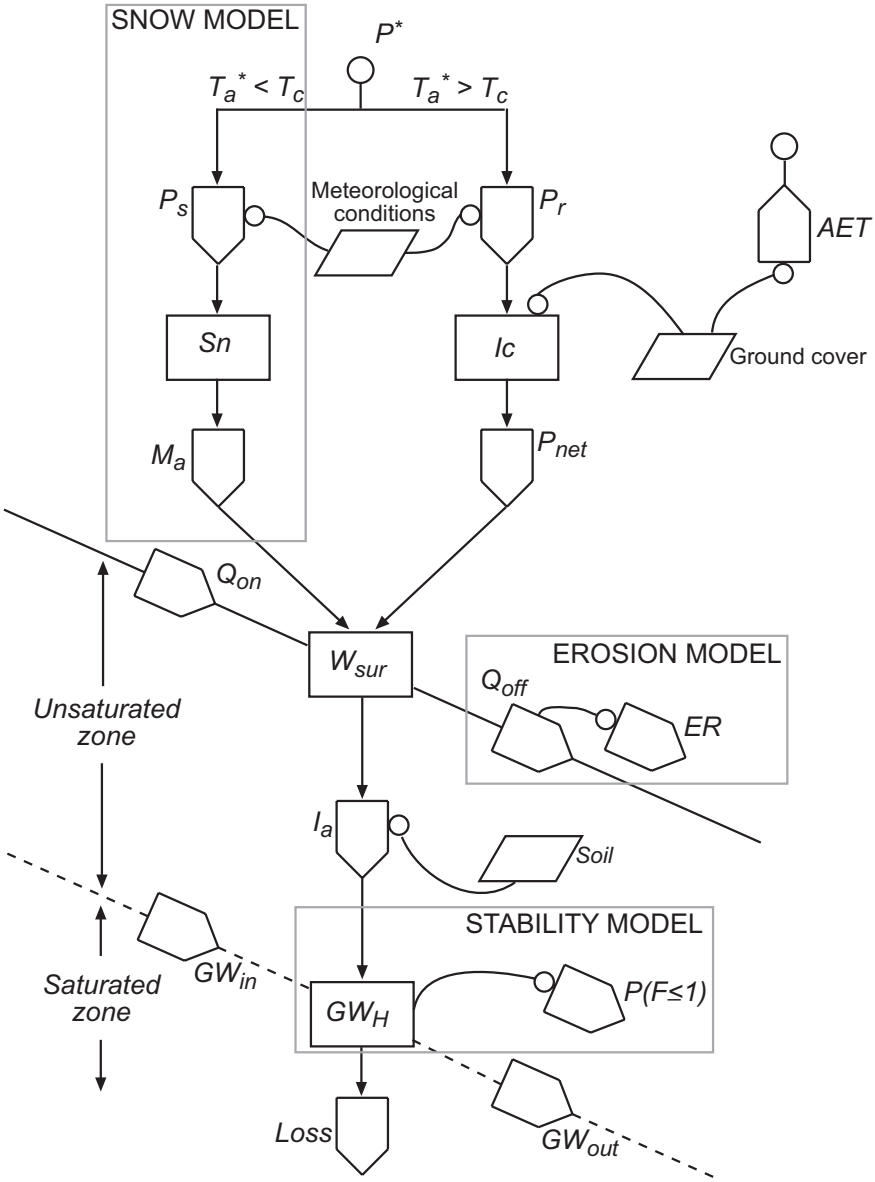

Figure 7.4 Components and modelling structure of the hydrological model; with, P^* the precipitation (m), T_a^* air temperature (ºC), T_c temperature threshold (ºC), P_s snow (m water slice), P_r rainfall (m), *Sn* snow thickness (m water slice), M_a the melt rate (m/time step), *Ic* the interception (m/time step), P_{net} the net rain supplied to the soil surface (m/time step), *AET* actual evapotranspiration (m/time step), W_{sur} the amount of water at the surface available for infiltration (m), Q_{on} the amount of water draining into a cell (m/time step), Q_{off} the amount of water leaving a cell as runoff (m/time step), I_a the actual infiltration (m/time step) into the soil, GW_H the groundwater level (m), GW_{in} groundwater flow draining into a cell (m/time step), G_{out} the groundwater flow to the downstream neighbour (m/time step), *ER* erosion (kg/m^2) and $P(F\leq1)$ (-) the probability of slope failure.

7.3.2 Interception

Interception is defined as the part of the rainfall ($P_r(t)$, Eq. 7.2.7) that is intercepted by vegetation, but never reaches the soil surface. The other part of the rainfall (throughfall) becomes available for infiltration or overland flow. Principally interception is determined by the vegetation type, the stage of development, and the intensity, duration, frequency and form of precipitation. For the HE-model, interception is represented by an equation (Merriam, 1973) similar to those used in event-based runoff models, with the difference that the rainfall accumulated on the vegetation (P_{cum}, m) can be emptied according to 7.3.2. For an area covered with vegetation, the amount of water in the interception store ($IcSt$, t) (m), at time step t is modelled as:

$$IcSt(t) = IcStM \cdot (1 - e^{\frac{-P_{cum}(t)}{I_cStM}}) \tag{7.3.1}$$

with, $IcStM$ (m) the maximal amount of water that can be stored on the vegetation type and $P_{cum}(t)$ (m) the cumulative amount of rainfall stored on the vegetation. The values of the maximal interception store, $IcStM$, depend on the vegetation type (Section 7.3.7, Table 7.3). For each time step, P_{cum} (t) is calculated as:

$$\begin{aligned} &P_{cum}(t) = P_{cum}(t-1) + P_r(t) && \text{if " t is not dry"} \\ &P_{cum}(t) = 0 && \text{if " t is dry"} \end{aligned} \tag{7.3.2}$$

with, “t is dry” representing a time step with $P_r(t\text{-}5, t\text{-}4, \ldots, t)$=0, particularly a continuous period of five hours without rainfall, and “t is not dry” otherwise. It has been assumed that all water in the interception store will have evaporated within five hours. Assuming a 100% vegetation cover, the water flux going to the interception store ($ToIc$(t), m/time step) within one time step is:

$$ToIc(t) = IcSt(t) - IcSt(t-1) \tag{7.3.3}$$

with, $IcSt(t)$ (m) the amount of water in the interception store at time t (Eq. 7.3.1) and $IcSt(t\text{-}1)$ the amount of water in the interception store at the antecedent time step (Eq. 7.3.1). For the HE-model, the amount of water in a grid cell that is intercepted by vegetation ($Ic(t_{HE})$, m/time step) is:

$$Ic(t_{HE}) = COV \cdot ToIc(t_{HE}) \tag{7.3.4}$$

with, t_{HE} the time step of the HE-model and COV the fraction of the land surface covered with vegetation (7.3.7, Table 7.3). For the HS-model, interception is assumed to be a part of the evapotranspiration rate (7.3.3). For each time step, the net rain supplied to the ground surface ($P_{net}(t)$, m/time step) is computed by:

$$P_{net}(t) = P_r(t) - Ic(t) \tag{7.3.5}$$

with, $P_r(t)$ the rainfall (m/time step, Equation 7.2.7).

7.3.3 Evapotranspiration

In many process-based models evapotranspiration is modelled using the Penman-Monteith equation (Monteith, 1965; Calder, 1977), which computes potential evapotranspiration. Since this equation needs many input data and parameter values, which are mostly not available in the framework of decision making and expensive to collect, a temperature-based approach (Thornthwaite, 1948) is used to assess potential evapotranspiration. For the HS-model potential evapotranspiration ($PET(t_{HS})$, m/time step) is computed on a daily base according to:

$$PET(t_{HS}) = 29.8 \cdot D \cdot (e_a^* \cdot T_a^*(t_{HS}) / (T_a^*(t_{HS}) + 273.2) \quad (7.3.6)$$

with, t_{HS} the time step of the HS-model (days), D the duration of day light (hours), $e_a^*(t)$ the saturated water pressure (kPa) and $T_a^*(t)$ the average air temperature (Eq. 7.2.5) during a day (ºC). It is assumed that the soil is sufficiently wet, and for that case actual evapotranspiration (AET, m/time step) can be assumed to be the same as PET. For the HE-model potential evapotranspiration ($PET(t_{HE})$, m/time step) was derived from the HS-model, assuming a constant evapotranspiration rate during one day:

$$PET(t_{HE}) = PET(t_{HS}) / 24 \cdot t_{HE} \quad (7.3.7)$$

with, t_{HE} the time step of the HE-model (hours).

7.3.4 Potential infiltration

Infiltration is the process of water penetrating from the ground surface into the soil according to a given infiltration rate. The potential infiltration rate ($I_p(t)$, m/time step) is the amount of water that can infiltrate in one time step when an excess of water is available at the surface. $I_p(t)$ depends on the hydrological conditions below the surface. The actual infiltration rate is determined by the potential infiltration rate and the amount of water at the surface available for infiltration. The latter is partly controlled by the runon from upstream areas and therefore explained in the section of surface water routing (7.3.5). Under unsaturated conditions of the soil, the potential infiltration rate is controlled by factors such as the condition and the type of the ground cover, the antecedent weather conditions and therefore the variable hydrological characteristics of the soil, the porosity of the soil and the saturated hydraulic conductivity of the soil. Physically based equations such as the Richard-equation (Richards, 1931) or Green-Ampt-equation (Green and Ampt, 1911) address all these factors, but have the disadvantage that they require many inputs. The model described here assumes that

potential infiltration under unsaturated conditions is equal to the saturated conductivity of the upper soil. This approach neglects higher potential infiltration rates at the start of a rainstorm as a result of suction force. It is assumed that this process is of minor importance.

Since alpine areas, in particular the research area, have very thin soils, also the filling up of the pore space in the soil, resulting in saturated conditions throughout the profile, needs be taken into account. Under saturated conditions, the potential infiltration rate equals zero and runoff occurs as saturated overland flow. Representing both infiltration under unsaturated conditions and saturated conditions, the potential infiltration rate ($I_p(t)$, m/time step) is modelled as:

$$\begin{aligned} I_p(t) &= K_{TS}(\mathrm{t}) && \text{if } Unsat(t) > K_{TS}(t) \\ I_p(t) &= Unsat(t) && \text{if } Unsat(t) \le K_{TS}(t) \\ I_p(t) &= 0 && \text{if } Unsat(t) = 0 \end{aligned} \qquad (7.3.8)$$

with $K_{TS}(t)$ the amount of water (m) that could theoretically be stored in the soil during one time step t and $Unsat(t)$ (m) the amount of water (m) that can be stored in the soil until saturation is reached. $K_{TS}(t)$ is:

$$K_{TS}(t) = K \cdot TS \qquad (7.3.9)$$

with, K the saturated hydraulic conductivity of the upper soil (m/h) and TS the duration of a time step (hours). The value of $Unsat(t)$ is derived by subtracting the thickness of the saturated zone from the soil thickness and taking into account the porosity of the soil:

$$Unsat(t) = (S_{Th} - GW_H(t)) \cdot \theta_s \qquad (7.3.10)$$

with, S_{Th} the soil thickness (m) (Section 7.3.7, Eq. 7.3.23), $GW_H(t)$ the thickness of the saturated zone (m) (Eq. 7.3.15), equivalent to the groundwater height, and θ_s the soil moisture storage (m^3/m^3).

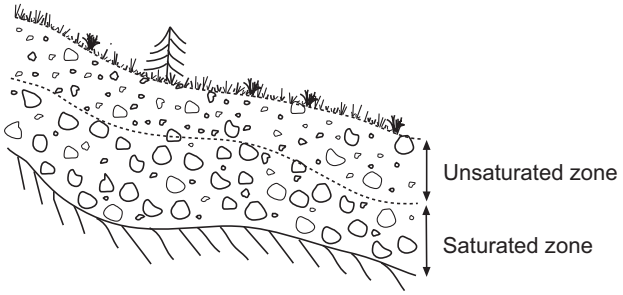

Figure 7.5 Division of the soil into saturated zone and unsaturated zone. The dashed line represents the groundwater level, which is controlled by the input to the soil, soil properties and the groundwater flow.

7.3.5 Surface water routing

Surface water routing deals with the movement of water along the surface to the downstream cells following the local drain direction. The local drain direction is the direction of the steepest downhill slope as determined from a gridded digital elevation model according to the D8 algorithm (Burrough and McDonnell, 1998; Moore et al., 1993; PCRaster, 1996). Event-based models usually use the kinematic wave model (Chow, 1988) for the transport of material. However, due to the limitations with respect to data, model-run time and therefore spatial and temporal resolution, the use of the kinematic wave model was not feasible. If we assume that within one time step all water above the surface reaches the outflow point of the catchment, we can use the PCRaster operation *accuflux* (PCRaster, 1996), which calculates the accumulated amount of water that flows out of a cell into its neighbouring downstream cell. This accumulated amount is the material in the cell itself plus the amount of material in all upstream cells of the cell. The topological linkages defining upstream and downstream neighbours are given by the local drain direction map. The transport of water was computed using the PCRaster function *accuthresholdflux*. This function only allows water to flow to the downstream neighbouring cell if the cell itself is saturated according to the threshold level (Figure 7.6).

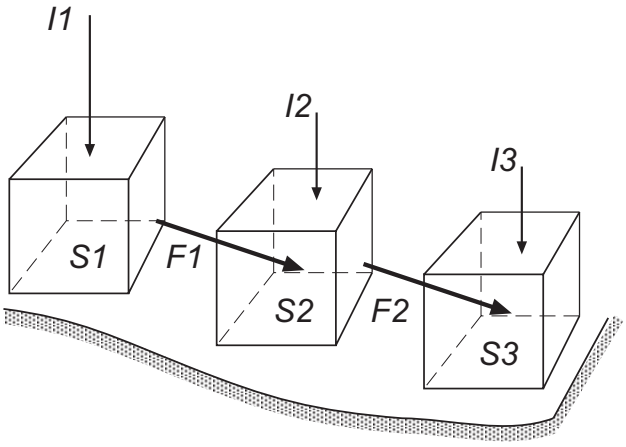

Figure 7.6 Interaction between inputs (I), storages (S) and fluxes (F) in simples systems (in: Burrough, 1998). If the storage capacity, i.e. the potential infiltration capacity ($I_p(t)$, is larger than the input to the cell, i.e. the surplus of water above the surface ($W_{sur}(t)$, m; Eq. 7.3.12), there is no flow downstream. Otherwise the difference between storage capacity and input ($W_{sur}(t)$-$I_p(t)$) is transported to the downstream neighbouring cell.

For each cell, *accuthresholdflux* assigns the amount of water at the surface that is draining to the neighbouring downstream cell (Q_{out}, m/time step, Eq. 7.3.14), while *accuthresholdstate* defines the amount that can actually infiltrate under unsaturated conditions until the cell is saturated. For each cell, the actual infiltration rate ($I_a(t)$, m/time step) is calculated by:

$$I_a(t) = \min\left(W_{sur}(t), I_p(t)\right) \tag{7.3.11}$$

with, $W_{sur}(t)$ the surplus of water above the surface (m) at time t available for infiltration and $I_p(t)$ the potential infiltration rate (m/time step) at time t (Eq. 7.3.8). The operation min(x,y) assigns the minimum value of x and y, in this case $I_a(t)$ is defined by the lower value of the water available for infiltration and the potential infiltration capacity. For a cell, the surplus of water ($W_{sur}(t)$, m) at time t is the sum of:

$$W_{sur}(t) = P_{net}(t) + M_a(t) + GW_{ab}(t) + Q_{on}(t) \tag{7.3.12}$$

with, $P_{net}(t)$ the net rainfall supplied to the surface (m/time step) at time t (Eq. 7.3.5), $M_a(t)$ the actual snow melt rate (m/time step) at time t, Equation 7.2.12, $GW_{ab}(t)$ the amount of exfiltration water above the surface (m) if the soil was saturated in the antecedent time step, Equation 7.3.22, and $Q_{on}(t)$ the amount of runon to the cell (m/time step), Equation 7.3.13. Figure 7.7 illustrates the concept of runon to a cell and runoff from a cell.

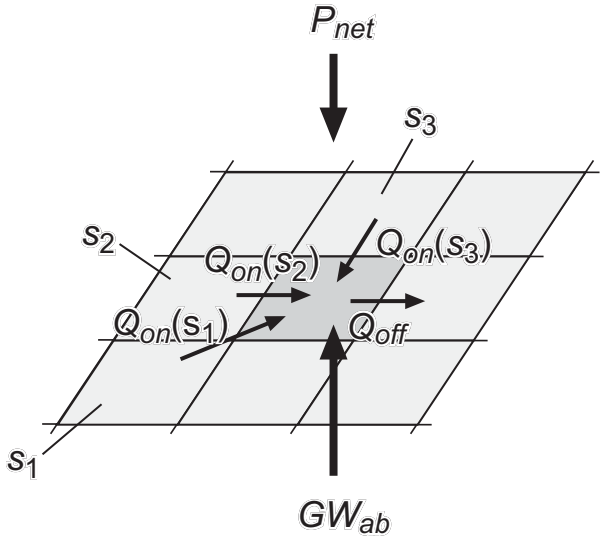

Figure 7.7 Interaction of neighbouring grid cells with respect to runoff is shown by a window of 3 by 3 cells; where, s_i, i=1,…,n and n between 1 and 7 an upstream neighbour, $Q_{on}(s_1)$ the amount of water coming from the upstream neighbour s_1 (m/time step), $Q_{on}(s_2)$ the amount of water coming from the upstream neighbour s_2 (m/time step), $Q_{on}(s_3)$ the amount of water coming from the upstream neighbour s_3 (m/time step), Q_{off} the amount of water flowing to the downstream neighbour (m/time step), P_{net} the input to the surface, i.e. net rain (m/time step), and GW_{ab} groundwater exfiltration above the surface (m).

Accordingly, runon (Q_{on}, m/time step) to a cell under consideration is defined as:

$$Q_{on}(t) = \sum_{i=1}^{n} Q_{out}(s_i, t) \tag{7.3.13}$$

with, $Q_{out}(s_i,t)$ (m/time step) the runoff received from the upstream neighbouring cells s_i, with i=1,...,n, and n between 1 and 7. A neighbouring upstream cell is a cell draining into a cell following the local drain direction. For each cell s_i, the outflow ($Q_{out}(s_i,t)$, m/time step) at time t is:

$$Q_{out}(s_{i,}t) = W_{sur}(s_i,t) - I_a(s_i,t) \tag{7.3.14}$$

In the case of total saturation, exfiltration from the groundwater ($GW_{ab}(t)$ m/time step) may occur, which is considered in Equation 7.3.21.

Since all water that remains at the surface after infiltration is brought to the outflow point of the catchment within one time step, it is not possible to include travel time, resulting in an overestimation and underestimation of the discharge.

7.3.6 Saturated zone and groundwater flow

The spatial and temporal dynamics of the groundwater height are determined by soil moisture storage, the percolation rate (assumed to be equal to infiltration, $I_a(t)$, m/time step), the inflow from the upstream area and the groundwater flow to the downstream area. It is assumed that groundwater flow follows the topology of the bedrock, controlled by the height of the groundwater, the saturated conductivity of the subsoil and the slope of the bedrock. The slope of the bedrock is derived by applying the slope function (Horn, 1981; PCRaster, 1996) to the elevation model of the bedrock, which is generated by subtracting the estimated soil thickness (Section 7.3.7, Eq. 7.3.23) from the elevation at the top of the surface. For each time step, the calculation of the groundwater height is determined in several steps: first the potential height of the groundwater level is determined according to the actual water volume present in the saturated zone (7.3.15 and 7.3.16), followed by the description of the groundwater flow to the down stream area and (7.3.17) and the groundwater inflow from the upstream area (7.3.18). Finally, the groundwater height is defined in terms of the intermediate groundwater fluxes and states (7.2.19).

The groundwater height, controlled by the soil moisture storage, is expressed as:

$$GW_H^{*}(t) = GW^{*}(t) / \theta_s \tag{7.3.15}$$

with, $GW_H^*(t)$ the groundwater height (m), $GW^*(t)$ the amount of water (m water slice) in the saturated zone without a soil matrix, and θ_s the soil moisture storage (m^3/m^3), and where $GW^*(t)$ is given by its state in the antecedent time step and the vertical fluxes according to:

$$GW^{*}(t) = GW(t-1) + P_c(t) - PET(t) \tag{7.3.16}$$

with, $GW(t\text{-}1)$ the amount of water in the saturated zone in the previous time step (m water slice) and P_c the percolation rate (m/time step) assumed to be equivalent to actual

infiltration (I_a(t), m/time step, Eq. 7.3.11). For a cell, the groundwater flow to the downstream neighbour is controlled by the saturated hydraulic conductivity of the saturated zone and the slope imposed by the bedrock:

$$GW_{out}(s_i, t) = K_s \cdot GW_H^*(t) \cdot b \cdot \tan S \tag{7.3.17}$$

with, $GW_{out}(s_i,t)$ the groundwater flow (m/time step) to the downstream area, K_s the saturated hydraulic conductivity of the saturated zone (m/time step) (c.f. Section 7.3.7, Table 7.3), b the width of a grid cell (m) and S the slope (degrees) imposed by the relief of the bedrock. The principle of the groundwater flow is shown in Figure 7.8.

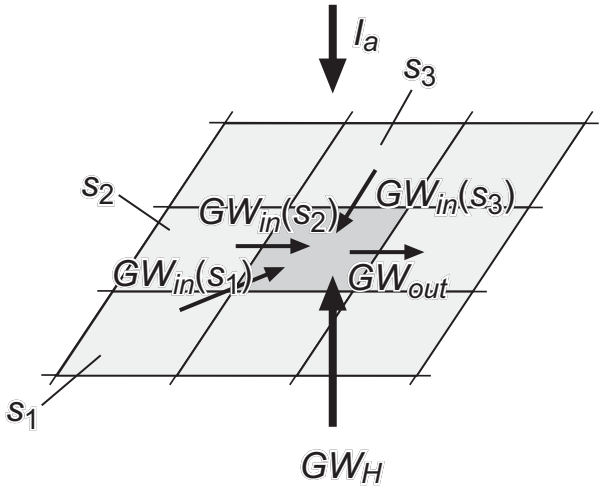

Figure 7.8 Interaction of neighbouring grid cells with respect to groundwater flow is shown by a window of 3 by 3 cells; where, s_i, i=1,…,n and n between 1 and 7 an upstream neighbour, $GW_{in}(s_1)$ the groundwater flow from the upstream neighbour s_1 (m/time step), $GW_{in}(s_2)$ the groundwater flow from the upstream neighbour s_2 (m/time step), $GW_{in}(s_3)$ the groundwater flow from the upstream neighbour s_3 (m/time step), GW_{out} groundwater flow to the downstream neighbour (m/time step), I_a the input to the soil, i.e. actual infiltration rate (m/time step), and GW_{ab} groundwater level (m).

For a cell, the total inflow of groundwater (GW_{in}, m/time step) from upstream neighbouring cells is:

$$GW_{in}(t) = \sum_{i=1}^{n} GW_{out}(s_i, t) \tag{7.3.18}$$

with, $GW_{out}(s_i,t)$ (m^3/time step) the groundwater flow received from upstream neighbouring cells s_i, with i=1,..,n the upstream neighbouring cells and n between 1 and 7. For each cell, the total thickness of the saturated zone ($GW_{Tot}(t)$, m) at time t is:

$$GW_{Tot}(t) = GW_H^*(t) + (GW_{in}(t) - GW_{out}(t)) / \theta_s \tag{7.3.19}$$

with, $GW^*_H(t)$ the groundwater height at time t without groundwater flow, $GW_{in}(t)$ the groundwater inflow (m/time step) at time t from the upstream neighbouring cells (Eq. 7.3.18), $GW_{out}(t)$ the groundwater flow (m/time step) leaving the cell at time t and θ_s the soil moisture storage (m^3/m^3) of the subsoil. Under saturated conditions, exfiltration to the surface may occur:

$$Seep(t) = \max(GW_{Tot}(t) - STh, 0) \tag{7.3.20}$$

with, $Seep(t)$ the part of the groundwater height that is above the surface (m). Since the groundwater height is a function of the pore volume, the absolute water height above the surface of a grid cell is:

$$GW_{ab}(t) = Seep(t) \cdot \theta_s \tag{7.3.21}$$

with, $GW_{ab}(t)$ the amount of groundwater exfiltration at the surface (m) and needed to compute saturated overland flow (Eq. 7.3.12) For each cell, the water height of the saturated zone ($GW(t)$, m) at time t is:

$$GW(t) = \left(GW_{Tot}(t) - Seep(t)\right) \cdot \theta_s \tag{7.3.22}$$

$GW(t)$ (m) is required for the following time step in Equation 7.3.16.

7.3.7 Model implementation and calibration

The HE-model is computed for every hour of the snow melt period and the HS-model is run on a daily time step covering one year (c.f. Chapter 6, Figure 6.2). Spatial information on site factors is retrieved from the common database (c.f. Chapter 6), while meteorological conditions are supplied by the SN-model (7.2), both for the HE-model and HS-model. Ski runs scenarios require possible locations of simulated ski runs and the modified digital elevation model. These data are provided by the ski run model, which has been discussed in Chapter 3. Soil maps of alpine areas are sparse, especially above an elevation that is not suitable for farming. Moreover, soil thickness of such a heterogeneous terrain is difficult to map. To this end soil thickness was modelled as a quadratic function of the slope:

$$\begin{aligned} STh &= \frac{y-b}{S_c^{\,2}} \cdot S^2 + b \qquad \text{if } S < S_c \\ STh &= d \qquad\qquad\qquad\quad \text{if } S \geq S_c \end{aligned} \tag{7.3.23}$$

with, STh the soil thickness (m), y a constant of the quadratic function, b the maximum soil thickness derived by calibration, S the slope angle (degrees), S_c the critical slope angle (degrees) above which the soil is assumed to be constantly thin and d the soil

thickness (m) that was assigned to very steep slopes. The choice for this function originates from the fact that the potential for soil formation is very little on steep slopes, while in flatter terrain the role of slope angle is of little importance.

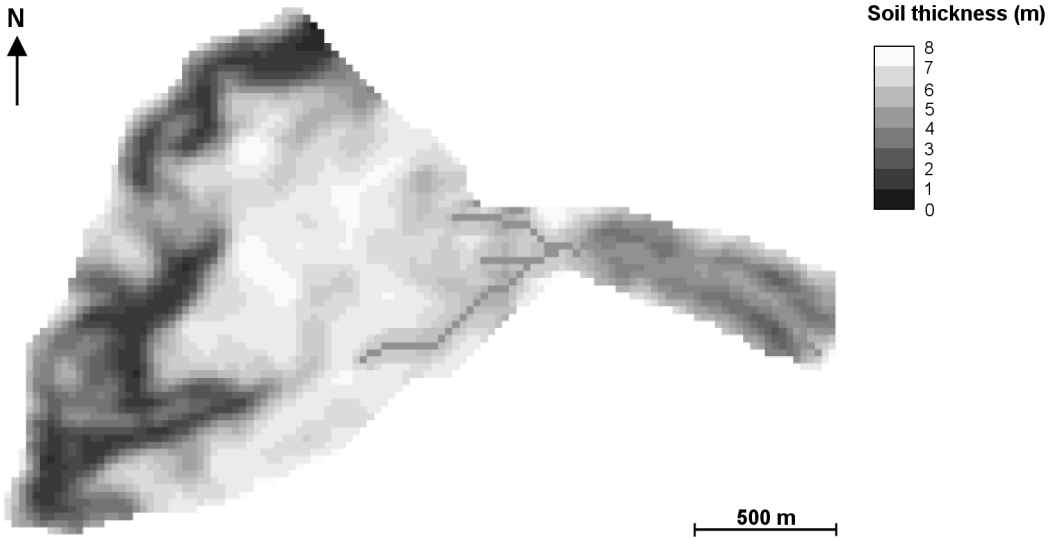

Figure 7.9 Estimated soil thickness (m). The gradual change of the grey scale from light to dark represents the decrease in soil thickness, which is assumed to decrease with increasing slope angle according to a quadratic function. The maximal soil thickness was used as a calibration factor and defined with 8 m.

Calibration parameters and other model input were retrieved from literature, measurements and by calibration, shown in Table 7.3 and Table 7.4.

Table 7.3 Parameter values for the HE-model.

Parameter	Symbol	Value	Unit	Source
Maximum soil thickness	*b*	8	m	calibrated
Hydraulic conductivity for infiltration	*K*	0.18	m/h	measured
Saturated hydraulic conductivity	K_s	0.5	m/h	calibrated
Density of vegetation cover	*COV*	Table 7.4.	(-)	estimated
Maximum interception store	*IcStM*	Table 7.4	m	Morgan (1998)

The vegetation cover is classified according to the vegetation map (Chapter 6), and each vegetation type is assigned a value for maximal interception store *IcStM* and coverage *COV*.

Table 7.4 Density of land cover and maximal interception store for each vegetation type.

Vegetation type	COV (-)	Source	IcStM (-)	Source
Alpine grass	0.9	estimated	0.23	Morgan (1998)
Alpine meadow	0.9	estimated	0.23	Morgan (1998)
Alpine heaths	0.95	estimated	0.15	Morgan (1998)
Forest	0.4	estimated	0.25	Morgan (1998)

Model calibration was done using the measured discharge data (Chapter 4) for the snow melt season of 2000 (see Figure 7.10). The timing of the peak could be modelled quite accurately, since the discharge of the river responded quickly to rainfall, but modelled peak runoff was three times as high as the measured peaks, the fluctuation of the baseflow was also considerable high.

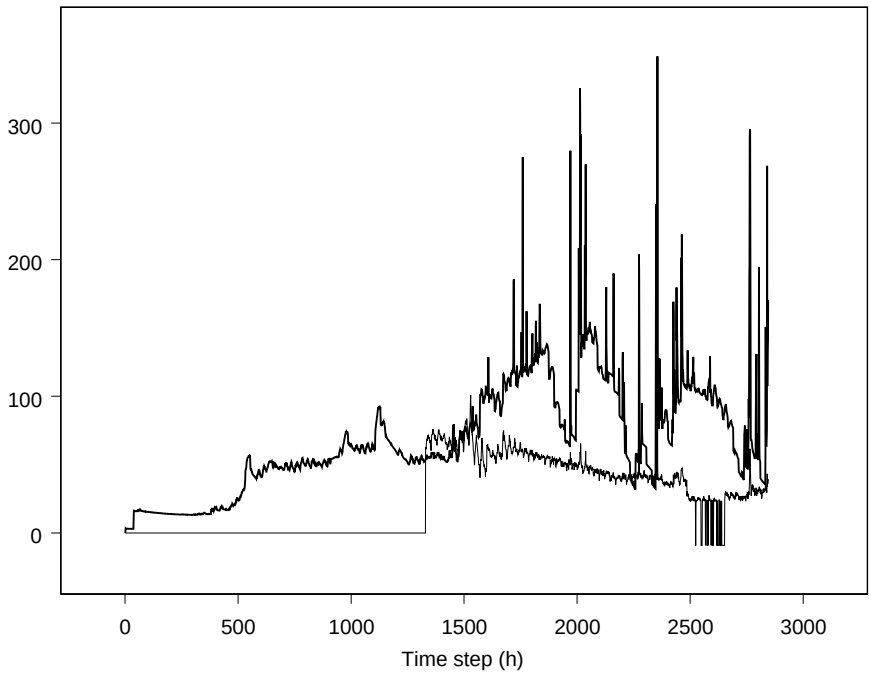

Figure 7.10 Discharge ($Q(t)$, l/s), calculated by the HE-model – the thinner line represents the measured discharge and the thicker line shows the simulated one. In the first part of the modelling period the line representing the measured discharge is constantly 0 because for that period no measurements were available. The same holds for the strange values after time step 2500.

Relevant model results are shown in the Figures 7.11 and 7.12. Figure 7.11 illustrates the change of the groundwater level, represented by the change of the difference between the soil thickness and the groundwater height, both at the beginning of the snow melt season and at the end. The groundwater level is an important driving force in predicting unstable slopes. The comparison of these two maps shows that at the end of the snow melt season

the groundwater is much higher than in the beginning, especially where concentrated flow is dominating. Increase in groundwater implies an increase of the risk of slope instability. The concentrated flow is also reflected by Figure 7.12, which displays the overland flow after a rain event. Overland flow is one of the causal factors for the occurrence of erosion.

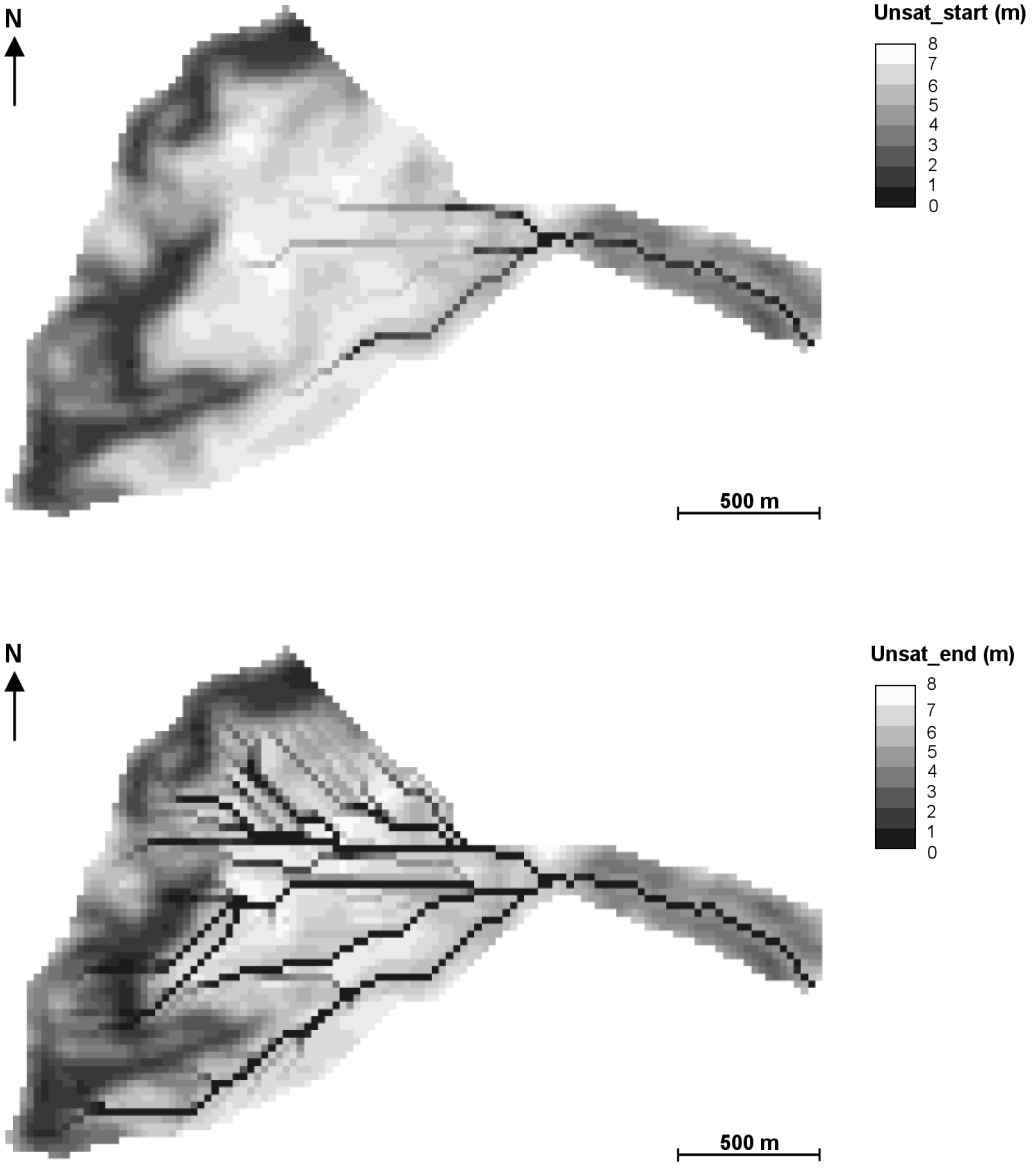

Figure 7.11 At the top the difference between the soil thickness and the groundwater height (*Unsat*, m) at the beginning of the snow melt season ($GW_H(t$=1April 2000), m) is shown, and at the bottom at the end (t=21 June 2000). The low groundwater level and therefore a larger difference between soil thickness and groundwater height at the start of the melt period reflect the break of hydrological processes during winter.

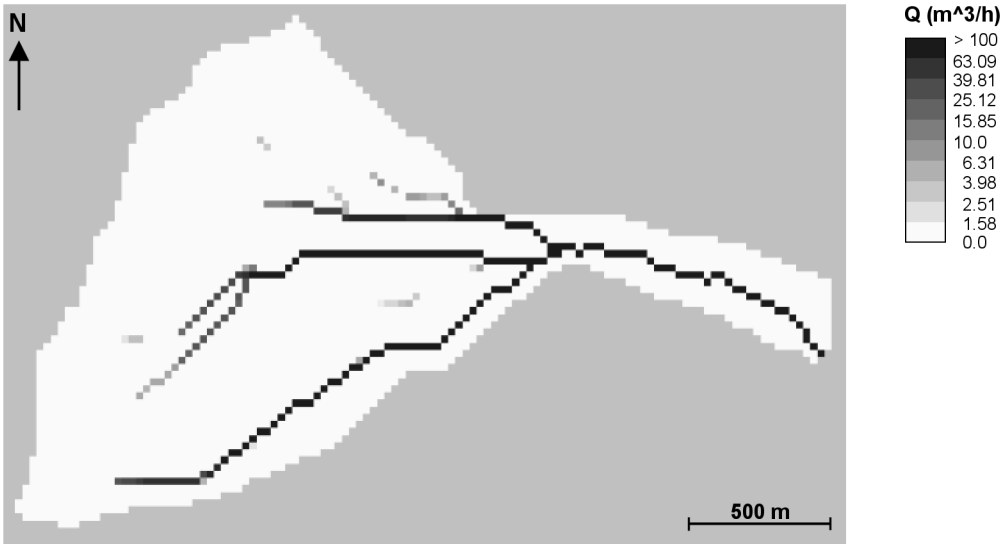

Figure 7.12 Overland flow after a rain event (Q, m^3/h). A logarithmic scale was chosen to improve visibility. Overland flow clearly concentrates along the local drain direction due to the use of the PCRaster operation *accuthresholdflux,* resulting in very high peaks of the discharge at the outflow point of the catchment, also shown by the simulated hydrograph in Figure 7.10.

7.3.8 Discussion and conclusion

Both versions of the hydrological model, the HE-model and the HS-model, represented the annual or seasonal variation of the hydrological cycle. The strong correspondence between rainfall and peak discharge (Figure 7.10) showed the strong response of discharge to rainfall. The gradual increase of the baseflow due to continuous snow melt, also observed in the field, was fairly captured by the model. Nevertheless, the model assists in understanding the hydrological regime of an alpine terrain, i.e. the hydrological differences between winter season and summer season, and the model can also be used to determine the response of hydrological characteristics to different inputs and site conditions, important when analysing the impact of ski pistes on the environmental system. Since the models can be applied with general data, they can be easily applied to another alpine environment. However, calibration parameters have to be fit again. This may involve the acquisition of hydrological data to which the model output can be calibrated. The main disadvantage of using general data and large time steps is that it was not possible to use a physically based approach for surface water routing. The use of *accuflux* or *accuthresholdflux* means that all the water above the surface reaches the outflow point within one time step, which causes travel time to be overestimated in the HE-model, and underestimated in the HS-model. Moreover, it leads to concentrated flow along the local drain directions and gives an immediate response to rainfall. Furthermore, it is not considered that the morainic material can store a lot of water and release it gradually to the outflow point. The inclusion of this process might buffer the high peaks of the discharge, however, it is very difficult to acquire the information about this and to include it in the model. A weakness of the spatial scale is that the width of the mountain

stream is also represented as a grid cell of 25 m, while in reality it is just about one metre. Nevertheless, the HE-model and the HS-model are useful tools to investigate the hydrological behaviour of a catchment and to compare potential sites for ski runs in the first stage of a planning process. At a later state, when choosing a certain location among few feasible alternatives, more detailed models could be used to optimise the decision making process because the acquisition of input data for a few ski runs could be feasible as a part of an overall socio-economic plan.

8 MODELLING HAZARDOUS PROCESSES

8.1 Modelling soil erosion

Soil erosion is an unwanted, but frequently observed feature at ski pistes, especially if the vegetation cover is scarce and the topographical slope smooth. It is controlled by three factors, 1) the erosivity - the energy provided by rain, runoff and wind able to cause erosion, 2) the erodibility - the resistance of the soil imposed by its mechanical and chemical properties including slope and slope curvature and, 3) the protection of the soil by vegetation. The very critical condition for triggering erosion is caused by the cumulative effect of heavy and long rain events during the snow melt season. The amount of erosion is determined by three processes, 1) detachment of the soil by the erosive agents, 2) transport capacity to move the detached material, and 3) deposition in the case that the sediment load exceeds the transport capacity. Due to the spatial variability of the controlling factors the erosion rate varies in space. In order to predict the amount and the spatial pattern of erosion a simple erosion model based on the revised Morgan-Morgan-Finney model (Morgan, 2001) was linked to the HE-model. While the Morgan-Morgan-Finney model predicts annual soil loss by water for the catchment as a whole, the erosion model used here calculates the annual soil loss for each grid cell of 25 m by 25 m. In order to predict annual erosion with the revised Morgan-Morgan-Finney model (Morgan, 2001), annual rainfall and runoff data are needed. To this end model results received from the HE-model were scaled up to one year according to the procedure described in 8.1.1 and all precipitation is assumed to be rainfall.

In correspondence with the dynamics involved in the process of erosion, the technical description of the model is divided into five parts. The first part deals with the estimation of appropriate input data. The second and the third part explain the detachment of the soil by rain drops or overland flow, followed by the description of the transport capacity. The last part is concerned with the estimation of deposition and net erosion (Figure 8.1, p. 124).

8.1.1 Estimation of input data

For each time step, the HE-model provides the net rain supplied to the surface (P_{net}, m/time step; Chapter 7, Eq. 7.3.5) and the overland flow or runoff under saturated conditions (Q_{out}, m/time step, Chapter 7, Eq. 7.3.14). However, annual totals are needed for the revised Morgan-Morgan-Finney method. Consequently, the values per time step are summed up for the total modelling period of the HE-model, resulting in total rain (*PTot*, m/modelling period) and total overland flow (*QTot*, m/modelling period). Having daily rain records for the duration of one year at one's disposal, the ratio of the rain falling during the snow melt period and the annual rainfall can be calculated from this annual time series of daily rain. For example, if annual rain in the valley is 800 mm and from this 800 mm 380 mm fell during the period to which the runoff of the snow melt period corresponds, the ratio is 0.475. It is assumed that this relation can be used to

estimate annual input values for each grid cell from the totals provided by the HE-models. The amount of annual rainfall (*PAnn*, mm/year) is estimated by:

$$PAnn = \left(PTot \cdot 1000\right) / a \tag{8.1.1}$$

with, *PTot*, the total amount of net rain during the period for which precipitation was measured in the field (m/modelling period of HE-model) and *a* the conversion factor to estimate annual rainfall. In order to estimate annual runoff, it is assumed that the ratio of the rain that fell during the period for which the runoff of the measurement period corresponds and of the annual rain holds for annual runoff. Accordingly, annual runoff (*QAnn*, mm/year) is:

$$QAnn = (QTot \cdot 1000) / b \tag{8.1.2}$$

with, *b* the conversion factor to estimate annual runoff and *QTot* the total runoff for the snow melt period (m/modelling period of HE-model).

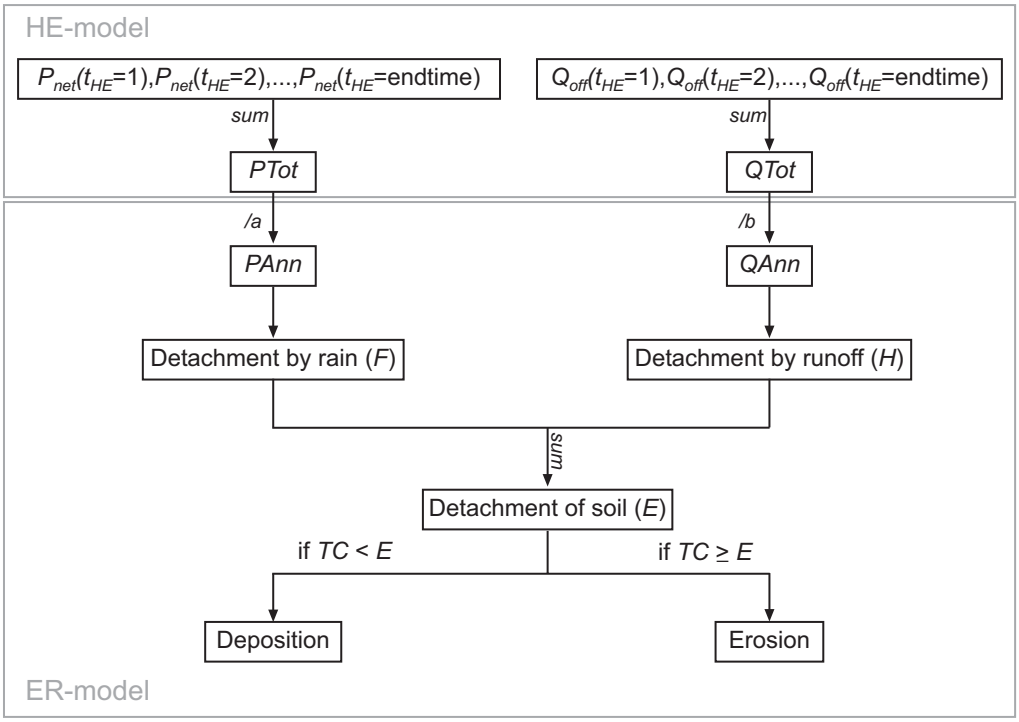

Figure 8.1 Flowchart of erosion model, where, $P_{net}(t_{HE}=j)$ the net precipitation (m/time step) supplied to the soil at time step *j* with $j=1,\ldots,n$, $Q_{off}(t_{HE}=j)$ the surface runoff at time step *j* with $j=1,\ldots,n$ (m^3/time step), *PTot* the sum of net rain during the modelling period of the HE-model (m), *QTot* the sum of runoff during the modelling period of the HE-model (m), *PAnn* the annual rainfall (mm), *QAnn* the annual amount of runoff (mm), *F* the detachment of soil by rain (kg/m^2), *H* the detachment of soil by runoff kg/m^2) and *E* the total amount of erosion (kg/m^2).

8.1.2 Detachment of the soil by rain drops

Soil may be detached by rain due to the kinetic energy of the rain drops. The kinetic energy of rainfall depends on the amount of net rain, the rain intensity and the height and the density of the vegetation. For areas covered with vegetation, annual net rainfall is divided into direct throughfall and leaf drainage, for which the kinetic energy is estimated separately. Leaf drainage from the vegetation depends on the density of the vegetation cover and is given by:

$$LD = PAnn \cdot COV \tag{8.1.3}$$

with, LD the amount of leaf drainage (mm/year) and COV the fraction of a grid cell covered with vegetation (-), also used in the HE-model (Chapter 7). Knowing the amount of leaf drainage, direct throughfall (TF, mm/year) can be calculated according to:

$$TF = PAnn - LD \tag{8.1.4}$$

The kinetic energy of direct throughfall is for the greater part determined by the amount of net rainfall and the rain intensity. It can be described by an empirical function proposed by Morgan (2001) for temperate zones:

$$Q_{kin}TF = TF \cdot \left(11.9 + 8.7 \cdot \log_{10}(I)\right) \tag{8.1.5}$$

with, $Q_{kin}TF$ the kinetic energy supplied by the rainfall directly reaching the ground cover (J/m^2) and I the estimated rain intensity (mm/h, see Table 8.1). Conversely, the kinetic energy of leaf drainage depends solely on the height of the vegetation cover:

$$Q_{kin}LD = \left(15.5 \cdot H^{0.5}\right) - 5.87 \tag{8.1.6}$$

with, $Q_{kin}LD$ the kinetic energy of rain draining from the vegetation (J/m^2) and H the average height of the vegetation (m, see Table 8.2). The total kinetic energy (Q_{kin}, J/m^2) supplied by rainfall is:

$$Q_{kin} = Q_{kin}LD + Q_{kin}TF \tag{8.1.7}$$

The detachment of soil by rain drops is a function of the kinetic energy of rain and the erodibility of the soil:

$$F = B \cdot Q_{kin} \cdot 10^{-3} \tag{8.1.8}$$

with, F the detachment of the soil (kg/m^2) and B the erodibility factor of the soil (g/J).

8.1.3 Detachment of the soil by runoff

The detachment of soil by runoff is controlled by the resistance of the soil, the slope and the density of the vegetation cover. The resistance of the soil is defined as a function of the cohesion of soil particles:

$$Z = 1/(0.5 \cdot COH) \tag{8.1.9}$$

with Z the resistance of the soil (kPa) and COH the soil cohesion (kPa) (Table 8.1). Assuming an exponential relation between runoff and erosion, detachment of soil by runoff can be computed by:

$$H = Z \cdot QAnn^{b} \cdot \sin\alpha \cdot (1 - COV) \cdot 10^{-3} \tag{8.1.10}$$

with H the detachment rate of the soil (kg/m^2), $QAnn$ the annual runoff (mm/year), b an empirical derived factor (Section 8.1.4, Table 8.1), α the slope in degrees and COV the fraction of the ground covered with vegetation.

8.1.4 Erosion

Integrating the detachment of soil by rainfall and the detachment of soil by runoff, for each cell, the total amount of potential erosion (E, kg/m^2 per year) is:

$$E = F + H \tag{8.1.11}$$

with F the amount of soil detached by rainfall (kg/m^2 per year, Eq. 8.1.8) and H the amount of soil detached by runoff (kg/m^2 per year, Eq. 8.1.10). The actual erosion is a function of the potential erosion rate and the transport capacity of annual runoff. For each cell, the transport capacity (TC, kg/m^2 per year) is given by:

$$TC = C \cdot (QAnn^{d}) \cdot \sin\alpha \cdot 10^{-3} \tag{8.1.12}$$

with, C the crop management factor according to the USLE (Wischmeier and Smith, 1962) and d an empirically derived factor (Table 8.1). Deposition of eroded material at a certain location is controlled by the transport capacity: if the transport capacity is lower than the amount of detached soil, a part of the eroded material is deposited, otherwise the total amount of eroded material is transported along the local drain direction (c.f. Chapter 7, surface water routing) to the downstream neighbour (Figure 8.2). For each cell, the amount of eroded material that can be transported by runoff is:

$$E_{out} = \min(E, TC) \tag{8.1.13}$$

with, E_{out} the amount of eroded material (kg/m^2) that is transported to the downstream cell over the local drain direction, where the function min(x,y) assigns the minimum value of x and y. Accordingly, the amount of eroded material that is received from the upstream neighbouring cells is:

$$E_{in} = \sum_{i=1}^{n} E(s_i) \tag{8.1.14}$$

with, E_{in} the amount of eroded material (kg/m^2) received from the neighbouring upstream cells s_i, with i=1,…,n, the neighbouring upstream cells and n between 1 and 7. The flow of eroded material is shown in Figure 8.2. For each cell, net erosion (E_{net}, kg/m^2 per year) is:

$$E_{net} = E + E_{in} - E_{out} \tag{8.1.15}$$

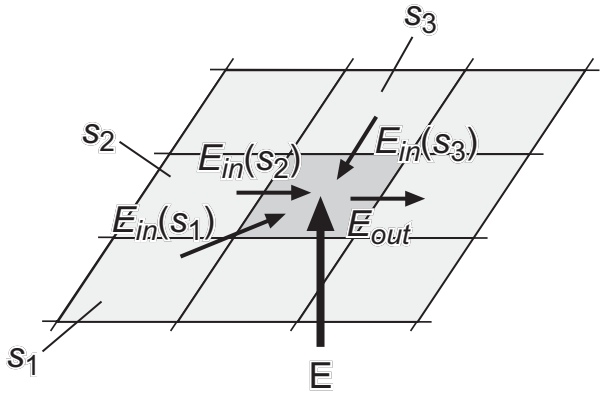

Figure 8.2 Flow of eroded material. Erosion (E) at a cell depends on the erosion received from the neighbouring upstream cells, the detached material at the cell and the transport capacity of the overland flow to transport the material to the downstream neighbour.

Table 8.1 Model parameters for the erosion model for a ski piste scenario and the situation without ski piste.

Parameter	Symbol	Unit	Value	Source
Conversion factor rain	a	-	0.6	estimated
Conversion factor runoff	b	-	0.5	estimated
Rain intensity	I	mm/h	10	Morgan (2001)
Cohesion	c	kPa	3	Morgan (2001)
Cohesion at ski piste	c_p	kPa	2.5	estimated
Erodibility factor	B	g/J	0.3	Morgan (2001)
Erodibility factor for piste	B_p	g/J	0.5	estimated
Crop factor	C	-	0.01	estimated
Crop factor piste	C_p	-	1	estimated
Bfactor	b	-	1.5	Morgan (2001)
Dfactor	d	-	2	Morgan (2001)

Table 8.2 Height and density of various vegetation types.

Vegetation type	Density (-)	Source	Height (m)	Source
Alpine meadow	0.9	estimated	0.15	estimated
Alpine grassland/low	0.9	estimated	0.10	estimated
Alpine grassland/high	0.8	estimated	0.05	estimated
Alpine heaths	0.95	estimated	0.4	estimated
Alpine heaths (calluna vulgaris)	0.95	estimated	0.25	estimated
Forest	0.4	estimated	7	estimated

Annual erosion is calculated for both the total catchment and for any possible ski run location. Just like the hydrological model, the erosion model has been developed to assess differences between the performance of different ski runs rather than for computing absolute values required to design mitigation measures to prevent serious erosion.

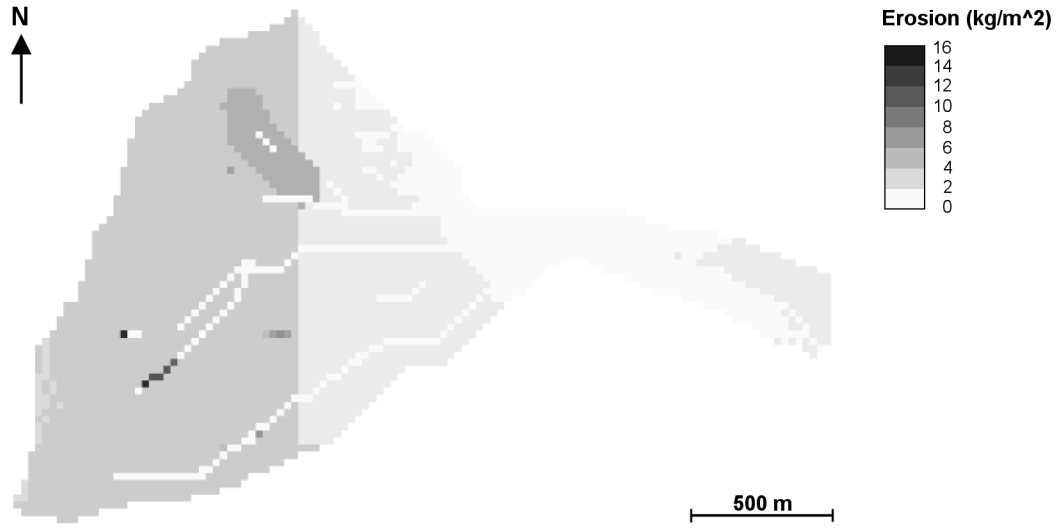

Figure 8.3 Spatial distribution of annual erosion (kg/m^2). The high values on the ski run are a consequence of the assumption that a ski piste is bare (Chapter 10, Table 10.1). The sharp transition is caused by the vegetation type map which was used to determine ground cover because bare areas have not been mapped.

8.1.5 Discussion and conclusion

The erosion model predicts the spatial distribution of annual erosion, which makes it possible to compare ski runs because for each ski run average annual erosion or maximum annual erosion can be derived from the model output, assuming a bare soil surface at each potential site for a ski piste. The temporal variation of rainfall and surface runoff is considered by deriving the input to the erosion model from the HE-model, which computes hydrological fluxes and states for every hour. An event based erosion

model would give more accurate information for the risk of single events, especially when mitigation measures have to be designed to prevent erosion. However, due to the conditions with respect to data and computer run-time it is not feasible to apply an event-based model for each ski run alternative. Since the aim is to compare the performance of each ski run rather than to derive absolute values required for designing mitigation measures, the erosion model is a useful tool to be used in this kind of decision framework.

It was assumed that all runoff occurring during the snow melt period refers to the precipitation that fell as snow including the rainfall during the snow melt period. When using the decision model for an initial site investigation to identify potential sites for ski runs and to compare them with each other, the erosion model is a useful tool. However, if absolute erosion values are required, for example for making the final decision whether to build the new ski run or not, the erosion model needs to be replaced by a model that is able to take into account snow covered periods.

8.2 The slope stability model

8.2.1 Introduction

In general, triggering of landslides is controlled by the strength of the soil and the geometry of a slope, (Lee et al., 1983). Landslides may be triggered by a rise of pore pressure in the slope that decreases the resistance of a slope and therefore increases the risk of *slope failure*. Failure is mainly induced by the decrease in strength, which is unable to support the weight of the soil. Free draining water does not substantially add to the disturbing forces acting on a slope. In natural hill slopes, the higher pore pressure is often induced by raised groundwater levels after prolonged or excessive rain or snowmelt. In order to predict hydrologically driven slope instability, the stability model derives information from the HS-model to take into account the impact of spatial and temporal groundwater fluctuations.

8.2.2 Model building

The stability model, described in this section, is a simplified version of the stability model PROBSTAB developed by Van Beek (2002). It aims to estimate the probability that the area covered by a given ski run might be threatened by slope failure. The stability of a ski slope can be expressed in terms of a *safety factor*, which is the ratio of the resisting or stabilising force (capacity) to the driving or disturbance force (demand). It is assumed that the failure plane of the landslide runs parallel to the slope of the bedrock, calculated on the basis of the digital elevation model and the estimated soil thickness (Chapter 7, Eq. 7.3.23). For each grid cell, the safety factor F_s , (-) is:

$$F_s = \frac{MC}{MD} \tag{8.2.1}$$

with, *MC* the capacity (kN/m^2) and *MD* the demand (kN/m^2). Failure is likely to occur for the case that the demand is greater than or equal to the capacity. The difference between capacity and demand is known as the safety margin (M_s, kN/m^2):

$$M_s = MC - MD \tag{8.2.2}$$

Positive values of the safety margin indicate a stable situation. The shearing resistance should balance the shear stress, which is the down slope component of the weight of the soil and any surcharge to avoid failure. Therefore, it is neither the shear stress nor the normal stress that causes failure, but a certain combination of them (Lee et al., 1983). (Figure 8.4)

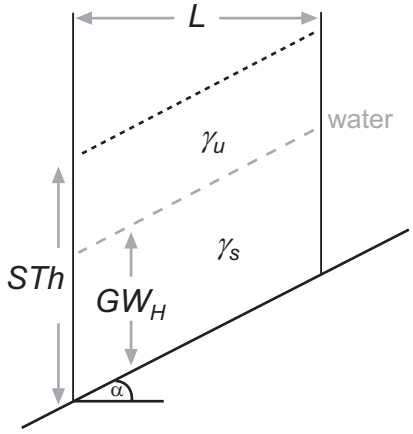

Figure 8.4 Relation of components controlling the stability of a grid cell where α the slope angle (degrees), *STh* the soil thickness (m), GW_H the groundwater level (m), γ_u the bulk density of the unsaturated soil (kN/m^2), γ_s the bulk density of the saturated soil (kN/m^2) and *L* the length of a grid cell (m).

For each cell, the maximum resistance at time *t* is given by the capacity (*MC*, kN/m^2):

$$MC(t) = c' + \sigma'(t) \cdot \tan\varphi \tag{8.2.3}$$

with, *c'* the effective cohesion of the soil (kN/m^2) (Table 8.3), $\sigma'(t)$ the effective normal stress (kN/m^2) and φ (degrees) the angle of internal friction. Under saturated conditions, pore water carries a proportional part of the imposed load. This reduces the normal stress ($\sigma'(t)$, kN/m^2) that effectively contributes to the frictional component of Equation 8.2.3 according to:

$$\sigma'(t) = \sigma(t) - u(t) \tag{8.2.4}$$

with, $\sigma(t)$ the total normal stress (kN/m^2) and $u(t)$ the pore water pressure (kN/m^2) at time t. Assuming that the weight of the soil, controlled by the thickness of the soil, the groundwater height and other soil properties, is the only force acting on an grid cell of a given length L, the total normal stress at time t ($\sigma(t)$, kN/m^2) is expressed in terms of:

$$\sigma(t) = \left(\gamma_u \cdot \left(S_{Th} - GW_H(t)\right) + \gamma_s \cdot GW_H(t)\right) \cdot \cos^2 \beta \tag{8.2.5}$$

with, γ_u the bulk density of the unsaturated soil (kN/m^2), γ_s the bulk density of the saturated soil (kN/m^2), S_{Th} (m) the estimated thickness of the soil (Chapter 7, Eq. 7.3.23), $GW_H(t)$ the groundwater height (m) (Chapter 7, Eq. 7.3.15) and β the slope angle (degree) of the bedrock. To determine the pore pressure it is assumed that the seepage is parallel to the failure plane and the topographic surface. The pore pressure ($u(t)$, kN/m^2) at a certain location is given by:

$$u(t) = \gamma_w \cdot GW_H(t) \cdot \cos^2 \beta \tag{8.2.6}$$

with, γ_w the bulk density of water (kN/m^2) and $GW_H(t)$ the ground water level above the failure plane (m) equivalent to $GW_H(t)$ in Equation 7.3.15 (Chapter 7). Assuming that the weight of the soil is the only force acting on a grid cell of a given length (L), the demand ($MD(t)$, N/m^2) at time t for each cell is given by:

$$MD(t) = \left(\gamma_u \cdot \left(S_{Th} - Sat_{Th}(t)\right) + \gamma_s \cdot Sat_{Th}(t)\right) \cdot \cos\beta \cdot \sin\beta \tag{8.2.7}$$

The factor of safety is a deterministic measure to predict instability if the demand is larger than the capacity. It is a useful measure to predict instability on a local scale, that means of a hill slope or a grid cell. However, it is a poor estimate for predicting slope instability on a regional scale such as a ski area because it is single valued and does not account for the inherent variability of site conditions (Mulder, 1991). To this end a probabilistic approach was implemented, namely the probability of failure, which 1) allows comparison over between areas, which is impossible with the safety factor, 2) it takes into account the uncertainty that surrounds the local estimate of slope instability, and 3) it gives relatively easy an idea about the reliability of the estimate, with consideration of the natural variability of relevant variables. Relevant variables are parameters, which are characterised by a large variability having a significant effect on the safety factor. To examine when failure is likely to occur, we need to assess the likelihood that the capacity is smaller than the demand, in particular $P(F \leq 1)$. This is expressed mathematically by (Lee et al., 1983):

$$P(F \leq 1) = P[C < D] = \int_{-\infty}^{+\infty} G_C(D) g_D(D) dD \tag{8.2.8}$$

with, $G_C(D)$ the cumulative distribution function of the capacity C and $g_D(D)$ the probability distribution function of the demand D. If we assume that the demand and the capacity are normally distributed, the probability of failure is given by (Lee et al., 1983):

$$P(F \leq 1) = 1 - G_F\left(\frac{M[C] - M[D]}{\sqrt{V[C] - V[D]}}\right) \tag{8.2.9}$$

with, G_F the cumulative probability of the standard normal distribution that the demand is greater than the capacity, $M[C]$ and $M[D]$ the respective mean of capacity and demand, and $V[C]$ and $V[D]$ the respective variance to characterise the normal distribution of C and D. Usually, the variability in the demand is smaller than that in the capacity (Lee et al., 1983; Van Beek, 2002). Consequently, only the variance of the capacity was considered in the estimation of the probability, specifically the variance of soil cohesion c and the variance of the angle of internal friction (φ). If the sum y of a number of random variables is defined as:

$$y = \sum_{i=1}^{n} \alpha_i x_i \tag{8.2.10}$$

with, α_i a constant for i=1,…,n and x_i a random variable, then the mean M_y and the variance V_y of the sum y are:

$$M_y = \sum_{i-1}^{n} \alpha_i M_{x_i} \tag{8.2.11}$$

$$V_y = \sum_{i=1}^{n} \alpha_i^2 V_{x_i} \tag{8.2.12}$$

with, M_{x_i} the mean and V_{x_i} the variance of the random variable x_i. Applying Equation 8.2.11 and 8.2.12 to the variables controlling the capacity, the variance of the capacity (V_C) is given by:

$$V_C = V_c + \sigma'^2 \cdot V_{\tan\varphi} \tag{8.2.13}$$

with, V_c the variance of the cohesion and $V_{\tan\varphi}$ the variance of the angle of internal friction. To determine the area below the probability distribution, the z-score can be estimated on the basis of the safety margin and the variance of the capacity:

$$z = \frac{M_s(t)}{\sqrt{V_C}} \tag{8.2.14}$$

with, z the z-score required to examine the probability that the safety margin is less then zero, and $M_s(t)$ the safety factor at time t. According to probability theory, the probability density $g_F(z)$ for the standard normal curve is

$$g_F(z) = \frac{1}{\lambda} \cdot e^{-0.5z^2} \tag{8.2.15}$$

with, λ equal to $\sqrt{V_C} \cdot 2\pi$. $g_F(z)$ is usually solved numerically. However, to avoid iterations outside the main dynamic loop, a parameterised function $G_F(z)$ is used which approximates the cumulative standard normal curve by

$$G_F(z) = \frac{1}{2} + \frac{a\tan\{z \cdot (C_1 + C_2 \cdot z^2)\}}{\pi} \tag{8.2.16}$$

with C_1 ˜ 1.253 and C_2 ˜ 0.579. This function deviates slightly from the true probability at the extremes of the curve, but the difference is negligible (<0.01) (Van Beek, 2002). So $G_F(z)$ and the principle of Equation 8.2.9 are used to calculate the likelihood that the capacity is smaller than the demand. Figure 8.5 shows one output of the ST-model, in particular the spatial distribution of the maximal probability that failure might occur at a location during the year under consideration. The probability of failure is large where the groundwater level is close to the surface.

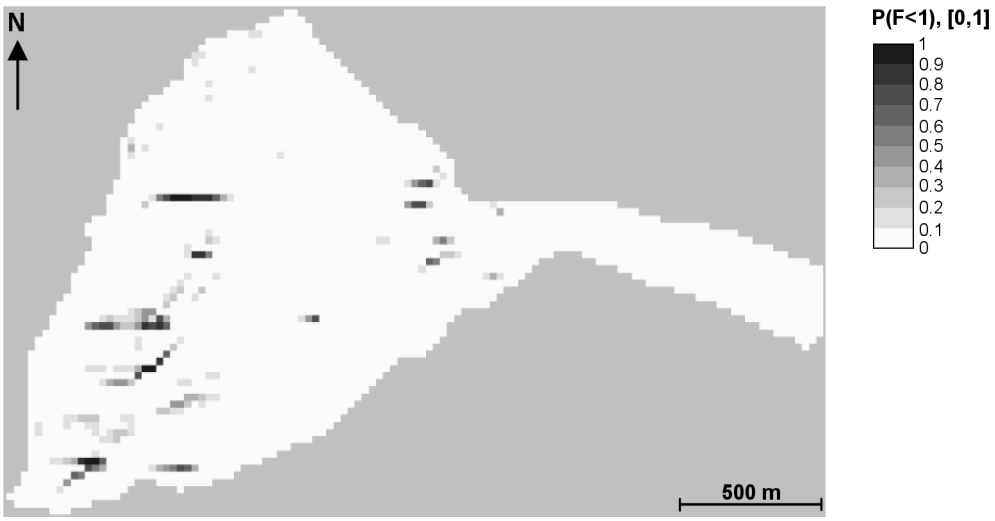

Figure 8.5 Spatial distribution of the maximal probability of failure ($P(F \leq 1)$) at each location; the difference between low probability and high probability is represented by the change of the grey shade from light to dark.

Table 8.3 Model parameters for the slope stability model.

Parameter	Symbol	Unit	Value	Source
Soil cohesion	c'	kN/m^2	8.58	measured
Variance of cohesion	V_c	kN/m^2	4.6	derived
Angle of internal friction	tan(φ)	degrees	0.61	measured
Variance of angle of internal friction	$V_{\tan\varphi}$	degrees	0.0036	derived
Bulk density of unsaturated soil	γ_u	kN/m^3	10	measured
Bulk density of saturated soil	γ_s	kN/m^3	16	measured
Bulk density of water	γ_w	kN/m^3	18	measured
Constant for cumulative PDF	C_1	-	1.253	Van Beek, 2000
Constant for gaussian distribution function	C_2	-	0.579	Van Beek, 2002

8.2.3 Discussion and conclusion

Model results of the stability model depend very much on the slope angle and the results of the HS-model since the daily groundwater level, which is assumed to have an impact on the safety factor, is retrieved from that model. The impact of the HS-model on the ST-model is confirmed by grid cells on steep slopes which are subject to saturated overland flow, and which also display a high probability of failure.

There are two reasons to use the ST-model in the proposed decision model for the planning of ski runs. First, it can be implemented with data that are generally available, which can be derived from literature or for which the expense to collect these data in the field is possible within the framework of decision making. For example, taking soil samples and analysing them in the laboratory to determine site-specific parameters such as soil cohesion or the angle of internal friction is costly. Second, the incorporation of the probability of failure makes it possible to compare a set of potential ski runs because for each alternative the probability that the ski run might be exposed to failure can be computed by aggregating the probability of slope instability for each location. So the choice of site for a new ski run with respect to the risk of landslides can be tailored.

9 MODELLING PLANT GROWTH IN ALPINE TERRAIN

with Roy Frings and Mikie Castenmiller

9.1 Introduction

The establishment of a new ski run often causes the area selected to be flattened and to be disturbed. A poor vegetation cover on these long and smooth slopes is one of the main factors for the occurrence of erosion features on the ski run. If a ski run is located where a satisfactory vegetation cover can be easily restored, the impact caused will be less then if it is established at a site where the regeneration of vegetation is constrained by bad growing conditions.

In alpine terrain the snow cover has a considerable impact on the growth of vegetation: 1) the disappearance of the snow, driven by the energy input of solar radiation and rising temperature, defines the start and the length of the growing period, 2) snow melt water influences the soil water content, and 3) in the beginning of the growing period the grass is rather brown, for the greater part caused by the duration of the snow cover and the reduced oxygen conditions below the snow cover (Chapter 2). The regeneration of grass stimulated by solar radiation, which is the main source for the process of photosynthesis, and temperature, starts with the biomass production below the ground surface, in particular the development of roots and the germination of seeds stored in the ground. Because of the energy present in the roots and seeds the first green leaves above the ground surface can develop and photosynthesis starts, which is limited to periods when plants have green stems and leaves. The main elements involved in the process of photosynthesis are water, carbon dioxide and minerals. The process of photosynthesis converts carbon dioxide of the air into carbohydrate, expressed by the overall reaction (Van Heemst, 1986):

$$6\,CO_2 + 6\,H_2O \text{ --------> } C_6H_{12}O_6 + 6\,O_2 \qquad (9.1.1)$$

with, CO_2 the carbon dioxide, H_20 water, $C_6H_{12}O_6$ the carbohydrate and O_2 oxygen. This process, also called CO_2-assimilation, determines the development of biomass. If influence factors, specifically soil water content, temperature, carbon dioxide concentration and the nutrient content, are not too low, photosynthesis is approximately a linear function of the incident energy amount up to a certain point. Beyond this point the plant becomes light saturated and the photosynthetic rate remains constant (Henderson-Sellers and Robinson, 1994). However, temperature and nutrient availability become less favourable with increasing elevation, for the greater part caused by extreme climatic conditions and less developed soils, especially on steep slopes. Solar radiation principally increases with increasing elevation, but the major influence on solar radiation in mountainous areas is the aspect: south-facing slopes receive much more radiation than north-facing slopes. The soil water content is indirectly controlled by aspect and elevation because of the strong impact of solar radiation on evapotranspiration and the dependence of precipitation on elevation. So a simple rule could be formulated to take

into account the indirect dependence of vegetation on topographic attributes, for example that plant growth decreases with increasing elevation, increasing slope angle and north-facing slopes which receive less solar radiation. A rule based approach returns a rough estimate for comparing ski runs with respect to spatial differences in their expected growing potential, but it does not integrate temporal variation of factors which have an impact on the process of plant growth such as temperature and water supply. However, the increase in biomass depends to a large extent on what happens during the growing season, that is to say whether water supply is always optimal and whether temperatures are always favourable. To overcome this weakness, a process-based spatio-temporal model may be used to model the process of plant growth in space and time with respect to the spatial heterogeneity and temporal variation of prevailing environmental conditions such as solar radiation, temperature, water supply, nutrient conditions and human interference.

9.2 Model building

As with the other models the plant growth model (PG-model) has to meet the modelling conditions defined for the decision framework (c.f. Chapter 6). It describes the spatial and temporal dynamics of grass growth, including sedge, for one growing season in an alpine area. If not specified differently, grass cover always refers to a vegetation cover that consists of grass and sedge. Other components of the vegetation cover such as moss, herbs, shrubs and heather are neglected because of having different growth characteristics. It is assumed that there is no impact of grazing, mowing and insect pests. Another assumption is that nitrogen is the only nutrient that constrains the growth of grass while there is no growth constraint due to the lack of carbon dioxide.

Biomass production is actually a small-scale process, both with respect to space and time. However, due to practical reasons and data constraints it is not possible to model the growth process at the high resolution required. Therefore the model computes growth processes for every six hours and calculations are carried out on grid cells with a cell size of 25 by 25 m; it is run twice, once for the current situation and a second time for a potential ski run defining a number of constraints (Chapter10). This makes it possible to assess the impact caused by a potential ski run and to compare the suitability of each ski run with respect to environmental quality.

The growth model has three components, 1) the radiation model equivalent to the radiation model of the SN-model (c.f. Chapter 7, Equation 7.2.8), 2) the water balance model, and 3) the biomass model including nutrient balance. These three parts assist in modelling the physiological principles of grass growth, specifically CO_2-assimilation, growth and maintenance respiration and the increase in biomass, commonly referred to as accumulation of dry matter. Moreover, the impact of environmental factors, specifically of radiation ($Q_c(t)$), air temperature ($T_a^*{}_{,c}(t)$), water supply ($SM_c(t)$), supply of nitrogen (N_c), land use (L_c), absorption of light ($F_c(t)$) and ageing of plants ($O_c(t)$), upon the assimilation rate is taken into account. Figure 9.1 shows the main components of the PG-model.

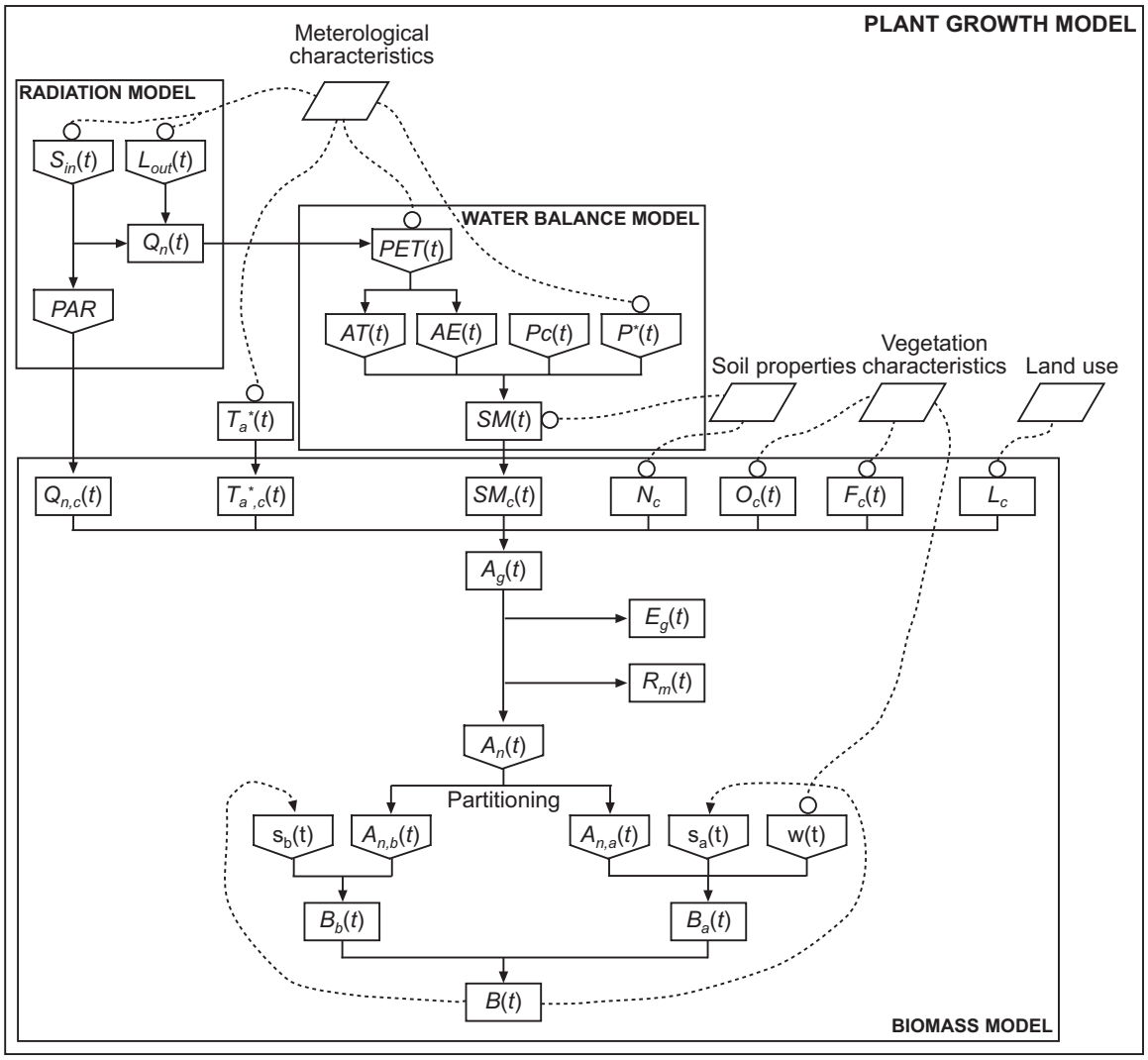

Figure 9.1 Axioms of the plant growth model. The model consists basically of three parts, 1) the radiation model, 2) the water balance model and the 3) biomass model. These models generate important input to determine the environmental factors such as radiation ($Q_c(t)$), air temperature ($T_a^*{}_{,c}(t)$), water supply ($SM_c(t)$), supply of nitrogen (N_c), land use (L_c), absorption of light ($F_c(t)$) and ageing of plants ($O_c(t)$) which control to a large extent the net carbohydrate assimilation rate ($A_n(t)$, the most important input for the development of biomass.

9.2.1 Radiation model

Solar radiation controls two processes, 1) the process of photosynthesis, and 2) the evapotranspiration rate. Only the visible part of the incoming solar radiation is photosynthetic reactive; evapotranspiration is influenced by the net flux of incoming radiation at all wavelengths, defined as net radiation. Net radiation, ($Q_n(t)$), ($J \cdot m^{-2} \cdot$time step^{-1}) is computed in the same way as described in Chapter 7:

$$Q_n(t) = S_{in}(t) - S_{out}(t) + L_{in}(t) - L_{out}(t) \quad (9.2.1)$$

with, $S_{in}(t)$ incoming shortwave radiation (J·m^{-2}·time step^{-1}), $S_{out}(t)$ outgoing shortwave radiation (J·m^{-2}·time step^{-1}), $L_{in}(t)$ incoming longwave radiation (J·m^{-2}·time step^{-1}), $L_{out}(t)$ outgoing longwave radiation (J·m^{-2}·time step^{-1}). For the derivation of the components of Equation 9.2.1 the reader is referred to Chapter 7 in which the radiation model is described (Eq. 7.2.9 to Eq. 7.2.13). The part of the incoming solar radiation that can be used for photosynthesis is called photosynthetic radiation. For each cell, photosynthetic radiation (PAR, J·m^{-2}·time step^{-1}) at time t is (Penning de Vries and Van Laar, 1982):

$$PAR(t) = \left(0.1 \cdot \left(Cl(t)\right) + 0.5\right) \cdot S_{in}(t) \quad (9.2.2)$$

with, $S_{in}(t)$ the incoming shortwave radiation (J·m^{-2}·time step^{-1}) at time t, equivalent to $S_{in}(t)$ in Chapter 7 (Equation 7.2.9) and $Cl(t)$ the cloud cover (fraction) at time t, estimated in the field for the growing period.

9.2.2 Water balance model

The determination of the soil water content is derived from the water balance. The main fluxes of the water balance included in the PG-model are infiltration to the soil, evapotranspiration, and percolation to the groundwater. It is assumed that precipitation infiltrates completely and fluxes like ground water flow, capillary flow, lateral matrix flow through the unsaturated zone and flow through macro pores are neglected. To this end, soil water content ($SM(t)$, cm^3/cm^3) at time t is defined as:

$$SM(t) = \min\left(SM(t-1) + (P^*(t) - AT(t) - AE(t) - Pc(t))/d, \eta\right) \quad (9.3.1)$$

with, $SM(t\text{-}1)$ the soil water content at the antecedent time step (cm^3/cm^3), $P^*(t)$ the precipitation supplied to the surface (mm/time step), $AT(t)$ the actual transpiration (mm/time step), $AE(t)$ the actual evaporation (mm/time step), $Pc(t)$ the percolation to the groundwater (mm/time step), d the thickness of the rooting zone (Table 9.5), and η the porosity of the soil (cm^3/cm^3). The operation $\min(x,y)$ assigns the minimum value of x and y. It is assumed that the soil moisture does not exceed the porosity of the soil, otherwise the surplus of water, in particular the difference between the computed soil water content $SM(t)$ according to the part before the comma in Equation 9.3.1 and the porosity of the soil η, becomes overland flow or loss to the underground and is excluded from further consideration. Precipitation ($P^*(t)$, mm/time step) is derived in the same way as explained in the description of the snow model (Chapter 7, Equation 7.2.6) with the difference that it is calculated in mm, while the hydrological model uses m. Furthermore, snowfall is not taken into account.

The rate of actual transpiration and actual evaporation is derived from the potential evapotranspiration rate, the rate at which evapotranspiration would occur from a well-vegetated surface when moisture supply is not limiting. Potential evapotranspiration

(*PET*(*t*), mm/time step) is computed by the Penman-Equation (Penman, 1963):

$$PET(t) = \frac{\delta(t) \cdot Q_n(t) + \rho \cdot C_a \cdot \dfrac{e_s(t) - e_a(t)}{r_a(t)}}{\lambda \cdot (\delta(t) + \gamma)} \cdot 21600 \qquad \text{if } Q_n(t) > 0 \qquad (9.3.2)$$

$$PET(t) = 0 \qquad \text{if } Q_n(t) \le 0$$

with, $\delta(t)$ the gradient of the saturated vapour pressure curve (hPa/K), ρ the density of humid air (kg/m^3) (Table 9.1), C_a the specific heat of air (J·kg^{-1}·K^{-1}), $e_s(t)$ the saturated vapour pressure (hPa), $e_a(t)$ the actual vapour pressure (hPa), $r_a(t)$ the aerodynamic resistance of wind (s/m), λ the latent heat of vaporisation (J/kg) (Table 9.1) and γ the psychometric constant (hPa/K) (Table 9.1). The Penman-equation requires many input data, which are not expected to be generally available. However, water supply is a very important driving force for biomass production and needs to be described at a reasonable spatial and temporal resolution. Since the growing season was subject to a detailed data survey carried out by undergraduates of Utrecht University, the Netherlands, and due to the availability of spatially distributed net radiation data derived from the radiation model, it was possible to implement Penman's approach to model *PET*. Moreover, the Penman-equation, also successfully applied in other studies (Calder, 1977), is an appropriate method if evapotranspiration has to be determined for a terrain with varying aspects and if required input data are available. If these data are not available, *PET* needs to be approximated by a less data forcing approach such as Thornwaithe (1948), used in the hydrological model. The following five equations (Eq. 9.3.3 to Eq. 9.3.8) address the derivation of the components of the Penman-equation that vary in space and time. The first two components described are actual and saturated vapour pressure. Saturated vapour pressure at time *t* ($e_s(t)$, hPa/K), in particular the vapour pressure when the air is at the maximum moisture content for a given temperature, is in this model calculated by (Conrads and Van de Wal, 1999):

$$e_s(t) = e^{\frac{-\lambda}{R_w \cdot (T_a^*(t) + 273)} + i} \qquad (9.3.3)$$

with, R_w the gas constant for water vapour (J·kg^{-1}·K^{-1}) (Table 9.1) and *i* a constant (Table 9.1). Then the actual vapour pressure ($e_a(t)$, hPa/K) at time *t* is:

$$e_a(t) = RH(t) \cdot e_s(t) \qquad (9.3.4)$$

with, $RH(t)$ the relative humidity (fraction). Measured relative humidity was assumed to be representative for the total catchment. The gradient ($\delta(t)$, hPa/K) of the saturated vapour pressure curve between the dew-point temperature and the actual air temperature is:

$$\delta(t) = \frac{e_s(t) - e_a(t)}{\left(T_a^*(t) + 273\right) - T_d(t)} \qquad \text{if } T_a^*(t) + 273 > T_d(t)$$
$$\delta(t) = \frac{\lambda \cdot e_s(t)}{R_w \cdot (T_a^*(t))^2} \qquad \text{if } T_a^*(t) + 273 = T_d(t) \tag{9.3.5}$$

with, $T_d(t)$ the dew-point temperature (K), which indicates the temperature at which air would just become saturated at a given specific humidity. Assuming that $T_a^*(t) = T_d(t)$ and $e_s(t) = e_a(t)$. The dew-point temperature ($T_d(t)$, K) at time t becomes:

$$T_d(t) = \frac{\lambda}{R_w \cdot \left(i - \ln\left(e_a(t) + 0.1\right)\right)} \tag{9.3.6}$$

The last component of the Penman-equation to be described is the aerodynamic resistance. It is assumed that the aerodynamic resistance of a poorly vegetated area can be compared with the resistance of a bare soil. The aerodynamic resistance ($r_a(t)$, s/m) at time t is given by (Beven, 1979; Finch, 1998):

$$r_a(t) = \frac{\ln^2\left(\frac{H - 0.67 \cdot h_v(t)}{0.1 \cdot h_v(t)}\right)}{k_c^{\,2} \cdot u(t)} \qquad \text{if } h_v(t) > 0$$
$$r_a(t) = r_{a,b} \qquad \text{if } h_v(t) = 0 \tag{9.3.7}$$

with, $r_{a,b}$ the aerodynamic resistance of a bare soil (s/m) (Table 9.1), H the height of the anemometer (m) (Table 9.1), $u(t)$ the wind velocity (m/s), k_c the "Von Karman" constant (Table 9.1) and $h_v(t)$ the height of the vegetation (m), Equation 9.3.8.

Table 9.1: Model parameters for the derivation of the Penman equation (Eq. 9.3.2).

Parameter	Symbol	Unit	Value	Source
Density of humid air	ρ	kg/m^3	1.29	Beven, 1979
Specific heat of air	C_a	J·kg^{-1}·K^{-1}	1010	Beven, 1979
Latent heat of vaporisation	λ	J/kg	$2.47 \cdot 10^6$	Beven, 1979
Psychometric constant	γ	hPa/K	0.66	Van Keulen and Wolf, 1986
Gas constant for water vapour	R_w	J·kg^{-1}·K^{-1}		Henderson-Sellers and Robinson, 1994
Constant in Eq. 9.3.3	i	-	21.65	Henderson-Sellers and Robinson, 1994
Aerodynamic resistance of a bare soil	$r_{a,b}$	s/m	80	Ward and Robinson, 1990
Von Karman constant	k_c	-	0.41	Beven, 1979
Maximal vegetation height	$h_{v,max}$	m	0.2/0.5	estimated
Height of anemometer	H	m	2	measured

Just like for relative humidity it is assumed that the wind velocity measured at one location is representative for the total catchment. The height of the vegetation is determined by the development stage according to:

$$h_v(t) = 0.5 \cdot f(t) \cdot h_{v,\max} \tag{9.3.8}$$

with, $f(t)$ the development phase (c.f. Section 9.2.3, Equation 9.4.1) and $h_{v,max}$ the maximum height of vegetation (Table 9.1).

To derive the amount of evaporation from the land surface and the amount of transpiration from the vegetation, namely actual evaporation and actual transpiration, from potential evapotranspiration, first the potential amounts need to be defined. The allocation of *PET* among potential evaporation and potential transpiration depends on the vegetation cover and the leaf area index. Potential transpiration ($PT(t)$, mm/time step) is determined by:

$$PT(t) = l_i(t) \cdot COV \cdot PET(t) \tag{9.3.9}$$

with, $l_i(t)$ the fraction of light intercepted by the grass cover which increases with the leaf area index and *COV* the density of the vegetation cover (fraction), estimated in the field. Accordingly, the fraction of intercepted light is (Van Heemst, 1986):

$$l_i(t) = 1 - e^{-k \cdot LAI(t)} \tag{9.3.10}$$

with, k the light extinction factor (Table 9.4) and $LAI(t)$ the leaf area index at time t (m^2/m^2), assessed for every time step by:

$$LAI(t) = \frac{c \cdot B_a(t)}{COV_g} \tag{9.3.11}$$

with, c the specific leaf area index of grass and sedge (m^2/kg) (Table 9.4), $B_a(t)$ the biomass of grass and sedge above the ground surface (kg/m^2), Equation 9.4.19, and COV_g the density of the grass and sedge cover (fraction), estimated in the field. In fact, the LAI calculated with Equation 9.3.11 is only valid for grass and sedge, but it is assumed that it is also valid for mixed vegetation.

In correspondence to Equation 9.3.3 and 9.3.9, potential evaporation ($PE(t)$, mm/time step) is:

$$PE(t) = (PET(t) - PT(t)) \cdot (1 - s) \tag{9.3.12}$$

with, s the stoniness of the ground surface (fraction, estimated in the field) to incorporate the decline of evaporation due to the presence of stones.

A low soil water content may restrain evaporation from the ground surface. As a result actual evaporation ($AE(t)$, mm/time step) at time t is (Van Keulen, 1986):

$$AE(t) = \frac{SM(t-1) - SM_a(t)}{SM_0 - SM_a} \cdot PE(t) \qquad (9.3.13)$$

with, $SM(t\text{-}1)$ the soil water content (m^3/m^3) during the antecedent time step according to the principle of Equation 9.3.1, SM_0 the soil water content at a matric suction of 0 cm (cm^3/cm^3) (Table 9.2) and SM_a the soil water content of air dry material (m^3/m^3), equivalent to $SM_{16000} \cdot 0.33$ (cm^3/cm^3) where SM_{16000} indicates the soil water content at a matric suction of 16000 cm (Table 9.2). SM_0 and SM_{16000} were only measured at seven locations. To derive SM_0 and SM_{16000} at each location from the point measurements, Thiessen polygons were used for the interpolation (Burrough and McDonnell, 1998).

In order to assess the actual transpiration rate it is assumed that transpiration is not restricted by high soil water content and that this assumption does not have a significant impact on the biomass production since high soil water content was only observed during the snow melt period. Actual transpiration ($AT(t)$, mm/time step) at time t is for the greater part controlled by the specific soil moisture types and the air temperature at time t:

$$AT(t) = \alpha(t) \cdot T^*_{a,c} \cdot PT(t) \qquad (9.3.14)$$

with, $\alpha(t)$ the correction factor for the soil water content between 0 and 1 (Eq. 9.3.15) and $T^*_{a,c}(t)$ the correction factor for air temperature between 0 and 1 (Eq. 9.4.7). $\alpha(t)$ and $T^*_{a,c}(t)$ express the impact of water supply and air temperature on the transpiration. If they are optimal, that is to say if $\alpha(t) = 1$ and $T^*_{a,c}(t) = 1$, there is no impact and actual transpiration is equivalent to potential transpiration. The same correction factors determine gross CH_2O-assimilation (c.f. Eq. 9.4.7). $\alpha(t)$ [0,1] depends on the relation of the specific soil moisture types according to (Van Keulen, 1986):

$$\begin{aligned}
&\alpha(t) = 1 && \text{if } SM(t-1) \geq SM_{cr}(t) \\
&\alpha(t) = \frac{SM(t-1) - SM_{16000}}{SM_{cr}(t) - SM_{16000}} && \text{if } \mathrm{SM_{cr}}(t) > SM(t-1) > SM_{16000} \\
&\alpha(t) = 0 && \text{if } SM(t-1) \leq SM_{16000}
\end{aligned} \qquad (9.3.15)$$

with, $SM_{cr}(t)$ the critical soil water content at time t (cm^3/cm^3) at which the transpiration may be restricted and assessed by (Van Keulen, 1986):

$$SM_{cr}(t) = (1 - p(t)) \cdot (SM_{100} - SM_{16000}) + SM_{16000} \qquad (9.3.16)$$

with, $p(t)$ the fraction of soil moisture at time t that can be directly absorbed by plants, equivalent to $e^{-0.24 \cdot PT(t)}$, and SM_{100} the soil water content at a matric suction of 100 cm (cm^3/cm^3) (Table 9.2), determined in the same way as SM_0 and SM_{16000}.

Table 9.2 Soil moisture content at 0, 100 and 16000 cm matric suction, measured at seven locations.

Parameter	Loc1	Loc2	Loc3	Loc4	Loc5	Loc6	Loc7
SM_0	0.429	0.422	0.397	0.500	0.363	0.429	0.408
SM_{16000}	0.197	0.123	0.217	0.245	0.230	0.212	0.207
SM_{100}	0.014	0.007	0.003	0.029	0.027	0.020	0.027

Percolation is the vertical flux to the groundwater. It is assumed that the percolation stops when the soil reaches field capacity ($SM(t) = SM_{100}$). Percolation at time t ($Pc(t)$, mm/time step) is described by Darcy's law (Chow, 1988):

$$Pc(t) = \min\left[\left(K(t)\cdot\frac{\delta H(t)}{\delta z}\right),\left(SM(t-1)-SM_{100}\right)\cdot d\right] \tag{9.3.17}$$

with, $K(t)$ the unsaturated hydraulic conductivity (mm/time step), and $\frac{\delta H(t)}{\delta z}$ the hydraulic gradient, assumed to be approximately 1 (Kutilek & Nielson, 1994). $K(t)$ responds strongly to the soil moisture. Therefore an average value is taken for the given time interval according to:

$$K(t) = \sqrt{K_a(t)\cdot K_b(t)} \tag{9.3.18}$$

with, $K_a(t)$ the unsaturated hydraulic conductivity (mm/time step) at the beginning of the time interval and $K_b(t)$ the estimated unsaturated hydraulic conductivity at the end of the time interval (mm/time step). $K_a(t)$ at time t is (Leibenzon, 1947, applied by Kutilek and Nielson, 1994):

$$K_a(t) = K_s\cdot 2.5\cdot\left(\frac{SM(t-1)-SM_r}{SM_0-SM_r}\right)^q \tag{9.3.19}$$

with, K_s the saturated hydraulic conductivity (mm/time step) (Table 9.4), SM_r the residual soil water content (cm^3/cm^3) and q an exponent derived by calibration. In correspondence to the determination of $K_a(t)$, $K_b(t)$ is assessed by the same principle using an estimated soil moisture content at the end of the time interval:

$$K_b(t) = K_s\cdot 2.5\cdot\left(\frac{SM_a(t)-SM_r}{SM_0-SM_r}\right)^q \tag{9.3.20}$$

with, $SM_a(t)$ the estimated soil water content according to:

$$SM_a(t) = \min\left(SM(t-1)+\left(P(t)-AE(t)-AT(t)-P_{c,a}(t)\right)/d,\eta\right) \tag{9.3.21}$$

with, $P_{c,a}(t)$ the percolation rate at time t (mm/time step), determined on the basis of the unsaturated hydraulic conductivity at the start of the given time interval (mm/time step) (see also Eq. 9.3.17).

9.2.3 Biomass model

The aim of the biomass model is to determine biomass production on the basis of genetic and environmental factors, which control the process of assimilation, respiration and biomass production at each development stage. The amount of biomass in time is controlled by the initial amount of biomass, in particular the biomass that is present below the ground surface at the beginning of the growing season, the amount of biomass that can be formed from the storage below the ground surface, and biomass production as a function of CH_2O-assimilation, respiration and the death rate. According to the hierarchical development of grass organs we can distinguish three development stages, 1) the vegetative stage, 2) the reproductive stage, and 3) the maturity stage, illustrated in the figure below.

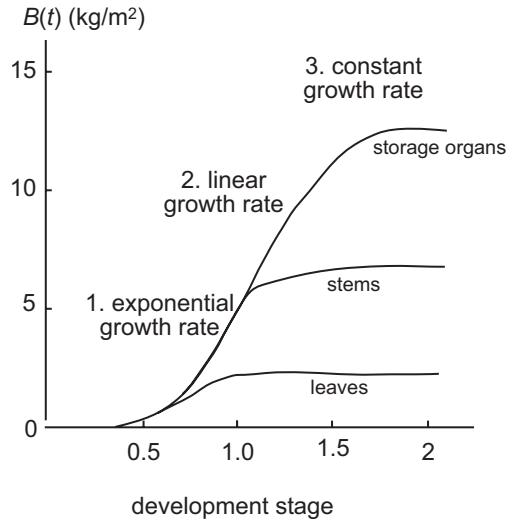

Figure 9.2 The development stages during one growing period. The vegetative phase is characterised by exponential growth rate, the reproductive by a linear growth rate, and the maturity phase by a constant growth rate and decreasing amount of biomass due to the death rate.

The start of each stage is characterised by the order and the rate of the appearance of vegetative and reproductive organs such as leaves, nodes and stems (Van Heemst, 1986). The appearance of these organs is for the greater part controlled by temperature and the day-length (Van Keulen, 1986). The vegetative stage includes both the biomass production below the ground surface and the development of leaves and stems, characterised by an exponential growth because with the increase of the leaf area more light can be intercepted, and consequently more grass can be produced. The transition from the vegetative stage to the reproductive phase is determined by the start of the flowering of the grass. Additionally, there is a shift from the initially exponential plant

growth to a nearly linear plant growth because at a certain leaf area the amount of intercepted light remains constant. At the end of the reproductive stage the growth rate declines. In the maturity stage the amount of biomass remains constant until the leaf area and its photosynthetic activity decrease due to the death rate.

Determination of the development stages. The start of each phase differs for each season and in space because of the impact of environmental factors which may vary in space and time. The timing of the start and the duration of a phase are estimated by (Van Keulen, 1986):

$$\begin{aligned} f(t) &= 0 && \text{if } D < v_d \\ f(t) &= \frac{D - v_d}{r_d - v_d} && \text{if } v_d < D < r_d \\ f(t) &= 1 + \frac{D - r_d}{m_d - r_d} && \text{if } v_d < D < m_d \\ f(t) &= 2 && \text{if } D > m_d \end{aligned} \qquad (9.4.1)$$

with, *f(t)* the development stage between 0 and 2, *D* the day number, which is zero at the beginning of the modelling period and increases with one every modelled day (in this case every four time steps), v_d is the day at which the vegetative phase starts, r_d indicates the start of the reproductive phase and m_d determines the start of the maturity phase, all counted from the beginning of the modelling period. The spatial variation of the start of the vegetative phase and the reproductive phase was estimated in the field, while the start of the maturity phase was estimated by the start of the reproductive plus two weeks, in particular $m_d=r_d+14$. The impact of the air temperature and the length of the day were neglected in the definition of the development phases. The development stages have an impact on the height of vegetation (Eq. 9.3.8), required for the computation of *PET*, on the ageing of biomass (Eq. 9.4.10), and on the allocation of carbohydrates to the plant parts above and below the soil surface (Eq. 9.4.14).

Modelling biomass production from the storage below the ground surface. In the beginning of the growing period biomass production mainly takes place below the ground surface, stimulated by the energy stored in the roots and the seeds that are still present in the soil. The initial amount of biomass below the ground surface ($B_b(t)$, kg/m^2) is estimated by:

$$B_b(t = 0) = B_{ini} \cdot COV_g \qquad (9.4.2)$$

with, t=0 the start of the modelling period, B_{ini} the initial amount of biomass below the ground surface (kg/m^2), derived by calibration for an area with a grass cover of 100% (Table 9.5), and COV_g the density of the grass cover (fraction), estimated in the field. A mathematical formulation for biomass production from the energy stored in the roots together with the seeds present in the soil could not be found in available literature (Frings, 2001). With respect to the theory that biomass production on the basis of the storage below the ground surface declines with time (Hijmans et al., 1994), the amount of

biomass that can be produced from the energy storage in the roots and the seeds below the ground surface ($w(t)$, kg/m^2) can be estimated by:

$$w(t) = g_w \cdot \left((w_{\max} \cdot COV_g) - w_{som}(t-1) \right) + c_w \quad (9.4.3)$$

with, w_{max} the maximum amount of biomass that can be produced from the energy storage below the ground surface that is present in the beginning of the growing period (kg/m^2, derived by calibration), $w_{som}(t\text{-}1)$ the total amount of biomass that has been formed from the energy storage below the ground surface at the end of the antecedent time interval, and g_w and c_w are constants. Consequently, the total amount of biomass that has been produced ($w_{som}(t)$, kg/m^2) from the energy storage below the ground surface at time t is:

$$w_{som}(t) = w_{som}(t-1) + w(t) \quad (9.4.4)$$

Four assumptions justify the use of this approach: 1) during the night there is no biomass production because of negative energy input, 2) for the case that the temperature is lower than the minimal temperature required for assimilation, there is no biomass production from the storage below the ground surface, 3) there is no growth respiration during the production of $w(t)$, 4) the amount of biomass $w_{som}(t)$ that has been produced in this way cannot exceed w_{max}.

Modelling CH_2O-assimilation. If all environmental conditions are optimal, the actual rate of gross assimilation of carbohydrates is equivalent to the potential one, which is, however, nearly impossible. So the decrease in gross assimilation if growing conditions are not optimal is included by a correction factor for each environmental condition such as solar radiation, temperature, soil moisture, nitrogen, land use, ageing of the plant, absorption and maximum CO_2-assimilation rate. They are assumed to be equally important for the CH_2O-gross assimilation. For each grid cell, CH_2O-gross assimilation ($A_g(t)$, kg·m^{-2}·time step^{-1}) at time t is:

$$A_g(t) = Q_{n,c}(t) \cdot T^*_{a,c}(t) \cdot SM_c(t) \cdot N_c \cdot L_c \cdot \left(F_c(t) \cdot O_c(t) \cdot A_{\max} \right) \cdot z \quad (9.4.5)$$

with, $Q_{n,c}(t)$ the correction factor for solar radiation (Eq. 9.4.6), $T_a^*{}_{,c}$ (t) the correction factor for temperature (Eq. 9.4.7), $SM_c(t)$ the correction factor for soil moisture (Eq. 9.4.8), N_c the correction factor for nitrogen (Table 9.3), L_c the correction factor for land use (Table 9.3), $O_c(t)$ the factor for natural ageing of grass (Eq. 9.4.10), $F_c(t)$ the absorption factor (Eq. 9.4.9), A_{max} the maximum rate of CO_2-assimilation at a high light intensity (kg CO_2·m^{-2}·h^{-1}) (Table 9.5), determined by calibration, and z a conversion factor from CO_2-assimilation (kg/m^2·h) to CH_20-assimilation (kg/m^2·time step) (Table 9.4). The value of all constraint factors but solar radiation varies between 0 and 1; 0 indicates total constraint of CO_2-assimilation and a value of 1 shows that there is no constraint.

Table 9.3 Correction factors that may have an impact on the CH_2O-assimilation rate.

Correction factors	Symbol	Value	Source
Solar radiation	$Q_{n,c}(t)$	Eq. 9.4.6	Penning de Vries and Van Laar, 1982
Temperature	$T_{a,c}(t)$	Eq. 9.4.7	calibrated
Soil moisture	$SM_c(t)$	Eq. 9.4.8	Van Keulen and Wolf, 1986
Nitrogen	N_c	1	calibrated
Land use (ski piste)	L_c	0.875	estimated
Land use (no ski piste)	L_c	1	estimated
Absorption	$F_c(t)$	Eq. 9.4.9	Van Keulen and Wolf, 1986
Ageing	$O_c(t)$	Eq. 9.4.10	Van Keulen and Wolf, 1986

Usually a light response curve is constructed to determine the gross CO_2-assimilation at various radiation intensities. However, when using this curve, the effect of different radiation intensities on the assimilation cannot be represented by a value between 0 and 1. As a result the light response curve was divided by the maximum rate of CO_2-assimilation at a high light intensity, A_{max}. If the photosynthetic active radiation (*PAR;* Eq. 9.2.2) is very low, the light response curve becomes negative due to the increase of dark respiration and the low rate of gross CO_2-assimilation. Therefore, the value of the correction value lies between 1 and -1 instead of 1 and 0. Assuming that assimilation is not constrained at very high light intensities, the correction factor for solar radiation can be determined by (Penning de Vries and Van Laar, 1982):

$$Q_{n,c}(t) = \frac{(A_{\max} + R_d) \cdot \left(1 - e^{\frac{-PAR(t)\cdot\varepsilon}{A_{\max}+R_d}}\right) - R_d}{A_{\max}} \qquad (9.4.6)$$

with, R_d the dark respiration ($kg \cdot m^{-2} \cdot h^{-1}$) (Table 9.4), $PAR(t)$ ($J \cdot m^{-2} \cdot$time step^{-1}) the photosynthetic active radiation, Equation 9.2.2, and ε the light use efficiency (Table 9.4).

The influence of temperature on the CO_2-assimilation has already been studied, (Feddes et al., 1978), however, in other areas than alpine terrain, and results differed greatly. Therefore an empirical curve, where the initial shape of the curve was derived from an approach suggested by Feddes et al. (1978) and adjusted according to the correspondence of predicted biomass production and the field data (Frings, 2001; Castenmiller, 2001), was used to determine the constraint of CO_2-assimilation if temperatures are too low, represented by the correction factor for temperature ($T^*_{a,c}(t)$, [0,1]):

$$\begin{aligned} T^*_{a,c}(t) &= 0 && \text{if } T^*_a(t) < 0.4 \\ T^*_{a,c}(t) &= 0.25 \cdot \ln(T^*_a(t)) + 0.3 && \text{if } 0.4 \le T^*_a(t) \le 16.4 \\ T^*_{a,c}(t) &= 1 && \text{if } T^*_a(t) > 16.4 \end{aligned} \qquad (9.4.7)$$

with, $T_a^*(t)$ the air temperature (ºC) at time t.

In dry periods there might not be enough water in the soil that could be absorbed through the roots, but transpiration of the plants above the surface continues. Due to the shortage of water in the plant the stomata closes, and consequently assimilation of carbohydrates is constrained because there is no input of carbon dioxide anymore, which can only be supplied through the stomata. If we assume that the influence of soil moisture on CO_2-assimilation is equal to the influence of transpiration, the correction factor for soil moisture ($SM_c(t)$, [0,1]) can be estimated by:

$$SM_c(t) = \alpha(t) \tag{9.4.8}$$

with, $\alpha(t)$ [0,1] the restriction of transpiration due to dry conditions.

A number of correction factors had to be determined by calibration because of insufficient information about the relation between the factor and the assimilation rate. These are the nitrogen correction factor, N_c [0,1], which was given a 1 in the case that satisfactory nitrogen conditions were known, and the correction factor for land use, L_c [0,1], which was assigned a 1 in natural areas and 0.875 on potential ski runs. Gross assimilation is also influenced by an absorption factor ($F_c(t)$, [0,1]), which was included to correct for the amount of light interception that is not absorbed by the grass cover (Van Keulen, 1986):

$$F_c(t) = \left(1 - e^{-k \cdot LAI(t-1)}\right) \cdot COV_g \tag{9.4.9}$$

with, $1 - e^{-k \cdot LAI(t-1)}$ the fraction of light intercepted by the grass cover at time t and COV_g the density of the grass cover, equivalent to the parameters defined in Eq. 9.3.10 and Eq. 9.3.11.

When defining the influence of the ageing factor on the assimilation rate, it is assumed that the effect can be neglected in the vegetative phase and that the influence increases gradually with the development phases. The impact of the age of the biomass on the assimilation rate ($O_c(t)$, [0,1]) can be represented by a similar approach as suggested by Feddes (1978) and Thimann (1980):

$$\begin{aligned}
&O_c(t) = 1 && \text{if } f(t) < 1 \\
&O_c(t) = 1.143 - 0.143 \cdot f(t) && \text{if } 1 \le f(t) \le 1.7 \\
&O_c(t) = 3.167 - 1.330 \cdot f(t) && \text{if } 1.7 < f(t) < 2 \\
&O_c(t) = 0.5 - 0.004 \cdot (D - m_d) && \text{if } f(t) = 2
\end{aligned} \tag{9.4.10}$$

with, $f(t)$ the development stage, D (days) the day number and m_d the start day of the maturity state (Eq. 9.4.1).

Modelling actual biomass production. At the beginning of the growing period (t=0) it is assumed that there is no biomass above the ground surface. For each following time step, the biomass above the ground surface ($B_a(t)$, kg/m^2) at time t is to a large

extent controlled by the assimilation of carbohydrates (CH_20). For each grid cell, the net CH_20-assimilation rate ($A_n(t)$, kg·m^{-2}·time step^{-1}) at time t is expressed in terms of:

$$A_n(t) = E_g(t) \cdot \left(A_g(t) - R_m(t)\right) \tag{9.4.11}$$

with, $E_g(t)$ the conversion efficiency at time t (kg/kg), correcting for the consequences of both the growth respiration, which denotes the use of energy for the conversion of primary photosynthetic products into structural plant material, and the respiration due to the transport of ions, and $R_m(t)$ the maintenance respiration at time t (kg·m^{-2}·time step^{-1}), representing the use of energy for the maintenance of ionic gradients and re-synthesis of degrading structural material. The maintenance respiration ($R_m(t)$, kg·m^{-2}·time step^{-1}) is determined by (Van Keulen and Wolf, 1986):

$$R_m(t) = r(t) \cdot B(t-1) \tag{9.4.12}$$

with, $r(t)$ the relative maintenance respiration rate (kg·kg^{-1}·time step^{-1}) of grass and $B(t\text{-}1)$ the total biomass at the previous time step ((kg/m^2, c.f. Eq. 9.4.18). The relative maintenance respiration rate ($r(t)$, kg·kg^{-1}·time step^{-1}) depends on the air temperature (De Jong and de Kabat, 1990):

$$\begin{aligned} r(t) &= r_v \cdot 0.25 \cdot e^{0.0693 \cdot T_a^*(t)} && \text{if } f(t) < 1 \\ r(t) &= r_r \cdot 0.25 \cdot e^{0.0693 \cdot T_a^*(t)} && \text{if } f(t) \geq 1 \end{aligned} \tag{9.4.13}$$

with, r_v the relative maintenance respiration rate (kg·kg^{-1}·time step^{-1}) in the vegetative phase by 20° C and r_r the relative maintenance respiration rate (kg·kg^{-1}·time step^{-1}) in the reproductive and maturity phase by 20° C, both estimated by calibration, and T_a^*(t) the air temperature (°C), determined according to the same concept described in Chapter 7 (*meteorological model*). Besides it is assumed that differences in the nitrogen balance, the pH value of the soil and the soil moisture do not have an impact on the respiration rates and the ageing.

Among other things, the development stages principally determine the partitioning of carbohydrates over the individual organs. While in the beginning, after germination, most assimilates are converted to roots and leaves, at a later phase they are allocated to stems. At the transition from the first stage to the second the allocation to the roots stops. The computation of the distribution of the available carbohydrates over the different parts of the plant is based on crop data from Van Keulen (1986) with the assumption that they are also valid for the development of grasses and sedges. The fraction distributed to the individual parts of the plants at time t is estimated by:

$$\begin{aligned} n_b &= 0.4 \cdot f^2(t) - 0.9 \cdot f(t) + 0.5 && \text{if } f(t) < 1 \\ n_b &= 0 && \text{if } f(t) \geq 1 \\ n_a &= 1 - n_b \end{aligned} \tag{9.4.14}$$

with, n_a the fraction of the carbohydrates that is allocated to the parts of the plant above the ground surface, n_b the fraction allocated to the parts of the plant below the ground surface and $f(t)$ the development stage (see Eq. 9.4.2). Accordingly, the amount of net CH_2O-assimilation distributed over the individual plant parts at time t becomes:

$$\begin{aligned} A_{n,a}(t) &= n_a \cdot A_n(t) \\ A_{n,b}(t) &= n_b \cdot A_n(t) \end{aligned} \tag{9.4.15}$$

with, $A_{n,a}(t)$ the net CH_2O-assimilation allocated to the part of the grass above the ground surface at time t (kg·m^{-2}·time step^{-1}) and $A_{n,b}(t)$ the net CH_2O-assimilation allocated to the parts of the grass below the ground surface at time t (kg·m^{-2}·time step^{-1}).

Modelling the decline of biomass. Biomass declines due to the dying of parts of the grass. The determination of the death rate is based on three assumptions: 1) the death rate of the biomass below the ground surface is rather small compared to the death rate of biomass above the ground surface, 2) the lack of soil water is the only factor that has an impact on decline rate, and 3) the death rate differs in each development phase. This results in:

$$\begin{aligned} S_a(t) &= s(t) \cdot B_a(t-1) \\ S_b(t) &= x \cdot s(t) \cdot B_b(t-1) \end{aligned} \tag{9.4.16}$$

with, $S_a(t)$ the death rate of the biomass above the ground surface at time t (kg·m^{-2}·time step^{-1}), $S_b(t)$ the death rate of biomass below the ground surface at time t (kg·m^{-2}·time step^{-1}), $B_a(t)$ the biomass above the ground surface (kg/m^2) (Eq. 9.4.19), $B_b(t)$ the biomass below the ground surface (kg/m^2), x the ratio between the biomass above the ground surface and the one below the ground surface and $s(t)$ the relative death rate (kg·kg^{-1}·time step^{-1}), specified for each development stage:

$$\begin{aligned} s(t) &= s_w - (s_w - s_0) \cdot SM_c(t) && \text{if } f(t) < 1 \\ s(t) &= s_w - (s_w - s_1) \cdot SM_c(t) && \text{if } 1 \le f(t) < 2 \\ s(t) &= s_w - (s_w - s_2) \cdot SM_c(t) && \text{if } f(t) = 2 \end{aligned} \tag{9.4.17}$$

with, s_w the relative death rate for the case that there is not enough water (kg·m^{-2}·time step^{-1}), s_1, s_2 and s_3 the death rate (kg·m^{-2}·time step^{-1}) in the vegetative phase, the reproductive phase and the maturity phase, respectively, determined by calibration, and $SM_c(t)$ the correction factor for the soil water content. The development of the total biomass in time is defined as:

$$B(t) = B_a(t) + B_b(t) \tag{9.4.18}$$

with, $B(t)$ the total biomass at time t (kg/m^2). The biomass above the ground surface ($B_a(t)$, kg/m^2) is expressed in terms of:

$$B_a(t) = B_a(t-1) + \left(A_{n,a}(t) - S_a(t)\right) + w(t) \quad (9.4.19)$$

with, $w(t)$ the growth rate of grass on the basis of energy stored in roots and from seeds present in the soil at time t (kg/m^2) (Eq. 9.4.3), thereby assuming that the energy stored in roots and from seeds present in the soil is entirely allocated to the biomass production above the ground surface, and $A_{n,a}(t)$ and $S_a(t)$ according to Equation 9.4.15 and 9.4.16. The biomass below the ground surface ($B_b(t)$, kg/m^2) is:

$$B_b(t) = B_b(t-1) + \left(A_{n,b}(t) - S_b(t)\right) \quad (9.4.20)$$

with, $A_{n,b}(t)$ and $S_b(t)$ according to Equation 9.4.15 and 9.4.16.

Table 9.4 Model input to the plant growth model.

Parameter	Symbol	Unit	Value	Source
Rooting depth	d	M	2	measured
Porosity of the soil	η	cm^3/cm^3		measured (equal to SM_0)
Light extinction factor	k	-	0.65	Van Heemst, 1986
Specific leaf area index for grass and sedge	c	m^2/kg	20	Penning de Vries and Van Laar, 1982
Hydraulic gradient	$\frac{\delta H(t)}{\delta z}$	-	1	Kutilek and Nielson, 1994
Saturated hydraulic conductivity	K_s	mm/h	18	measured
Start vegetative phase	v_d	days		estimated
Start reproductive phase	r_d	days		estimated
Start maturity phase	m_d	days		calculated
Conversion factor in 9.4.5	z	-	$(30 \cdot 44^{-1}) \cdot 6$	Van Keulen, 1996
Light use efficiency	ε	-	$4 \cdot 10^{-5}$	Penning de Vries and Van Laar, 1982
Dark respiration	R_d	kg·s^{-1}·h^{-1}·J^{-1}	1/9-1/10 of A_{max}	Keulen and Wolf, 1986
Conversion efficiency in vegetative phase	$E_{g,v}(t)$	kg/kg	0.7	Van Keulen and Wolf, 1986
Conversion efficiency in reproductive phase	$E_{g,r}(t)$	Kg/kg	0.8	Van Keulen and Wolf, 1986

The typical development of the biomass above the ground surface (kg·m^{-2}·time step^{-1}), rapid increase at the beginning and slow decrease at the end of the growing period, is shown in Figure 9.3 for one measurement site of the study area.

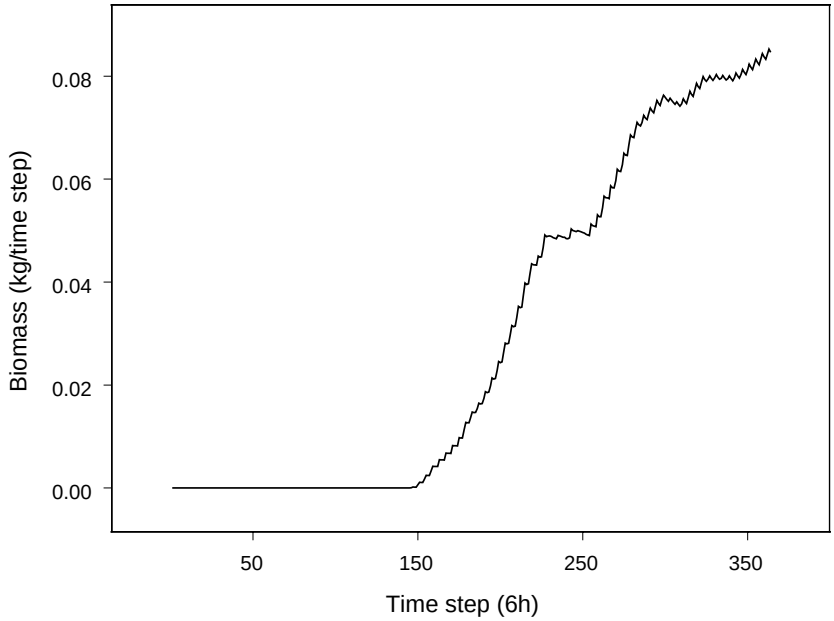

Figure 9.3 The seasonal development of biomass above the ground surface (kg·m^{-2}·time step^{-1}) at one potential ski run location in the ski area of Sölden. One time step represents 6 hours.

For every location of the catchment, Figure 9.4a shows the spatial distribution of the maximum amount of biomass above the ground surface (kg/m^2) that can be expected during the growing period of one year, Figure 9.4b represents the initial density of vegetation (fraction, mapped in the field), and Figure 9.4c the estimated fraction of stones in the upper soil layer, also mapped. The comparison of these three maps shows that the spatial differences of the vegetation density and the stoniness have a large effect on the amount of biomass (Figure 9.4a) because at the patches with a small amount of biomass, a low density of vegetation and a large fraction of stones have been observed.

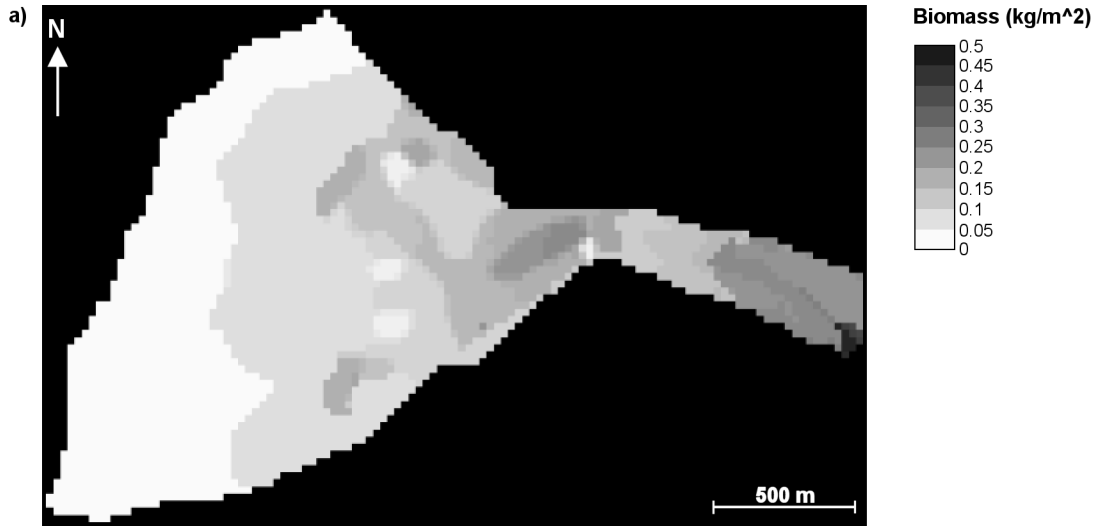

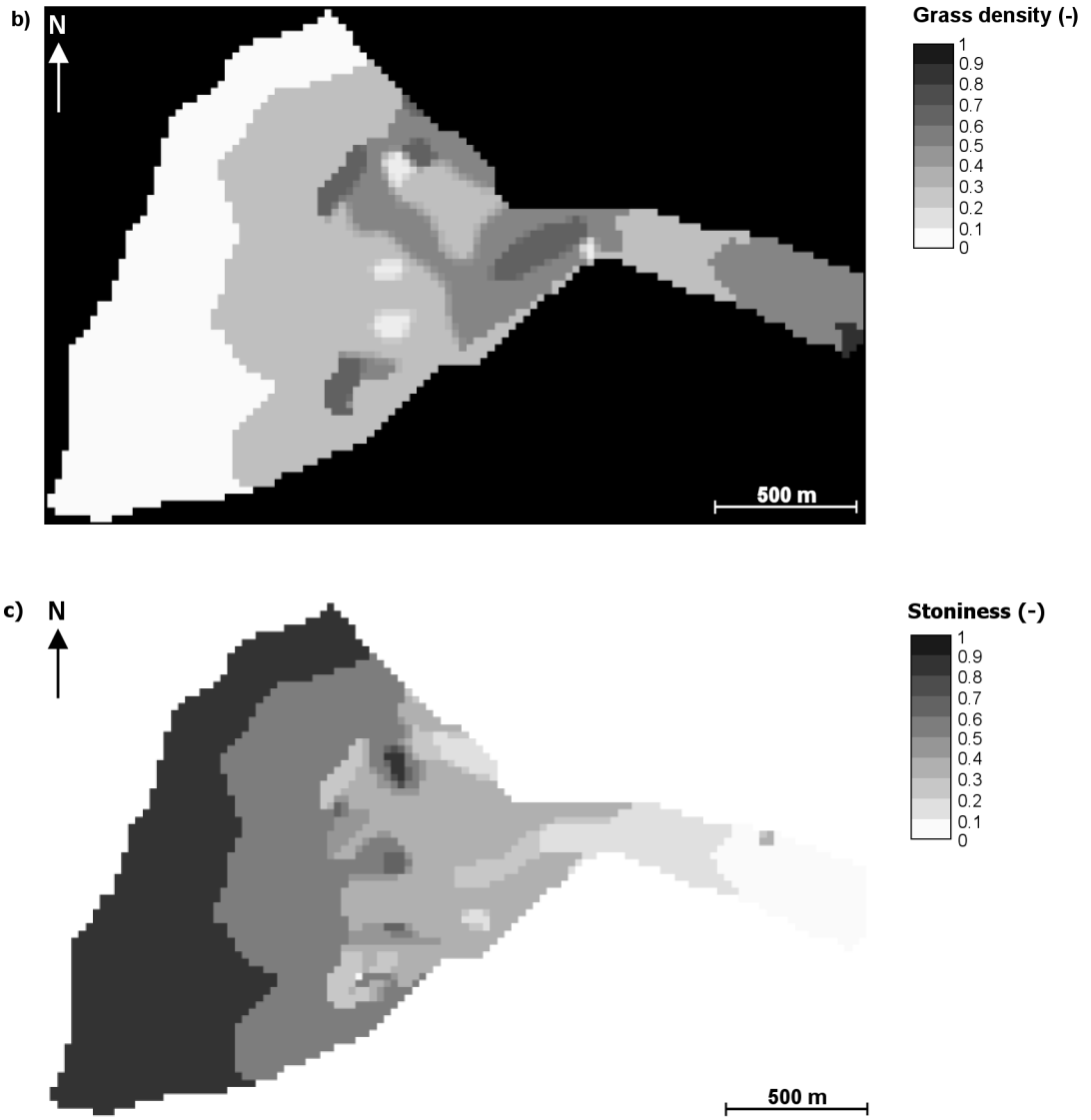

Figure 9.4 a) Spatial distribution of the maximum amount of biomass above the ground surface (kg/m^2), b) initial density of grass (-), observed in the field, and c) fraction of stones, estimated in the field. The patchy structure of the biomass above the ground surface is related to the observed spatial differences of grass density (-) and stoniness (-).

9.3 Model implementation, calibration and significant model parameters

As with the other process based models, the set of operations is computed for each grid cell of the catchment and each time step of the growing period (Chapter 6, Figure 6.2). The model was calibrated according to maximum correspondence between field data and model predictions at seven locations in the catchment. Therefore several calibration parameters (Table 9.5) were selected, where a single parameter or a certain combination of parameters was expected to have an effect on intermediate model results and the increase in biomass. For example the exponent q (Eq. 9.3.20) was selected to achieve

maximum correspondence between measured soil moisture characteristics and predicted soil moisture characteristics. From the model parameters of the light response curve (Eq. 9.4.6), i.e. the maximum assimilation rate by light saturation (A_{max}), the dark respiration (R_d) and the light use efficiency (ε), turned out to be most sensitive with respect to a change in the amount of biomass. The impact of other parameters like the conversion efficiency in different phases ($E_{g,v}(t)$, and $E_{g,r}(t)$) and the spatial information on stoniness, grass density and the density of vegetation may not be neglected.

The analysis of the impact of the correction factors on the assimilation rate identified the radiation factor to have largest influence, followed by the correction factor for temperature.

For more details about model calibration and the significance of other model input the reader is referred to Frings (2001) and Castenmiller (2001).

Table 9.5: Calibration parameters to achieve maximum correspondence between field data and predictions.

Calibration parameter	Symbol	Unit	Value	Equation
Exponent in Eq. 9.3.20	q	-	5	9.3.20
Initial biomass	B_{ini}	kg/m^2	0.3	9.4.2
Biomass to be built from storage below the surface	w_{max}	$kg \cdot m^{-2} \cdot h^{-1}$	0.03	9.4.3
Constant in Eq. 9.4.3	g_w	-	0.075	9.4.3
Constant in Eq. 9.4.3	c_w	-	0.001	9.4.3
Maximum assimilation rate by light saturation	A_{max}	$kg \cdot m^{-2} \cdot h^{-1}$	$4 \cdot 10^{-3}$	9.4.5
Relative maintenance respiration factor in v_d	r_v	$kg \cdot kg^{-1} \cdot$time step^{-1}	0.0015	9.4.13
Relative maintenance respiration factor in r_d	r_r	$kg \cdot kg^{-1} \cdot$time step^{-1}	0.0015	9.4.13
Ratio between $S_a(t)$ and $S_b(t)$	x	-	0.05	9.4.16
Death rate in vegetative phase	s_0	$kg \cdot kg^{-1} \cdot$time step^{-1}	0	9.4.17
Death rate in reproductive phase	s_1	$kg \cdot kg^{-1} \cdot$time step^{-1}	0.0015	9.4.17
Death rate in maturity phase	s_2	$kg \cdot kg^{-1} \cdot$time step^{-1}	0.00425	9.4.17
Relative death rate in dry periods	s_w	$kg \cdot kg^{-1} \cdot$time step^{-1}	0.006	9.4.17

9.4 Discussion and conclusion

The plant growth model is a complex tool, which requires model input that is usually not available. This includes information about specific vegetation characteristics such as composition of plant species, leaf area index or density of vegetation cover and soil properties. To a large extent these values can be derived from the literature (see Table 9.1, 9.3 and 9.4), especially if they are rather general values such as specific leaf area index. However, input parameters with large spatial and temporal variation, a strong impact on the model output, and which are site specific, need to be acquired in the field. This includes the measurement of meteorological data, the collection of soil samples and their analysis in the laboratory, the investigation of the average rooting depth and the observation of site specific and season specific characteristics like the ratio of grass and total vegetation cover, the density of the vegetation cover, the start of the growing season and of each development phase at different elevations and the stoniness. So, to produce reasonable model results when modelling plant growth processes, this information has to

be acquired in the field. However, since the aim of this study is to compare a set of ski runs in order to identify the best one, data, which are assumed to be constant for the entire study area, such as the majority of meteorological data, are of minor importance. Emphasis needs to be put on the acquisition of the information with a large spatial variation and a strong impact on the biomass production such as the mapping of stoniness, grass density and density of vegetation cover. To this end, the plant growth model cannot completely meet the modelling conditions that were imposed in Chapter 6, i.e. using simple models which can be run with general data. However, it is assumed that the effort for collecting necessary field data is reasonable within the planning of new ski runs.

Besides the determination of biomass production for the current situation, the plant growth model can be used to predict the amount of biomass for different environmental conditions, for instance to predict the impact of a ski run on the growth of grass. Impact identification and assessment can be done by changing some parameters of the plant growth model, specifically the correction factor for land use, the initial amount of biomass above the ground surface, the delay of the vegetation period because of a longer duration of the snow cover and the soil thickness at a potential site for a ski run. Accordingly, the plant growth model is a useful tool that can be used in environmental impact assessment and the MCDM for planning ski runs, if minimal data requirements can be met.

10 SPATIO-TEMPORAL MULTI CRITERIA DECISION MAKING FOR PLANNING SKI RUNS: APPLICATION AND RESULTS

10.1 Introduction

Identifying potential locations for the establishment of environmentally sound ski runs, thereby striving for the least environmental impact on the sensitive components of the environmental system, requires consideration of several issues:

1. Ski runs are a spatial object, which may have an impact both at the site where they are put and on their surroundings.
2. There may be various possibilities for locating a new ski run, having the same socio-economic benefits, but different consequences for the environment.
3. Environmental processes vary in space and are controlled by the temporal variation of driving forces.
4. Different environmental concerns represented by environmental criteria need to be systematically brought together.

These aspects were the driving forces for the development of the decision framework introduced in Chapter 3 and represented in the general approach in Figure 10.1.

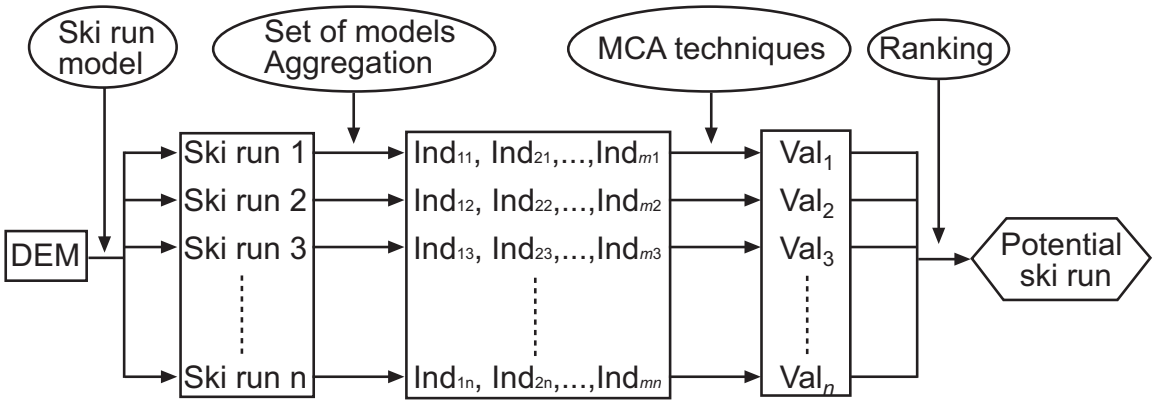

Figure 10.1 Simplified scheme of spatio-temporal multicriteria decision making (c.f. Chapter 3). The main principles are the generation of the set of ski runs, the application of environmental models to each generated ski run, and the aggregation of their results to characterise each ski run by means of indicator values and the combination of those indicators by means of multicriteria analysis.

The main steps in this framework are 1) ski run modelling to generate spatial objects representing possible ski runs (ski run 1,…, ski run *n*), described in Chapter 3, 2) environmental modelling to compute attribute maps for the environmental characterisation of each ski run, to a large extent covered by the Chapters 6, 7, 8 and 9, 3) the aggregation of the model output to a set of indicators, (Ind_{11},…,Ind_{mn}), and 4) combining the aggregated model output to a score for each ski piste (Val_1,…,Val_n) by

means of multicriteria analysis (MCA). For reasons of clarity some principles of the four steps, which have already been explained in previous chapters, will be repeated:

Step 1 - Generation of ski pistes. The only inputs to the ski run model were the digital elevation model, having a grid cell size of 25 by 25 m, and a set of feasible starting points, which are represented by a single grid cell (black dots in Figure 10.2). From each of these grid cells ski runs of the same length and width were generated, oriented downhill according to the local drain direction (c.f. Chapter 3). The topography of each ski run so obtained was smoothed because a ski run with a large change in slope over a short distance is not desirable with respect to the safety of skiers and the preferences of the average skier. The output of the ski run model was 83 overlapping ski pistes, distributed over the area suitable for skiing. In the figure below only the starting points are shown.

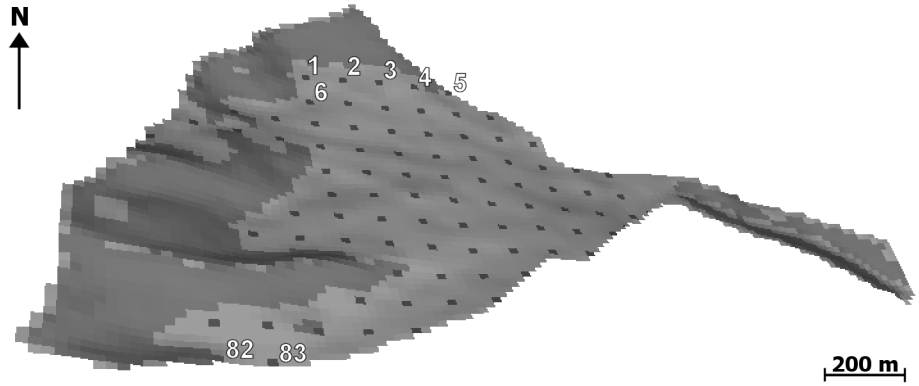

Figure 10.2 Black spots indicate starting points for each ski piste, and the numbers the order of simulation (1-83). The dark grey area displays the area of the catchment that is considered to be too steep for skiing and light grey the area that is suitable for new ski runs with respect to the slope of the terrain.

The number of ski pistes to be analysed in the decision framework was restricted to 83 because the evaluation of all possible ski runs was not feasible through lack of computational power. The number 83 resulted from the regular grid that was assigned to the area suitable for skiing from which the feasible starting points were selected in a stratified way. Ski pistes were numbered in ascending order from the left to the right and from the top to bottom.

Step 2 – Modelling. The second step deals with the application of the set of spatio-temporal environmental models to each ski run, consisting of the snow model (SN-model, Chapter 7), the hydrological models (HS-model and HE-model, Chapter 7), the erosion model (ER-model, Chapter 8), the stability model (ST-model, Chapter 8) and the plant growth model (PG-model, Chapter 9). These models were used to describe the environmental processes at the potential ski run that are relevant for the planning and to identify and quantify a change caused by a ski run, both in space and time. Each model generates a series of maps for different moments, in previous chapters referred to as a stack of maps (Chapter 3 and Chapter 6). An overview of the selected environmental processes and their numerical representation by means of spatio-temporal environmental models was provided in part D of this thesis (Chapters 6, 7, 8 and 9). In addition, a statistical vegetation type model (VT-model, Chapter 5) was developed which predicted

the vegetation type map, from which the degradation of vegetation communities could be derived for each ski piste.

Step 3 – Spatio-temporal aggregation. For each environmental criterion, attribute maps (a stack of maps or a single map) were computed by the various models (*step 2*). In order to combine the environmental criteria by a method known as compensatory evaluation (Jankowski, 1995; Malczewski, 1999), these attribute maps need to be aggregated to a single value. The different methods for aggregating the spatial and temporal component (c.f. Chapter 3) resulted in nine scores for each ski piste, with each score representing the state of a ski piste with respect to one of the nine environmental criteria.

Step 4 – MCA. The last step deals with the application of multicriteria analysis techniques to balance the importance of the different environmental criteria and to achieve a rank order of the ski pistes with respect to those criteria. The MCA consists of three parts, first the standardisation of the indicator value to a common scale, second the assignment of priorities to impose a preference for a certain criterion and third the use of different decision rules to obtain the rank order of the ski pistes.

The main aim of this Chapter is to apply the principles of steps 2, 3 and 4 to the Sölden case study. First, the different methods for predicting the impact will be explained. This is followed by the description of how the spatial and temporal model results were aggregated to a single value, defined here as the *indicator value*. Then the different parts of MCA with respect to the Sölden case study are explained, divided into 1) standardisation techniques, 2) assignment of priorities, and 3) decision rules. Finally the results of the different methods and steps are presented and discussed. The sensitivity of the rank order to the selected methods and techniques is analysed in the following chapter (Chapter 11).

10.2 Methods

10.2.1 Prediction of the impact of a ski piste

The review of environmental impacts of ski pistes and skiing (Chapter 2) showed that human activities such as flattening of the surface of a ski piste, slope preparation by means of piste caterpillars and artificial snow, and the action of skiing are responsible for unfavourable changes in the landscape. In this thesis, these changes are called *impacts*, which represent the absolute difference between the environmental situation before the establishment of a ski piste and afterwards, illustrated by Figure 10.3. In order to predict the impact likely to caused by a new ski piste and to determine the future state of the environmental system because of the impacts of a ski piste, in this thesis referred to as the *overall environmental situation or state,* hypothetical human activities and estimated negative effects of these activities on the site conditions (Table 10.1) were included in the modelling. The hypothetical activities (measures) and effects (changes) were expressed in the script of the respective environmental model. Each model was computed first for the situation without ski piste (original situation) and then for each piste scenario in order to identify the impact likely to be caused by a future ski run and to determine the overall environmental state of each criterion.

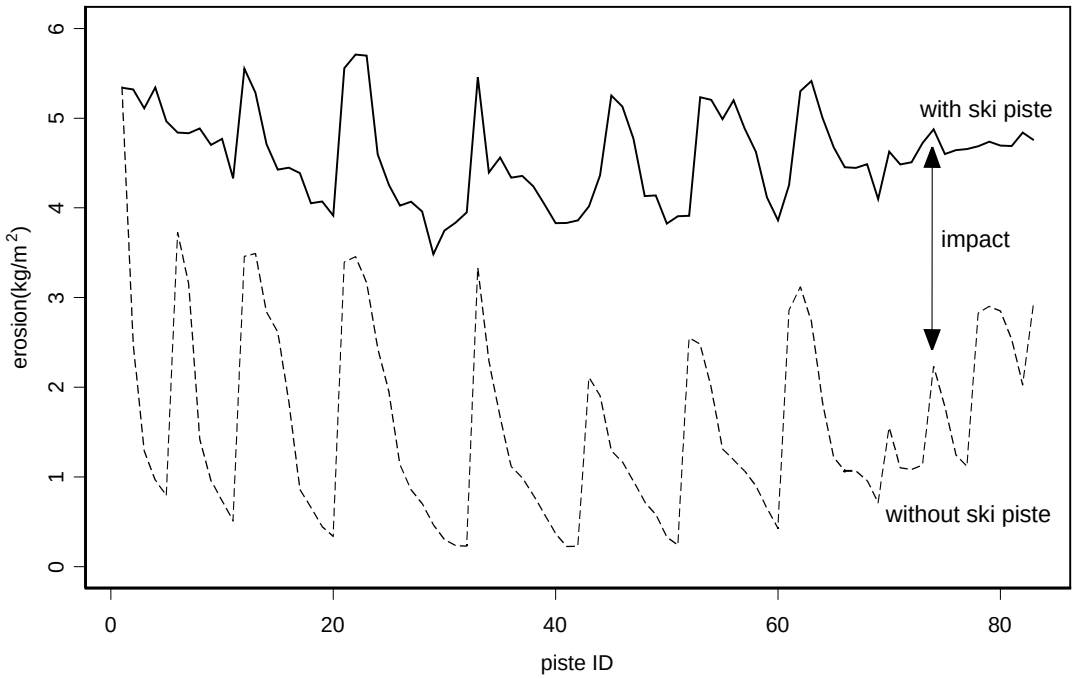

Figure 10.3 Illustration of the normal situation without the impact of a ski piste (dashed line), the impact brought about by a ski piste (distance between the two lines) and the future state to which an environmental factor was changed (closed line), illustrated for the criterion "erosion on a ski piste". The periodicity is caused by the order of simulation.

Table 10.1: Measures and changes applied to a potential ski run, specified for each environmental model.

Model	Measure/Change
Ski run model	Surface corrections (smoothing)
SN-model	Addition of artificial snow
HE-model/HS-model	Reduced hydraulic conductivity (K, Eq. 7.3.9) at the surface
	Ground cover at ski piste: bare
ER-model	Ground cover at ski piste: bare
	Higher erodibility (B, Eq. 8.1.8)
	Weaker soil cohesion (COH, Eq. 8.1.10)
	Higher Crop management factor (C, Eq. 8.1.12)
PG-model	Later start of the vegetative phase (v_d, Eq. 9.4.1)
	Lower land use correction factor (L_c)
	Less soil because of surface corrections, effect on water balance
ST-model	No direct changes; controlled by hydrological properties

The following sections describe how the hypothetical changes and estimated consequences were included in the different environmental models (Chapters 5, 7, 8 and 9).

Impacts through surface corrections. Smoothing of surface irregularities over short distances to provide the conditions skiers and the skiing company want, have an impact on the soil, regolith or bedrock. The impact caused by the smoothing of the

surface irregularities, in particular the destruction of soil, regolith and bedrock and the filling up of depression, is simulated by the ski run model, which computes the difference between the elevation (m) of each grid cell before the smoothing (i.e. without the impact of a ski piste) and the elevation of each cell after the smoothing of the surface of a ski piste using block kriging (Chapter 3). Figure 10.4 shows the location of one ski piste and the elevation difference (m) caused by the smoothing.

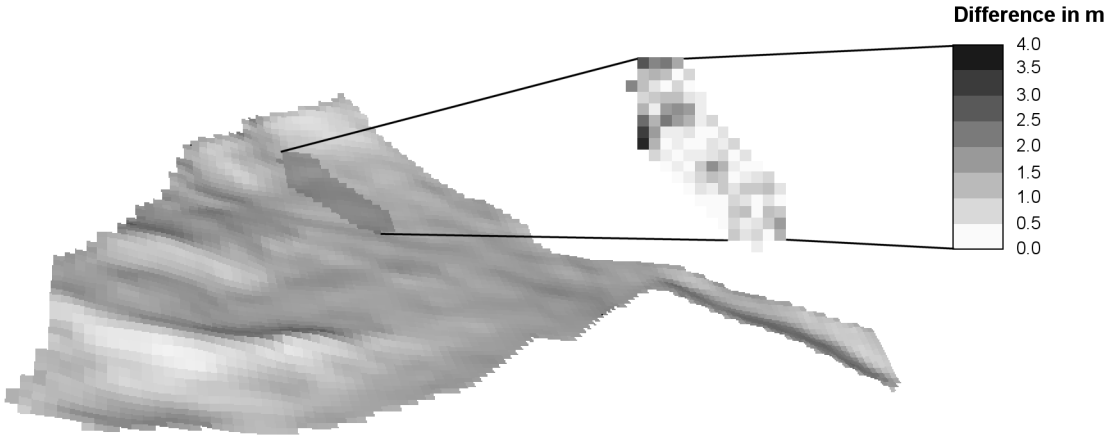

Figure 10.4 Location of ski piste 1 and the difference in the elevation (m) for ski piste 1 after smoothing.

The destruction of soil, regolith or even bedrock can have a considerable effect on the soil properties and other site conditions, which control the hydrological processes, the amount of erosion and the slope stability. The probable differences of the soil properties and the other site conditions were expressed in the different models by a lower infiltration capacity of the soil in form of a reduced hydraulic conductivity (*K*, Chapter 7, Eq. 7.3.9.), a weaker soil cohesion (*COH*, Chapter 8, Eq. 8.1.9), a higher erodibility of the soil (*B*, Chapter 8, Eq. 8.1.8), a bare surface at the potential ski run locations (*COV*=0, Chapter 7, Eq. 7.3.4; Chapter 8, Eq. 8.1.3) and therefore a higher crop management factor (*C*, Chapter 8, Eq. 8.1.12). Furthermore, the growth of grass and sedge was also considered to be constrained by the destruction of the upper soil layer. This was taken into account by assigning a thinner soil to the ski piste when computing grass growth (Chapter 9). Moreover, vegetation communities were assumed to disappear. This impact was expressed by assigning a degradation value to each vegetation class of the vegetation type map (Chapter 5).

Impacts due to slope preparation by means of piste caterpillars. Piste caterpillars are considered to be responsible for soil compaction, and therefore also a lower infiltration capacity. This impact has already been addressed by surface corrections.

Impacts of slope preparation by means of artificial snow. The impact of artificial snow is considered both in the snow model and in the plant growth model. The snow model predicts the state of the snow cover and also indicates when meteorological conditions are suitable for adding artificial snow (Chapter 2) in the case of a ski piste. This can be used to investigate potential changes of the state and availability of snow with respect to the situation without ski piste and with ski piste. Because of a longer

duration of the snow cover due to the addition of artificial snow and snow compaction, the vegetative phase (v_d, Chapter 9, Eq. 9.4.1) was assumed to start later in the case of a ski piste.

Impacts through skiing. The action of skiing especially affects the regeneration of grass. The impact on the grass growth was expressed by a reduced land use correction factor in the plant growth model (L_c, Chapter 9, Eq. 9.4.5).

The incorporation of the hypothetical measures and changes in each environmental model made it possible to compute the environmental situation in the case of a ski piste, but also to identify the impact likely to be caused by a new ski piste (Section 10.3.1). As already mentioned before, the impact of a ski piste is the difference between the original situation (without ski piste) and the state of the environmental criteria in the case of a ski piste.

The term *performance* is used to express the environmental suitability of a ski piste compared to the suitability of the other ski pistes, either with respect to the impact caused by a ski piste on a criterion or according to the overall environmental state of the criteria. *Overall performance* expresses the performance of a ski piste with respect to how well it meets the environmental criteria that were selected for the decision analysis, the higher the overall performance, the better a ski piste. To evaluate the *performance* or *overall performance* of a ski piste by means of MCA, the overall environmental state of the criteria was used rather than the impact of a ski piste on the criteria.

10.2.2 Aggregation of model results

The environmental criteria were divided into three main groups, 1) vegetation, 2) land degradation and 3) snow condition, and further analytically decomposed in one or two sub groups (c.f. Chapter 3, Figure 3.8). This resulted in nine environmental criteria, each represented by their indicator value (Table 10.3, column 3) that was used for the MCA. For each environmental criterion, except for the criteria "fraction of disturbed soil" and the "degradation of vegetation communities", a stack of attribute maps was calculated with the respective environmental model (Chapter 6, Figure 6.1). To provide a measure for the other two criteria, attribute maps were derived from static models, namely from the ski run model (SR-model, Chapter 3) and the vegetation type model (VT-model, Chapter 5). The computation of the attribute maps was repeated for every ski run. Since the aim of this study is to integrate the set of environmental criteria for every ski run by *compensatory evaluation*, the map information content of the stacks (time series) of maps or of the static maps need to be synthesised to a single value, in this thesis defined as *indicator value* (10.5) as already mentioned before. So both the spatial and temporal component need to be aggregated.

Figure 10.5 Aggregation of a stack of maps for different moments to a single value which is assumed to be representative for the stack of maps; the complete theoretical framework is shown in Figure 3.6 (Chapter 3).

Chapter 3 discussed the different strategies (Method A, B and C, Figure 3.6) to aggregate the model results, which may vary in space and time to provide the MCA with a measure (indicator values) for each environmental criterion and ski run. From these methods only A and B were considered to be appropriate for the case study described in this thesis. To carry out the aggregation in space or in time standard techniques were applied to the different model results, shown in Table 10.2. The choice for a certain method is based on the knowledge of the relation between the indicator and the environmental suitability of a ski run. The aggregation of each criterion was done within the script of each respective model.

Table 10.2 Standard aggregation techniques for aggregating the model results to an indicator value I_v; x can be both a grid cell and a time step.

Aggregation technique	Operation	Example
Total sum	$I_v=x_1+x_2+\ldots+x_n$	Total runoff
Arithmetic mean	$I_v=(x_1+x_2+\ldots+x_n)/n$	Average erosion on the ski run
Minimum/maximum method	$I_v=\max(x_1,..,x_n)$	Maximum probability of failure
Weighted average	$I_v=w_1 \cdot x_1+w_2 \cdot x_2+\ldots+w_n \cdot x_n$	Maximum average biomass
Fraction	$I_v=A_{deg}/A_{tot}$	Fraction of degraded soil
Rule based	I_v=if…then…	Number of days with snow cover

In the following sections it is described how the model results were aggregated by means of the standard techniques of Table 10.2. In all computations, the meaning of the letters and terms are as follows: m is the number of time steps, n is the number of cells of the ski piste or the catchment, $\hat{s}_i$ is the cell of a ski piste, s_i is the cell of a catchment, p denotes the ski piste and *cat* the catchment:

10.2.2.1 Vegetation

The criteria group "vegetation" (*Veg*) involves both the "potential for a satisfactory regeneration of the vegetation cover" on the ski piste (*VegOne*) and the "destruction of valuable vegetation types" that are present at the potential ski run location (*VegTwo*). It has been assumed that the maximum amount of biomass that can develop during one growing season, averaged for the ski piste area, provides a measure for the "potential of satisfactory regeneration". *VegOne* was derived from the PG-model, which computed for each time step t the amount of biomass that was present above the ground surface ($B_a(t)$, kg/m^2). For each grid cell of the ski piste, the maximum amount of biomass within one growing season ($B_{a,max}(\hat{s}_i)$, kg/m^2) was filtered according to:

$$B_{a,\max}(\hat{s}_i) = \max(B_a(t_k, \hat{s}_i)) \qquad (10.1)$$

with, $\hat{s}_i$, i=1,…,n, a grid cell of the ski run, n the number of grid cells into which the ski run is divided, and $B_a(t_k, \hat{s}_i)$ the amount of biomass on the ski run for each time step t_k of the modelling period and of each grid cell $\hat{s}_i$ of the potential ski run with k=1,…,m, and m the number of time steps. Aggregating the map so derived by:

$$B_{a,\max,av,p} = B_{a,\max}(\hat{s}_i) \cdot CA / A_{piste} \quad (10.2)$$

results in the average maximum amount of biomass at the ski piste p ($B_{a,max,a,v,p}$, kg/m^2), with CA the cell area (m^2) of a grid cell, and A_{piste} the area of the potential ski run (m^2). It has to be noted that all ski pistes have the same area.

The second environmental criterion (*VegTwo*) is the degradation of vegetation if a certain vegetation community is going to be disturbed because of a ski piste is. In order to include this impact in the comparative analysis, the vegetation class map generated by the statistical vegetation type model (Chapter 5, Figure 5.5) was converted to a degradation map by assigning a number between 1 (low degradation) and 9 (high degradation) to each vegetation class. From this map, the average degradation was derived by:

$$Veg_{av,p} = \left(\sum_{i=1}^{7} V_i \cdot A_i \right) / A_{piste} \quad (10.3)$$

with, $Veg_{av,p}$ the average degradation of vegetation for the respective ski piste p, V_i the number assigned to the vegetation class i, with i=1,…,7, and A_i (m^2) the particular area of the vegetation class i that belongs to the potential ski run.

10.2.2.2 Land degradation

The criteria group "land degradation" (*Deg*) was split up in four sub groups, specifically "erosion" (*DegEr*), "slope instability" (*DegSl*), expressed by the probability of failure, "flooding" (*DegFl*), described by the maximum discharge at the outflow point (*FlOne*) and "surface corrections" (*DegSf*), expressed by the fraction of disturbed soil (*SfOne*) due to the smoothing of irregularities over short distances. Erosion and slope instability were further divided into erosion or stability (*ErOne, SlOne*) on the ski run and erosion or stability in the catchment (*ErTwo, SlTwo*). The impact on the catchment was included because the aim is to identify potential sites for a future ski run that are environmentally sound with respect to both the site conditions on a ski run and its surroundings, represented by the catchment. For the criteria group land degradation indicator values were only determined for the 3rd attribute level (c.f. Chapter 3, Figure 3.8), that is to say for *ErOne*, *ErTwo*, *SlOne*, *SlTwo*, *FlOne* and *SfOne*), the 1st and 2nd levels control the assignment of priorities (Section 10.2.3.2).

Erosion. Indicator values for the two erosion criteria (*ErOne, ErTwo*) were derived from the annual erosion map ($Er(t)$, kg/m^2, t = 1 year), computed by the erosion model. The output of the erosion model (Chapter 8) varies only in space because it was calculated for just one time step t. Accordingly, only the spatial component had to be aggregated. Since the average sediment load on a ski run was considered to be representative for the sensitivity of a ski run to erosion, for each piste p the average erosion rate ($Er_{av,p}$, kg/m^2) was computed by:

$$Er_{av,p} = \left(\sum Er(\hat{s}_i) \cdot CA \right) / A_{piste} \quad (10.4)$$

with, $Er(\hat{s}_i)$ the amount of erosion at each grid cell $\hat{s}_i$ of the ski piste, i=1,…,n and n the number of the grid cells in which the ski run is divided. Following the same principles as demonstrated for erosion at the ski piste, for each potential ski run, average erosion in the catchment ($Er_{av,cat}$, kg/m^2) is:

$$Er_{av,cat} = \left(\sum Er(s_i) \cdot CA \right) / A_{cat} \quad (10.5)$$

with, $Er(s_i)$ the amount of erosion at each grid cell s_i of the catchment, i=1,…,n and n the number of grid cells by which the catchment is represented. If one is more concerned about the maximum amount of erosion than the average sediment load, $Er_{av,p}$ and $Er_{av,cat}$ can be replaced by the maximum erosion on the ski piste ($Er_{max,p}$, kg/m^2) and the maximum erosion in the catchment ($Er_{max,cat}$, kg/m^2) according to

$$Er_{\max,p} = \max(Er(\hat{s}_i)) \quad (10.6)$$

and

$$Er_{\max,cat} = \max(Er(s_i)) \quad (10.7)$$

Slope instability. The slope stability model (Chapter 8) was used to estimate the risk of unstable cells on a potential ski run (*SlOne*) or in the catchment (*SlTwo*). For each time step this model computed the probability of failure (PF(F≤1)) that a grid cell might become unstable with respect to the given site conditions. The advantage of using the probabilistic approach is that for each grid cell it returns an estimate about the risk of slope failure, and therefore grid cells may be compared with each other, and moreover aggregated. Unstable slopes are a hazard, and so the worst case needs to be considered in the multicriteria decision framework. In order to identify for each grid cell of the piste the highest probability of slope failure ($PF_{\max}(\hat{s}_i)$, the maximum method was applied to the dynamic stack of maps that was generated by the stability model for each time step:

$$PF_{\max}(\hat{s}_i) = \max(PF(t_k, \hat{s}_i)) \quad (10.8)$$

with, $PF(t_k, \hat{s}_i)$ an estimate for the probability of failure for each grid cell $\hat{s}_i$ of the ski piste and each time step t_k, where i=1,…,n and k=1,…,m. The map so derived was aggregated to a single value by:

$$PF_{[F\leq 1],p} = PF_{\max}(\hat{s}_i) \cdot CA / A_{Piste} \quad (10.9)$$

where $PF_{[F\leq 1],p}$ represents the average probability of failure on the ski piste. The same aggregation method was applied to determine the indicator value to estimate the risk of unstable cells in the catchment for any future ski run. Just like in Equation 10.8, the highest probability of failure for each grid cell s_i in the total catchment ($PF_{max}(s_i)$) is:

$$PF_{\max}(s_i) = \max(PF(t_k, s_i)) \tag{10.10}$$

with, $PF(t_k, s_i)$ the probability of failure for each grid cell s_i of the catchment and each time step t_k, with i=1,…,n and k=1,…,m. From the map computed in 10.10 the average probability of failure in the catchment ($PF_{[F\leq 1],cat}$) was determined by:

$$PF_{[F\leq 1],cat} = PF_{\max}(s_i) \cdot CA / A_{cat} \tag{10.11}$$

Given that one is interested in large probabilities, the dynamic stack of maps computed by the stability model for each ski piste can first be transformed to a boolean map which represents whether, at a certain grid cell, the probability of failure was once or several times above 0.5 during the total modelling period ($PF_{[F\geq 0.5]}(\hat{s}_i)$):

$$\begin{aligned} PF_{[F\geq 0.5]}(\hat{s}_i) &= 1 \qquad \text{if } PF(t_k, \hat{s}_i) \geq 0.5 \\ PF_{[F\geq 0.5]}(\hat{s}_i) &= 0 \qquad \text{if } PF(t_k, \hat{s}_i) < 0.5 \end{aligned} \tag{10.12}$$

where $PF_{[F\geq 0.5]}(\hat{s}_i)$ is a boolean map, in which 1 represents risk areas, while 0 denotes no or little risk, and $PF(t_k, \hat{s}_i)$ is the probability of failure for each grid cell $\hat{s}_i$ of the ski piste and each time step t_k, with i=1,…,n and k=1,…,m. Then the boolean map can be aggregated to a single value by:

$$PF_{[F\geq 0.5],p} = PF_{[F\geq 0.5]}(\hat{s}_i) \cdot CA / A_{piste} \tag{10.13}$$

where $PF_{[F\geq 0.5],p}$ is an indicator value, which is assumed to represent the probability that the ski slope fails. The same procedure holds when we want to compute the probability of slope failure in the total catchment ($PF_{[F\geq 0.5],cat}$). Aggregation in time, that is to say reducing the time series of maps to one map, is done by:

$$\begin{aligned} PF_{[F\geq 0.5]}(s_i) &= 1 \qquad \text{if } PF(t_k, s_i) \geq 0.5 \\ PF_{[F\geq 0.5]}(s_i) &= 0 \qquad \text{if } PF(t_k, s_i) < 0.5 \end{aligned} \tag{10.14}$$

where $PF_{[F\geq 0.5]}(s_i)$ is a boolean map, in which 1 represents risk areas in the catchment, while 0 denotes no or little risk. $PF(t_k, s_i)$ is the probability of failure for each grid cell s_i of the catchment and each time step t_k, with i=1,…,n and k=1,…,m, with the probability restricted to an interval between 0.5 and 1. Consequently, the risk of instability in the total catchment ($PF_{[F\geq 0.5],cat}$) is determined by:

$$PF_{[F\geq 0.5],cat} = PF_{[F\geq 0.5]}(s_i) \cdot CA / A_{cat} \tag{10.15}$$

Flooding: The maximum discharge that occurred during the modelling period of the HE-model was assumed to be representative for the risk of flooding. The HE-model computed for every time step the discharge at the outflow point of the catchment (*FlOne*). Since this map provided information for a single grid cell, we only had to aggregate in time. In risk assessment one is interested in the worst case, and therefore the maximum discharge (Q_{max}, l/s) during the total modelling period was extracted by:

$$Q_{\max} = \max(Q_{out}(t_k)) \tag{10.16}$$

with, $Q_{out}(t_k)$ the discharge at the outflow point for each time step t_k, k=1,…,m.

Degradation of the soil: Besides the natural degradation, triggered by natural or human changes, degradation of the soil (*SfOne*) caused by surface corrections was included. As mentioned in the introduction and in 10.2.1, the surface of each possible location for a future ski run has been smoothed, which resulted in a slightly different topography for each ski run. The impact caused by the flattening can be described by:

$$Dem_{Dif}(\hat{s}_i) = \left| Dem(\hat{s}_i) - Dem_{Piste}(\hat{s}_i) \right| \tag{10.17}$$

with $Dem_{Dif}(\hat{s}_i)$ the relative difference (m) between the original elevation $Dem(\hat{s}_i)$ (m) of a grid cell $\hat{s}_i$ and the elevation of the grid cell $\hat{s}_i$ in the case of a ski piste $Dem_{Piste}(\hat{s}_i)$ (m), caused by the smoothing procedure. If the elevation difference (m) exceeds a certain threshold d (m), it is assumed that the difference is a considerable impact. Grid cells on the ski piste, where the threshold is exceeded, can be identified by:

$$\begin{aligned} Dem_{im}(\hat{s}_i) &= 1 \quad \text{if } Dem_{Dif}(\hat{s}_i) > d \\ Dem_{im}(\hat{s}_i) &= 0 \quad \text{if } Dem_{Dif}(\hat{s}_i) \le d \end{aligned} \tag{10.18}$$

with $Dem_{im}(\hat{s}_i)$ a boolean map, where 1 indicates the grid cells with a considerable impact and 0 denotes no and very little impact. The fraction of the ski piste area with a considerable impact ($Dem_{im,p}$) is:

$$Dem_{im,p} = Dem_{im}(\hat{s}_i) \cdot CA / A_{Piste} \tag{10.19}$$

The indicator value so obtained is assumed to be a measure for the land degradation caused by surface corrections.

10.2.2.3 Snow conditions

The environmental criterion “snow conditions” is principally a benefit criterion, which means principally the more snow, the better for the protection of the vegetation, and the less artificial snow needs to be produced to meet a satisfactory snow cover. However, a

too long duration of the snow cover is not favourable for the regeneration of vegetation. This constraint will be taken into account when standardising the snow criterion to a value between 0 and 1 as explained in Section 10.2.3.1.

It was assumed that the number of days with a satisfactory snow cover (*SnOne*) is a good measure for the characterisation of snow conditions. The snow cover of a ski piste was assumed to be satisfactory, if a certain fraction of the ski piste (*a*) is covered with *z* m of snow. For each time step *t*, the time series of snow cover maps (*Sn*(*t*), m) was confined to a time series of boolean values by:

$$\begin{aligned} Sn_z(\hat{s}_i, t) &= 1 \quad \text{if} \quad Sn(\hat{s}_i, t) > z \\ Sn_z(\hat{s}_i, t) &= 0 \quad \text{if} \quad Sn(\hat{s}_i, t) \le z \end{aligned} \tag{10.20}$$

with, $Sn_z(\hat{s}_i,t)$ a boolean map for each time step *t* to identify the grid cells of the ski run with a satisfactory snow thickness, $Sn(\hat{s}_i,t)$ the snow thickness at each grid cell $\hat{s}_i$ of the ski run for each time step *t* as predicted by the snow model and z the threshold to distinguish between satisfactory snow cover and unsatisfactory conditions. From the boolean map, the fraction of the ski piste where the snow thickness is satisfactory ($Sn_x(\hat{s}_i,t)$) is:

$$Sn_x(\hat{s}_i, t) = Sn_z(\hat{s}_i, t) \cdot CA / A_{Piste} \tag{10.21}$$

For each time step *t*, those time steps need to be identified, for which the fraction with a satisfactory snow thickness exceeds the fraction that needs to be covered (*a*) to meet the required snow conditions:

$$\begin{aligned} Sn_{sat,p}(t) &= 1 \quad \text{if } Sn_x(\hat{s}_i, t) \ge a \\ Sn_{sat,p}(t) &= 0 \quad \text{if } Sn_x(\hat{s}_i, t) < a \end{aligned} \tag{10.22}$$

with, $Sn_{sat,p}(t)$ a boolean value for each time step *t*, where 1 denotes the presence of a satisfactory snow cover at time step t and 0 refers to too little snow or no snow. To derive the number of days with a satisfactory snow cover ($Sn_{sat,p,d}$),, the boolean values need to be summed up:

$$Sn_{sat,p,d} = \sum_{k=1}^{m} Sn_{sat,p}(t_k) \tag{10.23}$$

with t_k, k=1,…,m the number of time steps.

The results of the aggregation of the attribute maps in space and time to indicator values are summarised in Table 10.3. Since 83 ski pistes are evaluated, each indicator has 83 entries. Accordingly, the decision matrix consists of 9 columns (indicators for each environmental criterion) and 83 rows (ski pistes).

Table 10.3 Model output per criteria group, aggregated output in form of the indicator and its description.

Model output	Indicator	Description
Vegetation (1st group)		
Biomass above ($B_a(t)$, kg/m^2)	$B_{a,max,av}(p)$	Maximum average biomass on the piste
Vegetation classes	$Veg_{av}(p)$	Average degradation of vegetation (1=low, 9=high)
Land degradation (2nd group)		
Erosion load (Er, kg/m^2)	$Er_{av,p}$	Average erosion – piste
	$Er_{max,p}$	Maximum erosion – piste
Erosion load (Er, kg/m^2)	$Er_{av,cat}$	Average erosion – catchment
	$Er_{max,cat}$	Maximum erosion – catchment
Likelihood of unstable cells ($PF(t)$)	$PF_{[F\leq1],p}$	Average maximum probability of failure – piste
	$PF_{[F\geq0.5],p}$	Fraction of piste area with P[F>0.5]
Likelihood of unstable cells ($PF(t)$)	$PF_{[F\leq1],cat}$	Average maximum probability of failure – catchment
	$PF_{[F\geq0.5],cat}$	Fraction of catchment area with P[F>0.5]
Peak discharge (Q_{out}, l/s)	Q_{max}	Maximum peak discharge at the outflow point
Elevation difference ($DemDif$, m)	$Dem_{im,p}$	Fraction of piste with more than 0.5m soil degradation
Snow (3rd group)		
Snow thickness ($Sn(t)$, m)	$Sn_{sat,p,d}$	Number of days with a certain snow cover

10.2.3 Multicriteria analysis (MCA)

10.2.3.1 Standardisation techniques

In MCA standardisation techniques are used to bring *indicator values* that have been measured on different scales to a commensurate scale (Malczewski, 1999, Sharifi, 2002). For example, average erosion at a ski piste was computed in kg/m^2, while peak discharge was expressed in l/s. In order to combine these two criteria by means of *compensatory evaluation*, they need to be transformed to a common scale, for example to a value between 0 and 1. Several standardisation techniques such as linear transformation functions, value or utility functions (Beinat, 1995), probabilistic techniques and fuzzy membership functions can be used for the standardisation, each method having its advantages and disadvantages.

In this thesis, both *linear transformation functions* and *value functions* were applied to the selected environmental criteria. Linear standardisation of the vector X, which consists of an indicator value for each ski piste with respect to one environmental criterion (with X equivalent to one column of the decision matrix), was done according to:

$$\overline{X} = \frac{X - X_{\min}}{X_{\max} - X_{\min}} \qquad \text{if } X \textit{ a benefit criterion}$$
$$\overline{X} = 1 - \frac{X - X_{\min}}{X_{\max} - X_{\min}} \qquad \text{if } X \textit{ a cost criterion} \tag{10.24}$$

with, $\overline{X}$ [0,1] the standardised vector containing the transformed indicator value for each ski piste, X_{min} the minimum value of the vector X, and X_{max} the maximum value of it. This method assigns the maximum value of the original vector X a "1", and the minimum value is transformed to "0". When using this method, it is assumed that the increase of a benefit or the decrease of a cost is linear. However, for certain aspects the assumption of the linear relationship is not appropriate. In order to transform *indicator values* according to an individual assessment, value functions can be used (Beinat, 1995). These functions, which are a mathematical representation of human judgement, can be defined by 1) direct rating in form of assigning a score that corresponds to a given value or 2) by directly selecting a curve that fits to the human judgement (c.f. Beinat, 1995). In this thesis *indicator values* were standardised according to the second method, particularly by exponential functions assuming that the increase of a benefit or the decrease of a cost have either the form of a concave curve or of a convex function or of an S-shaped curve. The exact shape of those curves was determined by direct rating, which means that after imposing $f(X_{min})=0$ and $f(X_{max})=1$, with X_{min} the minimum value of the vector X and X_{max} its maximum value, the curve has one degree of freedom which can be used to fit the curve to a directly rated value (Beinat, 1995). For example, X is the vector that represents the environmental criterion "potential for revegetation" (kg/m^2) for each ski piste. Given, that this criterion is a *benefit criterion* because a better vegetation cover is advantageous for an environmentally sound ski run, the starting point S is set at (X_{min} ,0) and the end point E of the curve at (X_{max} ,1). Further it is assumed that this criterion follows the shape of a convex curve expressed by:

$$\overline{X} = a + b \cdot e^{c(X-d)} \tag{10.25}$$

with, a, b, and c parameters, where $c<0$, since it is a benefit criterion, and d the difference between the minimum value of the vector X and 0 to ensure that the environmental criterion is scaled to a value between 0 and 1. In order to fit the curve and to obtain the parameter values a, b and c, the *midvalue point* point was determined, namely $P=(X_P,0.5)$, which determines that X_P is half as important as the maximum value of the vector X. This resulted in indicator scores between 0 and 1, where 0 represents the lowest average biomass and 1 the largest amount (Figure 10.6, upper left corner). Conversely, *cost criteria* were for the greater part transformed according to:

$$\overline{X} = 1 - (a + b \cdot e^{c(X-d)}) \tag{10.26}$$

with, a, b, c and d according to Equation 10.25, and where $c<0$ because of being a cost criterion (Figure 10.6, upper right diagram). Moreover, standardised indicator scores $\overline{x}$ ($\overline{x} \in \overline{X}$) for the environmental criterion "snow conditions' were derived by applying an S-shaped curve to the original indicator values (X) according to:

$$\overline{X} = e^{-\left(\frac{X-d}{a}\right)^2} \tag{10.27}$$

with, a the parameter obtained by fitting the curve to selected data points, d equivalent to

Equation 10.25, illustrated in the lower right diagram of the Figure below. In order to standardise the criterion "snow conditions" by means of Equation 10.27, the indicator values had to be modified by determining an optimum and subtracting the difference between the optimum and the indicator value from the optimum if indicator values were larger than the optimum.

The lower left diagram in Figure 10.6 was obtained by applying linear transformation function illustrated in Equation 10.24 to the environmental criterion "surface corrections".

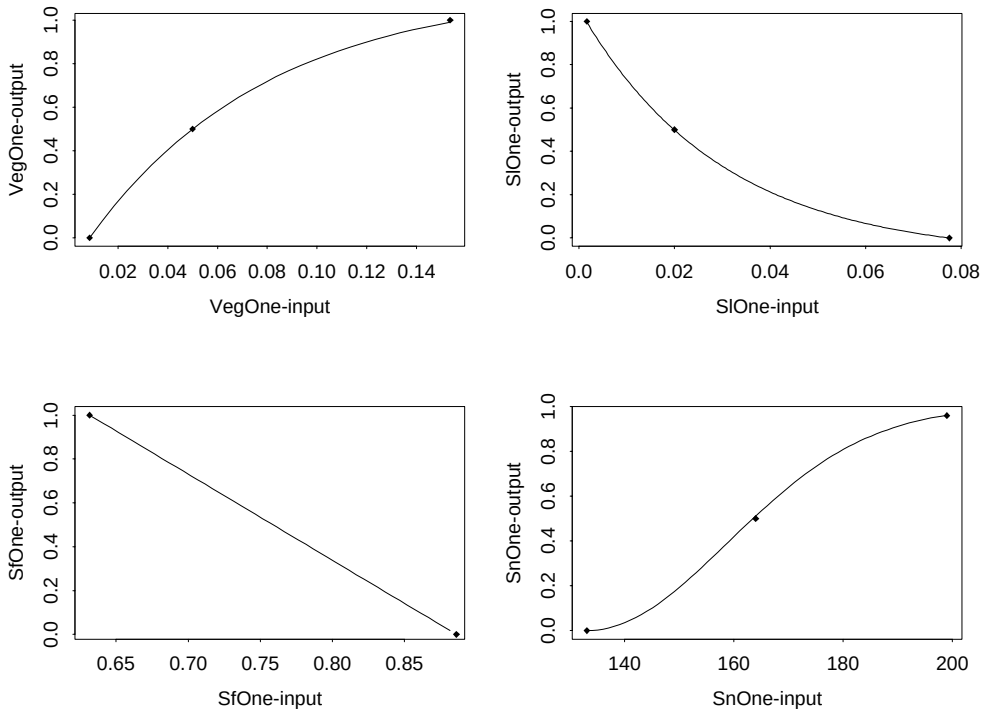

Figure 10.6 Standardisation functions for selected criteria, in particular for *VegOne*, *SlOne*, *SfOne*, *SnOne,* to demonstrate the concept of both linear transformation function and value function. The indicator values are standardised to a value between 0 and 1. The black diamonds, indicated along each value function, illustrate the points to which the functions were fit.

Using value functions, one can tailor the importance of an environmental criterion to the decision problem. Within this procedure three decisions need to be made, 1) the choice for a specific function, 2) the determination of the values which are standardised to 0 or 1, and 3) the selection of the midvalue point (X_P).

A convex function (Eq. 10.25) was used for those *benefit criteria*, for which the difference between indicator values is of larger concern if they are low, while above a certain threshold the difference of the scores is less important (see Figure 10.6, upper left graph). For example, if the ground cover is sparse, any additional amount of vegetation will increase protection against natural hazard. At a certain threshold, a ski slope is not anymore exposed to hazardous processes, and the additional increase in biomass is of little concern.

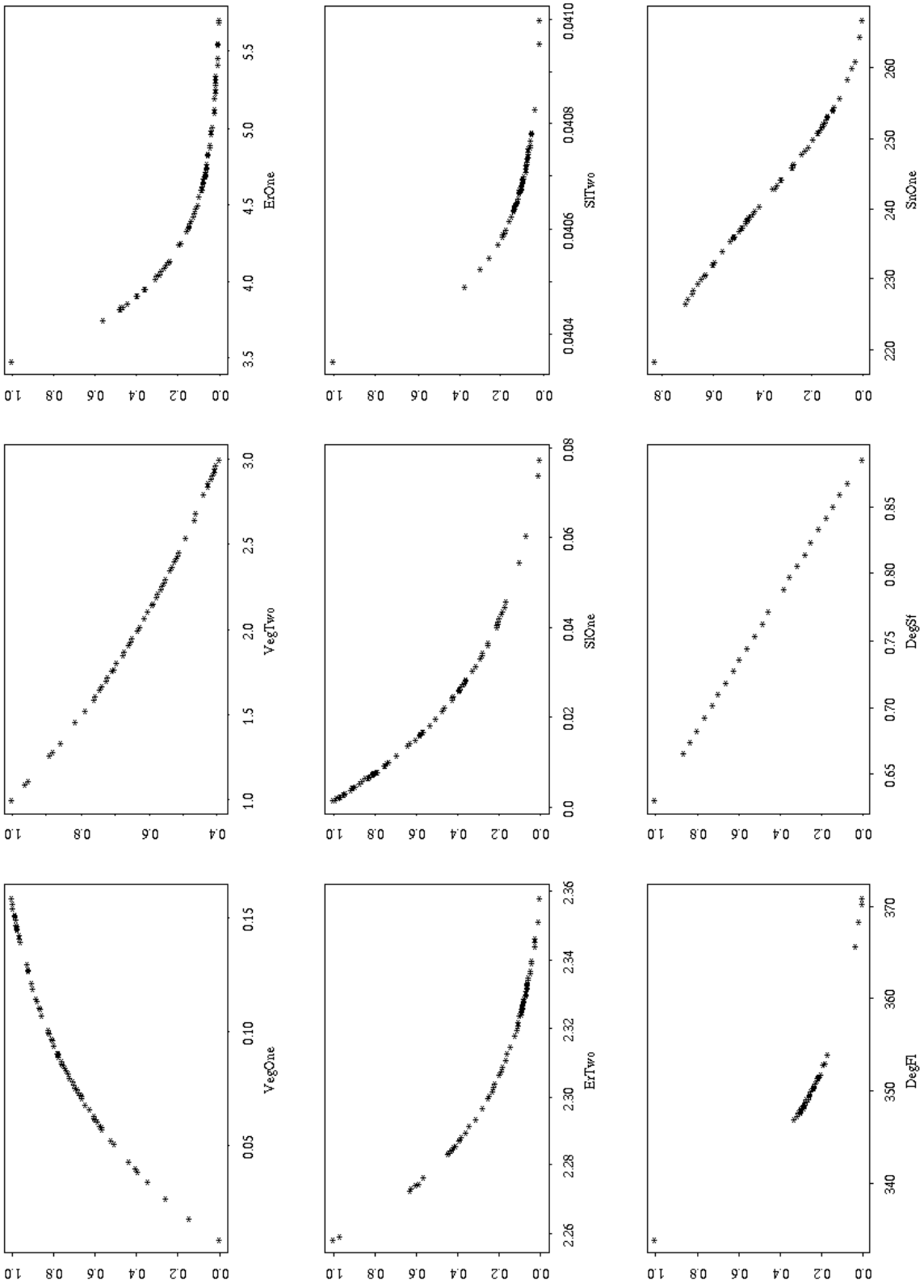

Figure 10.7 Standardisation functions in order to standardise indicator values to a commensurate scale. (The figure needs to be turned clockwise.)

In order to emphasise the importance of little impact or natural hazard and to assign a very low value to unfavourable conditions, a concave function was applied to all *cost criteria* (Eq. 10.26), in particular to the second vegetation criterion (*VegTwo*), the erosion criteria (*ErOne* and *ErTwo*), the slope stability criteria (SlOne and SlTwo) and the flooding criterion (*FlOne*), but not to the criterion "surface corrections" (*SfOne*) because the impact of the latter was assumed to be linear. On the one hand, the concave function causes a strong separation of ski pistes with a little impact or little risk of possible hazard, which helps to optimise the identification of the best ski piste. On the other, it will result in considerable low values for those ski pistes which may cause a high impact or which are exposed to a high risk of natural hazard.

The construction of the value function for the *benefit criterion* "snow conditions" was different because, besides the midvalue point, the minimal value and the maximum value, the function also requires the determination of an optimum, in this case the optimal number of days with a good snow cover. This is because on the one hand, snow protects the vegetation from freezing and the mechanical impact of skiing, but on the other hand a too long duration of the snow cover is disadvantageous for the regeneration of vegetation. A bell-shaped curve was considered an appropriate function to implement these characteristics. In order to use the S-shaped function (half of the bell-shaped curve) to standardise the snow criterion, the difference between the indicator value and the optimum were subtracted from the optimum for those indicator values that were above the optimum.

The various value functions to standardise the indicator values of all environmental criteria are shown in Figure 10.7 (p. 172). They were not only applied to the overall environmental conditions (original situation + impact), but also to the impact caused by potential ski pistes.

10.2.3.2 Assignment of priorities

In multicriteria decision making (MCDM) the importance of selected environmental criteria for the decision making process can be expressed by assigning different priorities to them. The specification of priorities or weights is a subjective procedure because the objectives of individuals or groups of individuals often differ. For example, an enterprise might be more concerned about the minimisation of costs than the protection of valuable species. Conversely, an environmentalist will assign higher weights to those criteria that favour environmental sustainability. To determine priorities among various criteria or indicators, pairwise comparison was used (Saaty, 1980). This procedure requires the comparison of a pair of criteria at one time and repeating this for all pairs within each hierarchical level of the decision tree (Chapter 3, Figure 3.8) to derive a weight for each criterion. The advantage of this method is that it considers each hierarchical level into which a decision problem is decomposed, and moreover, it strives for a consistent judgement by comparing just a pair of criteria at one moment rather than all criteria together. The consistency of the judgement is expressed by the consistency ratio (CR), which can be derived for each set of comparison at various levels of the decision tree.

In order to analyse the subjectivity of pairwise comparison, the opinion of other people was acquired, in this case of several researchers of the Department of Physical

Geography (Utrecht University, The Netherlands), who are considered to be experts of environmental processes. This was done by distributing a questionnaire with a short description of the decision problem, background information about pairwise comparison and the Table 10.4, which they were asked to fill in.

Table 10.4 Part of the questionnaire for deriving weights by means of pairwise comparison. Each row contains a pair of criteria that had to be compared, specified for each sub group.

Pairs of criteria	Weight
1st group	
Vegetation-Land degradation	
Vegetation-Snow conditions	
Snow conditions-Land degradation	
2nd group	
Potential for revegetation-Degradation of vegetation	
Erosion-Slope instability	
Erosion-Flooding	
Erosion-Degradation of soil surface	
Slope instability-Flooding	
Slope instability-Degradation of soil surface	
Flooding-Degradation of soil surface	
3rd group	
Growth of grass-conservation of vulnerable species	
Erosion on the ski run -Erosion outside the ski run	
Slope instability on the ski run-Slope instability outside the ski run	

To each pair of criteria (Table 10.5) a weight between 1 and 9 had to be assigned, where 1 expressed "equal importance" and 9 "much more important". The meaning of the intermediate values is shown in Table 10.5. If the first criterion of the criteria pair was less important than the first one, the inverse weight had to be given, again a 1 for "equal importance", but 1/9 when it was "much less important".

Table 10.5: Possible weights that can be assigned to a pair of criteria and their interpretation; only every second graduation is represented.

Weight	Interpretation	Weight	Interpretation
1	Equal importance	1	Equal importance
3	A little bit more important	1/3	A bit less important
5	Moderately more important	1/5	Moderately less important
7	Clearly more important	1/7	Clearly less important
9	Much more important	1/9	Much less important

10.2.3.3 Decision rules

A decision rule provides the basis for ordering the set of ski pistes and choosing the best ski piste according to the *overall performance* of each ski piste. As already mentioned before (Section 10.2.1), the *overall performance* of a ski piste expresses the environmental suitability of a ski piste compared to the environmental suitability of the other ski piste with respect to all environmental criteria. The overall performance is based on the state of the selected environmental criteria and assigned priorities. In MCA there are several possibilities to achieve a ranking of alternatives, 1) *non-compensatory evaluation*, 2) *partial compensatory evaluation* and 3) *compensatory evaluation* (c.f. Chapter 3, Figure 3.4) to achieve a ranking of alternatives. As a consequence of the large number of ski pistes, only *compensatory evaluation*, in particular Simple Additive Weighting (SAW) and the Technique for Order Preference by Similarity to Ideal Solution (TOPSIS, Hwang and Yoon, 1981) and *partial compensatory evaluation*, specifically Elimination of Choice Translating Reality (ELECTRE, Benayoun, 1966), were used in this thesis to integrate the standardised indicator values and to achieve a ranking of the ski pistes. The selection of these decision rules was based on the ease of implementation of the rule for the large number of alternatives.

SAW, uses the concept of weighted averages:

$$A_i = \sum_{j=1}^{n} w_j x_{ij} \tag{10.28}$$

with, A_i the overall performance of the ski piste i, i=1,…,83, w_j the weight, in this case derived by pairwise comparison, assigned to the criterion j, j=1,…,n, n equal to 9 and x_{ij} the standardised indicator value with respect to ski piste i and criterion j. The ranking of ski pistes was derived by ordering the ski pistes according to their overall performance A_i in descending order because the MCA aimed at the identification of the ski pistes with the highest performance. The advantage of SAW is its easy application, however, it assumes independence of criteria, and moreover, that the increase or decrease of the indicator value is linear (Malczewski, 1999).

TOPSIS identifies the best ski piste as the one that is simultaneously closest to the ideal solution and farthest away from the worst solution, known as negative ideal point. In this thesis the ideal solution was characterised by the best performance of each environmental criterion, while the minimum indicator value of each criterion determined the worst solution. First, the separation of a ski piste to the two solutions needs to be calculated. The distance of the ski piste i, i=1,…,83, to the ideal solution (s_{i+}) was determined by:

$$s_{i+} = \left[\sum_{j=1}^{n} (v_{ij} - v_{j+})^2 \right]^{0.5} \tag{10.29}$$

with, v_{ij} the standardised weighted indicator value of the ski piste i and v_{j+} the maximum indicator value of criteria j, j=1,..,n and n equal to 9, also standardised and weighted.

Then the same principle was applied to determine the separation of the ski piste i to the negative ideal solution (s_{i-}):

$$s_{i-} = \left[\sum_{j=1}^{n} (v_{ij} - v_{j-})^2 \right]^{0.5} \tag{10.30}$$

with, v_{j-} the standardised and weighted minimum indicator value of criterion j. Subsequently, the proximity (c_{i+}, $0 < c_{i+} < 1$) of the ski piste to the best solution was derived by:

$$c_{i+} = \frac{s_{i-}}{s_{i+} + s_{i-}} \tag{10.31}$$

Ski pistes were ranked according to minimum difference between c_{i+} and 1. The application of TOPSIS results in a complete ranking of the ski pistes, and moreover, it is especially suitable for decision problems for which it is difficult to identify independent criteria, as were encountered in this study.

ELECTRE is a concordance method that is based on the pairwise comparison of alternatives (Benayoun et al, 1966), in this case ski pistes. The advantage of this method is that each ski piste is compared with every other ski piste with respect to the standardised indicator value. For example ski piste 1 was compared to piste 2. For all indicators for which piste 1 scored better, the weights of the respective criteria were summed to provide a measure for the performance of piste 1 with respect to piste 2. This procedure was repeated for every combination of ski pistes, resulting in a performance matrix that contained the performance measure for each piste with respect to every other one. At the end, ski pistes were ranked according to the overall performance, which was derived by summing the performance measures for each piste. The implementation of this method is quite laborious for a large number of alternatives. However, a small script written with the cartographic modelling language of PCRaster and the conversion of tables to maps in raster form, where the x-coordinate expressed the rows of a table and the y-coordinate the columns, made it possible to apply this decision method to a large number of ski pistes. There is also professional computer software to carry out this method, but it was not available. The advantage of ELECTRE is that the rank is based on the pairwise comparison with respect to each criterion. However, it does not necessarily provide a complete ranking (Malczewski, 1999), and moreover, since it is an ordinal ranking, it only shows that ski piste 1 is preferred to ski piste 2, but not by how much.

10.3 Results

10.3.1 Prediction of the impact of a ski piste and overall environmental state of a piste

The model tree presented in Chapter 6 (Figure 6.2) was repeated for each piste scenario to predict the effect of the measures and hypothetical changes (Table 10.1) on the

environmental processes for each piste. The impact of a future ski piste was identified by comparing the results computed for the original situation (situation without the impact of a ski piste) and the output from each piste scenario, that is to say for all 83 alternatives. In order to compare the performance of a ski piste with respect to the impact on the environmental system likely to be caused by a ski piste and the overall environmental situation on a ski run, the average impact of a ski piste on the environmental criteria and the average environmental situation in the case of a piste were computed. So for each environmental criterion, the indicator values, representing either the impact of a ski piste on an environmental criterion or the overall environmental state of the respective criterion, were standardised by means of linear transformation. Then the standardised indicator values were combined by SAW, assuming equal importance for all criteria. To obtain the average impact or environmental situation for each ski piste (Figure 10.8), the outcome was divided by the number of the criteria.

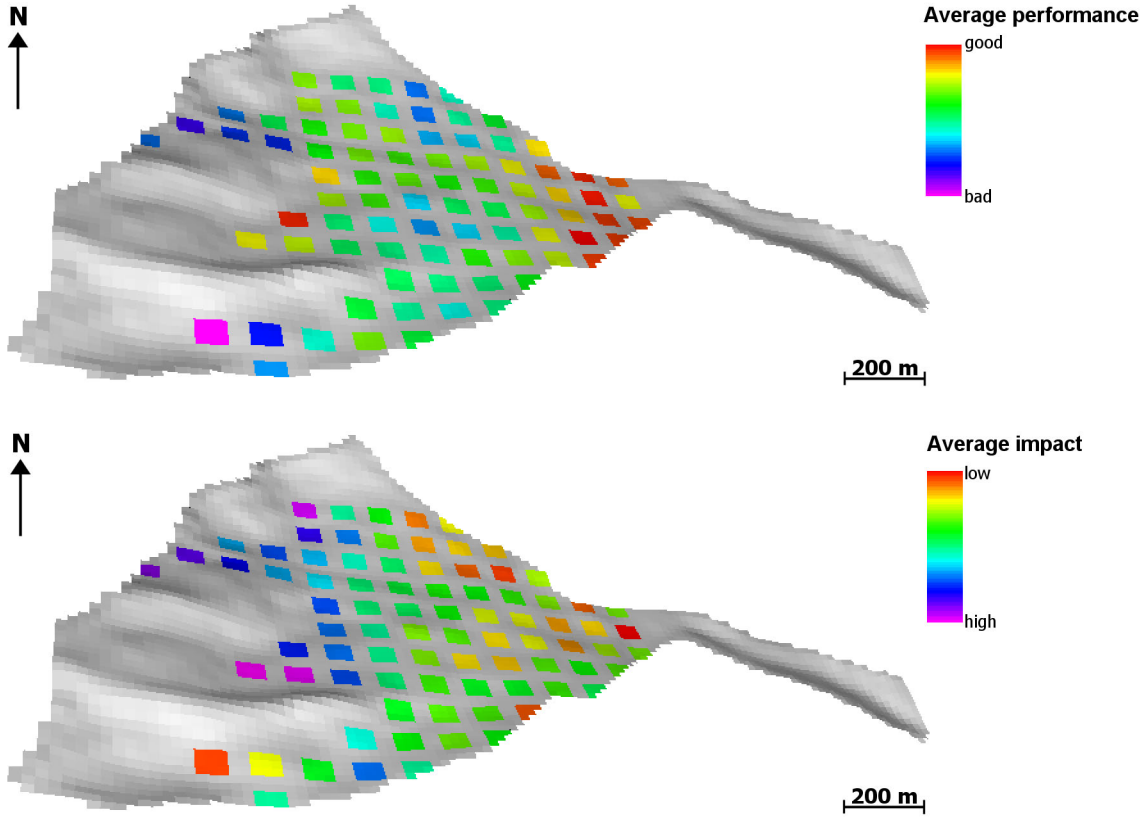

Figure 10.8 The upper map shows the average performance of each ski piste with respect to the overall environmental situation and the lower one the average impact of each ski piste. Ski pistes are represented by their starting point which was enlarged to a block of 3 by 3 grid cells to improve visibility. Ski pistes with a high impact can still perform well because of their originally high environmental suitability.

The figure shows that a bad performance is not necessarily related to a high impact because some ski pistes with an originally very good performance can still buffer the impact.

In the following paragraphs the impact of the changes brought about by a ski piste on the various environmental criteria is described briefly:

Potential for revegetation: The hypothetical changes included in the plant growth model (Table 10.1) resulted in less biomass of grass and sedge for each ski run. The magnitude of the impact differs for each ski piste because it is controlled by both the proposed changes and the original situation. Although the impact is considerable for ski pistes with an originally high amount of biomass, they still have a higher potential for revegetation than ski pistes with a lower impact, but originally bad growing conditions.

Degradation of vegetation: Negative consequences on the vegetation types were derived from only one source, specifically the vegetation type map (c.f. Chapter 5), which was transformed to a degradation map by assigning a degradation value to each vegetation class according to the typical species composition of such a class. For each ski piste the average degradation was calculated. Accordingly, the degree of degradation expressed by this map is clearly a function of the input map; it depends to a large extent on the degradation values that were assigned to each vegetation class, and moreover, on the quality of the map derived from the mapping procedure.

Erosion: Looking at the original situation of a potential site for a ski piste, serious erosion features were mainly predicted for bare areas, or areas, exposed to concentrated overland flow. As a consequence of the changes brought about by a ski piste, the impact in areas that had originally a small sediment load is considerable higher than the impact of ski pistes that had originally a large amount of erosion. This was mainly caused by the assumption that a potential ski piste is bare. The increase of overall erosion in the total catchment is very small, being largely controlled by the amount of erosion on future ski pistes.

Slope instability: The impact of a ski piste on the risk of slope instability was very little, obtained by comparing the aggregated value of the probability of slope failure in space and time for the normal situation to the one of the changed situation. Moreover, for some ski pistes even a positive impact was observed, probably caused by smoothing irregularities over a short distance. The overall impact of a ski piste on the risk of slope failure within the total catchment is negligible, and again, it is mainly caused by the unstable grid cells on the ski pistes.

Flooding: The peak discharge at the outflow point of the catchment hardly differs for the changes brought about by a ski piste. Just some areas in higher elevations seemed to contribute to a higher discharge for the case of a future ski piste.

Surface corrections: The degree of soil degradation was solely determined by the topography of the physical terrain of a selected ski piste and the aggregation rule for the translation of the impact to a single value. The fraction of soil that is going to be disturbed is rather large, independent from the aggregation rule.

Snow conditions: The impact of the addition of artificial snow and the smoothing of the surface of a ski piste had a negligible effect on the number of days with satisfactory snow conditions. The impact could partly be compensated by the spatio-temporal aggregation of the model results, or, if natural snow conditions were reasonable, that there was just no need for artificial snow.

10.3.2 MCA

In order to obtain a rank order of the 83 alternatives, several choices had to be made with respect to the 1) aggregation method to provide the MCA with a value for each indicator, 2) the standardisation function to bring the indicator values to a common scale, 3) the determination of weights, and 4) the decision rules to combine the standardised and weighted indicator values. Table 10.6 illustrates the methods that were eventually applied to each environmental criterion to be able to combine them by means of simple additive weighting (SAW). The weights, w_i ($\sum_{j=1}^{n} w_j = 1$, n=9), were derived by means of pairwise comparision with a consistency ratio (CR) of 0.008 (a CR above 0.1 means inconsistent judgement).

Table 10.6 Characteristics of the environmental criteria and selected methods to carry out the MCA.

Criterion	Effect	Indicator value, derived by aggregation	Standardisation	Weight
VegOne	Benefit	Average maximum biomass (Eq. 10.2)	Convex curve	0.36
VegTwo	Cost	Average degradation (Eq.10.3)	Concave curve	0.18
ErOne	Cost	Average erosion (piste) (Eq. 10.4)	Concave curve	0.0135
ErTwo	Cost	Average erosion (catchment) (Eq.10.5)	Concave curve	0.0135
SlOne	Cost	Average maximum failure (piste) (Eq.10.9)	Concave curve	0.018
SlTwo	Cost	Average maximum failure (catchment) (Eq.10.11)	Concave curve	0.018
FlOne	Cost	Maximum discharge (Eq.10.16)	Concave curve	0.042
SfOne	Cost	Fraction of piste disturbed (10.19)	Linear function	0.078
SnOne	Benefit	Number of days with snow (10.23)	S-shaped curve	0.277

Since the overall environmental situation of a ski piste was considered to be more important than the actual impact caused by a piste, the ski pistes were evaluated with respect to the overall state of each environmental criterion (i.e. original situation plus the impact) and not according to the impact on each indicator caused by the changes brought about by a ski piste. The sum of the procedural steps to obtain the performance of each ski piste resulted in a better performance for ski pistes in lower elevation, represented in Figure 10.9 (p.180) in form of the starting point of each piste, which was enlarged to a block of 3 by 3 cells to improve visibility.

The good performance of the ski pistes at lower altitudes was to a large extent caused by the nearly linear correlation of biomass and snow conditions with elevation and the higher weight that was assigned to them. From the performance of each ski piste the average performance for each grid cell, which falls in the area of at least one ski piste, was computed (Figure 10.10). The average performance of each grid cell illustrates the same spatial variation as the overall performance for each piste. So the evaluation of 83 pistes has made it possible to obtain the spatial pattern of the environmentally suitable areas that optimise the choice of a site for a new ski run.

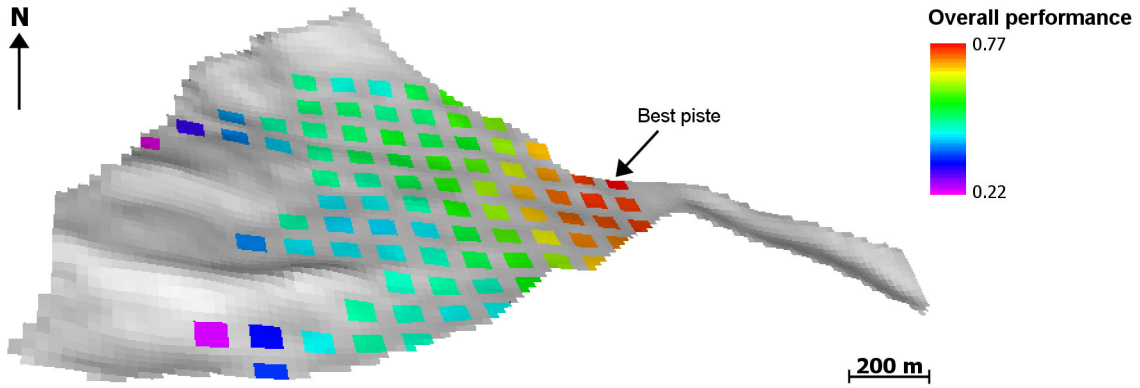

Figure 10.9 Overall performance of each ski piste obtained by SAW according to the methods of Table 10.6, represented by the starting point of each piste which was enlarged to a block of 3 by 3 grid cells to improve visibility. The starting point of a piste only indicates the start of a piste and not its total area (c.f. Chapter 3, Figure 3.11)

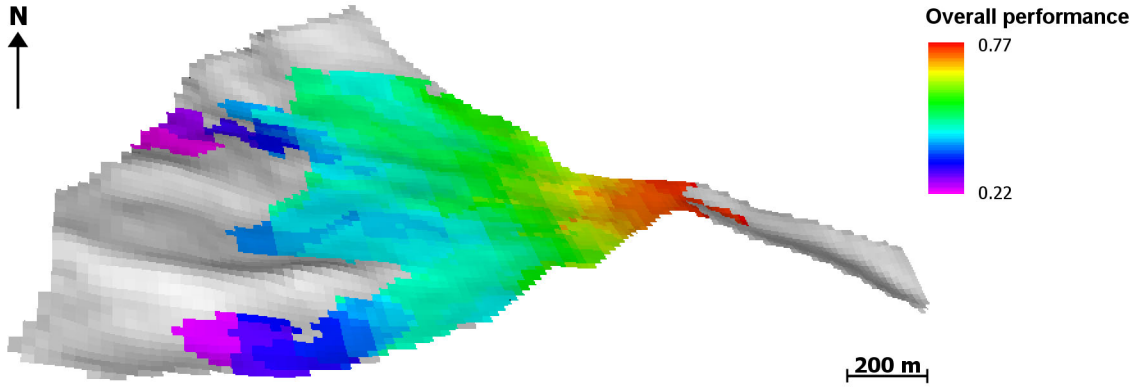

Figure 10.10 Average overall performance for each grid cell that is part of at least one ski piste, derived from the overall performance of each ski piste.

The outcome of SAW can be used to achieve a complete ranking of the ski pistes with respect to overall performance of each ski piste to provide the decision maker with the best ski piste (Figure 10.9). The other decision rules TOPSIS and ELECTRE are considered in Chapter 11.

10.4 Discussion and conclusions

The comparison of potential sites for ski pistes with respect to 1) the original situation at those sites, 2) the situation in the case of a new ski run and the magnitude of the possible impact at these sites showed that the final ranking of ski pistes depends largely on the input to the MCA, which can be either the overall state of an environmental criterion for a

ski piste or the impact. However, in order to take into account the original situation plus the impact, for example the amount of erosion without the impact of a ski piste plus the increase of the sediment load due to the changes brought about by a ski piste, MCA was based on the overall state of the environmental criteria such as the total or maximum sediment load of a ski piste. Nevertheless, in the decision making process for a new ski run both aspects should be considered. The identification of the more acceptable ski piste needs to be tailored to both the minimal impact likely to be caused by a ski piste and the maximum performance of a ski piste with respect to the state of the environmental criteria in the case of a ski run.

The outcome of the MCA showed that the performance and therefore the rank order of ski pistes was strongly influenced by the preference for an environmental criterion. This was clearly illustrated by the indicator "growth of grass" or "snow conditions", which were given a higher priority and which had a significant effect on the final ranking of the ski pistes. The definition of preferences gives the opportunity to tailor the planning of ski runs to the decision problem and the needs of individuals or groups of individuals. However, the assignment of priorities has a distinct effect on the final ranking and can cause the selection of an alternative that performs badly with respect to criteria which were assigned a low weight. For example, giving a high priority to vegetation combined with a low one to the triggering of slope instability can result in the selection of a ski piste that has a high potential for revegetation, but also a high risk of slope failure because the ranking was to a large extent determined by the good vegetation conditions.

A shortcoming of the study was that the weight, which was assigned to each environmental criterion, was assumed to be valid for each ski piste. However, in reality the importance of an environmental criterion has a spatial variation, in the mountains to a large extent controlled by elevation. Therefore it would be sensible to include the spatial variation of the relevance of an environmental criterion in the assignment of priorities. However, it was not done in this thesis, because, since the assignment of weight has a strong effect on the overall performance of a ski piste, it requires detailed information, which was beyond the scope of this study.

Another shortcoming was the use of compensatory evaluation to identify the best ski piste because it allows for the compensation of bad performances by good performances. This can cause that a ski piste is considered to be the best solution despite the presence of unfavourable conditions. In order to avoid the selection of such a ski piste, the rank order of the ski piste and the performance of the ski piste with respect to each environmental criterion has to be carefully evaluated.

Nevertheless, MCA made it possible to combine the model results and to identify environmentally suitable areas for locating new ski runs with respect to the choices that have been made in all steps of the decision framework. Moreover, it is a useful method for integrating the objectives of individuals or groups of individuals to balance the decision making process.

Since the choice of methods for aggregating the model results, for standardising the indicator values to a common scale, weighting the criteria and obtaining a ranking of the alternatives is very subjective, a sensitivity analysis needs to be carried out to investigate the impact of the several choices on the final ranking of the ski pistes. This will be demonstrated in the following chapter.

11 SPATIO-TEMPORAL MULTICRITERIA DECISION MAKING FOR PLANNING SKI RUNS: SENSITIVITY ANALYSIS

11.1 Introduction

MCDM requires several decisions to achieve a ranking of the ski pistes, which are related to the selection of the environmental criteria, the input to the MCA, the choice for the standardisation method, assigning a weight and finally the application of a decision rule to obtain a rank order of the ski pistes. In each procedural step uncertainty is involved, and therefore the sensitivity of the final rank order of the ski pistes has to be evaluated with respect to each step of the decision framework. The starting point for each scenario of the sensitivity analysis is the evaluation of Chapter 10 according to the settings of Table 10.6, for which the overall environmental state of a criterion was used in the MCA, in the following part referred to as *base evaluation*.

11.2 Sensitivity to the input to the MCA

The ranking of the ski pistes obtained by compensatory evaluation depends to a large extent on the input to the MCA. In the MCA carried out in this thesis the input can differ with respect to 1) whether the overall environmental state of a ski piste was evaluated or the impact likely to be caused by a ski piste (Chapter 10), 2) the aggregation method to aggregate a stack of maps to an indicator value (Chapter 10), and 3) the assignment of a degradation value to the different units of a map such as the classes of the vegetation type map (Chapter 5). In the following sections the sensitivity of the rank order to the input to the MCA will be presented. In all scenarios the best ski piste is equivalent to rank position 1, while the worst ski piste is ranked in position 83.

11.2.1 Rank order according to the impact of a ski piste

In the MCA carried out in Chapter 10 the overall environmental state of a potential site for a ski piste was considered to be more important than the impact likely to be caused by a ski piste. However, for certain aspects the magnitude of the impact may be of higher concern, for example if additional measures have to be established to prevent or mitigate natural hazard. And moreover, if the aim is to identify the ski piste with minimum impact and most favourable environmental conditions, the rank order of the ski pistes with respect to the environmental impact has to be evaluated as well. Therefore, the performance of the 83 ski pistes was evaluated according to the magnitude of the impact of each ski piste on the environment.

For all environmental criteria the impact was computed by comparing the state of the environmental criteria with ski piste and without ski piste. To compute the rank order of ski pistes with respect to the indicator values that represent the impact of a ski piste on each environmental criterion, the same standardisation functions, fitted to the magnitude

of the impact of a ski piste on each criterion, and the same weights were used.

Ranking the ski pistes with respect to the "impact of a ski piste on a criterion" rather than according to the "overall environmental state of that criterion" results in a quite different rank order. Therefore, when specifying the impact of ski pistes on each environmental criterion as the input to the MCA, led to a quite different rank order as well. However, since the criterion "potential for revegetation" was assigned a rather high weight, the ranking of the ski pistes with respect to the impact of a ski piste on each environmental criterion was to a large extent controlled by the magnitude of the impact on this criterion.

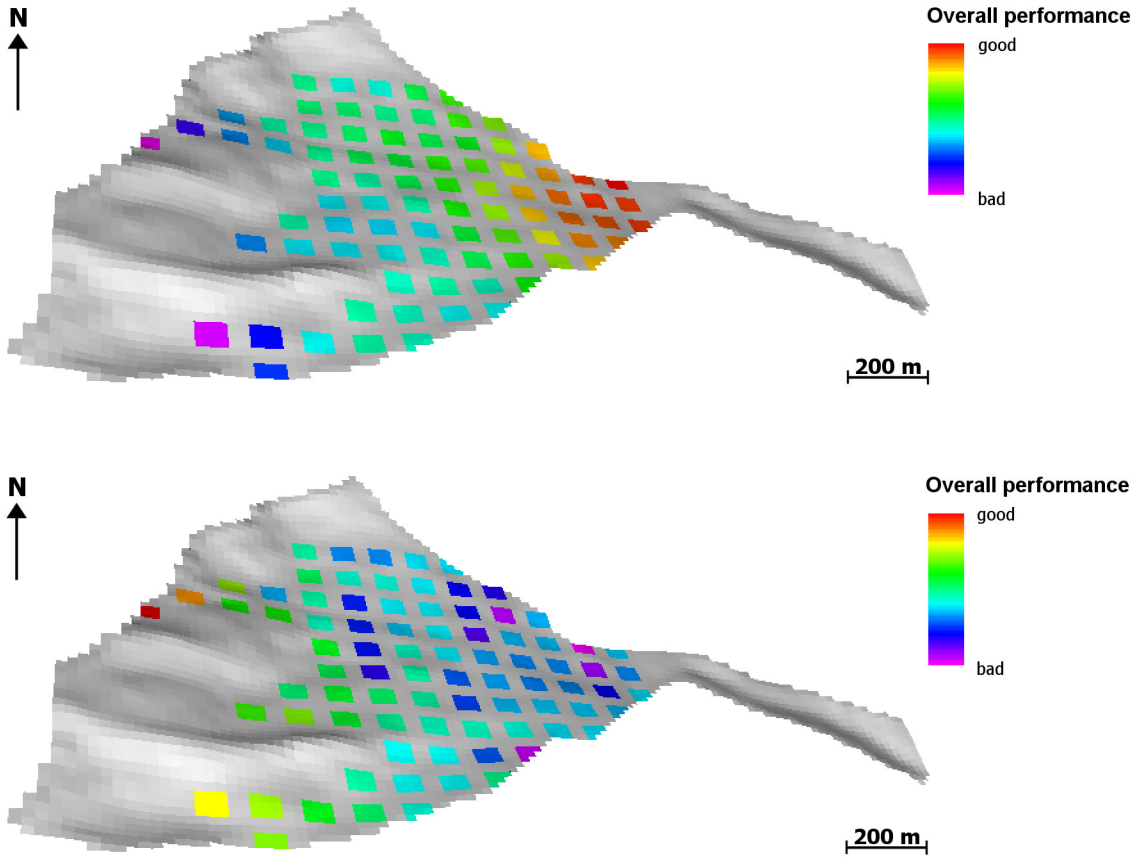

Figure 11.1 The upper map shows the overall performance of each ski piste according to the state of each environmental criterion, and the lower one the overall performance of each ski piste with respect to the impact of a ski piste on each criterion. In both maps a ski piste is represented by its starting point, enlarged to a block of 3 by 3 cells.

11.2.2 Effect of the aggregation method

The aggregation of the spatial and temporal component of the different stacks of maps was determined by the estimated importance of an environmental criterion for the

planning of environmentally sound ski runs. However, since the selection of a certain aggregation method is very subjective, the sensitivity of the ranking of the ski pistes was evaluated for another aggregation method for selected environmental criteria, in particular the "erosion" criteria (*ErOne*, *ErTwo*), the "slope instability" criteria (*SlOne*, *SlTwo*), the criterion "surface correction" and the criterion "snow conditions".

Spatial aggregation of erosion. In the base evaluation (Chapter 10) the erosion status of a ski piste was described by the average annual erosion on the ski piste or in the catchment, both derived from the annual erosion map. However, the erosion status could also be expressed by the maximum erosion rate for the spatial extent in consideration as mentioned in Chapter 10 (Equation 10.6 and 10.7). The application of the second aggregation method to the annual erosion map led to a different pattern of the state of erosion on a ski piste or in the catchment than was obtained in the base evaluation (Figure 11.2).

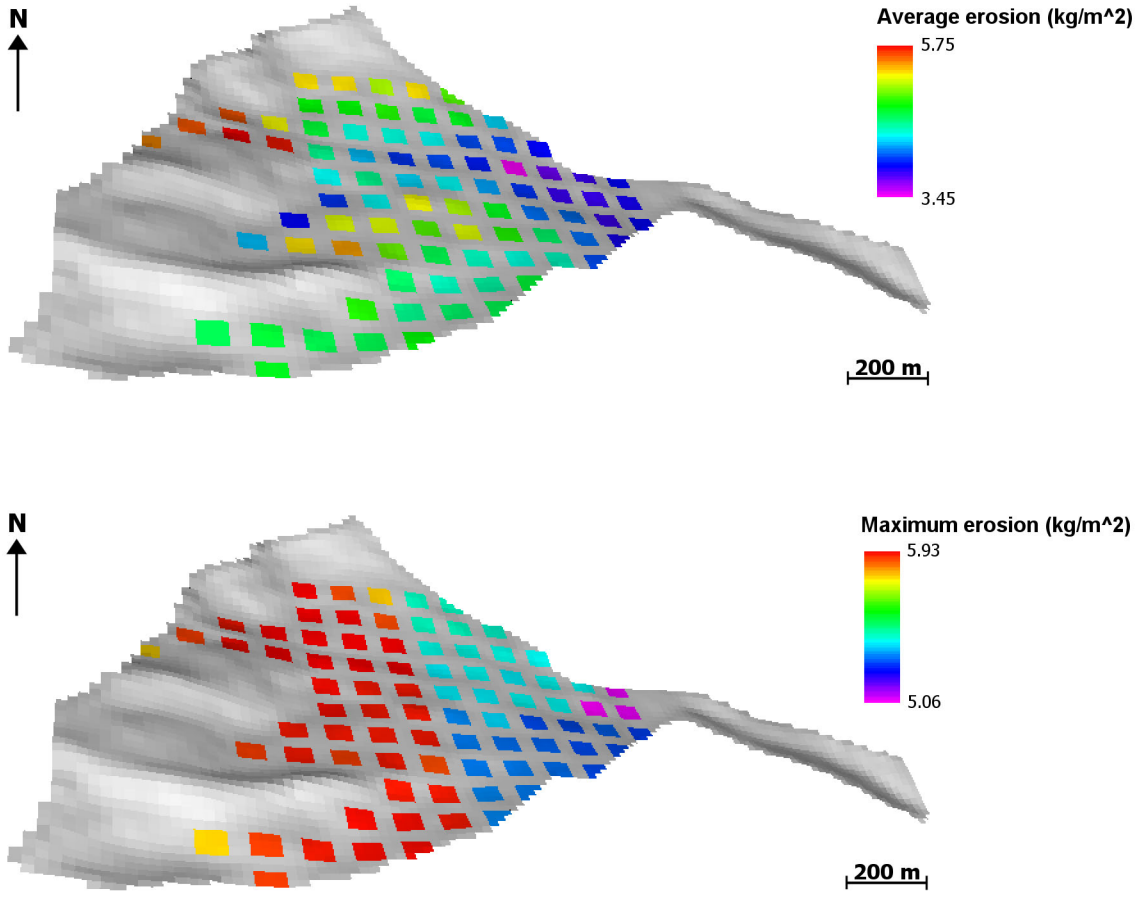

Figure 11.2 The upper map illustrates the state of erosion on each ski piste, represented by the average erosion (kg/m^2) and the lower one indicates the state of erosion in form of maximum erosion on a ski piste (kg/m^2). The different range of the scale needs to be taken into account.

Replacing “average erosion” on the ski piste and in the catchment by “maximum erosion” in the entire MCA according to Table 10.6 of Chapter 10 resulted in approximately the same rank order of the ski pistes because, as a consequence of compensatory evaluation, the overall trend was determined by the standardised and weighted indicator value of other criteria such as “potential for revegetation” rather than by another aggregation method for the erosion criteria. The choice of aggregation method had little effect on the performance of the best and the worst ski pistes, although there were changes in the rank order of ski pistes of average performance.

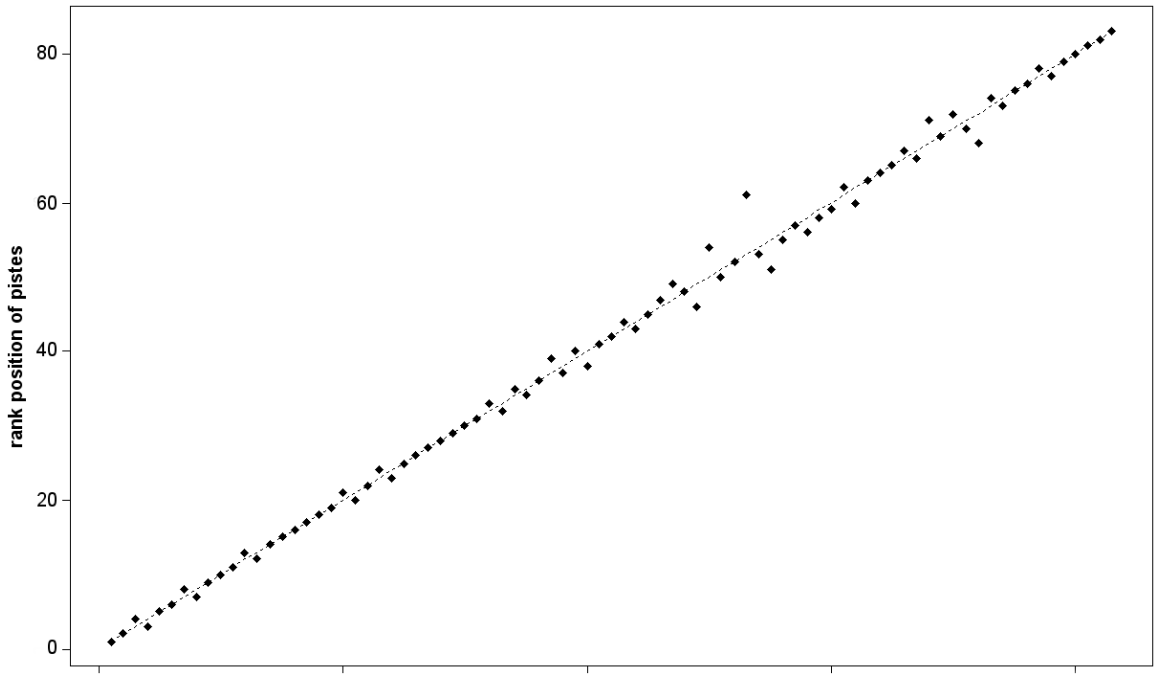

Figure 11.3 Consistency of rank positions (y-axis) using another aggregation method for the output of the erosion model, represented by the deviation of the points (rank position of a ski piste when aggregating to maximum erosion rate) from the dashed line (rank position when aggregating to average erosion). The x-axis represents the ski pistes, sorted according to the rank order obtained in the base evaluation.

Spatio-temporal aggregation of probability of failure. To represent the risk of slope instability on a ski piste or in the catchment by a single value, the temporal variation of the spatial distribution of the probability of slope failure was aggregated by computing the spatial average of the maximum probability of failure during one year (probabilistic method, Chapter 10, Eq. 10.9 to 10.11). However, in the previous chapter a second consideration was introduced, in particular to indicate slope instability by the fraction of the ski piste area for which at least once a probability of failure above 0.5 was predicted (deterministic method, Chapter 10, Eq. 10.12 to 10.15). Just as was the case for erosion, the deterministic method led to a different rank order of the ski pistes according to the

aggregated indicator value for the slope criterion. However, the outcome of the entire MCA resulted for both indicators in more or less the same rank positions of the ski pistes.

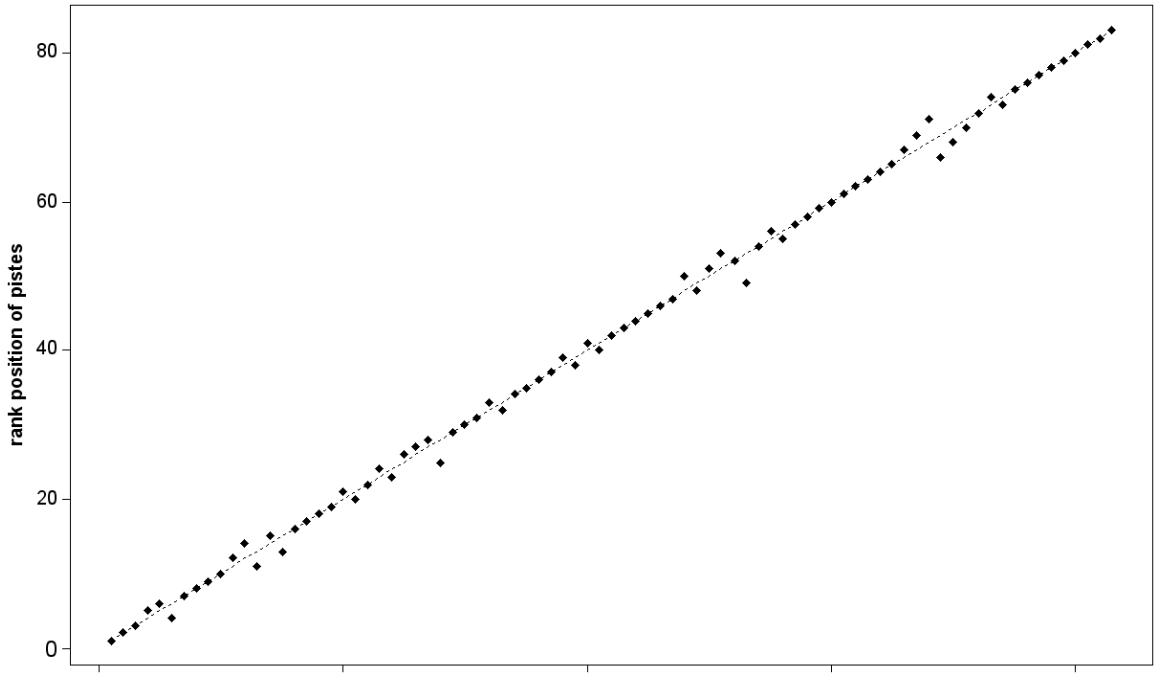

Figure 11.4 Consistency of rank positions using another aggregation method for the output of the slope stability model, represented by the vertical deviations of the points (rank positions of ski pistes when restricting to probabilities greater than 0.5) from the dashed line (rank positions when using all probabilities). The x-axis represents the ski pistes, sorted according to the rank order obtained in the base evaluation.

Determination of the impact of surface corrections. The impact of surface corrections on the soil, regolith and bedrock was expressed by the fraction of the ski piste area where the removal of soil or filling up of depressions exceeded the threshold d (Chapter 10, Eq. 10.17 to 10.19). In order to analyse the sensitivity of the outcome of the MCA to the determination of d, d was assigned three different thresholds, resulting in three different indicator values representing the impact of surface corrections of the soil, regolith or bedrock. Repeating the MCA according to the settings of Table 10.6, each time with a different indicator value for the criterion "surface corrections", led to approximately the same rank order of the ski pistes. With respect to the outcome of the entire MCA, the different threshold had a small effect on the ranking of ski pistes, it caused only small changes of the rank positions of the ski pistes within a short range of the rank order.

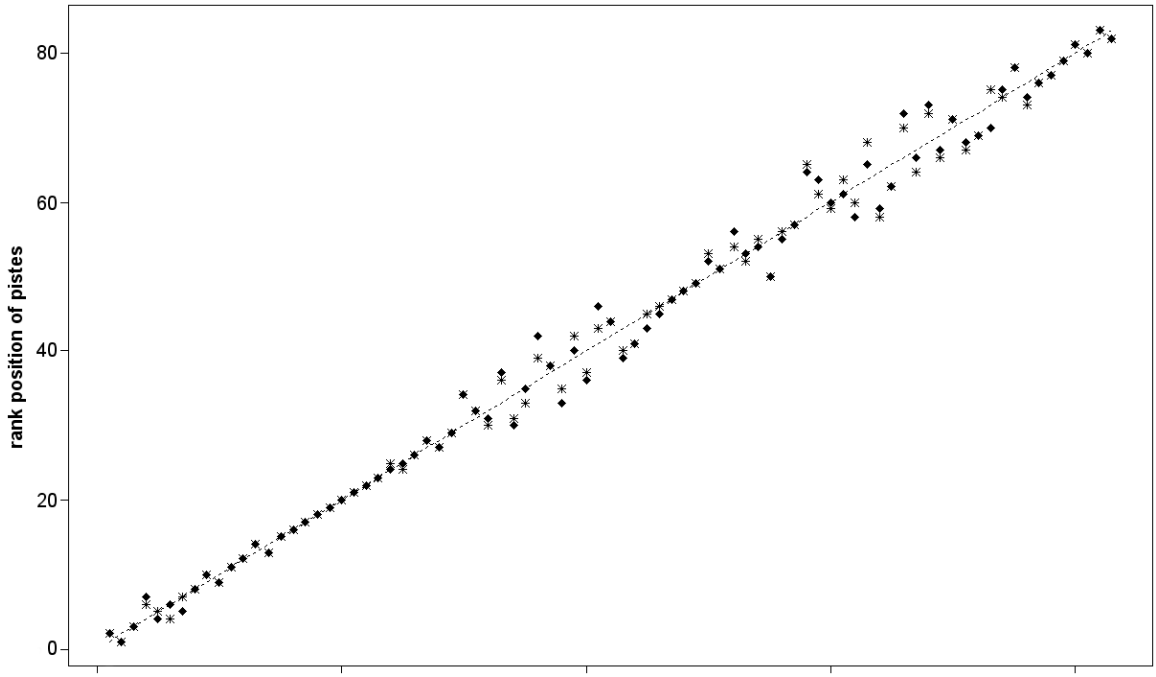

Figure 11.5 Sensitivity of the ranking to the aggregation rule in order to express the impact of surface corrections on the soil, regolith or bedrock. For each scenario a different threshold *d* was selected, represented by the vertical deviations of the stars, (*d*=0.25) and diamonds (*d*=0.75) from the dashed line (*d*=0.5; default). The x-axis represents the ski pistes, sorted according to the rank order obtained for *d*=0.5.

Spatial and temporal aggregation of snow conditions. The aggregation of snow cover maps for different moments to a single value required the definition of a satisfactory snow cover at the ski piste (c.f. Chapter 10). A snow cover was assumed to be satisfactory when at a certain fraction of the ski piste area (*a*) a defined snow thickness (*z*) could be observed. In further scenarios both *a* and *z* were assigned a higher and a lower threshold, resulting in nine indicators representing snow cover conditions. Using each time a different indicator to represent the snow cover conditions in the MCA showed that the aggregation rule had a small effect on the rank positions (Figure 11.6).

The analysis showed the aggregation method to have a small effect on the final rank order of the ski pistes, for which all criteria were combined. Moreover, the effect on the worst or best ski pistes was negligible. However, since the final rank order is the result of the performance of the ski pistes with respect to all criteria, the uncertainty involved in the aggregation method can determine the short range variation of the rank positions as illustrated by the deviations from the closed line in the Figures 11.3 to 11.6. Nevertheless, the analysis of the individual criteria showed the state of a ski piste with respect to one of the considered criteria to be different when using another aggregation method (Figure. 11.2), although this difference becomes unimportant for criteria which are given a low weight because the ranking is in the first order determined by the criterion which was given the highest weight.

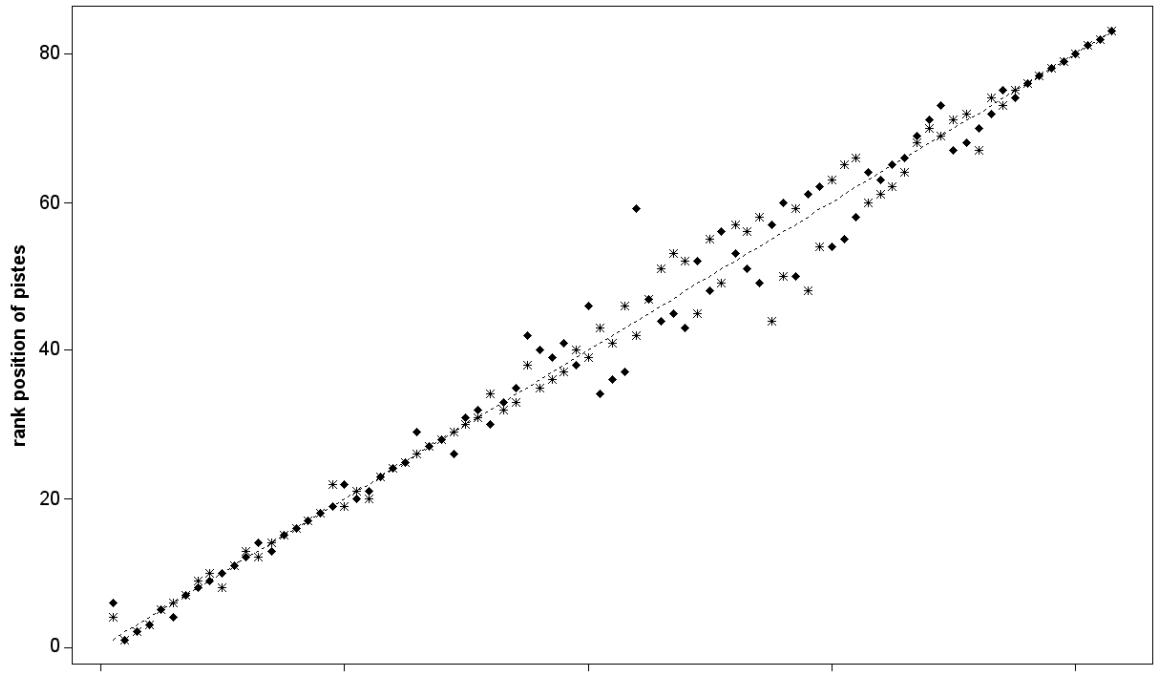

Figure 11.6 Sensitivity of the rank order to the method for aggregating snow cover maps to an indicator value. The ranking with respect to a thin snow cover (diamonds), an average snow cover (dashed line) and a thick snow cover (stars) was similar. Ski pistes, represented at the x-axis, are sorted according to the rank order obtained for the average snow cover.

11.2.3 Determination of the degree of degradation

The assignment of a number between 0 and 9 to a vegetation class to express the degradation of the vegetation when a certain vegetation community is going to be disturbed by a future ski run is subjective. In order to analyse the sensitivity of the ranking of the ski pistes to the assignment of the degradation value, four further scenarios were carried out, each scenario with another degradation map that has been aggregated to an average degradation value. The maps differed only in one property from the degradation map that was used in the base evaluation. Ascribing a higher degradation of vegetation to "the man-made" vegetation at higher altitudes (2nd scenario) resulted in a considerable better ranking of ski pistes with just a slightly greater degradation because of the worse performance of ski pistes with a significantly greater degradation with respect to the base evaluation, partly driven by using SAW to obtain the rank order where low indicator values can be compensated by higher ones. The rank order of the other scenarios hardly differed from the outcome obtained in the base evaluation except for small changes between the base evaluation and the second scenario which are related to the assignment of a greater impact value to the vegetation class that was occupied with species that were not found in other vegetation communities (c.f. Chapter 5). Nevertheless, the best and the worst ski pistes kept their rank position in all scenarios.

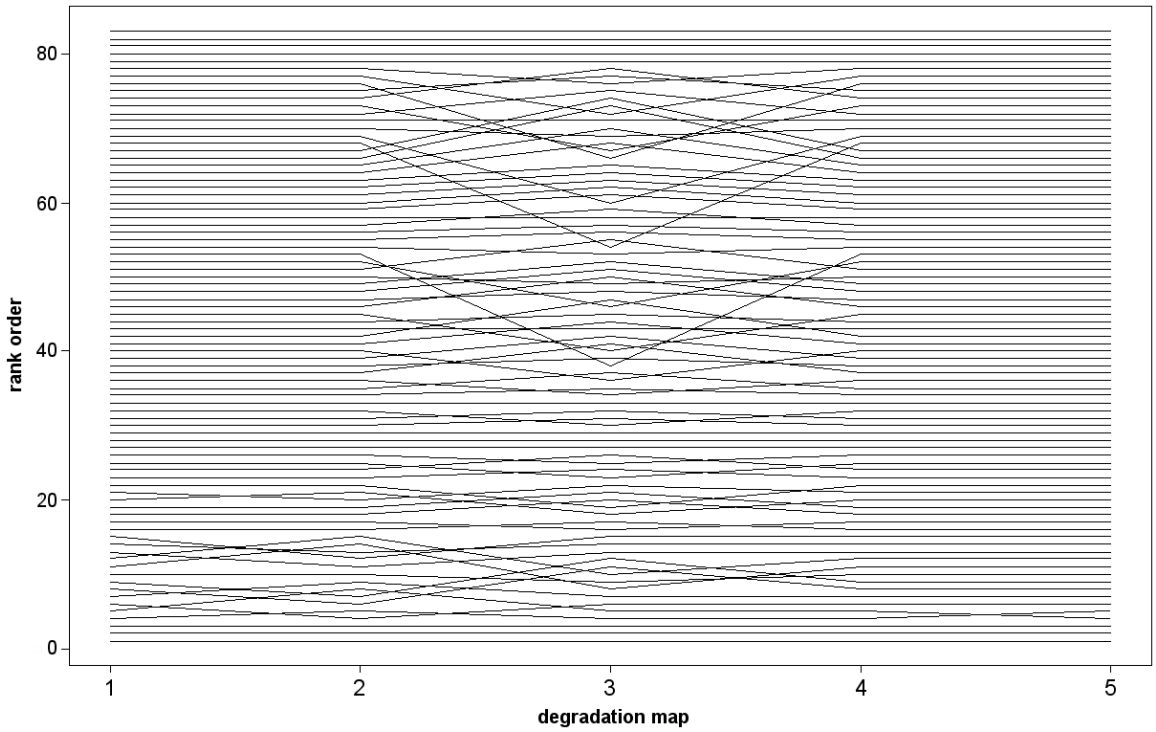

Figure 11.7 Rank order of ski pistes according to different degradation maps. 1 represents the rank order obtained by the base evaluation, 2, 3, 4 and 5 further scenarios, each time with a different degradation map.

11.3 Sensitivity to the standardisation method

Chapter 10 described among other methods three kinds of standardisation techniques (Eq.10.24 to 10.27) to standardise the *indicator values*. Because of the presumably different objectives of individuals, their knowledge of the decision problem and their position in the decision making process, the selection of the standardisation techniques and the exact shape of a non-linear standardisation function (value function) can be biased. Consequently, the uncertainty involved in the choice for a certain technique and the determination of the midvalue point when using value functions can have a considerable effect on the ranking of the ski pistes. Therefore the sensitivity of the ranking of the ski pistes to these decisions needs to be analysed. This was done by comparing the rank order of the ski pistes obtained in the base evaluation (Chapter 10) with the rank order of each further scenario described in the following sections for which just one setting was changed at one time.

11.3.1 Sensitivity to the choice of a standardisation technique

The choice of a linear transformation function or convex or concave value functions for each criterion to standardise the values of an indicator to a common scale led to approximately the same ranking of the ski pistes. Also when applying the S-shaped curve

to standardise the erosion criteria or slope stability criteria, the rank order hardly differed with respect to the rank order obtained in the evaluation of Chapter 10. However, standardising the criterion "potential for revegetation", the criterion "surface corrections" and the criterion "snow conditions" according to an S-shaped curve had a large effect on the final ranking of the ski pistes compared to the rank order when standardising these criteria by means of another standardisation techniques. The use of another standardisation method to standardise the criterion flooding resulted in a quite stable ranking, except for the significant different rank position of the two ski pistes, whose indicator value was assigned a 0 or a 1 in each scenario.

The ranking of the ski pistes with respect to the criterion "degradation of vegetation communities (*VegTwo*)" turned out to be more sensitive to the impact assigned to each vegetation class than to the transformation method (Figure 11.7).

In general, standardising the indicator value by means of linear transformation function and convex or concave value functions leads to approximately the same rank order for all environmental criteria. However, just like for the sensitivity of the ranking to the aggregation method, the sensitivity of the ranking to the standardisation method is considerable for those criteria which were given a high priority, namely "potential for revegetation ", and a slightly lower weight to the criteria "surface corrections" and "snow conditions".

11.3.2 Sensitivity to the shape of a value function

In order to fit the general value functions to the individual criteria, a *midvalue point* had to be determined. The midvalue point (X_P, Chapter 10) is the point, whose indicator value is expected to be half important as the maximum value of the indicator in consideration. Just like with all other decisions, the selection of this point is subjective. Accordingly, to consider the uncertainty involved in the selection of a midvalue point for fitting a value function, the sensitivity of the ranking of the alternatives to the determination of the midvalue points was examined by repeating the MCA several times, each time for a different midvalue point, but the same environmental criterion. The procedure was carried out for all environmental criteria that were standardised according to a convex, concave or S-shaped curve.

Convex or concave value function. The effect of the determination of the midvalue point on the ranking of ski pistes in the case of a convex or concave function revealed rank positions to be quite stable, except for the criterion "potential for revegetation" which was assigned a considerable high weight. The significant change in the rank positions can be explained by on the one side the strong separation of ski pistes with a low indicator value because there the slope of the value function is very steep, and on the other, the choice for compensatory evaluation, which can balance the performance of the environmental criteria. Accordingly, when standardising a criterion according to this kind of value function, low indicator values are more sensitive to the slope of the curve than high values of an indicator, which resulted in a larger effect on the weighted sum, and consequently also on the final ranking. In addition, just like when using a different standardisation technique to standardise the flooding criterion, the rank positions of the same two ski pistes changed significantly for a different midvalue point.

Again the sensitivity of the rank order of ski pistes is also related to the assignment of the weight, which means that the rank order of ski pistes to the determination of a different midvalue point is more sensitive for those criteria which were given a considerable high weight, as for instance shown for the criterion "potential for revegetation" (Figure 11.8). The selection of a different midvalue point rather affected the change of rank positions within a small range of the rank order.

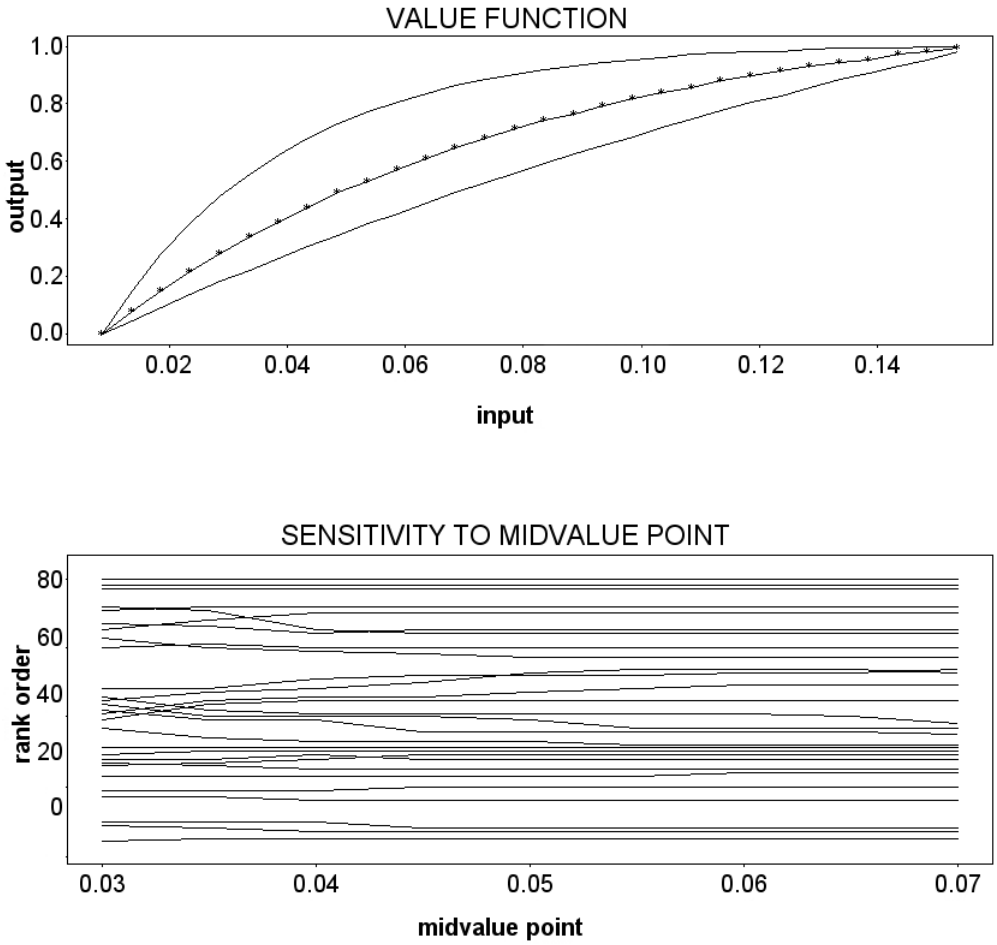

Figure 11.8 Sensitivity of the rank positions to the determination of the midvalue point (kg/m^2) when standardising the criterion "potential for revegetation"; top: convex transformation function, bottom: ranking of ski pistes with respect to the midvalue point (kg/m^2) according the outcome of the MCA.

S-shaped value function. To standardise the criterion "snow conditions" by means of an S-shaped curve, the determination of both a midvalue point and an optimum was required. When analysing the sensitivity of the ranking of ski pistes to the shape of the S-shaped curve, the selection of a different optimum led to more changes in the rank position than when carrying out a sensitivity analysis for the midvalue point.

In addition, the sensitivity of the rank order to the fitting of an S-shaped function was also examined for the other criteria that were originally (in the base evaluation)

standardised according to a convex or a concave function. When using an S-shaped curve in the standardisation procedure, the effect of a different midvalue point on the rank order of ski pistes was similar to the outcome of the sensitivity analysis with respect to the midvalue point that has been carried out for a convex or concave value functions. Again, rank positions of ski pistes changed a lot when using a different midvalue point to fit the value function to the indicator values of the criterion ”potential for revegetation”. An S-shaped curve with a rather steep slope for low indicator values, fitted for example to the indicator values of the criterion ”erosion at the ski piste”, caused the change of few rank positions because of the strong effect of the standardised value of ski pistes with a low indicator value, in this case little erosion, on the weighted sum. Furthermore, a different midvalue point for the construction of an S-curve can also have a strong effect on ski pistes with an average performance with respect to the environmental criterion in consideration. This was for instance shown for the criterion “slope instability on the ski piste”, where the shift in rank positions was to a large extent related to the variation of the indicator values of ski pistes with an average impact on slope stability. Sensitivity analysis of the effect of the midvalue point to fit an S-shaped curve to the indicator values of the flooding criterion on the overall performance of ski pistes led to the same result as in the previous scenarios.

The various scenarios showed that the rank order was more sensitive to the determination of the midvalue point when standardising the values of an indicator according to an S-shaped curve than by means of a concave or convex function.

In general, the rank positions of ski pistes with a very good performance or a very bad performance are considerable stable, independent from the transformation function or the shape of the standardisation curve.

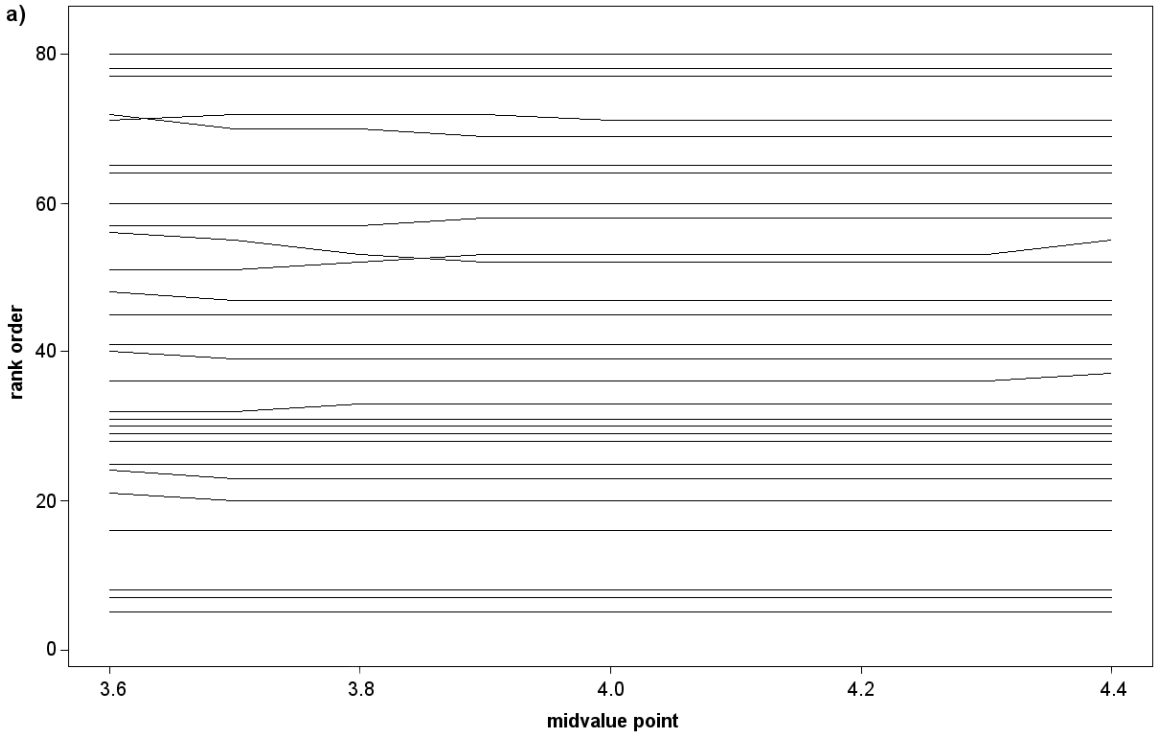

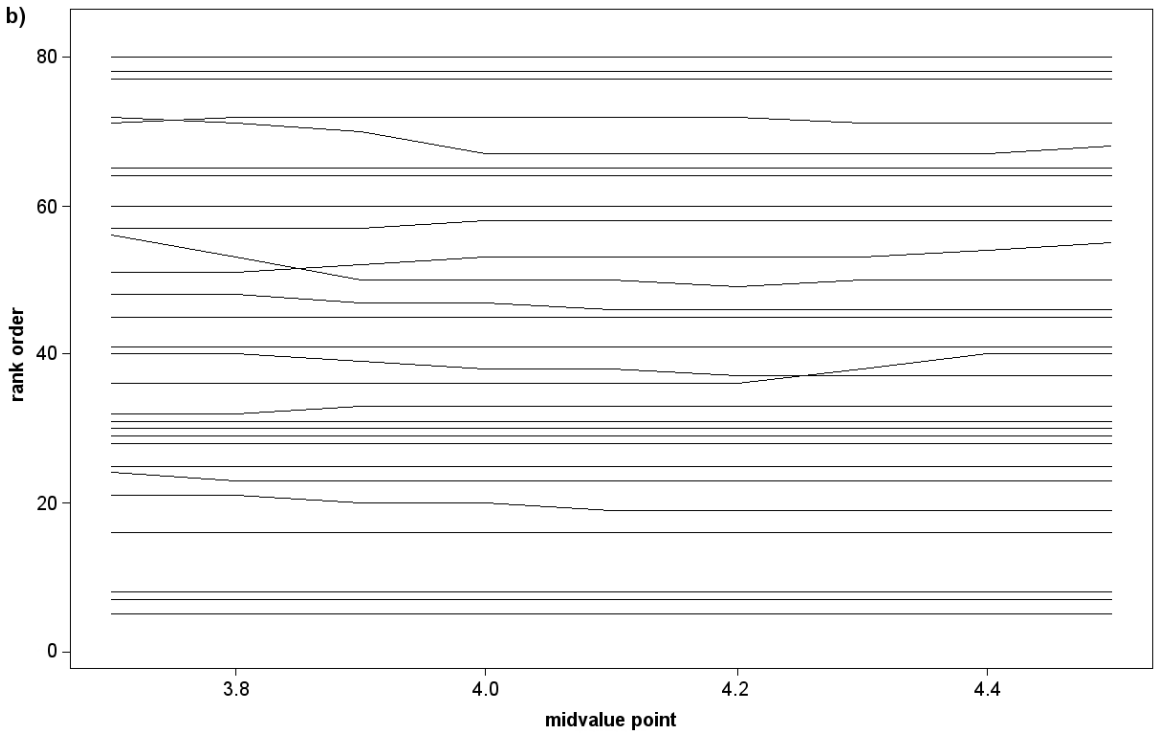

Figure 11.9 a) Consistency of the rank order for choosing a different midvalue point (kg/m^2) to standardise the indicator values of the criterion "erosion on a ski piste" by mean of a concave function. b) Consistency of the rank order for choosing a different midvalue point to standardise the indicator values of the criterion "erosion on a ski piste" according to an S-shaped function. Rank orders show little variation.

11.4 Sensitivity of the ranking of ski pistes to the assignment of priorities

In the MCA described in Chapter 10 priorities among various indicators were assigned by ascribing weights that were derived from pairwise comparison. The sensitivity analysis of the rank order to the choices made with respect to the input to the MCA and the standardisation technique already showed the assignment of the weight to be more important than the other two choices. Nevertheless, the effect of assigning priorities was analysed in a separate procedure by carrying out the MCA four times with different options. In the first scenario linear transformation was used to standardise all environmental criteria, which were eventually combined by SAW, assuming equal importance for all environmental criteria. The second scenario was equivalent to the first one, except for the difference that the criteria were assigned different weights. In the third scenario environmental criteria were brought to a common scale by means of value functions (i.e. according to the meaning of an environmental criterion for the planning of a ski pistes), however, assuming equal importance for all environmental criteria. The fourth scenario was equivalent to the base evaluation of Chapter 10, that is to say, standardisation in form of a value function and ascribing different weights to the environmental criteria. In the first scenario, no significant correlation was observed between the ranking of a ski piste and the standardised indicator values of the individual

criteria which were assumed to be equal important. However, assigning priorities to all criteria derived by pairwise comparison caused criteria that were given a higher weight to have a larger effect on the rank positions. In the case of the criterion "potential for revegetation", which was given a high priority, this means that a higher indicator value was the driving force for the higher rank position of a ski piste. The third scenario, represented by Figure 11.10 c, showed the rank order of the ski pistes to a certain extent to be controlled by the shape of the value function; deviations from the general trend of the correlation of an indicator value and the rank order of the ski pistes were related to the better performance of a ski piste with respect to another criterion because of the use of compensatory evaluation which can balance the effect of the standardised indicator values on the performance of ski pistes. However, the correlations are less clear than when using value functions and direct weights derived from pairwise comparison like in the fourth scenario; the assignment of weights resulted in a shape very similar to the shape of the value function, especially when assigning a large weight. For example, standardising the criterion "potential for revegetation" according to a linear standardisation results in a very weak correlation with the final rank positions of ski pistes. However, ascribing a weight to all criteria increased this correlation. Maximum correlation between the criterion "potential for revegetation" and the final rank positions was observed by using a convex function and a considerable preference for this criterion (Figure 11.10). A similar trend was identified for the criterion "snow conditions" which was also given a higher weight than was assigned to the remaining criteria.

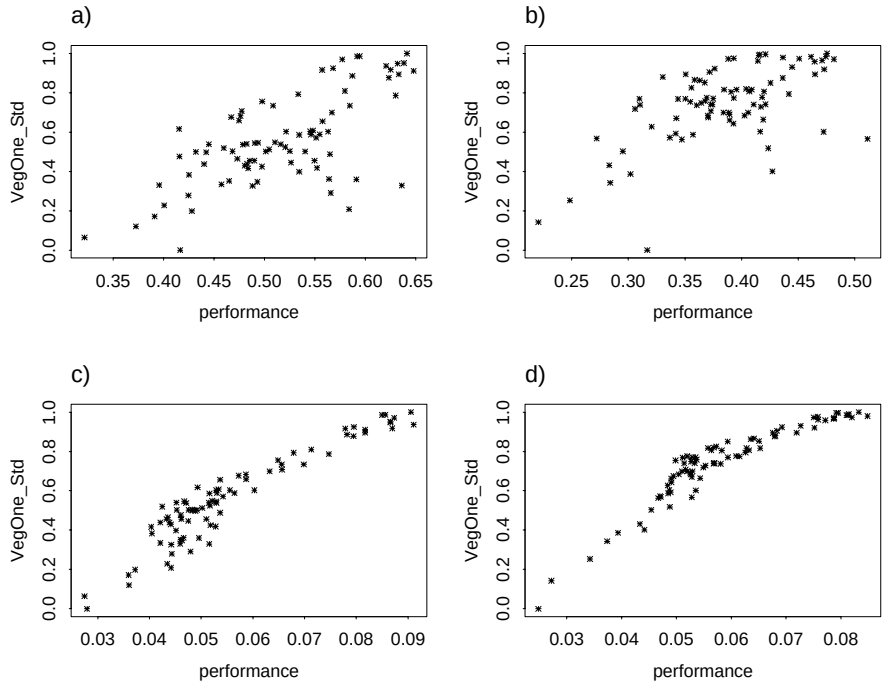

Figure 11.10 Correlation of the criterion "potential for revegetation" and the total performance of ski pistes of four different scenarios; a) linear standardisation, no priority assigned; b) standardisation according to a value function, no priority assigned; c) linear standardisation, direct weighting; d) standardisation according to value functions, direct weighting;

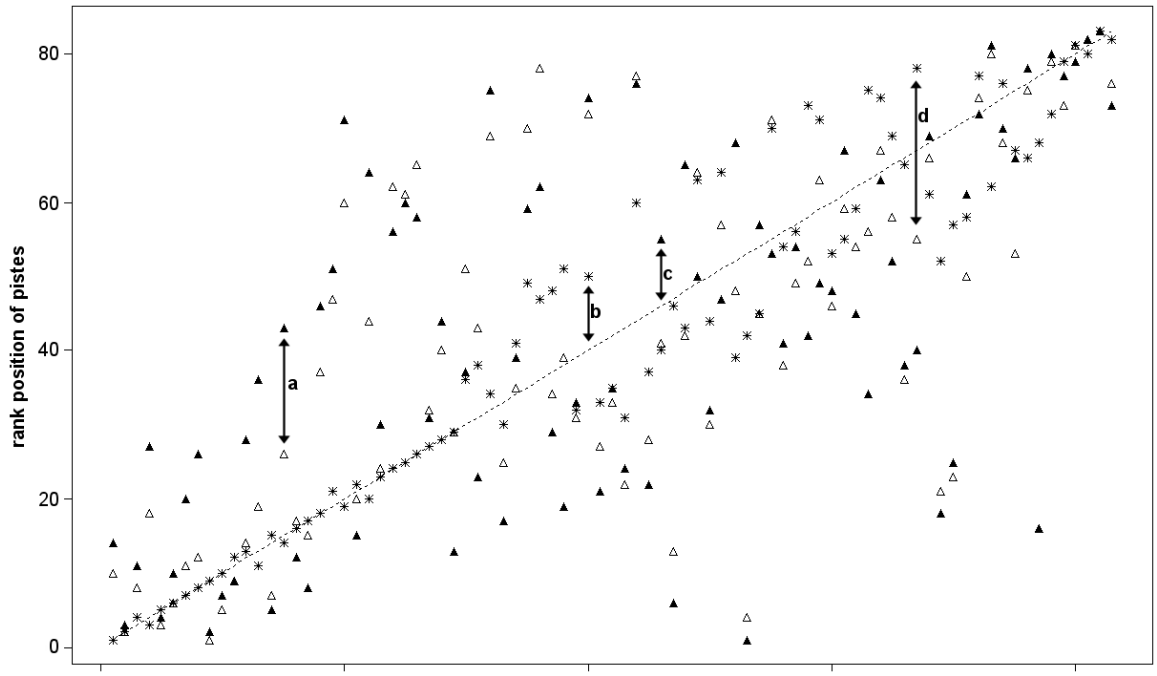

Figure 11.11 Sensitivity of the ranking of ski pistes with respect to the assignment of a weight; the dashed line represents the rank order obtained in the base evaluation, i.e. standardisation according to a value function plus the assignment of weights, **a** represents the difference between the assignment of weights (filled triangle) and no priorities (empty triangle) in the case of linear standardisation, **b** illustrates the difference between the assignment of weight (dashed line) and no priorities (star) for value functions, **c** shows the difference between linear standardisation and value function without the determination of priorities and **d** indicates the difference between linear standardisation and value functions in the case of priorities. The x-axis represents the pistes, sorted according to the rank order obtained in the base evaluation.

Furthermore, as already mentioned in Chapter 10, the MCA was also repeated for different weight combinations which were acquired in form of a questionnaire that was given to several researchers of the Department of Physical Geography (Utrecht University, the Netherlands) who were assumed to be reliable experts in the field of environmental processes. Two problems were encountered: First, the description of the decision problem that was included in the questionnaire seemed to be not sufficiently clear, the assignment of weights was to a large extent inconsistent. Second, carrying out the questionnaire by means of a form to acquire the preference structure restricted the ease of repeating the pairwise comparison in case of an inconsistent judgement. Moreover, the assignment of weights by those experts (only consistent judgement was included in the analysis) resulted in very different rank positions of ski pistes (Figure 11.12, p. 197).

The analysis of the ranking of ski pistes to the assignment of priorities showed the priorities to have a strong impact on the outcome of the MCA. However, giving priorities makes it possible to include human judgement such as the objectives of individuals or groups of individuals to balance the final decision according to the different objectives. In order to select the more acceptable solution, the aspiration level of the solutions obtained by the different preference structures needs to be compared.

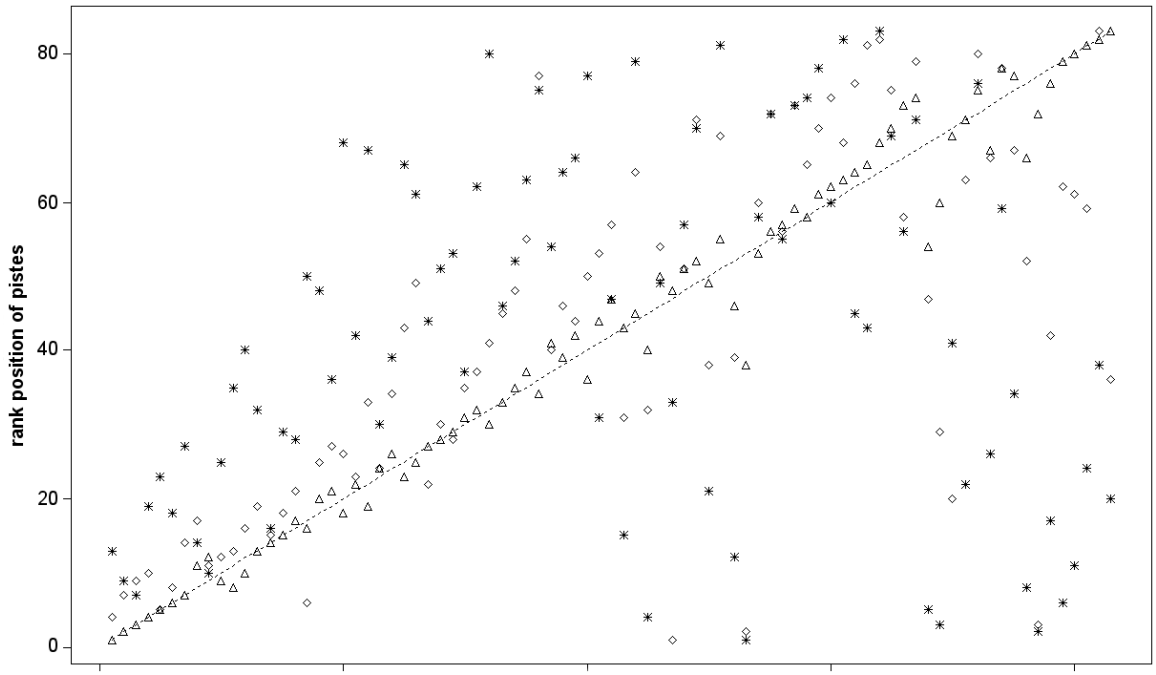

Figure 11.12 Sensitivity of the ranking of ski pistes with respect to the judgement of various experts. The x-axis represents the pistes, sorted according to the rank order obtained in the base evaluation.

11.5 Sensitivity to the decision rule

In the base evaluation, the standardised indicator values were combined by means of SAW, using weights that were derived from pairwise comparison. However, since the decision for this method is to a large extent based on its easy use, especially when analysing a large number of alternatives, two other decision methods were applied to determine the rank order of the ski pistes, namely TOPSIS and ELECTRE (Chapter 10). Both methods used the same input as was used in the base evaluation. In general, more or less the same rank positions were obtained for the ski pistes with the best and the worst performances. However, rank positions of ski pistes with an average performance turned out to be quite unstable with respect to the decision rule. For the case of TOPSIS, a better rank position is probably related to a very small separation of the majority of criteria to the ideal solution, or in the case of a worse performance, a small separation to the negative ideal solution. The different rank positions when using ELECTRE is caused by the fact that ski pistes are compared with respect to their performance, but not in reference to the magnitude of the better performance. For example, using SAW, ski pistes 7 and 9 were ranked in the positions 44 and 40, thus both having an average performance. Conversely, with ELECTRE ski piste 7 gets a higher rank position (from 44 to 30), while piste 9 seems to be a bad solution (from 40 to 60). Comparing these two ski pistes with each other, ski piste 7 performs slightly better with respect to the majority of the environmental criteria, and also with respect to the criterion to which a larger weight was assigned. For that reason piste 7 was assigned a better rank position when using

ELECTRE, since this method solely looks at a better performance, but not at the magnitude of the better performance.

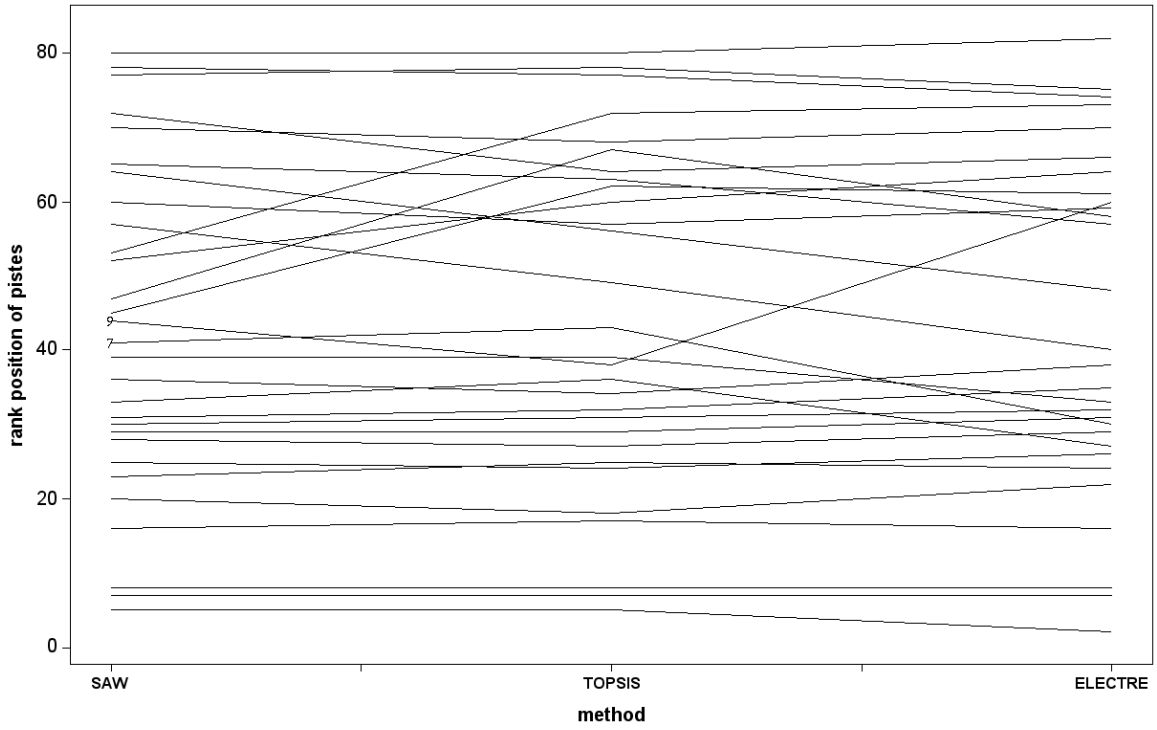

Figure 11.13 Sensitivity of the rank position of ski pistes to the decision rule, in particular SAW, TOPSIS and ELECTRE.

11.6 Discussion and conclusions

As one would expect, the analysis of the sensitivity of the rank positions to the input to the MCA, the standardisation techniques, the assignment of weights and the use of decision rules showed that the rank order of ski pistes is strongly controlled by the preference for an environmental criterion, significantly more than by all other choices. This was clearly illustrated by the indicator "biomass production of grass" or "snow conditions", which were given a higher priority and which had a significant effect on the final ranking of ski pistes in the majority of the scenarios. For instance, when analysing the sensitivity of the rank order of ski pistes to a different standardisation technique or a different midvalue point, the variation in the rank positions was considerable for the criterion "potential for revegetation". For the other criteria, however, the ranking seemed to be quite stable, especially for the erosion criteria or the stability criteria that were given a lower weight. This is because the variation of the standardised indicator values was dominated by the importance of the criteria that were assigned a higher priority.

Furthermore it was shown that the assignment of a 1 to the minimum (if cost criterion) or maximum (if benefit criterion) indicator value can have a strong effect on the final rank order because this indicator value will always be assigned a 1, independent from the standardisation method, and therefore the corresponding ski piste will always have the same weighted sum, while the weighted sum of the other ski pistes can be different. Thus the uncertainty involved in the determination of the minimum or maximum value to fit a value function should get the same consideration as the selection of the midvalue point.

The analysis of the ranking of ski pistes to the assignment of priorities revealed the priorities to have a strong impact on the outcome of the MCA. Besides the strong impact of the assignment of priorities on the final rank order, it was also shown that objectives and preferences of individuals differ significantly, even if they are all concerned about the environmental suitability of an area for a project. Furthermore, carrying out pairwise comparison by means of a form containing the questionnaire had the disadvantage that an inconsistent assessment of preferences could not be easily repeated.

As a consequence of using compensatory evaluation, the sensitivity of the rank positions to the choice of the input to the MCA, the standardisation technique and the selection of the midvalue point or optimum to define the exact shape of a value function is not only controlled by the standardised indicator score for the environmental criterion in consideration, but also by the performance of the ski pistes with respect to the remaining criteria and the weights that were assigned to each criterion. To this end, the rank order of ski pistes that is achieved by *compensatory evaluation* requires careful evaluation because a bad performance of an environmental criterion can be compensated by a good one. In order to avoid the choice for a ski piste with an overall good performance, but unfavourable conditions with respect to few criteria, we need to compare the outcome of the MCA with the input to the MCA, in particular with the environmental properties of the selected ski runs. Moreover, since, there is no common agreement for the suitability of a certain MCA technique, different decision rules need to be implemented to evaluate the final rank order from different viewpoints.

To this end, MCA is a useful method to combine different criteria and to integrate the preferences of individuals or groups of individuals to balance the final decision according to the different criteria and objectives, which is very important when including social and economical objectives in the decision framework. Nevertheless, when using MCA in the decision making process, the uncertainty involved in the various procedural steps and its effect on the selection of the more acceptable ski piste needs to be thoroughly studied.

12 DISCUSSION AND CONCLUSIONS

12.1 Introduction

It is clear that ski pistes and skiing affect the alpine environment, but despite the awareness of possible consequences, human activities in the mountains continue, driven to a large extent by socio-economic forces. To balance social and economical demands with environmental limitations requires methods for assisting the planning of environmentally sound ski runs.

The aim of the work carried out in this thesis was to explore methods for optimally choosing new ski runs by combining 1) experiences with respect to the environmental impact of ski pistes and skiing, 2) the understanding of environmental processes, 3) normally available data, and 4) modern geographical information technology. In order to reach the goal, the general research aim was decomposed in smaller parts, each referring to one of the issues addressed in the objectives.

12.2 Selection of environmental criteria

The first issue addresses the identification of environmental criteria that are important for the planning of ski runs in an alpine area. The general review of impact studies, which discussed the negative consequences of ski pistes, gave a reasonable understanding of the environmental impact likely to be caused by ski pistes and skiing. This literature study showed that the geo-ecological factors soil, plant species, forest and geomorphological forms, and consequently, also hydrological processes are most susceptible to human activities. In addition, ski pistes may be endangered by natural hazards such as rock falls, landslides or avalanches, for which mitigation measures need to be set up. However, the relevance of these factors and possible consequences for environmental processes depend to a large extent on the geographical characteristics of an area. For example, deforestation is of no importance if a new ski piste is going to be built above the timberline, areas in higher elevations with negligible soil formation are not sensitive to the triggering of soil erosion, and the impact of ski pistes and skiing on the vegetation is unimportant in areas which are mainly covered with debris. To this end, the selection of environmental criteria relevant for the planning of new ski runs had to be tailored to the possible consequences for the environment with respect to the geographical settings of the study site. The analytical hierarchical process (AHP) turned out to be helpful for the systematic decomposition of the decision problem in smaller understandable parts, and therefore for the selection of environmental criteria. While the first hierarchy of the decision tree (Chapter 3, Figure 3.8), being composed of vegetation, land degradation and snow, could be applicable to any environmental impact assessment for new ski runs, the second and the third hierarchy were specifically formulated for the Sölden case study. Since the catchment in consideration is quite small, the decision tree so obtained was assumed to be valid for the total study area. However, if the evaluation has to be carried out for a larger area in the mountains, the spatial variation of the sensitivity of environmental factors and

processes to a new development, which is to a large extent controlled by elevation, needs to be integrated both in the selection of environmental criteria and the assignment of priorities to each indicator value.

12.3 Benefits and problems of spatio-temporal models for planning ski runs

There is no doubt that the establishment and maintenance of ski pistes, and the action of skiing itself have an impact on environmental factors and processes. Clearly, for improvements to be made in the planning of ski runs in alpine terrain, a good understanding of the environmental system and the response of environmental processes to a new development are necessary. On the one hand spatio-temporal environmental models proved to be useful for describing the spatial and temporal variation of an environmental process. Moreover, these models helped to identify and quantify the environmental impact likely to be caused by a new development. This was shown in Chapter 10, in which the situation without the impact of a ski piste (original situation) was compared with each of the 83 possible, different ski piste scenarios in order to evaluate the various solutions. In addition, the integration of the temporal component and therefore the dynamic or forward representation of an environmental process is a peculiar characteristic of this type of models because it also supports the temporal analysis of cause-effect relations. However, using spatio-temporal environmental models in MCDM for planning ski runs was subject to several constraints. These are related to 1) the availability of spatial and temporal data to feed the models and to calibrate them, 2) the required computer run-time of the models for the given spatial and temporal resolution, and 3) both the error in the models, that is to say the simplification of real world processes to be able to use them for the decision framework proposed in this thesis, and the uncertainty in the input data.

Data. Chapter 6 discussed the principles of using spatio-temporal environmental models in MCDM for planning ski runs. In order to develop a modelling framework that can assist the planning of socio-economic infrastructure and that can also be re-used for other case studies, emphasis was put on the use of models that can be run with normally available data without additional field campaign because alpine areas are difficult to access and field data collection is expensive. However, the restriction to normally available data could not be completely realised. First, for mountainous terrain, high-resolution data are sparse. Site-specific information such as soil and vegetation properties, an important input to characterise the environmental processes in consideration, are not generally acquired for high altitudes of alpine areas. Accordingly, these data had to be collected in the field (Chapter 4). Second, dynamic models require continuous temporal data. General acquired data such as daily rainfall do not correspond with the temporal resolution of each environmental model. Moreover, these data are mostly just acquired at one location in the study area. In order to improve the availability of temporal data, two meteorological stations at different locations were installed. However, the measurements were just carried out for a short period, and not for the total modelling period because of logistic problems and costs. In order to feed the models with the required data, the general data had to be interpolated for the time steps and locations,

for which no measurements were available. Third, when using models, one is interested in the reliability of model predictions, especially when they are used for risk or impact assessment. Therefore process-specific data such as the measurement of the water table to calibrate the temporal variation of the discharge computed by the hydrological model (Chapter 4, Section 4.5.3), the collection of snow samples (Chapter 4, Section 4.4) to compare them with the predicted snow water equivalent (SWE_c), and the survey and measurements of growth characteristics to optimise the model results of the plant growth model (Chapter 4, Section 4.3.2) are needed. Just like for the input data, these are not normally available and had to be acquired in the field.

From this it can be concluded that it is not possible to rely solely on normally available data if we want to obtain reasonable information by means of spatio-temporal environmental models to describe environmental processes at a specific site. However, attempts could be made to direct data collection towards the right balance between the required data and costs, as for example demonstrated for mapping of vegetation types (Chapter 5).

Computer run-time. In the current procedure of planning ski runs mostly just one solution is proposed to the decision maker, neglecting that there could be another alternative with a higher environmental suitability, but the same socio-economic satisfaction. To overcome this shortcoming, this thesis aimed at the evaluation of a number of possible solutions to optimise the choice of site for a new ski piste, that is to say to identify the ski piste with most favourable environmental conditions. However, one ski piste scenario required considerable computing time on a standard PC, even though the spatial resolution was quite coarse with respect to the environmental process that was modelled. This was because of 1) the evaluation of long periods such as a season or even a year, 2) the use of run-time intensive sub modules, specifically the radiation model using an hourly time step, and 3) the lack of important input data such as a snow cover map ($Sn(t=0)$, c.f. Figure 6.2) and a groundwater height map ($GW_H(t=0)$, c.f. Figure 6.2) at the start of the modelling period which had to be estimated by two additional model runs. As a consequence of the long computing time and since the individual environmental models had to be repeated for each ski piste scenario, it was not feasible to evaluate all possible ski piste locations. The number of ski pistes to be evaluated was tailored to a reasonable computer run-time.

In order to consider all solutions with respect to the given ski run model, the computer run-time of the individual models needs to be reduced. This can be achieved by 1) evaluating shorter periods than determined in the modelling framework, 2) using a larger temporal resolution, 3) the use of simpler, but still reliable model operations or 4) faster hardware and software. A shorter evaluation period has the disadvantage that not all seasonal characteristics are integrated in the model prediction. However, to optimise on the one hand the computer run-time, and on the other the representation of the seasonal characteristics, the selection of the period could be tailored to the season which is assumed to be most important for each environmental process, as for instance already implemented for the hydrological model (HE-model). The temporal resolution was already adapted to the characteristics of the respective environmental process and the required computer run-time, thus a larger temporal resolution is not recommendable. Improvements to optimise computer run-time could take place with respect to model

operations. For example, using the degree-day index for computing the daily snow melt rate still gives a reasonable idea about the daily snow conditions, but its reliability for the HE-model is questionable. Thus simplifying model operation will reduce computer run-time, but may have a negative effect on the various model results. Accepting all the consequences, computer run-time could be improved by optimising the individual components that slow down the calculation process.

Model error and error of input data. A well-known problem of the representation of environmental processes by means of models is the uncertainty involved in both the model and the input to the model. The model error is to a large extent caused by the simplifications that have to be made with respect to the availability of data and computer run-time. The model error was for example obvious with respect to the concentrated flow that has been computed by the HE-model (Chapter 7). This was to a large extent caused by the assumption that within one time step the entire amount of water that is available for surface runoff is routed to the outflow point. The bad correspondence of predicted SWE and computed SWE is probably related to the error in the precipitation data that were used for the snow cover development. Carrying out an error propagation procedure for all models and all model parameters that have been used in the modelling framework is a study by itself and requires an enormous computer run-time because each model needs to be run for several realisations of each parameter, and this needs to be repeated for each piste scenario. With available computer run-time and research time it was not feasible to determine the model error and the error in the input data of the individual models.

Beyond the deficiencies, model results of the individual environmental models, tailored to the use for planning ski runs, were reasonable with respect to the given input (c.f. Chapter 7, 8 and 9). Especially for the computation of the snow cover development (Chapter 7) and the calculation of biomass production (Frings, 2001), the mean error between model predictions and measured data was quite low. As a consequence of the model error involved in the surface water routing and the precipitation data, the predictions of the hydrological model were less good. For the erosion and the stability model the performance could only be judged according to the impression obtained in the field. A distinctive characteristic of the modelling framework was the tight coupling of the different models (c.f. Chapter 6), which facilitated the performance of the scenarios and optimised the total computing time as a consequence of the efficient use of intermediate model results. The importance to link several environmental models and to re-use data and model components within environmental decision support systems has already been addressed by Rizzoli et al. (1998) and Taylor et al. (1999).

12.4 Methods to improve the estimation of spatial input data

The previous section addressed the problem of data constraints for mountainous areas. Nevertheless, when carrying out an environmental impact assessment or describing environmental processes by means of models in such a terrain, we need to acquire information on various site factors. Since data collection in mountainous terrain is difficult and expensive, new methods need to be developed to use field data more

efficiently. This was tested by correlating the attribute to be mapped, in particular vegetation observations, with derivatives of a high-resolution digital elevation model (Chapter 5). The mapping procedure, consisting of different statistical techniques, was demonstrated to be a promising tool for mapping environmental factors for which a significant correlation with the topographical attributes can be identified. However, two problems were encountered: First, a considerable number of samples need to be acquired for each topographical attribute for which a significant correlation with the respective environmental factor is expected. These units can for example be determined by fuzzy *k*-means classification (Burrough et al., 2001). Second, in alpine terrain field observations are difficult to geo-reference. The determination of the geographical location by means of a hand-held global positioning system (GPS) is questionable for alpine terrain due to the shadow effect of the mountains. Accordingly, field measurements were for the greater part based on the field maps derived from available topographical maps, and so there can be some uncertainty in locating the vegetation observations. Furthermore, using just derivatives of the digital elevation model in the mapping procedure restricts its applicability to those environmental factors, which are controlled by topographical attributes such as vegetation communities or the spatial variation of precipitation. Integrating additional site information such as geological properties would extend the possibilities to apply the proposed mapping procedure also to other environmental factors.

12.5 Using multicriteria analysis for spatio-temporal information

Multicriteria analysis (MCA) is to a large extent regarded as a systematic, transparent approach that increases objectivity and generates results that can be reproduced (Bonte et al., 1997, 1998, cit. in Janssen, 2001). MCA techniques have been applied to various decision problems, for which the combination of multiple aspects was a major concern, for example for the determination of appropriate input parameters for environmental models (Mackay and Robinson, 2000), the performance of integrated assessments (Bell et al., 2001; Wenzel, 2001), the implementation of environmental impact assessments (Janssen, 2001), or for land use management (Beinat and Nijkamp, 1998). This thesis aimed at using MCA techniques for combining the output of spatio-temporal environmental models to support the choice of a site for a new ski run because the entire information provided by these models for 83 ski pistes is very complex, which made it difficult to draw conclusions about a suitable location for a new ski run. The choice of using MCA for the integration of the environmental information to provide a discrete measure for each ski piste demanded the aggregation of the spatial and temporal component to a single value because MCA techniques are originally designed for single values. Accordingly, some trade-offs had to be taken into account. First, as a consequence of the spatial and temporal aggregation, the temporal component, which is a peculiar characteristic of the models used in this thesis, was removed. Furthermore, the information provided by the indicator value that resulted from the spatial and temporal aggregation is less objective than the model output provided by the individual spatio-temporal environmental models because there are different ways to aggregate in space

and time (c.f. Chapter 10), each having a different effect on the final rank order of the ski pistes. For example, the performance of ski pistes with respect to the criterion ”erosion on the ski piste” differed depending on whether it was assumed that the average erosion rate represents the erosion situation on a ski piste or the maximum erosion rate. The same holds for the remaining model results such as the probability of failure or the fraction of disturbed soil. Another trade-off is the application of standardisation and weighting methods to single values. Due to the availability of modern geographical information systems which make it possible to use algebraic operations for each spatial unit into which the study area is divided, it is principally possible to apply standardisation functions and the assignment of weights to the individual criteria maps (Malczweksi, 1999) rather than to single values. However, in the study described in this thesis criteria maps were first aggregated to a single value because ski pistes do not only affect the site where they are going to be established, but may also have an effect on its surroundings. Consequently, there are two different maps, namely the map representing the ski pistes and the map representing the catchment, which cannot be combined because of their different map attributes. Therefore it was not feasible to keep the spatial component for applying standardisation and weighting methods. Aggregating first the spatial and temporal component before combining the individual environmental criteria had also an advantage because the aggregation rules could be tailored to the relevance of the individual criteria.

To this end, accepting the trade-offs involved in the aggregation of spatio-temporal information, it is possible to include spatio-temporal environmental models for multicriteria decision making (MCDM), however, the selection of the aggregation method needs to be adjusted to both the characteristics of the study area and the importance of an environmental criterion for the entire equilibrium of the environmental system.

12.6 Benefits and constraints of MCA

MCA has frequently been used to combine different aspects to provide the decision maker with discrete information. Just like for every other method, the use of MCA has both advantages and disadvantages which are related to the input to the MCA, the standardisation methods, the assignments of weights and the achievement of a rank order by means of decision rules.

First, the use of MCA made it possible to base the decision for a certain ski piste on the selected environmental criteria and the priorities that were assigned to them. In this thesis priorities were introduced by ascribing a direct weight that has been derived by means of pairwise comparison. As is commonly known, the assignment of weights revealed to be a significant factor in the determination of the final rank order (chapters 10 and 11). The combination of the individual criteria required the transformation of the indicator values to a commensurate scale. In general, there is no standard rule about the suitability of a certain method. Nevertheless, the sensitivity analysis showed that the choice of the transformation method can have an effect on the final rank positions. Furthermore, the application of decision rules such as simple additive weighting (SAW)

or technique for order preference by similarity to ideal solution (TOPSIS) assisted in achieving a complete rank order of the alternatives in consideration with respect to their overall performance. Principally, there is no restriction for the number of alternatives if compensatory evaluation is chosen for the integration of the individual environmental criteria, and therefore it was assumed to be an appropriate method for this study. However, the use of compensatory evaluation can cause that an alternative with a very bad performance with respect to one criterion can still have an overall good performance because the bad performance of one criterion can be compensated by the good performance of another. Another disadvantage, which was already addressed in the previous section, is the need of single values when using MCA analysis to support the choice of a site for a new ski run. This caused the loss of the process-specific information that was provided by the individual environmental models because the detailed information had to be aggregated.

To this end, despite using MCA, which is regarded as a method for increasing objectivity, for supporting the choice of site for a new ski run, there is still much uncertainty involved with respect to the selection of the methods to finally achieve a rank order of the alternatives in consideration. Nevertheless, the evaluation of the 83 ski pistes and the sensitivity analysis of the rank order to the several decision that had to be made showed that MCA can be a useful method if there is clarity about the meaning and importance of an environmental criterion for the study area and the decision problem, even though the spatio-temporal maps had to be aggregated to single values. It was even possible to determine the spatial variation of the environmental suitability of each spatial unit (grid cell) into which the catchment was divided (Figure 10.10) by computing the average performance of each grid cell (c.f. Chapter 10).

12.7 Concluding remarks

In this thesis I have shown that it is possible to build a methodology for identifying environmentally suitable sites for new ski runs by combining the knowledge of environmental processes, available data and current GIS technology. The outcome of the MCA has shown that the decision framework can be a useful method for the first investigation of potential sites for new ski pistes with respect to selected environmental criteria and therefore a useful method for the first phase in an environmental impact assessment. However, for the final decision one must be aware that the outcome of the MCA depends to a large extent on the many choices that were made with respect to modelling principles and the MCA techniques. Both the comparison of the output of the MCA with the model results and a site investigation is therefore recommended. Moreover, since ski pistes and skiing are also related to social and economical aspects such as number of expected visitors to the ski piste or constructions costs, the socio-economic situation needs to be included in the decision model as well.

APPENDIX 1: SPECIES TABLES

Table A1.1 The presence of common species and their classification into general vegetation classes

Common species	General vegetation class
Antennaria dioica	Alpine grassland, Alpine heaths
Calluna vulgaris	Alpine heaths
Campanula barbarta	Alpine grassland
Carex species (above all Carex curvula)	Alpine grassland, Alpine heaths
Cladonia rangifera	Alpine heaths
Calluna vulgaris	Alpine heaths
Festuca species(above all Festuca varia)	Alpine grassland, Alpine heaths
Geum repens	Alpine grassland
Helictotrichon versicolor	Alpine grassland, Alpine heaths
Homogynae alpina	Alpine grassland
Islandica cetraria	Alpine heaths
Leontodan helveticus	Alpine grassland, Alpine
Leucanthemum alpinum	Alpine grassland
Luzula campestris	Alpine grassland, Alpine heaths
Nardus stricta	Alpine grassland, Alpine heaths
Phyteuma orbiculare	Alpine grassland, Alpine
Polytrichium species	Pioneer vegetation
Potentilla aurea	Alpine grassland,
Rhododendron ferrugineum	Alpine heaths
Trifolium alpinum	Alpine grassland
Vaccinium myrtillus	Alpine heaths
Vaccinium uliginosum	Alpine heaths
Vaccinium vitas-ideae	Alpine heaths

Table A1.2 Frequent species in each vegetation cluster

Cluster 1	Cluster 2	Cluster 3	Cluster 4
Alchemilla alpina	*Achillea millefolium*	*Cardamine resedifolia*	*Agrostis alpina*
Campanula scheuchzeri	*Alchemilla alpina*	*Carex curvula*	*Bryophyta species*
Carex species	*Campanula scheuchzeri*	*Centraria islandica*	*Calluna vulgaris*
Cerastium species	*Festuca species*	*Cerastium alpinum*	*Campanula barbarta*
Cladonia rangifera	*Myosotis alpestris*	*Cladonia rangifera*	*Cladonia rangifera*
Festuca species	*Phleum alpinum*	*Cladonia species*	*Empetrum hermaphroditum*
Geum repens	*Phyteuma betoniafolium*	*Festuca species*	*Festuca species*
Helictotrichon versicolor	*Potentilla aurea*	*Geum repens*	*Homogynae alpina*
Homogynae alpina	*Ranunculus species*	*Leontodan helveticus*	*Loiseleuriia procumbens*
Leontodan helveticus	*Rhinantus alectorolophus*	*Leucanthemopsis alpina*	*Potentilla erecta*
Leucanthemopsis alpina	*Rhododendron ferrugineum*	*Mutellina ligusticum*	*Rhododendron ferrugineum*
Mutellina ligusticum	*Rumex alpinus*	*Nardus strictus*	*Silene vulgaris*
Nardus strictus	*Silene vulgaris*	*Phyteuma orbiculare*	*Trifolium alpinum*
Phleum alpinum	*Taracum alpinum*	*Polytrichium*	*Vaccinium myrtillus*
Phyteuma orbiculare	*Trifolium pratense*	*Potentilla aurea*	*Vaccinium vitas-idaea*
Polytrichium species	*Vaccinium vitas-idaea*	*Salix herbacea*	
Potentilla aurea		*Sedum alpestre*	
Ranunculus species		*Sedum species*	
Taracum alpinum		*Sibbaldia procumbens*	
Trifolium alpinum		*Soldanella alpina*	
Trifolium pratense		*Vaccinium uliginosum*	
Vaccinium myrtillus		*Veronica belleoides*	
Vaccinium uliginosum			

`

Cluster 5	Cluster 6	Cluster 7
Campanula barbarta	*Antennaria dioica*	*Campanula scheuchzeri*
Campanula scheuchzeri	*Carex species*	*Carex species*
Carex species	*Carex curvula*	*Calluna vulgaris*
Cladonia rangifera	*Centraria islandica*	*Festuca species*
Festuca species	*Cladonia rangifera*	*Galium alpinum*
Geum repens	*Cladonia species*	*Gentiana kochiana*
Homogynae alpina	*Festuca species*	*Juniperus nana*
Leontodan helveticus	*Geum repens*	*Larix species*
Lotus cornulatus	*Helictotrichon versicolor*	*Lotus cornulatus*
Luzula campestris	*Homogynae alpina*	*Luzula alpino pilosa*
Nigritella nigra	*Leontodan helveticus*	*Luzula campestris*
Pedicularis foliosa	*Leucanthemopsis alpina*	*Picea abies*
Phyteuma betoniafolium	*Luzula campestris*	*Pinus species*
Phyteuma orbiculare	*Nardus strictus*	*Poa alpina*
Potentilla erecta	*Phyteuma orbiculare*	*Potentilla erecta*
Pulsatilla vernalis	*Polytrichium species*	*Trifolium pratense*
Ranunculus montanus	*Ranunculus montanus*	*Vaccinium vitas-ideae*
Rhododendron ferrugineum	*Trifolium alpinum*	
Trifolium alpinum	*Vaccinium myrtillus*	
Vaccinium myrtillus		
Vaccinium uliginosum		
Vaccinium vitas-idaea		

Table A1.3 Typical species in each vegetation cluster

Cluster 1	Cluster 2	Cluster 3	Cluster 4
Cardamine palustre	*Cardamine pratensis*	*Cerastium alpinum*	*Bryophyta species*
Cerastium palustre	*Chrysanthemum leucanthemum*	*Pohlia nutans*	*Dactylorhiza maculata*
Cirsium spinosissimum	*Geranium pratense*	*Primula glutinosa*	*Dianthus cartusianorum (rare)*
Eriphorum species	*Poa alpina*	*Salix herbacea*	*Gentiana punctata*
Heracleum sphondylium	*Trollius europeus*	*Sedum alpestre*	*Gramineae species*
Trifolium badium		*Sedum species*	
		Sibbaldia procumbens	
		Veronica alpina	

Cluster 5	Cluster 6	Cluster 7
Agrostis alpina	*Androsacae species*	*Melampyrum sylvaticus*
Aster alpinus	*Artemisiaspecies*	*Papaver alpina*
Carlina aucalis	*Bistorta vivpara*	*Picea abies*
Conium maculatum	*Carex firma*	
Dactylorhiza maculata	*Centraria islandica*	
Epilobium angustifolium	*Chamaebuxus alpestris*	
Galium species	*Cladonia pyxidata*	
Hieracium pilosella	*Galium alpinum*	
Nigritella nigra	*Gentiana clusii*	
Orchis militaris	*Geum repens*	
Parnassia palustris	*Graue Flechte*	
Pedicularis foliosa	*Homogynae alpina*	
Phyteuma betoniafolium	*Leucanthemopsis alpina*	
Pinus mugo	*Luzula lutea*	
Poa alpina	*Ranunculus montanus*	
Polygala amara	*Saxifraga muscoides*	
Pulsatilla apii	*Sedum alpestre*	
Senecio icanus	*Sempervivum montanum*	
Silene rupestris	*Pteridophyta species*	
Thymus pulegioides	*Viola biflora*	
Tripleurosperum perforatum		
Veronica species		

APPENDIX 2: SCATTER PLOTS OF TOPOGRAPHIC ATTRIBUTES AGAINST DCA SCORES

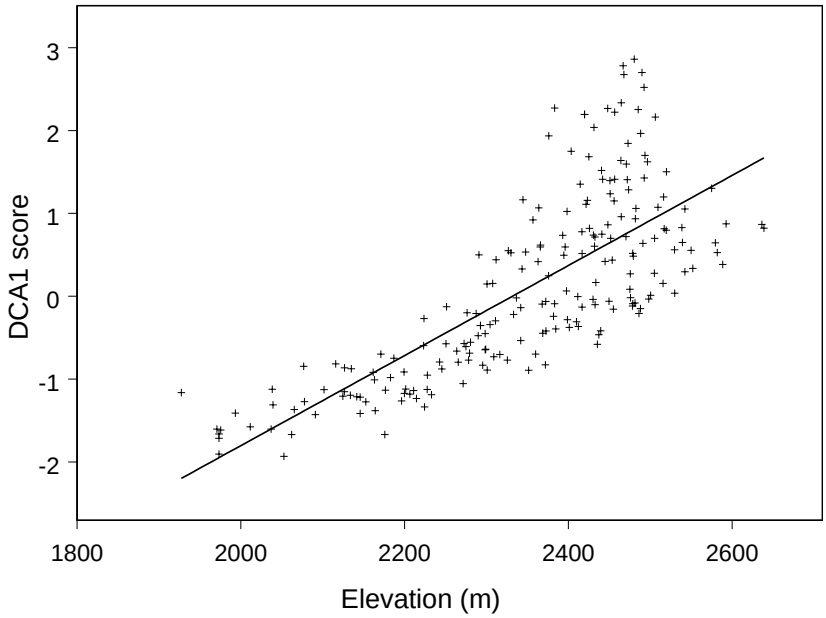

Figure A2.1 Scatter plot of elevation against scores of DCA 1

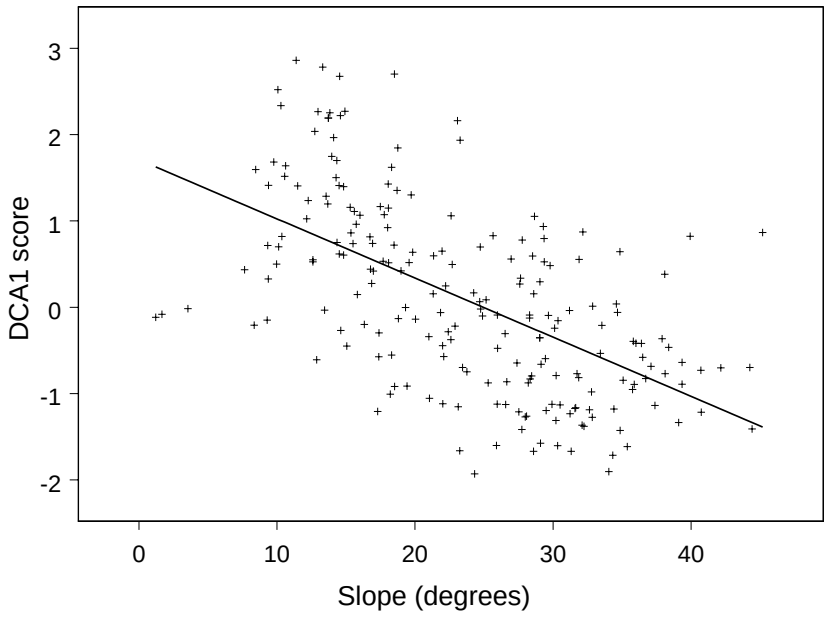

Figure A2.2 Scatter plot of slope against scores of DCA 1

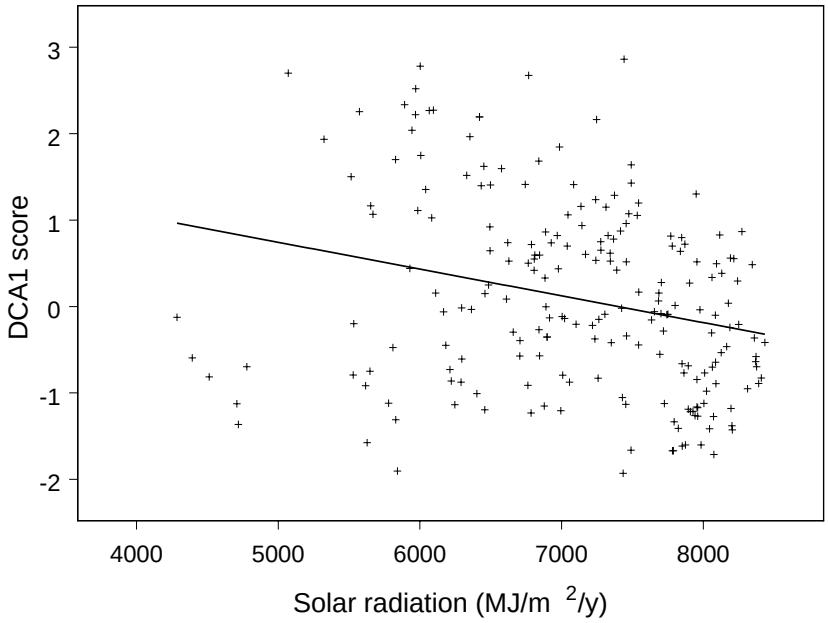

Figure A2.3 Scatter plot of solar radiation against scores of DCA 1

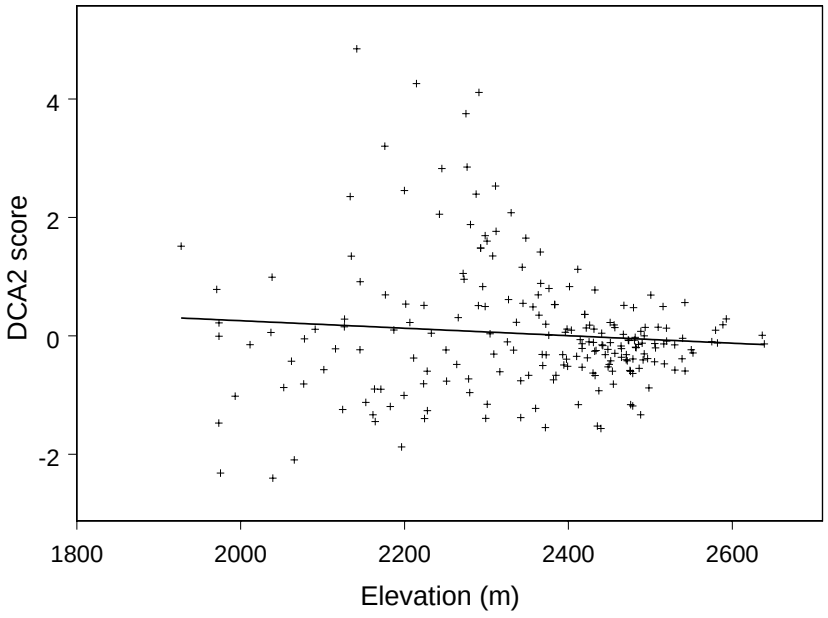

Figure A2.4 Scatter plot of elevation against scores of DCA 2

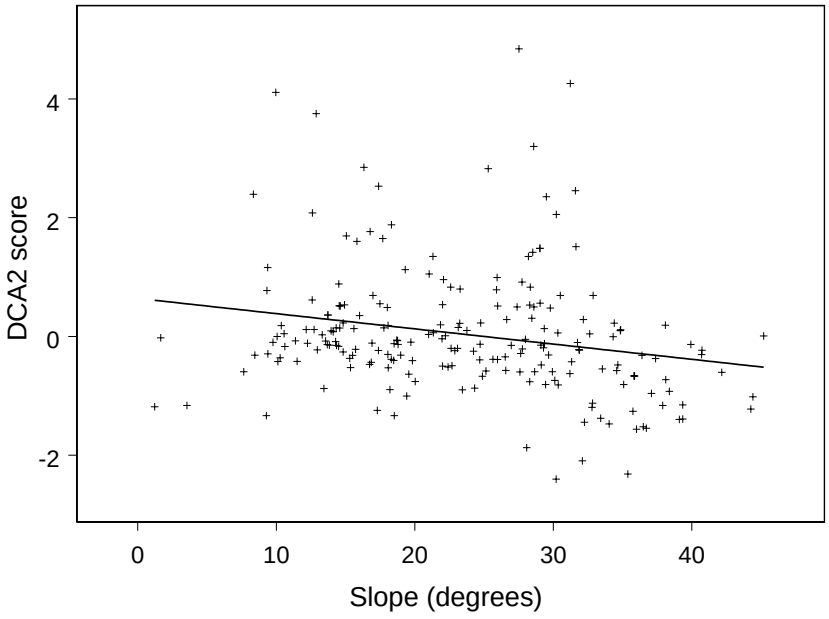

Figure A2.5 Scatter plot of slope against scores of DCA 2

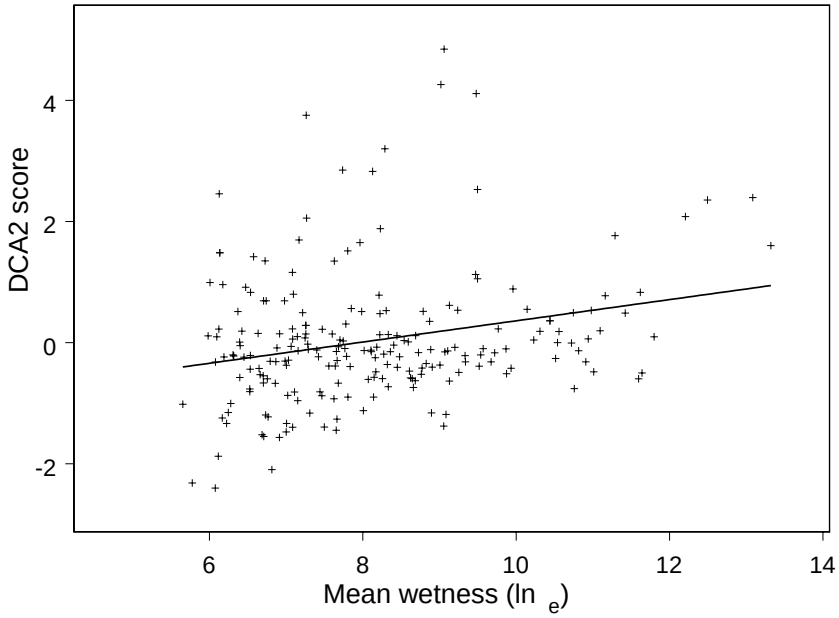

Figure A2.6 Scatter plot of elevation against scores of DCA 2

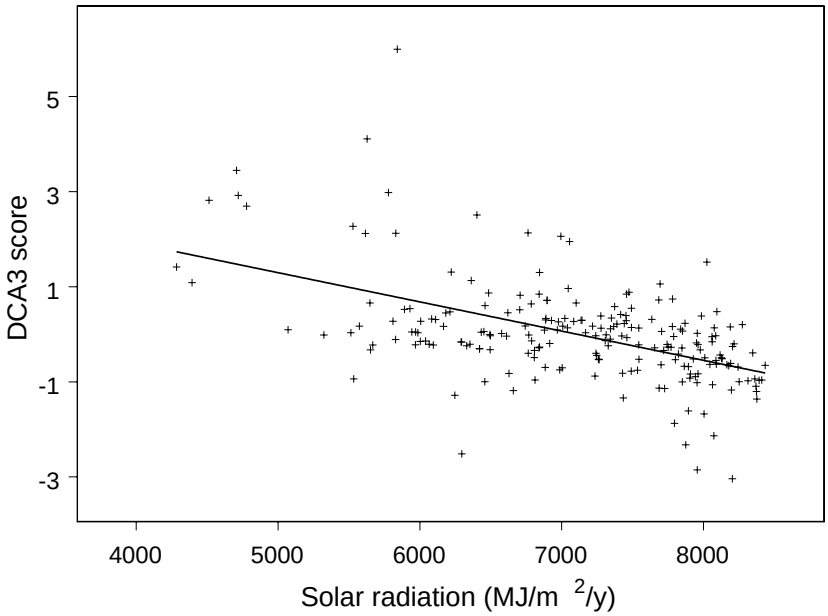

Figure A2.7 Scatter plot of solar radiation against scores of DCA 3

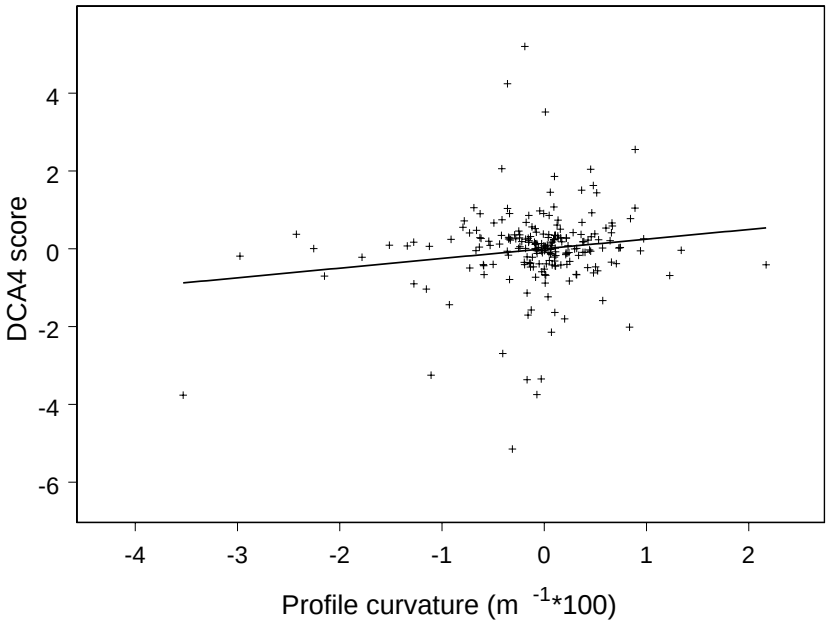

Figure A2.8 Scatter plot of profile curvature against scores of DCA 4

APPENDIX 3: CALIBRATION PLOTS (SN-model)

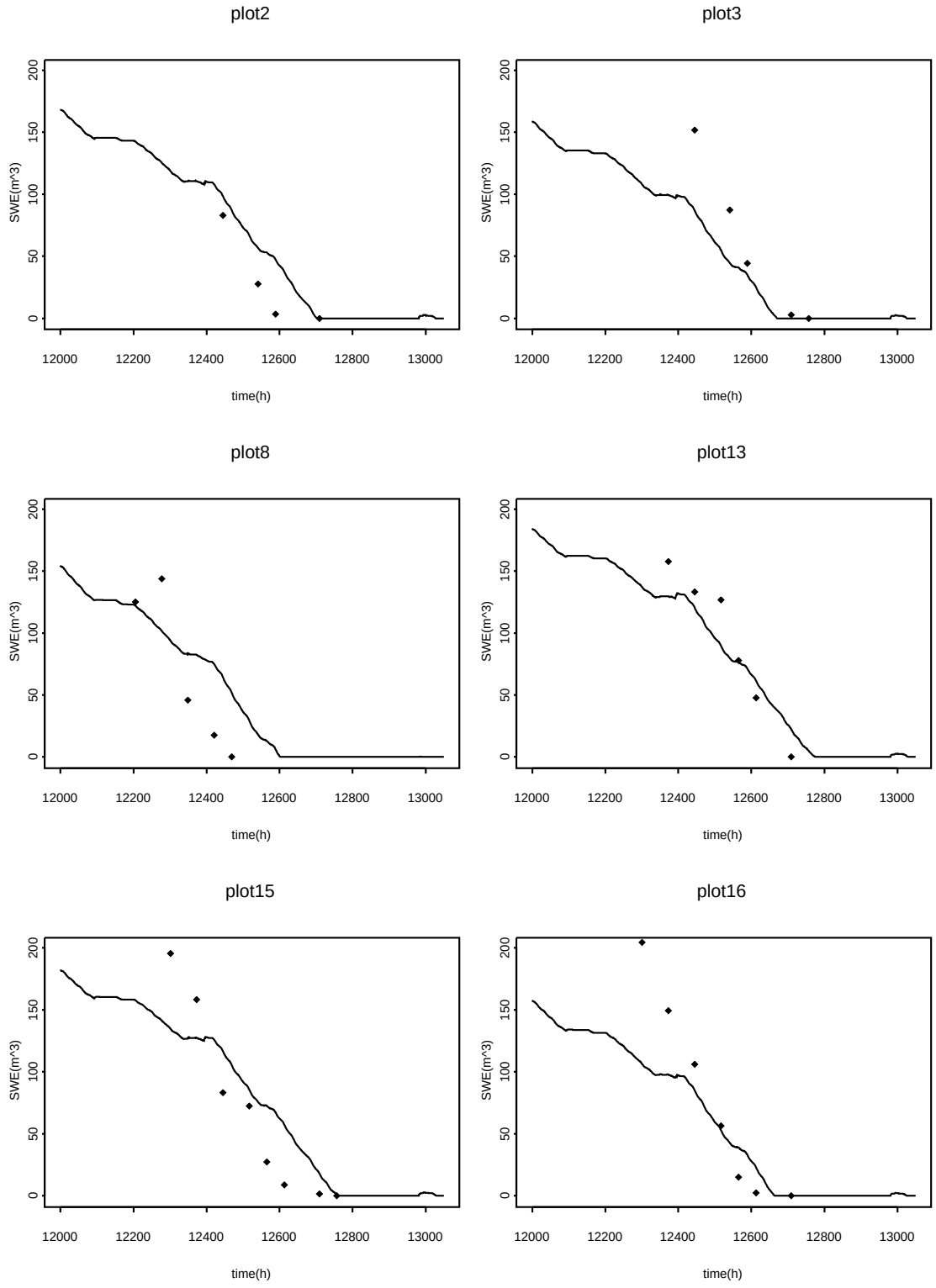

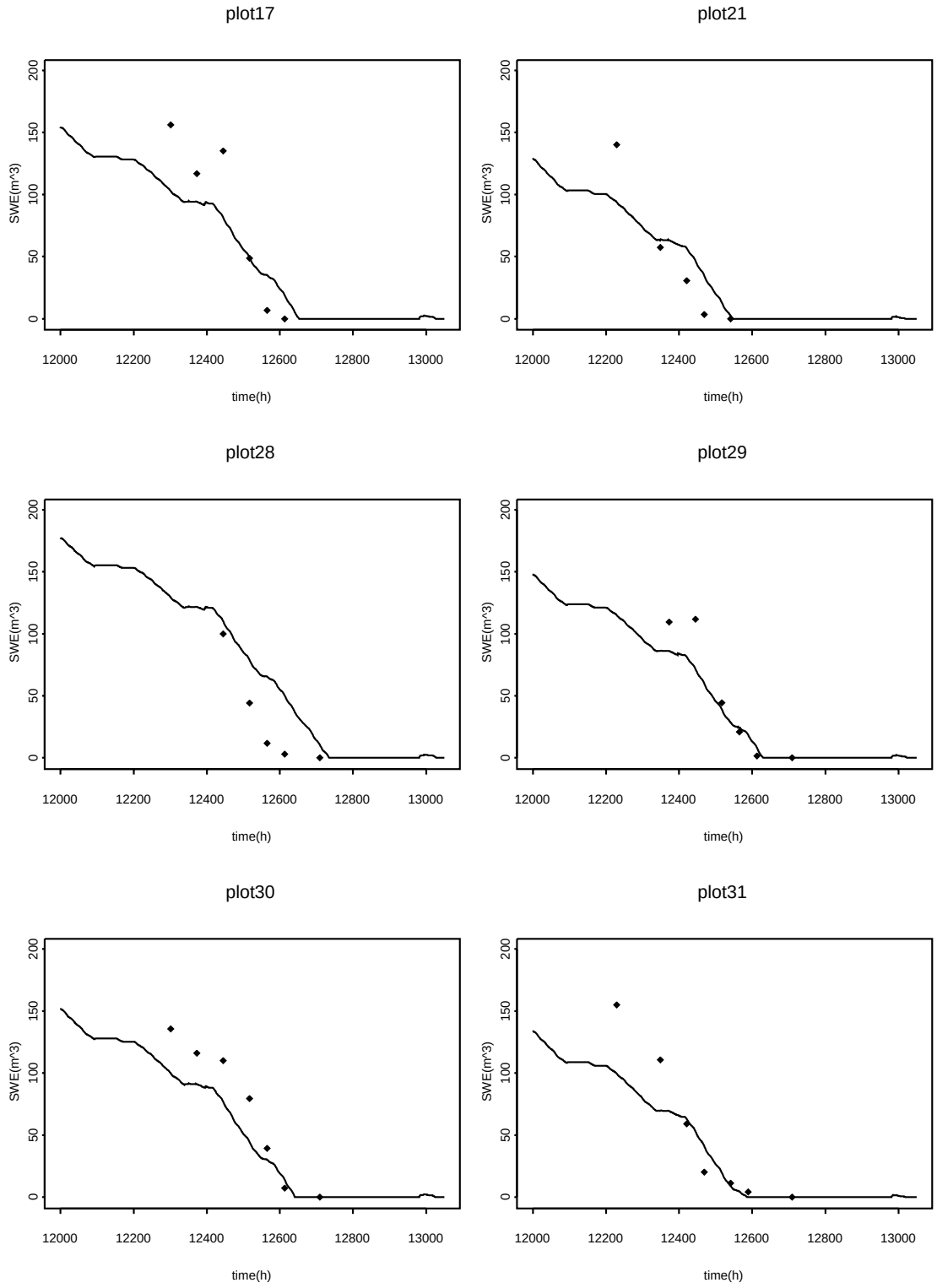

Figure A3.1 Correspondence of measured snow water equivalent (SWE_o, m^3/plot), indicated by the dots, and the simulated snow water equivalent (SWE_c, m^3/plot), represented by the closed line.

Summary

The construction of ski runs and skiing activities can cause a considerable modification of environmental factors or processes. This change is called their impact. The construction of ski runs very often results in a change of landforms (e.g. due to flattening of slopes etc.), change of soil characteristics and hydrological parameters as well as vegetation. The use of ski runs by skiing activities then requires very often the making of artificial snow and snow preparation by caterpillars. However, new ski runs continue to be developed. In order to minimise the negative effects on the environment, their environmental suitability needs to be considered as part of their planning. The aim of this thesis was the development of a generic methodology to support the choice of site for a new ski run with respect to prevailing environmental conditions in the area of consideration, taking account of the environmental impact likely to be caused by a new ski run. In this thesis the area in consideration is an alpine catchment of area of 3.6 km² in the ski area of Sölden, which is a popular skiing resort in the Austrian Tyrol.

The identification of the more acceptable site for a new ski run within the area of consideration required both the environmental characterisation of all possible sites in that area, taking into account the environmental impact possibly caused by a ski piste, and the ranking of those sites according to their overall environmental situation. To evaluate and to compare all possible sites for a new ski run a sequence of steps was formulated and carried out for the study area.

The first step was the investigation of all possible ski run locations within the area suitable for skiing, determined by the slope of the terrain. Within this area, a set of ski runs of the same length and width were generated with the ski run model. The only input to the ski run model was the digital elevation model and a set of feasible starting points from which the ski runs were generated.

Second, to characterise each of these possible ski run alternatives, relevant environmental criteria had to be determined. The determination of those criteria was controlled by knowledge of negative effects of ski runs and skiing reported in the literature, the prevailing environmental conditions in the study area and the impacts of ski runs and skiing investigated in the area. The construction of the criteria tree was supported by the analytical hierarchical process (AHP), which is a useful method to systematically decompose a decision problem into a small number of understandable or measurable parts. Vegetation, land degradation and snow conditions were selected as the most important criteria groups to find the ski run with minimal environmental disturbance. These three criteria groups were further decomposed to measurable elements, in this thesis called indicators, which formed the basis for the environmental characterisation of each possible ski run. The systematic decomposition of vegetation resulted in two vegetation indicators: the average maximum biomass production on a ski run and the average degradation of the valuable vegetation of a ski run. The degree of land degradation of a possible ski run was described by the average erosion on a ski run and its surroundings, the probability of slope failure on the ski run and its surroundings, the peak discharge at the outflow point of the catchment and the fraction of disturbed soil due to the flattening of the surface of a ski run. Snow conditions were expressed by the number of days with a continuous snow cover.

In the third step of the methodology a quantitative measure had to be found for each environmental indicator identified in step two, both for the situation without a ski run and the future situation under a scenario with a ski run. Therefore a set of spatio-temporal process-based environmental models consisting of a snow model, two hydrological models, an erosion model, a slope stability model and a plant growth model was applied to each ski run location. The models calculate the values of each of the indicators for the situations with and without a ski run in order to evaluate each possible location. In addition, a statistical model was developed, on the one hand to generate a high-resolution vegetation map to be used as an input to the environmental models, and on the other hand to generate a vegetation degradation map by assigning a value according to the environmental sensitivity and importance of a certain vegetation type. The vegetation degradation map was used to provide a measure for the degree of degradation of the vegetation on a ski run. Since spatio-temporal models are capable of simulating an environmental process in space and time, the output of those models is a time series of maps that had to be aggregated to a single value in order to rank the set of possible ski runs with respect to the environmental criteria. For the aggregation an existing approach was modified by adding the factor time.

The aim of the fourth step of the methodology was the integration of the aggregated model output (i.e. indicators calculated by the models) by means of multicriteria analysis (MCA) to characterise each possible ski run location by a single value. In order to combine the environmental indicators that had been measured on different scales, linear transformation functions and value functions were used to standardise the values to a common scale. Pairwise comparison resulted in a weight for each environmental indicator. The indicator values were integrated by means of simple additive weighting (SAW), using the weights obtained by pairwise comparison. Finally the possible sites for a new ski run were ranked according to the total value computed with SAW. The ranking of the best and worst ski runs was rather stable, however, it was to a large extent determined by the assignment of a weight, and less by the aggregation or standardisation method, as shown by the analysis of the sensitivity of the outcome to the choice of a certain method.

The application of the methodology to the ski area of Sölden demonstrated the methodology to be a useful method for exploring the environmental suitability of possible sites for a new ski run, where the outcome of the methodology needs to be considered as a support for making a decision and not as the decision. Using spatio-temporal models for planning ski runs is related to constraints in the availability of spatial and temporal data and the computing time. In addition, both the error in the models and the uncertainty in the input data must be considered. Moreover, when integrating the model output to a single value for each ski run, much subjectivity is involved with respect to the choice of a certain aggregation and standardisation method, the assignment of a weight and the method to achieve a ranking of the ski runs. Nevertheless, the methodology is a useful tool in the first phase of an environmental impact assessment (EIA) to investigate the necessity of an EIA and the generation of alternatives. In a further phase of the decision making process socio-economic criteria need to be integrated as well.

Samenvatting

De aanleg van skipistes en het skiën zelf heeft een negatief effect op het natuurlijk milieu. Er treedt een verandering op van de normale status van landschapsfactoren en processen naar een aangetaste status, vaak aangegeven met de term impact. De bodem, vegetatie, geomorfologie, en hydrologie zijn het meest gevoelig voor menselijke activiteiten op een ski piste zoals het vlakker maken van de helling, het prepareren van de piste met behulp van rupsvoertuigen of kunstmatige sneeuw, en de ski-activiteiten. Bij de planning van nieuwe skipistes is het dan ook van belang de milieueffecten van de skipiste mee te nemen bij het kiezen van de locatie van de nieuw te bouwen piste, aangezien het milieueffect van de piste per locatie zal verschillen. Het doel van dit proefschrift was het ontwikkelen van een generieke methode om de keuze van de locatie van een skipiste te bepalen, rekening houdend met de huidige landschappelijke situatie in een gebied en de te verwachten negatieve gevolgen voor het milieu. De methode werd getest in een 3.6 km^2 groot Alpien stroomgebied in het populaire skigebied Sölden, in Tirol, Oostenrijk.

Voor het vinden van de beste locatie voor een nieuwe skipiste binnen een bepaald gebied is het nodig om ten eerste alle mogelijke locaties voor de skipiste te beschrijven wat betreft de te verwachten impact op het milieu. Vervolgens dient met behulp van deze beschrijvingen een rangorde te worden aangebracht in deze alternatieve skipiste locaties, van een lage naar een hoge te verwachten impact. Deze benadering wordt in het proefschrift uitgewerkt tot een methode bestaande uit vier stappen.

De eerste stap omvat het vinden van alle mogelijke locaties voor de nieuw te bouwen skipiste binnen een bepaald skigebied. Hierbij worden met een computermodel mogelijke locaties van skipistes gegenereerd die zich steeds bevinden op delen van het gebied met een natuurlijke helling van het terrein die geschikt is voor skiën. Hierbij hebben alle mogelijk skipistes een gelijke lengte en breedte. Als invoer voor dit model, dat de verschillende mogelijke skipistes genereerd maakt, is alleen een digitaal hoogte model nodig.

In de tweede stap van de methode is het nodig relevante landschappelijke criteria te bepalen voor het karakteriseren van elk van deze alternatieve locaties voor de skipiste. Dit is gedaan op grond van in de literatuur beschreven negatieve effecten van skipistes op het milieu, de heersende landschappelijke condities in het studiegebied en de effecten op het milieu van skipistes en skiën waargenomen in het studiegebied. Het opstellen van de boom van criteria werd ondersteund door het gebruik van het analytisch hiërarchisch proces (“Analytical Hierarchical Process”, AHP), welke een vaak gebruikte methode voor Multi Criteria Analyse (MCA) is. Met AHP kan een beslissingsprobleem systematisch worden opgesplitst in een klein aantal eenvoudig te begrijpen, meetbare, onderdelen. De toepassing van AHP resulteerde in drie groepen van criteria, die het meest relevant zijn voor milieueffecten als gevolg van de aanleg van een piste, en de keuze van de piste locatie. Deze groepen zijn vegetatie, landdegradatie en sneeuwcondities. Elk van de groepen werd verder opgesplitst in meetbare elementen, in dit proefschrift indicatoren genoemd, die de basis vormen voor de karakterisering van elke mogelijke skipiste locatie wat betreft milieueffecten. De opsplitsing van vegetatie resulteerde in twee indicatoren voor vegetatie: de gemiddelde maximale productie van biomassa en de gemiddelde degradatie van waardevolle vegetatie op een skipiste. De mate van landdegradatie op een skipiste werd beschreven door de gemiddelde erosie op een skipiste en binnen het

stroomgebied waarin de piste ligt, de kans op een massabeweging op de piste of in het stroomgebied, de waarde van de maximale afvoer bij het uitstroompunt van het stroomgebied en de fractie van de bodem die gestoord wordt als gevolg van het vlakker maken van het oppervlak van de skipiste. De sneeuwcondities werden weergegeven met het aantal dagen waarop de piste geheel bedekt is met sneeuw.

In de derde stap van de methode dient een kwantitatieve maat te worden gevonden voor elk van de indicatoren die zijn gedefinieerd in de tweede stap, zowel voor de situatie zonder een skipiste op een bepaalde locatie, als voor de (mogelijke) toekomstige situatie mét een skipiste op een bepaalde locatie. Voor het verkrijgen van een dergelijke kwantitatieve waarde werd een set van deterministische temporele en ruimtelijke modellen gebruikt die processen die zich in het landschap afspelen simuleren. De modellen die toegepast werden voor elke alternatieve locatie van de skipiste zijn een sneeuwmodel, twee hydrologische modellen, een erosiemodel, een hellingstabiliteitsmodel en een plantgroeimodel. Deze modellen berekenen de waarde van elk van de indicatoren voor de situatie met en zonder ski piste, waarbij op deze manier iedere alternatieve skipiste locatie kan worden geëvalueerd. Tevens werd een statistisch model ontwikkeld ter verkrijging van een vegetatie kaart met een hoge resolutie, die kan worden gebruikt als invoer voor de hierboven genoemde deterministische modellen. Dit statistische model werd daarnaast gebruikt voor het maken van een vegetatiedegradatie kaart door middel van toekenning van waarden die de gevoeligheid en relevantie van een bepaald vegetatie type representeren. Deze vegetatiedegradatie kaart werd gebruikt voor het verkrijgen van een maat voor de degradatie van de vegetatie op een mogelijke locatie van de skipiste. Aangezien de gebruikte landschappelijke modellen processen simuleren in ruimte en tijd, diende de uitvoer van deze modellen, bestaande uit tijdseries van kaarten, te worden geaggregeerd naar één indicator waarde. Deze aggregatie werd uitgevoerd volgens een bestaande methode, die werd aangepast voor het werken met temporele gegevens. De op deze manier verkregen indicator waarden voor elke locatie van de skipiste kunnen vervolgens worden gebruikt voor het karakteriseren van elke locatie wat betreft de te verwachten milieueffecten.

In de vierde stap van de methode wordt een dergelijke karakterisering verkregen door de set van indicator waarden (berekend met behulp van de modellen) voor elke piste locatie te integreren met behulp van MCA, resulterend in één totaalwaarde die het geïntegreerde milieueffect van de piste op die locatie weergeeft. Aangezien de verschillende indicatoren, berekend met de modellen, niet allemaal zijn uitgedrukt in dezelfde eenheden, werden de indicatorwaarden eerst gestandaardiseerd naar een gemeenschappelijke schaal met behulp van verschillende typen transformatiefuncties. Vervolgens werden, voor elke skipiste locatie, de set van gestandaardiseerde indicatorwaarden geïntegreerd tot één totaalwaarde, door middel van gewogen sommering (“Simple Additive Weighting”, SAW). Hierbij werd aan elk type indicator een gewicht toegekend, bepaald met behulp van paarsgewijze vergelijking (“pairwise comparison”). Als laatste stap werden de verschillende mogelijke locaties voor de skipiste gerangordend naar milieueffect op grond van deze totaalwaarden, bekend voor elke piste locatie. Een gevoeligheidsanalyse gaf aan dat de gevonden rangordening van de pistes gevoelig was voor de keuze van de gewichten die aan de indicatoren worden toegekend, en in mindere mate voor de keuze van de aggregatie- of

standaardisatiemethode. Echter, de rangorde van skiruns met de hoogste en laagste milieueffecten was betrekkelijk stabiel.

De toepassing van de procedure op het skigebied van Sölden liet zien dat de methode goed bruikbaar is voor het evalueren van de landschappelijke geschiktheid van mogelijke locaties van een skipiste. De uitkomst van de methode dient echter altijd te worden beschouwd als beslissingsondersteunend en niet als de beslissing zelf. Het gebruik van deterministische ruimtelijke, temporele, landschappelijke modellen voor het plannen van skipistes gaat gepaard met beperkingen gerelateerd aan de beschikbaarheid van veldgegevens en de rekentijd op een computer. Daarnaast dient rekening te worden gehouden met de fout in de modellen en de onzekerheid in de invoergegevens. Tevens zijn er subjectieve factoren aanwezig in de methode. Bij de integratie van de uitvoeren van de modellen naar totale impactwaarden per locatie van de skipiste zijn zowel de keuze van de aggregatie- en standaardisatiemethode, als de keuze van de gebruikte gewichten voor de verschillende indicatoren subjectief. Ondanks de hierboven genoemde problemen, is de in dit proefschrift beschreven methode goed bruikbaar in de eerste fase van een milieueffectrapportage ter verkenning of de volgende fasen van een milieueffectrapportage nodig zijn en voor het genereren van alternatieven. In een latere fase van de besluitvorming dienen tevens socio-economische criteria te worden geïntegreerd.

Zusammenfassung

Der Bau und die Nutzung von Schipisten stellen einen beträchtlichen Eingriff in den Naturhaushalt der Alpen dar. Untersuchungen auf bestehenden Schipisten haben ergeben, dass vor allem der Boden, die alpine Vegetation, der Wald, geomorphologische Formen und hydrologische Prozesse von den Geländekorrekturen, der Erzeugung von Kunstschnee, der Pistenpräparierung und dem Schifahren selbst beeinträchtigt wurden. Es werden ständig neue Skipisten geplant und gebaut, vor allem in den höheren Bergregionen, und daher muss der Umweltverträglichkeit von Schipisten in deren Planung mehr Bedeutung zukommen, um die negativen Auswirkungen zu minimalisieren. Das Ziel dieser Dissertation war die Entwicklung einer allgemein gültigen Methode, um die Lage einer geplanten Schipiste in Bezug auf die Umweltverträglichkeit zu optimieren. Die Wahl der besten Lage für eine neue Schipiste, die die höchste Umweltverträglichkeit in dem Gebiet aufweist, das sich für eine neue Schipiste eignen würde, bedingt die Evaluierung der Umweltverträglichkeit von allen möglichen Lagen. Als Untersuchungsgebiet diente ein kleines alpines Einzugsgebiet in der Skiregion Sölden im Ötztal mit einer flächenhaften Ausdehnung von etwa 3.6 km². Um alle erdenklichen Lagen für eine neue Schipiste zu evaluieren, wurden mehrere Schritte in einer festgelegten Reihenfolge durchgeführt.

Der erste Schritt war die Entwicklung und Anwendung des Schipistenmodells ("ski run model"), um alle Alternativen, die eine zukünftige Schipiste im Einzugsgebiet darstellen könnten, zu simulieren. Dazu wurden sowohl ein digitales Höhenmodell von dem Einzugsgebiet als auch eine Anzahl von Startpositionen benötigt, von denen ausgehend eine Schipiste mit derselben Länge und Breite konstruiert werden konnte.

Weiters wurden verschiedene Kriterien definiert, die der Beschreibung der Umweltverträglichkeit einer simulierten Schipiste dienten. Sowohl die vorherrschenden Gebietseigenschaften als auch die Ergebnisse der Untersuchungen auf bestehenden Schipisten, unter anderem auch in Sölden, beeinflussten die Auswahl der bedeutenden Kriterien in Bezug auf die Umweltverträglichkeit. Die Zerlegung der gewählten Kriterien in verschiedene Untergruppen wurde unter Anwendung des analytischen hierarchischen Prozesses ("analytical hierarchical process", AHP) durchgeführt. Diese Methode ist eine häufig verwendete Vorgangsweise innerhalb von "Multicriteria Analyse" (MCA), um ein Entscheidungsproblem systematisch in verschiedene Teile zu zerlegen, die einfacher zu verstehen sind und qualitativ geschätzt oder quantitativ gemessen werden können. Vegetation, Beeinträchtigung der Landschaft und Schneeverhältnisse bildeten Großgruppen, die systematisch in kleine Elemente zerlegt wurden, in dieser Dissertation definiert als Umweltindikatoren. Die Umweltverträglichkeit einer Schipiste in Bezug auf die Vegetation wurde durch zwei Indikatoren charakterisiert: erstens durch die durchschnittliche maximale Wachstumsrate der alpinen Grasdecke und zweitens durch die Beeinträchtigung von Vegetationsgemeinschaften. Erosionserscheinungen auf der Schipiste und ihrer Umgebung, die eventuelle Gefahr von Hangrutschungen, der maximale Durchfluss des Gebirgsflusses am Aussfluss des Einzugsgebietes und der prozentuelle Anteil des zerstörten Bodens als Folge der Einebnung dienten der Beurteilung der Beeinträchtigung der Landschaft. Die Schneeverhältnisse wurden durch die Anzahl der Tage mit ausreichender Schneedecke beschrieben.

Der dritte Schritt der allgemein gültigen Methode behandelte die Quantifizierung der Umweltindikatoren, die im zweiten Schritt definiert wurden, sowohl für die Situation mit Schipiste als auch ohne Schipiste. Aus diesem Grund wurde ein Set von räumlich-zeitlichen Simulationsmodellen zusammengestellt, das aus einem Schneemodell ("snow model"), zwei hydrologischen Modellen ("hydrological models"), dem Erosionsmodell ("erosion model"), dem Stabilitätsmodell ("stability model") und dem Biomassemodell ("plant growth model") bestand. Mithilfe dieser Modelle konnten für jede Schipiste die Umweltindikatoren sowohl für die Situation ohne Landschaftseingriffe als auch mit den negativen Auswirkungen, die durch den Bau von Schipisten und den damit verbundenen Tätigkeiten verursacht wurden, berechnet werden. Zusätzlich wurde ein statistisches Pfanzengesellschaftenmodell entwickelt. Auf der einen Seite, um eine großmaßstäbige Vegetationskarte anzufertigen, die als Input für die räumlich-zeitlichen Simulationsmodelle verwendet werden konnte, und auf der anderen Seite, um eine Vegetationsbeinträchtigungskarte herzustellen. Dazu wurde jeder Pflanzengesellschaft entsprechend der Umweltverträglichkeit einer Schipiste ein Wert zugeordnet. Die Vegetationsbeeinträchtigungskarte diente der quantitativen Darstellung der Beeinträchtigung der Vegetationsgemeinschaften, die durch eine Skipiste hervorgerufen werden könnte. Da räumlich-zeitliche Simulationsmodelle Landschaftsprozesse in Raum und Zeit beschreiben können, wurden Karten von mehreren Zeitschritten erzeugt, die zu einem dimensionslosen Wert aggregiert werden mussten, um eine Rangordnung der untersuchten Schipisten erstellen zu können. Für die Aggregation wurde eine bestehende Methode mit dem Faktor Zeit erweitert.

Das Ziel des vierten Schrittes der Methode war die Integration der aggregierten Modellresultate (d.h. der Indikatoren, deren Wert mit den verschiedenen Modellen berechnet wurde) unter Verwendung von "Multicriteria Analyse" (MCA). Dies diente der Beurteilung der Umweltverträglichkeit jeder Schipiste. Um die verschiedenen Indikatoren, die in unterschiedlichen Einheiten gemessen wurden, zu kombinieren, wurden diese mithilfe von linearen und nichtlinearen Funktionen standardisiert. Anschließend wurden die standardisierten Indikatoren mittels numerischer Gewichtung ("simple additive weighting", SAW) für jede Schipiste aggregiert, wobei die Gewichte (Bedeutung eines Indikators) mit paarweisen Vergleichen ("pairwise comparison") ermittelt wurden. Anhand des Ergebnisses von SAW wurde die Rangordnung der untersuchten Schipisten erstellt. Die Rangordnung der Schipisten wurde vorwiegend durch die Zuerkennung unterschiedlicher Gewichte bestimmt, weniger durch die Wahl der Methode für die Standardisierung oder Aggregation, wie die Analyse der Sensitivität des Ergebnisses auf die Wahl einer bestimmten Methode gezeigt hatte. Der Rang der besten und der schlechtesten Schipisten war ziemlich stabil.

Die Anwendung dieser Methode auf das Untersuchungsgebiet Sölden hat gezeigt, dass es eine nützliche Methode ist, die Umweltverträglichkeit verschiedener Schipisten zu erforschen, wobei das Ergebnis als Entscheidungshilfe und nicht als die Entscheidung angesehen werden muss. Die Verwendung von räumlich-zeitlichen Simulationsmodellen für die Planung von Schipisten ist auf die Verfügbarkeit von gebietsbezogenen Daten und der verfügbaren Computer-Rechenzeit beschränkt. Weiters müssen die Fehler in der Modellbildung und die Fehler in den verwendeten Daten berücksichtigt werden. Darüber hinaus ist die Integration der Umweltindikatoren zu einem dimensionslosen Wert, der die Umweltverträglichkeit einer Schipiste darstellt, sehr subjektiv, da es in Bezug auf die

Standardisierungsmethode, der Aggregationsmethode, der Zuerkennung der Gewichte oder der Erstellung der Rangordnung viele verschiedene Möglichkeiten gibt. Wie dem auch sei, die Methode ist ein nützliches Hilfsmittel in der ersten Phase einer Umweltverträglichkeitsprüfung, um die eigentliche Notwendigkeit dieser Prüfung festzustellen und um verschiedene Alternativen zu entwerfen. In einer weiteren Phase des Entscheidungsfindungsprozesses müssen auch soziale und wirtschaftliche Aspekte einbezogen werden.

REFERENCES

Abott, M. B., J. C. Bathurst, J. A. Cunge, P. E. O'Connel and J. Rasmussen (1986), An introduction to the European Hydrological System - système hydrologique européen (SHE): 1. History and philosophy of a physically-based, distributed modelling sytem. Journal of Hydrology 87, pp. 45-59.

Aerts, J. (2002), Spatial decision support for resource allocation. Amsterdam: Institute of Biodiversity and Ecosystem Dynamics, University of Amsterdam (Ph.D. Thesis).

Albert, M. and G. Krajeski (1998), A fast, physically based point snowmelt model for use in distributed applications. Hydrological Processes 12, pp. 1809-1824.

Anderson, E. A. (1976), A point energy and mass balance model of a snow cover. U.S., Deparment of Commerce.

Anderson, M. G. and P. D. Bates (2001), Model validation: Perspectives in Hydrological Science. Chichester: John Wiley & Sons, Ltd.

Aulitzky, H. (1988), The summer 1987 floods in Tyrol - Natural disasters or absence of precautions. Österreichische Wasserwirtschaft 40, pp. 122-128.

Balk, B. and K. Elder (2000), Combining binary decision tree and geostatistical methods to estimate snow distribution in a mountain watershed. Water Resources Research 36, pp. 13-26.

Barbier, B. (1991), Problems of French winter sports resorts. Societe de Geographie de Marseille 91, pp. 18-33.

Beck, A. J., M. B. Jakeman and M. J. McAleer (1993), Construction and evaluation of models in environmental systems. In: Jakeman, A. J., M. B. Beck and M. J. McAleer, eds., Modelling Change in Environmental Systems. Chichester: John Wiley & Sons Ltd., pp. 3-35.

Beinat, E. (1995), Multiatttribute value functions for environmental management. Amsterdam: Faculty of Economy and Econometry, Free University of Amsterdam (Ph.D. Thesis, published in Tinbergen Institute Research Series 103).

Beinat, E., M. Bressan, M. Jones and K. Fabbri (1999), Geographical information systems and environmental impact assessment. Amsterdam (Optional EIA Module 1).

Beinat, E. and P. Nijkamp (1998), Multicriteria evaluation for land use management. Dordrecht: Kluwer Academic Publisher.

Belfroid, A. C., D. Sijm and K. Van Gestel (1996), Bioavailability and toxicokinetics of hydrophobic aromatic compounds in benthic and terrestrial invertebrates. Environ. Rev 4, pp. 276-299.

Bell, M. L., B. F. Hobbs, E. M. Elliott and Z. Robinson (2001), An evaluation of multi-criteria methods in integrated assessment of climate policy. Journal of multi-criteria decision analysis 10, pp. 229-256.

Bell, V. A. and R. J. Moore (1999), An elevation-dependent snowmelt model for upland Britain. Hydrological Processes 13, pp. 2067-2077.

Benayoun, R., B. Roy and B. Sussman (1966), ELECTRE: une méthode pour guider le choix en présence de points de vue multiples. Paris: SEMA (Metra International), Direction Scientifique.

Bergonzoni, M., A. Vezzani, J. I. Lugaresaresti, M. Soldati and D. Barani (1995), Environmental impact assessment studies in the regional park of Sassi di Roccamalatina (Northern Apennines, Italy). In: Marchetti, M., M. Panizza, M. Soldati and D. Barani, eds., Geomophology and environmental impact assessment. pp. 139-156.

Beven, K. (1979), A sensitivity analysis of the Penman-Monteith actual evapotranspiration estimates. Journal of Hydrology 44, pp. 169-190.

Beven, K. J. (1997), Distributed modelling in catchment hydrology: Application of the TOPMODEL concept. Chichester: John Wiley&Sons.

Bie, S. W. and P. H. T. Beckett (1973), Comparison of four independent soil surveys by air-photo interpretation, Paphos area (Cyprus). Photogrammetria 29, pp. 189-202.

Bio, A. M. F. (2000), Does vegetation suit our models?: data and model assumptions and the assessment of species distribution in space. Utrecht: Faculty of Geographical Sciences, Utrecht University (Ph.D. Thesis, published in Netherlands Geographical Studies 265).

Blöschl, G. (1991), The influence of uncertainty in air temperature and albedo on snowmelt. Nordic Hydrology 22, pp. 95-108.

Blöschl, G. and R. Kirnbauer (1991), Point snowmelt models with different degrees of complexity - internal processes. Journal of Hydrology 129, pp. 127-147.

Blöschl, G. and R. Kirnbauer (1992), An analysis of snow cover patterns in a small alpine catchment. Hydrological processes 6, pp. 99-109.
Blöschl, G., R. Kirnbauer and D. Gutknecht (1991), Distributed snowmelt simulations in an Alpine Catchment: 1. Model evaluation on the basis of snow cover patterns. Water Resources Research 27, pp. 3171-3179.
Blöschl, G., R. Kirnbauer and D. Gutknecht (1991), Distributed snowmelt simulations in an alpine catchment: 2. Parameter study and model predictions. Water Resources Research 27, pp. 3181-3188.
Braun, L. N. (1991), Modelling of the snow-water equivalent in the mountain environment. Proceedings of 1991, IAHS.
Broggi, F. and G. Willi (1989), Beschneiungsanlagen im Widerstreit der Interessen. CIPRA-Kleine Schriften 3, pp. 48.
Bunza, G. (1989), Oberflächenabfluss und Bodenabtrag in der alpinen Grasheide der hohen Tauern an der Grossglocknerstrasse. Innsbruck: Österreichische Akademie der Wissenschaften.
Burrough, P. A. (1989), Matching spatial databases and quantitative models in land resource assessment. Soil use and management 5, pp. 3-8.
Burrough, P. A. (1991), Sampling designs for quantifying map unit composition. In: Mausbach, M. J. and L. P. Wilding, eds., Spatial Variabilities of Soils and Landforms. Wisconsin, USA: Medison, pp. 89-125.
Burrough, P. A. (1998), Dynamic modelling and geocomputation. In: Longley, P. A., S. M. Brooks, R. McDonnell and B. MacMillan, eds., Geocomputation a Primer. New York: John Wiley & Sons, Ltd., pp. 165-191.
Burrough, P. A. and R. A. McDonnell (1998), Principles of Geographical Systems. Oxford: Oxford University Press.
Burrough, P. A., P. F. M. Van Gaans and R. A. MacMillan (2000), High-resolution landform classification using fuzzy k-means. Fuzzy Sets Systems 113, pp. 37-52.
Burrough, P. A., J. P. Wilson, P. F. M. Van Gaans and A. J. Hansen (2001), Fuzzy k-means classification of topo-climatic data as an aid to forest mapping in the Greater Yellowstone Area, USA. Landscape Ecology 16, pp. 523-546.
Calder, I. R. (1977), A model of transpiration and interception loss from a spruce forest in Plynlimon. Journal of Hydrology 33, pp. 247-265.
Carton, A., A. Cavallin, F. Francavilla, F. Mantovani, M. Panizza and G. B. Pellegrini (1993), Ricerce ambientali per l'individuazione dei geomorfologici. Metodi ed esempi. Il Quarternio 7, pp. 365-372.
Castenmiller, M. E. (2001), Grasgroei in de Alpen. Utrecht: Faculty of Geographical Sciences, Utrecht University (MSc Thesis).
Cavallin, A., M. Marchetti and M. Panizza (1996), Geomorphology and environmental impact assessment: a methodologic approach. In: Panizza, M., A. G. Fabbri, M. Marchetti and A. Patrono, eds., Geomorphologic analysis and evaluation in environmental impact assessment. pp. 308-310.
Cazorzi, F. and G. D. Fontana (1996), Snowmelt modelling by combining air temperature and a distributed radiation index. Journal of Hydrology 181, pp. 169-187.
Cernica, J. N. (1995), Geotechnical engineering - Soil mechanics. New York: John Wiley &Sons.
Cernusca, A. (1977), Ökologische Veränderungen im Bereich von Schipisten. In: Sprung, R. and B. König, eds., Das Österreichische Skirecht. Innsbruck: Universitätsverlag Wagner, pp. 81-150.
Cernusca, A. (1986), Ökologische Auswirkungen des Baues und des Betriebes von Skipisten und Empfehlungen zur Reduktion der Umweltschäden. Strassbourg: Europarat.
Cernusca, A. (1987), Wintersporterschließungen und Naturschutz - Ergebnisse einer Studie im Auftrag des Europarates. Verhandlungen der Gesellschaft für Ökologie pp. 173-181.
Cernusca, A. (1989), Zur Schneestruktur beschneiter Flächen - Einflussfaktoren und ökologische Auswirkungen auf Vegetation und Boden im Pistenbereich. Motor im Schnee 5, pp. 13-16.
Cernusca, A. (1990), Umweltverträglichkeitsprüfungen für Wintersporteinrichtungen. In: Cernusca, A., eds., Umweltverträglichkeitsprüfung: Theorie und Praxis. Innsbruck: Universitätsverlag Wagner, pp. 129-150.
Cernusca, A., H. Angerer, C. Newesely and U. Tappeiner (1989), Ökologische Auswirkungen von Kunstschnee - Eine Kausalanalyse der Belastungsfaktoren. Verhandlungen der Gesellschaft für Ökologie 19, pp. 746-757.
Chang, K. T. and Z. Li (2000), Modelling snow accumulation with a geographic information system. Int.J.Geographical Information Science 14, pp. 693-707.

Chow, V. T., D. R. Maidment and L. W. Mays (1988), Applied Hydrology. Singapore: McGraw-Hill.
Climaco, J. (1997), Multicriteria Analysis. Berlin: Springer Verlag.
Conrads, L. A. and R. Van de Wal (1999), College 'KLIM' 1999, basisdoctoraal Fysische Geografie. Utrecht: Instituut voor Marien en Atmosferisch Onderzoek Utrecht.
Coughlan, J. C. and S. W. Running (1997), Regional ecosystem simulation: A general model for simulating snow accumulation and melt in mountainous terrain. Landscape Ecology 12, pp. 119-136.
Cowlard, K. A. (1998), Decision-Making in Geography. London: Hodder & Stoughton.
Cremer, J. (2001), The invloed van ondiepe aardverschuivingen op het skigebied van Sölden. Utrecht: Faculty of Geographical Sciences, Utrecht University (MSc Thesis).
Cressie, N. A. C. (1993), Statistics for spatial data. New York [etc.]: John Wiley and Sons.
Daly, S. F., R. Davis, E. Ochs and T. Pangburn (2000), An approach to spatially distributed snow modelling of the Sacramento and San Joaquin basins, California. Hydrological Processes 14, pp. 3257-3271.
Davis, J. C. (1986), Statistics and Data Analysis in Geology. New York: John Wiley & Sons, Inc.
De Jong, R. and P. Kabat (1990), Modelling water balance and grass production. Soil Sciences Society of America Journal 54, pp.
De Roo, A. P. J., C. G. Wesseling and W. P. A. Van Deursen (1998), Physically-based river basin modelling within a GIS: The LISFLOOD model. Proceedings of Geocomputation 98. Bristol (UK): University of Bristol.
Department, I. Ilwis 2.1. for Windows - The intregrated land and water information system: User's guide. Enschede: ITC.
Dewey, J. (1910), How we think. New York: D.C. Heath.
Dingman, S. L. (2002), Physical Hydrology, 2nd edition. New Jersey: Prentice Hall.
Dorren, L. K. A. (2002), Mountain Geoecosystems-GIS modelling of rockfall and protection forest structure. Amsterdam: Institute of Biodiversity and Ecosystem Dynamics, University of Amsterdam (PhD. Thesis).
Edwards, R. (1996), Downhill all the way. In: New Scientist, 20 April, pp. 36-39.
Elder, K., W. Rosenthal and R. E. Davis (1998), Estimating the spatial distribution of snow water equivalence in a montane watershed. Hydrological Processes 12, pp. 1793-1808.
Ellenberg, H., H. E. Weber, R. Düll, V. Wirth, W. Werner and D. Paulissen (1991), Zeigerwerte von Pflanzen Mitteleuropas. Göttingen: Goltze.
Feddes, R. A., P. J. Kowalik and H. Zaradny (1978), Simulation of field water use and crop yield. Wageningen: Pudoc Wageningen.
Felber, H. U., M. Hirsch and P. Walther (1989), Skiportbedingte Landschafteingriffe: Richtlinien zu Projektierung, Bewilligung und Ausführung. Bern: Eidgenössisches Departement des Inneren/ Eidgenössisches Justiz- und Polizeidepartement.
Finch, J. W. (1998), Estimating direct groundwater recharge using a simple water balance model - sensitivity to land surface parameter. Journal of Hydrology 211, pp. 112-125.
Fischer, I. (1992), Beschneiungsanlagen in Österreich: Bestandserhebung und Literaturrecherche. Wien: Umweltbundesamt.
Franklin, J. (1995), Predictive vegetation mapping: geographic modelling of biospatial patterns in relation to environmental gradients. Progress in Physical Geography 19, pp. 474-499.
Franklin, J., P. McCullough and C. Gray (2000), Terrain variables used for predictive mapping of vegetation communities in southern California. In: Wilson, J. P. and J. C. Gallant, eds., Terrain Analysis: Principles and Application. New York [etc.]: John Wiley & Sons, Inc., pp. 331-353.
Frings, R. M. (2001), Ruimtelijke verschillen in de biomassaproductie van grassen en zeggen in alpiene gebieden. Utrecht: Faculty of Geographical Sciences, Utrecht University (MSc Thesis).
Ghinoi, A. (2002), A spatial prediction model for localising potential snow avalanche release areas: S.T.A.R.T.E.R. the prototype study of Sölden (Tyrol, Austria). Vienna: Institute of Geography, University of Vienna (Ph.D. Thesis).
Giessübel, J. (1988), Nutzungsschäden, Bodendichte und rezente Geomorphodynamik auf Skipisten der Alpen und Skandinaviens. Z.Geomorph.N.F. 70, pp. 205-219.
Goodchild, M. F., P. O. Parks and L. T. Steyaert (1993), Modeling with GIS. New York: Oxford University Press.
Gottfried, M., H. Pauli and G. Grabherr (1998), Prediction of vegetation patterns at the limits of plants life: a new view of the alpine-nival ecotone. Arctic and Alpine Research 30, pp. 207-221.

Grabherr, G. (1985), Damage to vegetation by recreation in the Austrian and German Alps. England: Wye College.
Green, W. H. and G. A. Ampt (1911), Studies on soil physics - The flow of air and water through soils. Journal of agricultural science 4, pp. 1-24.
Groenendijk, M. and T. Koerts (2001), Sneeuwsmelt en afvoer in een bergachtig gebied. Utrecht: Faculty of Geographical Sciences, Utrecht University (MSc Thesis).
Gruppo di lavoro per la cartografia geomorfologica Servizio Geologico Nazionale (1994), Carta Geomorfologica d'Italia 1:50.000: guida al rilevamento, Quaderni serie III 4.
Guisan, A., J. P. Theurillat and F. Kienast (1998), Predicting the potential distribution of plant species in an alpine environment. Journal of Vegetation Science 9, pp. 65-74.
Guisan, A., S. B. Weiss and A. D. Weiss (1999), GLM versus CCA spatial modeling of plant species distribution. Plant Ecology 143, pp. 107-122.
Guisan, A. and N. E. Zimmermann (2000), Predictive habitat distribution models in ecology. Ecological Modelling 153, pp. 147-186.
Güthler, A. (2002), Die Alpen im internationalen Jahr der Berge. Informationsdienst 65, pp. 5-6.
Haberli, W. (1982), Skipisten im alpinen Permafrost. Materialien zur Physiogeographie 4, pp. 59-61.
Hardisty, J., D. M. Taylor and S. E. Metcalfe (1993), Computerised environmental modelling: a practical introduction using Excel. Chichester: Wiley.
Henderson-Sellers, A. and P. J. Robinson (1994), Contemporary climatology. Essex (UK): Longman Scientific & Technical.
Hijmans, R. J., I. M. Guiking-Lens and C. A. Van Diepen (1994), WOFOST: User guide for the Wofost 6.0 crop growth simulation model. Wageningen: DLO Winand Staring Centre.
Hofer, H. (1981), Skipisten verändern die alpine Grasheide. Unterricht Biologie 55, pp. 55-62.
Holaus, K. and L. Köck (1992), Skipisten und Ökologie. Rinn: Landesanstalt für Pflanzensucht und Samenprüfung Rinn.
Holaus, K. and C. Partl (1994), Beschneiung von Dauergrünland - Auswirkungen auf Pflanzenbestand, Massenbildung und Bodenstruktur. Verhandlungen der Gesellschaft für Ökologie 23, pp. 268-276.
Horn, B. K. P. (1981), Hill shading and the reflectance map. Proceedings IEEE 69, pp. 14-47.
Hörsch, B., G. Braun and U. Schmidt (2002), Relation between landform and vegetation in alpine regions of Wallis, Switzerland. A multiscale remote sensing and GIS approach. Computers, Environment and Urban Systems 26, pp. 113-139.
Hühnerwadel, D., R. Rudin, W. Rüsch, F. H. Schwarzenbach, H. K. Stiffler, B. Wallimann and H. Weiss (1982), Skipistenplanierungen und Geländekorrekturen-Erfahrungen und Empfehlungen. Birmensdorf: Swiss Federal Institute of Forestry Research.
Huxham, M. and D. Sumner (2000), Science and Environmental Decision Making. Harlow: Pearson Education Limited.
Hwang, C. L. and K. Yoon (1981), Multiple attribute decision making: methods and applications. Berlin: Springer Verlag.
Illich, I. P. and J. R. Haslett (1994), Responses of assemblages of Orthoptera to management and use of ski slopes in upper sub-alpine meadows in the Austrian Alps. Oecologica 97, pp. 470-474.
Jakeman, A. J., M. B. Beck and M. J. McAleer (1995), Modelling change in environmental systems. New York: Wiley.
Jankowski, P. (1995), Integrating geographical information systems and multiple criteria decision-making methods. Int.J.Geographical Information Science 9, pp. 251-273.
Jansen, A. I. (1977), BINAS (Informatieboek VWO-HAVO voor het inderwijs in de natuurwetenschappen. Groningen: Wolters-Noordhoff.
Janssen, L. L. F. and H. Middelkoop (1991), Knowledge based image classification: the use of knowledge about crop rotations in a Thematic Mapper image classification procedure. Wageningen: The Winand Staring Centre.
Janssen, R. (1992), Multiobjective decision support for environmental management. Dordrecht: Kluwer Academic.
Janssen, R. (2001), On the use of multi-criteria analysis in Environmental Impact Assessment in The Netherlands. Journal of multi-criteria decision analysis 10, pp. 101-109.
Jongman, R., C. J. F. Ter Braak and O. F. R. Tongeren (1995), Data Analysis in Community and Landscape Ecology. Cambridge: Cambridge University Press.

Jørgensen, S. E. (1996), Handbook of environmental and ecological modelling. New York: Lewis Publishers.
Kammer, P. and O. Hegg (1989), Auswirkungen von Kunstschnee auf subalpine Rasenvegetation. Verhandlungen der Gesellschaft für Ökologie 19, pp. 758-767.
Karssenberg, D. (2002), Building spatial dynamic environmental models. Utrecht: Faculty of Geographical Sciences, Utrecht University (Ph.D. Thesis, published in Netherlands Geographical Studies 305).
Karssenberg, D. (2002), The value of hydrological environmental modelling languages for building distributed hydrological models. Hydrological Processes 16, pp. 2751-2766.
Keeney, R. L. (1996), Value-focused thinking: Identifying decision opportunities and creating alternatives European. Journal of Operational Research 92, pp. 537-549.
Kessler, J. and R. Oosterbaan (1974), Determining hydraulic conductivity of soils. Drainage principles and applications 16, pp. 253-296.
Köck, L. and R. Schnitzer (1980), Quantitative and qualitative Veränderung der Vegetation durch den Einfluss des Schisports. Zeitschrift für Vegetationstechnik 3, pp. 113-119.
Kuchment, L. S. and A. N. Gelfan (1996), The determination of the snowmelt rate and the meltwater outflow from a snowpack for modelling river runoff generation. Journal of Hydrology 179, pp. 23-36.
Kuchment, L. S., A. N. Gelfan and V. N. Demidov (2000), A distributed model of runoff generation in the permaforst regions. Journal of Hydrology 240, pp. 1-22.
Kuhn, M. and F. Pellet (1989), Basin precipitation as residual in alpine water balances. In: Sevruk, B., eds., Precipitation measurements. Zürich: Eidgenössische technische Hochschule, pp. 275-277.
Kustas, W. and A. Rango (1994), A simple energy algorithm for the snowmelt runoff model. Water Resources Research 30, pp. 1515-1527.
Kutilek, M. and D. R. Nielsen (1994), Soil hydrology. Cremlingen-Destedt: Catena-Verlag.
Lauterwasser, E. (1990), Skisport und Umwelt: Ein Leitfaden zu den Asuwirkungen des Skisports auf Natur und Landschaft. Weilheim: Stöppel.
Leavesley, G. H. (1989), Problems of snowmelt runoff modelling for a variety of physiographic and climatic conditions. Hydrologic Sciences 34, pp. 617-643.
Leavesley, G. H., R. W. Lichty, B. M. Troutman and L. G. Saindon (1983), Precipitation-runoff modeling system: user's manual. U.S. Geological Survey. Denver, Colorado: U.S. Geological SurveyWater-Resources Investigations Report.
Lee, I., W. White and O. G. Ingles (1983), Geotechnical Engineering. Boston: Pitman.
Leibenzon, L. S. (1947), Flow of natural liquids and gazes in porous medium (in Russian). Moscow: Gostekhisdat.
Leicht, H. (1993), Beschneiungsanlagen und Naturschutz - eine naturschutzfachliche Betrachtung der Situation in Bayern. Natur und Landschaft 68, pp. 52-57.
Leicht, H., T. Dietmann and U. Köhler (1993), Landschaftsökologische Untersuchungen in den bayrischen Skigebieten: Grundlagen zur Sicherung und Entwicklung der landschaftlichen Situation. Naturschutz und Landschaftsplanung 25, pp. 99-104.
Lillesand, T. M. and R. W. Kiefer (1994), Remote sensing and image interpretation. New York [etc.]: John Wiley and Sons, Inc.
Mackay, D. S. and V. B. Robinson (2000), A multiple criteria decision support system for testing integrated environmental models. Fuzzy Sets and Systems 113, pp. 53-67.
MacQueen, J. B. (1967), Some methods for classification and analysis of multivariate observations. Proceedings of CA: University of California,Press Berkely.
Malczewski, J. (1996), A GIS-based approach to multiple criteria group decision-making. Int.J.Geographical Information Science 10, pp. 955-971.
Malczewski, J. (1999), GIS and multicriteria decision analysis. New York: John Wiley & Sons, Inc.
Marchetti, M. and A. Rivas (2001), Geomorphology and Environmental Impact Assessment. Lisse: Balkema.
Markart, G. and B. Kohl (1991), Bodenphysikalische Charakterisierung der Böden des Skigebietes am Monte Bondone - Trient. Innsbruck: Aussenstelle für subalpine Waldforschung, Forstliche Bundesversuchsanstalt, Innsbruck.
Marks, D., J. Domingo, D. Susong, T. Link and D. Garen (1999), A spatially distributed energy balance snowmelt model for application in mountain basins. Hydrologic Processes 13, pp. 1935-1959.

Marks, D., J. Kimball, D. Tingey and T. Link (1998), The sensitivity of snowmelt processes to climate conditions and forest cover during rain-on-snow: a case study of the 1996 Pacific Northwest flood. Hydrological Processes 12, pp. 1569-1587.
Martinec, J. and A. Rango (1998), Snowmelt Runoff Model (SRM) User's Manual. Geographica Bernensia 83, pp.
Meentemayer, R. K. and A. Moodry (2000), Rapid sampling of plant species composition for assessing vegetation patterns in rugged terrain. Landscape Ecology 15, pp. 697-711.
Merriam, R. A. (1973), Fog drip form artificial leaves in a fog wind tunnel. Water Resources Research 9, pp. 1591-1598.
Mintzberg, H., D. Raisinghani and A. Theoret (1976), The structure of "Unstructured Decision Processes". Administrative Science Quarterly 21, pp. 246-275.
Monteith, J. L. (1965), Evaporation and environment. Proceedings of 19th Symposium of the Society for Experimental Biology. New York: Cambridge University Press.
Moore, I. D., R. B. Grayson and A. R. Ladson (1991), Digital terrain modelling: a review of hydrological, geomorphological, and biological applications. Hydrological Processes 5, pp. 3-30.
Moore, I. D., A. K. Turner, J. P. Wilson, S. K. Jenson and L. E. Band (1993), GIS and land surface-subsurface modeling. In: Goodchild, M. F., P. O. Parks and L. T. Steyaert, eds., Environmental modeling with GIS. New York: Oxford University Press, pp. 1996-230.
Morgan, R. P. C. (2001), A simple approach to soil loss prediction: a revised Morgan-Morgan-Finney model. Catena 44, pp. 305-322.
Morgan, R. P. C., J. N. Quinton, R. E. Smith, G. Govers, J. W. A. Poesen, K. Auerswald, G. Chisci, D. Torri and M. E. Styczen (1998), The European soil erosion model (EUROSEM): a process-based approach for predicting sediment transport from fields and small catchments. Earth Surface Processes and Landforms 23, pp. 527-544.
Mosimann, T. (1981), Geoökologische Standortsindikatoren für die Erosionsanfälligkeit alpiner Hänge nach Geländeeingriffen für Pistenanlagen. Geomethodica 6, pp. 143-174.
Mosimann, T. (1983), Landschaftsökologischer Einfluss von Anlagen für den Massensport: II. Bodenzustand und Bodenstörungen auf planierten Skipisten in verschiedenen Lagen (Beispiel Crap Sogn Gion/Laax GR). Basel: Institut für Geographie/Universität Basel.
Mosimann, T. (1985), Geo-ecological impacts of ski piste construction in the Swiss Alps. Applied Geography pp. 29-37.
Mosimann, T. (1985), Landschaftsökologischer Einfluss von Anlagen für den Massenskiport: III. Ökologische Entwicklung von Pistenflächen. Entwicklungstendenzen im Erosionsgeschehen und beim Wiederbewuchs planierter Pisten im Skigebiet Crap Sogn Gion/Laax GR. Basel: Institut für Geographie/Universität Basel.
Mosimann, T. (1986), Skitourismus und Umweltbelastung im Hochgebirge. Geographische Rundschau 38, pp. 303-311.
Mosimann, T. (1987), Schneeanlagen in der Schweiz. Materialien zur Physiogeographie 10, pp.
Mosimann, T. and P. Luder (1980), Landschaftsökologischer Einfluss von Anlagen für den Massenskisport: I. Gesamtaufnahme des Pistenzustandes (Relief, Boden Vegetation, rezente Morphodynamik) im Skigebiet Crap Sogn Gion/Laax GR. Basel: Institut für Geographie/Universität Basel.
Mulder, F. (1991), Assessment of landslide hazard. Utrecht: Faculty of Geographical Sciences, Utrecht University (Ph.D. Thesis).
Nagendra, H. (2001), Using remote sensing to assess biodiversity. International Journal for Remote Sensing 22, pp. 2377-2400.
Newesely, C. (1997), Auswirkungen der künstlichen Beschneiung von Schipisten auf Aufbau, Struktur und Gasdurchlässigkeit der Schneedecke, sowie auf den Verlauf der Bodentemperatur und das Auftreten von Dauerfrost. Innsbruck: Institut für Botanik, Universität Innsbruck (Ph.D. Thesis).
Newesely, C. and A. Cernusca (2000), Auswirkungen der künstlichen Beschneiung von Schipisten auf die Umwelt. Laufener Seminarbeiträge 6, pp. 29-38.
Newesely, C., A. Cernusca and M. Bodner (1994), Entstehung und Auswirkungen von Sauerstoffmangel im Bereich unterschiedlich präparierter Schipisten. Verhandlungen der Gesellschaft für Ökologie 23, pp. 277-282.
Österreichischer Wasser- und Abfallwirtschaftsverband (ÖWAV) (1998), Schipisten. Wien: Österreichisches Normungsinstitut.

Obled, C. (1990), Hydrological modeling in regions of rugged relief. Proceedings of Hydrology in Mountainous Regions. August 1990, Lausanne: IAHS.
Panizza, M. and S. Piacente (1993), Geomorphological Assets Evaluation. Z.Geomorph. N.F 87, pp. 13-18.
Pebesma, E. J. (1996), Mapping groundwater quality in the Netherlands. Utrecht: Faculty Geographical Sciences, Utrecht University (Ph.D. Thesis, published in Netherlands Geographical Studies 199).
Pebesma, E. J. and C. G. Wesseling (1998), GSTAT: a program for geostatistical modelling, prediction and simulation. Computers and Geosciences 24, pp. 17-31.
Penman, H. L. (1963), Vegetation and Hydrology. Harpenden: Commonwealth Bureau of Soil Science.
Penning de Vries, F. W. T. and H. H. Van Laar (1982), Simulation of plant growth and crop production. Wageningen: Pudoc Wageningen.
Pfeffer, K., D. Karssenberg, T. W. J. Van Asch and P. A. Burrough (2002), Application of spatio-temporal modelling and multicriteria analysis to optimise the planning of socio-economic infrastructure. Proceedings of iEMSs 2002. 24-27 June 2002, Lugano: International Environmental Modelling and Software Society.
Pfiffner, A. (1976), Landschaftsschäden und Entschädigungspraxis im Zusammenhang mit dem Schisport. Zollikofen: Schweizerisches landwirtschaftliches Technikum, Schweizerisches landwirtschaftliches Technikum (MSc Thesis).
Pfitzner, I. (1988), Auswirkungen von Schneeanlagen: Schipistenprojekt, Projektteil 1. Innsbruck: Universität Innsbruck/Institut für Geographie.
Pfitzner, I. (1988), Der Einfluss von Schipisten auf die Vorfluter: Schipistenproject, Projektteil 2. Innsbruck: Universität Innsbruck/Institut für Geographie.
Purtscheller, F. (1978), Ötztaler und Stubaier Alpen. Berlin: Gebrüder Borntraeger.
Raemaekers, J. (1991), Piste control: the planning and management of Scottish ski centres. Planner 77, pp. 6-8.
Ramskogler, K. (1987), Schierschliessungen-Auswirkungen auf Boden und Bestand am Beispiel des Schigrossraumes Gasteinertal. Österreichische Forstzeitung 6, pp. 5-8.
Reisigl, H. and R. Keller (1987), Alpenpflanzen im Lebensraum: Alpine Schutt- und Rasenvegetation. Stuttgart, New York: Gustav Fischer Verlag.
Richard, L. A. (1931), Capillary conduction of liquids through porous media. Physics 1, pp. 318-333.
Ries, J. B. (1996), Landscape damage by skiing at the Schauinland in the Black Forest, Germany. Mountain Research and Development 16, pp. 27-40.
Rivas, V., K. Rix, E. Francés, A. Cendrero and D. Brunsden (1996), Assessing impacts on landforms. In: Panizza, M., A. G. Fabbri, M. Marchetti and A. Patrono, eds., Geomorphologic analysis and evaluation in environmental impact assessment. pp. 342-344.
Rizzoli, A. E., J. R. Davis and D. J. Abel (1998), Model and data integration and re-use in environmental decision support systems. Decision Support Systems 24, pp. 127-144.
Rodewald, R. (1995), Schneekanonen-auf Knopfdruck Winter. Natur und Mensch 1, pp. 26-29.
Rohrer, M. B. and H. Lang (1990), Point Modelling of snow cover water equivalent based on observed variables of the standard meteorological networks. Proceedings of 1990, IAHS.
Rohrer, M. B. and H. Lang (1990), Point Modelling of snow cover water equivalent based on observed variables of the standard meteorological networks. Proceedings of 1990, IAHS.
Rutter, A. J., K. A. Kershaw, P. C. Robins and A. J. Morton (1971), A predictive model of rainfall interception in forests, 1. Derivation of the model from observations in a plantation of Corsican Pine. Agricultural Meteorology 9, pp. 367-384.
Saaty, T. L. (1980), The Analytical Hierarchy Process: Planning, priority setting and resource allocation. New York: McGraw-Hill.
Salm, B. and H. Gubler (1990), Berechnung von Fliesslawinen: Eine Anleitung für Praktiker. Mitteilungen des Eidgenössischen Institutes für Schnee- und Lawinenforschung 47, pp. 37.
Sambles, K. M. and M. G. Anderson (1994), Snowmelt Forecasting - Further cold region development of operational hydrological forecasting. London: U.S. Corps Engineers.
Schatz, H. (1990), Beurteilung von Beschneiungsanlagen aus naturschutzfachlicher Sicht. In: Cernusca, A., eds., Umweltverträglichkeitsprüfung: Theorie und Praxis. Innsbruck: Universitätsverlag Wagner, pp. 151-166.

Schatz, H. (1993), Auswirkungen des Wintertourismus auf Natur und Umwelt, insbesondere der Beschneiungsanlagen auf Flora und Fauna. Proceedings of Vortrag Fortbildungsveranstaltung Skisport und Ökologie. Berlin:
Schatz, H. (1993), Auswirkungen des Wintertourismus, insbesondere der Beschneiungsanlagen auf die Natur und Umwelt. GW Unterricht 52, pp. 119-123.
Schauer, T. (1981), Vegetationsveränderungen und Florenverlust auf Skipisten in den bayrischen Alpen. Jahrbuch des Verein zum Schutz der Alpen 46, pp. 149-171.
Schönthaler, K. E. (1985), Auswirkungen der Anlagen für den Massenschisport auf die Landschaft. Die Bodenkultur-Journal für landwirschaftliche Forschung 36, pp. 155-174.
Sharifi, A., M. Van Herwijnen and W. Van den Toorn (2002), Introduction to multiple criteria decision analysis. in press.
Sharifi, M. A. and E. Rodriguez (2002), Design and development of a planning support system for policy formulation in water resource rehabilitation. Journal of Hydro informatics 4, pp. 157-175.
Sharifi, M. A. and E. Rodriguez (2002), A planning support system for policy formulation in water resource rehabilitation, The case of Alcázar De San Juan District in the Aquifer 23, La Mancha, Spain. In: Geertman, S. and J. Stillwel, eds., Planning Support Systems in Practice. Berlin, New York: Springer, pp.
Shaw, E. M. (1994), Hydrology in Practice. London: Chapman and Hall.
Simon, H. A. (1960), The new science of management decision. New York: Harper & Row.
Singh, P., G. Spitzbart, H. Huebl and H. W. Weinmeister (1997), Hydrological response of snowpack under rain-on-snow events: a field study. Journal of Hydrology 202, pp. 1-20.
Skidmore, A. K. (1989), A comparison of techniques for calculating gradient and aspect from a gridded digital elevation model. International Journal of Geographical Information Systems 3, pp. 323-334.
Skidmore, A. K. (2002), Environmental modelling in GIS and RS. London: Taylor&Francis.
Sol, H. G. (1982), Simulation in information system development. Groningen: University of Groningen, University of Groningen (Ph.D. Thesis).
Sprague, R. H. (1980), A framework for development of decision support system. Management Information Science Quarterly 4, pp. 1-26.
Sprague, R. H. and H. J. Watson (1989), Decision Support Systems: Putting Thery into practice. New York: Prentice Hall, Englewood Cliffs.
Strik, L. A. (2001), Degradatie van skipistes door oppervlakkige landslides in skigebied Sölden, Tirol. Utrecht: Faculty of Geographical Sciences, Utrecht University (MSc Thesis).
Tappeiner, U., A. Cernusca and U. Pröbstl (1998), Die Umweltverträglichkeitsprüfung im Alpenraum. Berlin: Blackwell Wissenschaft.
Tappeiner, U., G. Tappeiner, J. Aschenwald, E. Tasser and B. Ostendorf (2001), GIS-based modelling of spatial pattern of snow cover duration in an alpine area. Ecological Modelling 138, pp. 265-275.
Tappeiner, U., E. Tasser and G. Tappeiner (1998), Modelling vegetation patters using natural and anthropogenic influence factors: preliminary experience with a GIS based model applied to an Alpine area. Ecological Modelling 113, pp. 225-237.
Tarboton, D. G., T. G. Chowdhury and J. T.H. (1994), A spatially Distributed Energy Balance Snowmelt Model. Utah Water Research Laboratory/Utah State University.
Tarboton, D. G. and C. H. Luce (1996), Utah Energy Balance Snow Accumulation and Melt Model (UEB)-Computer model technical descritpion and users guide. Utah Water Research Laboratory/Utah State University; USDA Forest Service Intermountain Research Station.
Tayler, K., G. Walker and D. Abel (1999), A framework for model integration in spatial decision support systems. 13 6, pp. 555.
Ter Braak, C. J. F. (1986), Canonical correspondence analysis: a new eigenvector technique for multivariate direct gradient analysis. Ecology 67, pp. 1167-1179.
Ter Braak, C. J. F. (1987), The analysis of vegetation-environment relationships by canonical correspondence analysis. Vegetatio 69, pp. 69-77.
Ter Braak, C. J. F. (1995), Unimodal Models to relate Species to Environment. Cambridge: Cambridge University Press.
Ter Braak, C. J. F. and P. Smilauer (1998), Canoco 4, Canoco Reference Manual and User's Guide to Canoco for Windows. Wageningen: Centre for Biometry Wageningen.

Thierer, M. and E. Hoh (1983), Skipisten gefährden die alpine Gebirgslandschaft. Praxis Geographie 12, pp. 36-43.
Thimann, K. V. (1980), Senescence in plants. Florida: CRC Press.
Thonon, I. (2001), The effect of skiing on soil, hydrology and erosion hazard in the ski area of Sölden, Tyrol, Austria. Utrecht: Faculty of Geographical Sciences, Utrecht University (MSc Thesis).
Thornthwaite, C. W. (1948), An approach toward a rational classification of climate. Geographical Review 38, pp. 55-94.
Todini, E. (1996), The ARNO-rainfall-runoff model. Journal of Hydrology 175, pp.
Trockner, V. and H. Kopeszki (1994), Auswirkungen der künstlichen Beschneiung auf Bodenverdichtung, Bodentemperatur, Ernteertrag und Collembolenfauna von Pistenböden. Verhandlungen der Gesellschaft für Ökologie 23, pp. 283-288.
Turpin, O., R. Ferguson and B. Johansson (1999), Use of remote sensing to test and update simulated snow cover in hydrologic models. Hydrological Processes 13, pp. 2067-2077.
Van Beek, R. (2002), Assessment of the influence of changes in land use and climate on landslide activity in a Mediterranean environment. Utrecht: Faculty of Geographical Sciences, Utrecht University (Ph.D. Thesis, published in Netherlands Geographical Studies 294).
Van Dam, O. (2001), Forest filled with gaps-Effects of gap size on water and nutrient cycling in tropical rain forest: A study in Guyana. Utrecht: Faculty of Geographical Sciences, Utrecht University (Ph.D. Thesis, published in Tropenbos-Guyana Series 10).
Van Deursen, W. P. A. (1995), Geographical information systems and dynamic models. Utrecht: Faculty of Geographical Sciences, Utrecht University (Ph.D. Thesis, published in Netherlands Geographical Studies 190).
Van Heemst, H. D. J. (1986), Physiological principles. In: Van Keulen, H. and J. Wolf, eds., Modelling of agricultural production: weather soils and crops. Wageningen: Pudoc Wageningen, pp. 13-24.
Van Herwijnen, M. (1999), Spatial decision support for environmental manangement. Amsterdam: Faculty of Economical Sciences and Econometry, Free University of Amsterdam (Ph.D. Thesis).
Van Keulen, H. and N. G. Seligman (1987), Simulation of water use, nitrogen and growth of a spring wheat crop. Wageningen: Pudoc Wageningen.
Van Keulen, H. and J. Wolf (1986), Modelling of agricultural production: weather soils and crops. Wageningen: Pudoc Wageningen.
Ward, R. C. and M. Robinson (1990), Principles of Hydrology. Maidenhead: McGraw-Hill.
Watson, A. (1985), Soil Erosion and Vegetation Damage near Ski Lifts at Cairn Gorm, Scotland. Biological Conservation 33, pp. 363-381.
Weber, J. (2002), Der Tourismus im Winter 2001/2002. Innsbruck: Amt der Tiroler Landesregierung/Raumordnung und Statistik.
Wenzel, V. (2001), Integrated assessment and multicrtieria analysis. Phys.Chem.Earth 26, pp. 541-545.
Wesseling, C. G., D. Karssenberg, W. P. A. Van Deursen and P. A. Burrough (1996), Integrating dynamic environmental model in GIS: the development of a dynamic modelling language. Transactions in GIS 1, pp. 40-48.
Whitehead, D. C. (1995), Grassland nitrogen. Wallingford: CAB International.
Williams, K. S. and D. G. Tarboton (1999), The ABC's of snowmelt: a topographically factorized energy component snowmelt model. Hydrological Processes 13, pp. 1905-1920.
Williams, P. W. (1997), Towards an environmental management system for ski areas. Mountain Research and Development 17, pp. 75-90.
Wilson, J. P. and J. C. Gallant (2000), Digital terrain analysis;. In: Wilson, J. P. and J. C. Gallant, eds., Terrain Analysis: Principles and Application;. New York [etc.]: John Wiley & Sons, Inc., pp. 1-27.
Wischmeier, W. H. and D. D. Smith (1968), Soil loss estimation as a tool in soil and water management planning. Int. Assoc. Scient. Hydrol. Pub. 59, pp. 148-59.
Zevenbergen, L. W. and C. R. Thorne (1987), Quantitative analysis of land surface topography. Earth Surface Processes and Landforms 12, pp. 47-56.

CURRICULUM VITAE

Karin Pfeffer was born on 31st of May in 1974 in Vöcklabruck, Austria. In June 1992 she obtained her A-level GCE (General Certificate of Education) at the Federal State Gymnasium Vöcklabruck. From 1992 to 1998 she studied Geography and Mathematics for teaching at the secondary school at the University of Vienna. In 1997 she followed for 6 months the Erasmus Exchange Program at the Faculty of Geographical Sciences at Utrecht University. From 1998 to 2002 she worked at the Department of Physical Geography at Utrecht University as a Ph.D. researcher. The research, which was funded by the European Research Network GETS (**G**eomorphology and **E**nvironmental Impact Assessment to **T**ransportation **S**ystems), aimed at the development and integration of environmental models and multicriteria decision making to support the planning of environmentally sound ski runs.

ACKNOWLEDGEMENTS

In October 1998 I came to the Netherlands to work at Utrecht University as a young researcher for the GETS project. The initial planning was to work 3 years for the project in the Netherlands and to get the degree of doctor at the University of Vienna. However, due to the effort of many people I was accepted for a PhD research at the Utrecht University. At this point I would like to mention my promotor from Vienna, Berthold Bauer, who gave me the opportunity for the research in the Netherlands and who supported me in the last four years in many different ways. A very important person in these four years was my co-promotor Theo van Asch. He helped me in finding my way in the field of applied physical geography and supported the work for the GETS project. At any time I could pass by at his office for discussions, questions or just a talk. Theo was always interested in the work I was doing. I had a lot of freedom within my research and he helped me a lot to finish my thesis in time. The successful finish of my PhD research was also thanks to the effort of my promotor Peter Burrough. He taught me how to analyse vegetation data and how to compile a piece of text in a structured way. He has spent many hours reading my long sentences and improving my Austrian English. Especially in the last phase he was a great support. I also honour the effort of Andrea Fabbri who motivated me to do the PhD in the Netherlands and who arranged everything to make GETS a successful project.

My background (I graduated as a teacher for geography and mathematics) was very different from that what was required for the research described in this thesis. Nevertheless, because of the support of many people I have learned a lot and successfully fulfilled the assignment: Thom Bogaard, my office mate in the beginning of the research, introduced me to the Dutch culture and habits, and was always available to resolve my downs and hydrological issues, or for other discussions. Rens van Beek, the second office mate at that time, got never tired of answering my questions or e-mails, he always took his time for finding the right answer or strategy although he had to work like hell for his own research. Rens also helped me with applying the stability model that he developed for his study area to the ski area of Sölden. Further I want to mention Simone van Dijck, whom I could always ask advises, especially in the beginning, and Oscar van Dam, who has given me his meteo station and who assisted me in applying the radiation model to my study area. Without the help of Derek Karssenberg I would not have been able to carry out the research in the way I finally did. Derek has spent many hours writing pieces of software, generating ideas, discussing the progress of my research, and explaining me technical things. Thanks to Kor de Jong I could carry out the modelling part at the Linux system of the PCRaster freaks. He kept the system up to date and was very patient in teaching me the basics for using it. Edzer Pebesma helped me a lot with the statistical analysis of my plant species and writing an article about it. Cees Wesseling supported me several times to solve problems related to the modelling work. Not to forget Raymond Sluiter for being a great office mate and friend in the second half of my research. I could ask him everything about computers and he always tried to cheer me up in bad moments, either with or without Pepsi light or Toblerone. Dinand Alkema assisted me in finding my way in the GETS project, with the data collecting in the field and many other things like critical reading of text. He was a very good discussion partner and knew how to cheer me up. I also want to mention Peter Mekenkamp and Aart Barendregt, and all the colleagues

from the Department of Physical Geography whom I did not yet cite, who made my stay in the Netherlands a pleasant one, in particular Esther Stouthamer, Pieter-Jan van Helvoort, Job Spijker, Ivo Thonon, Jiske Burema, Marlous van der Meer, Marcel van der Perk, Steven de Jong, Kim Cohen, Irene Esser, Annina Andriessen, Henk van Steijn, Anneke de Jode, Paola Almeida, Pieter Augustinus, Aart Kroon, Rudi Hessel, Rutger Dankers and many more.

The fieldwork could be done thanks to many people. First of all because of the effort of my co-promotor Theo and the field workers who collected most of the data that have been used in this thesis, in particular Ivo Thonon, who did numerous rainfall simulations in the high mountains together with his field mate Arthur Coevert and who did not get tired of explaining me essential things of physical geography and throwing salt in the mountain rivers during heavy rain; Liz-Anne Strik and Jaap Cremer, who drilled many holes in the ski pistes of Sölden to collect data for the stability model; Marleen Noomen, Christel Kooijman, Roy Frings, and Mikie Castenmiller for cutting many m² of grass that had to be sorted afterwards; Margriet Groenendijk and Tina Koerts, who had most of the time wet feet because of walking in the deep snow for sampling snow data. Thanks to Roy and Mikie I could include a sophisticated plant growth model in the decision analysis. I could also profit from the practical skills and knowledge of Martin Hendriks, Victor Jetten and Rens van Beek, who visited me and the students in the field. Annemarie van Asch took care of the mental support. A very important person in the field and also in the GETS project was Alessandro Ghinoi, with whom I have spent many hours mapping geomorphology and plant species, doing rainfall simulations, enjoying our rest after heavy field work and carrying out the Sölden case study for the GETS project. Furthermore, I appreciate very much all the help and technical support of the people from the laboratory of the Department of Physical Geography in Utrecht, especially Kees Klawer, Hassan Aarab, Marcel van Maarseveen and Bas van Dam. The fieldwork was also supported by the Ötztal Arena, which provided us with free tickets for the ski lift and other useful information. The workers of this company were very friendly and co-operative. We were further supported by the major of Sölden, the family Grüner, Karl-Heinz Gstrein, Ewald Schöpf, and local farmers. I do not want to forget Joy Burrough and Renske Eck, who helped me identifying plants.

The data set could be extended thanks to the help of several institutes in Austria providing to a large extent free data and additional information. These were several departments of the "Landesregierung", in particular "Gruppe Landesbaudirektion", "Gruppe Landesforstdirektion", "Gruppe Raumordnung, Bau und Umwelt" and "Gruppe Schule, Kultur und Sport", "Lawinenwarndienst" in Innsbruck, the "Institut für Lawinen- und Wildbachverbauung" in Imst, "Alpenverein" in Innsbruck, meteorological service of Austria (ZAMG) and "Ingenieursgemeinschaft AVT" in Imst. I also want to acknowledge Alexander Cernusca, Gernot Patzelt, Christian Newesely and Thomas Nagler from the University of Innsbruck for their cooperation.

It was fun to be a young researcher in the GETS project, I learned a lot, I got to know many nice people and I had a great time during the meetings. I want to point out Alessandro Ghinoi, my wonderful partner within the Sölden team, Ali Sharifi, the motivator to keep the direction of the research and to hurry up with the analysis, and Alfred Wagtendonk, the multimedia guru. He has put a lot of effort in connecting the network partners and publishing the results of the project on the Web. We had a very nice

meeting with several experts of different departments of the “Provincia Autonomia di Trento”, thanks to Francesca Defranceschi and Gianluca Tommasi who organised it for Alessandro and me.

Being an international PhD student has the advantage to get to know people from around the world. I had a great time and lots of nice food with my friends Lorna, Dave, Federica, Luciano, Alireza, Øystein, Marika, Marketa, Frank, Sandra, Carola, Cielito, Ana Maria and many more. Lorna was and still is not only a very good friend; she has also provided important input to my work, both as editor and as discussion partner.

In these four years my friends in Austria did not forget me, Alexandra, Joseph, Lisa, Guiseppe. Doris, Josef, Sabine, Hans, Christa and Walter supported me from far away and trusted that once I would finish my thesis.

I appreciate the trust, motivation and interest from my parents Anna and Werner, Derek, who had to stand all my moods, Roman and Verena (thanks for editing the German summary), Gudrun and Henk (thanks for all the hospitality), Birgit and Raimund, Ulli and Thomas, O.Alfred, Jitske and Ferd, Ana and Tim, Berend and many more.

Finally I want to thank all these people for the support in the last four years, both scientifically and mentally.